Functional renormalization group approach to strongly-correlated moiré materials

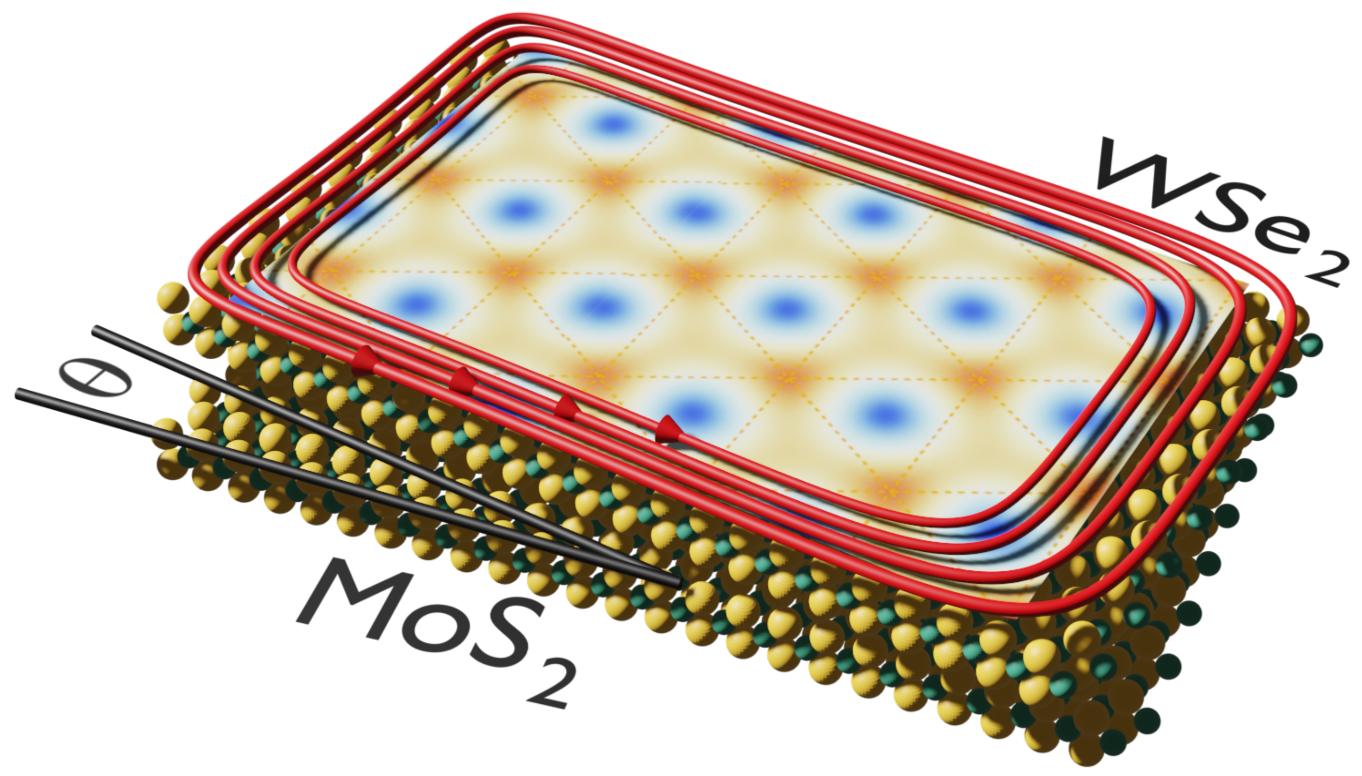

Michael M. Scherer

Ruhr-University Bochum

Oct 31, 2022 @ YITP

Introduction & motivation

- **graphene**: flat single layer of C atoms on honeycomb lattice
  - 2D material
  - excellent conductor, mechanically strong, flexible,...

- **emergent symmetries** → massless Dirac electrons:

$$i\hbar\gamma^{\mu}\partial_{\mu}\psi = 0$$

  - unusual Landau-level sequence $\epsilon_n \propto \mathrm{sgn}(n)\sqrt{B|n|}$
  - half-integer QHE, Klein tunneling,...

- band theory works very well → **no sign of strongly-correlated behavior**!

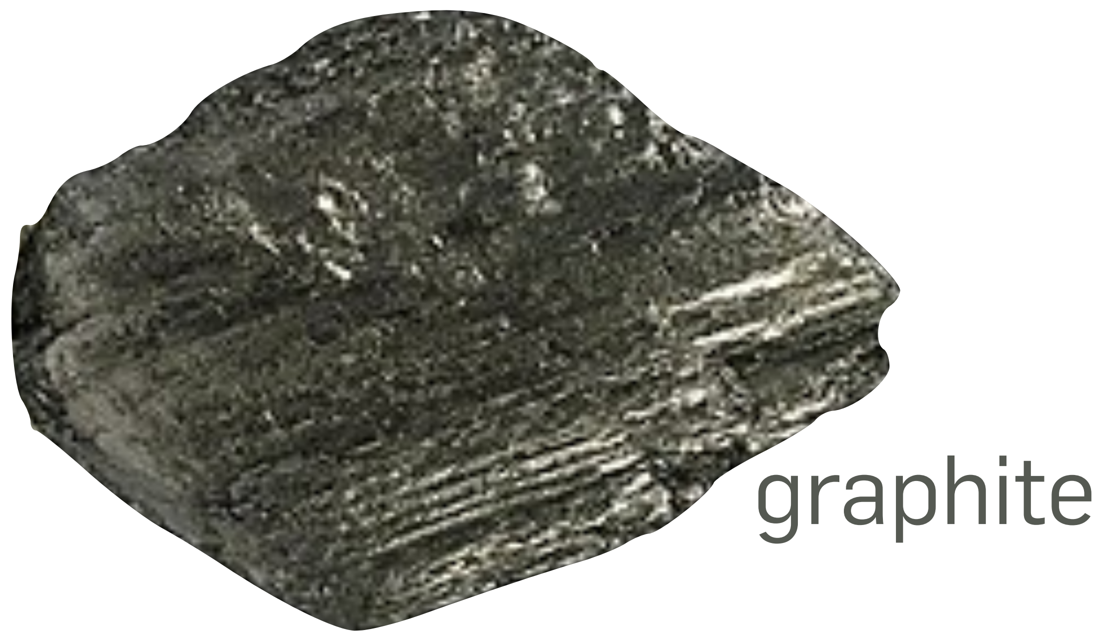

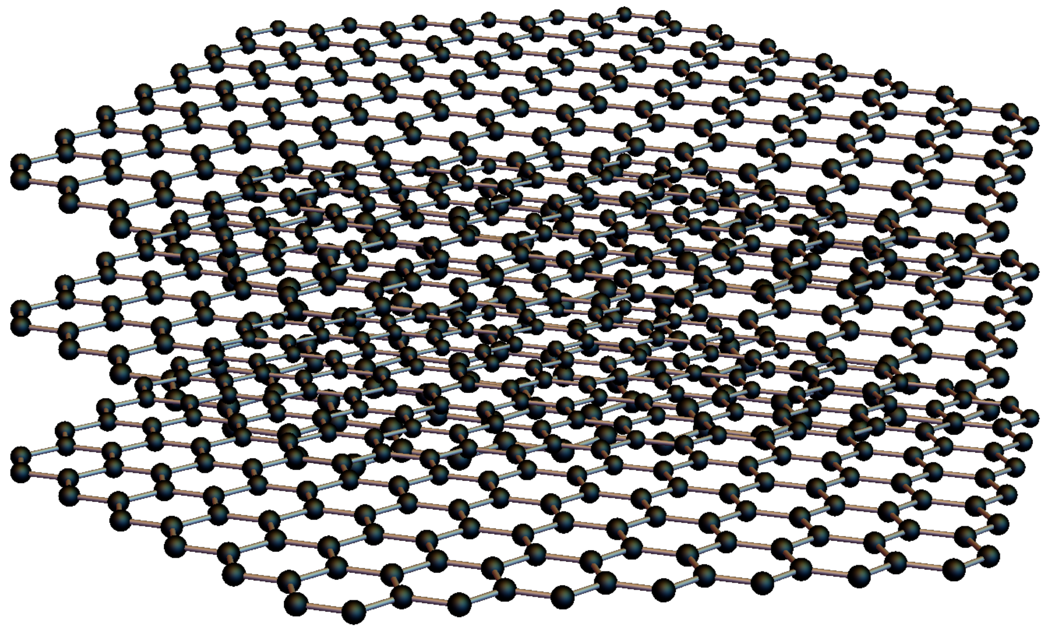

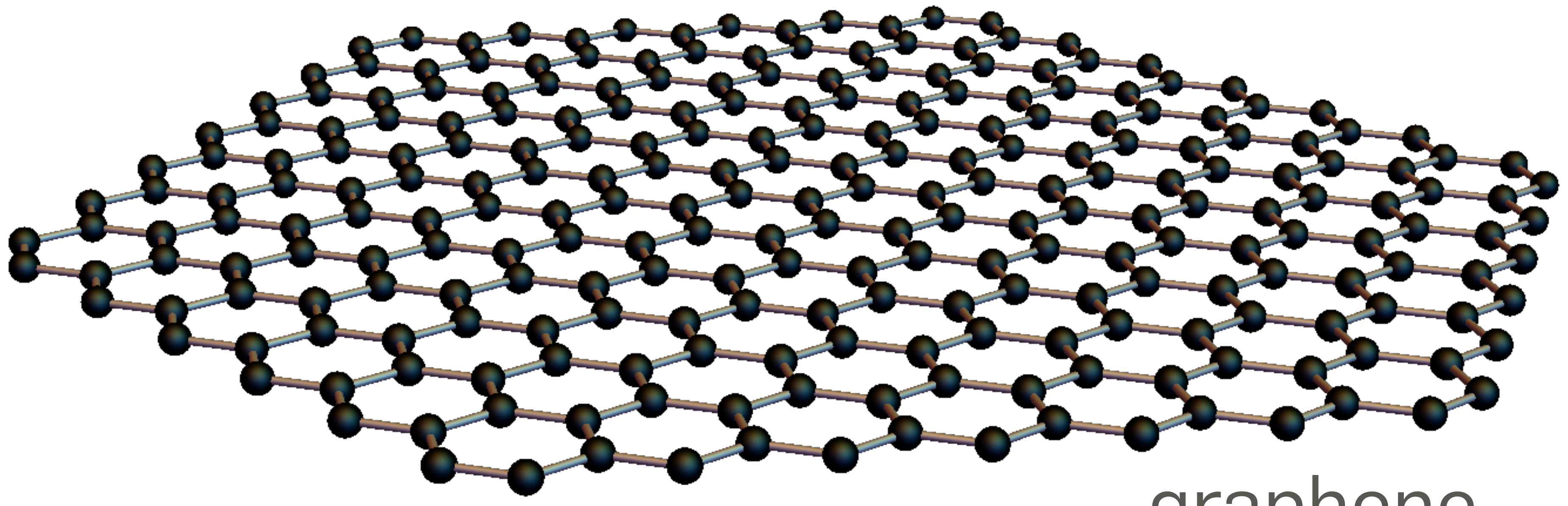

Introduction & motivation

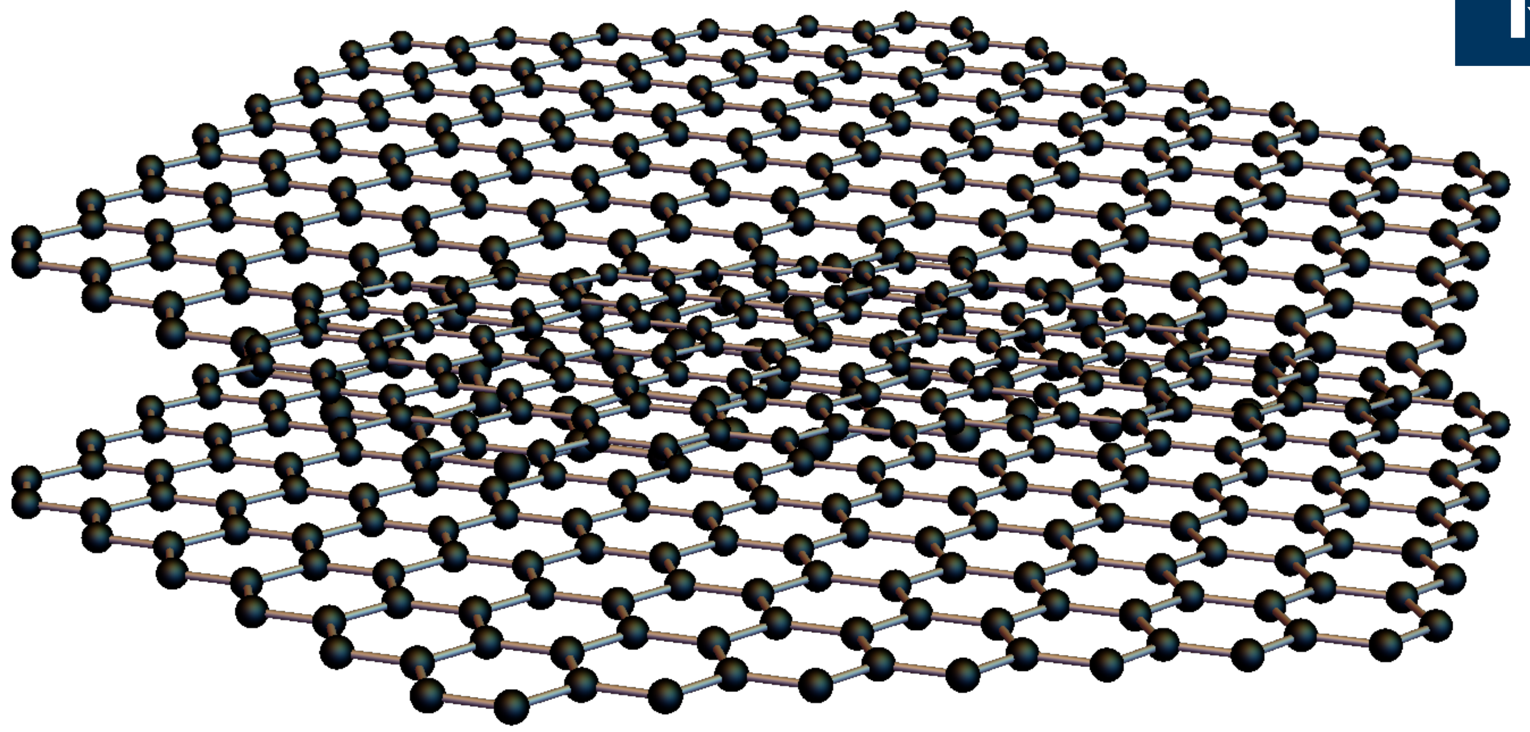

- **bilayer** graphene
  - layers weakly coupled via van der Waals interactions
  - experiments at small twist angle $\theta \sim 1^\circ$ → **strongly-correlated behavior**

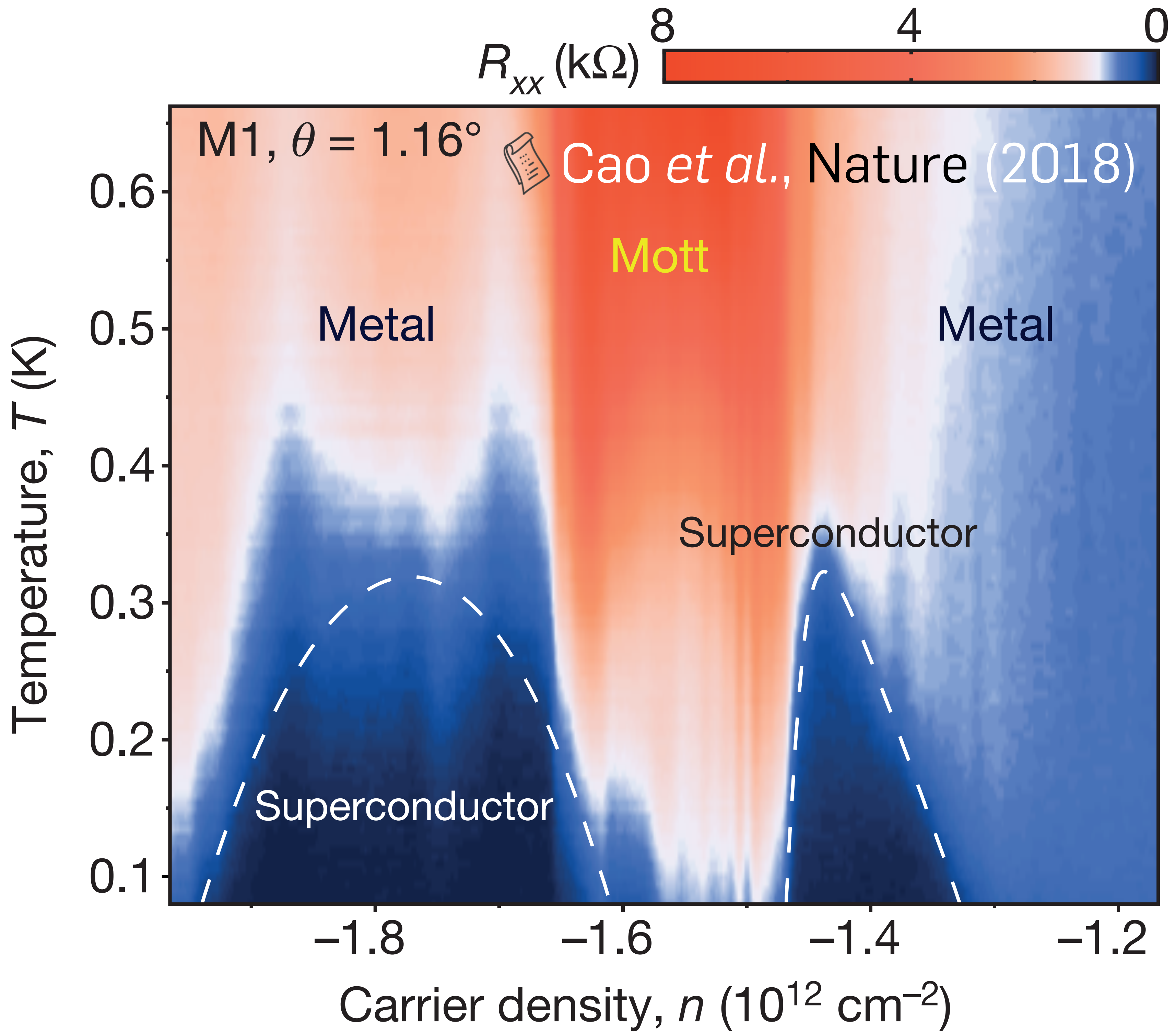

- phase diagram reminiscent of hight-T_c cuprates/pnictides,...
- new platform for study of strongly-correlated materials

  #twistronics #moiré-materials

Introduction & motivation

RUB

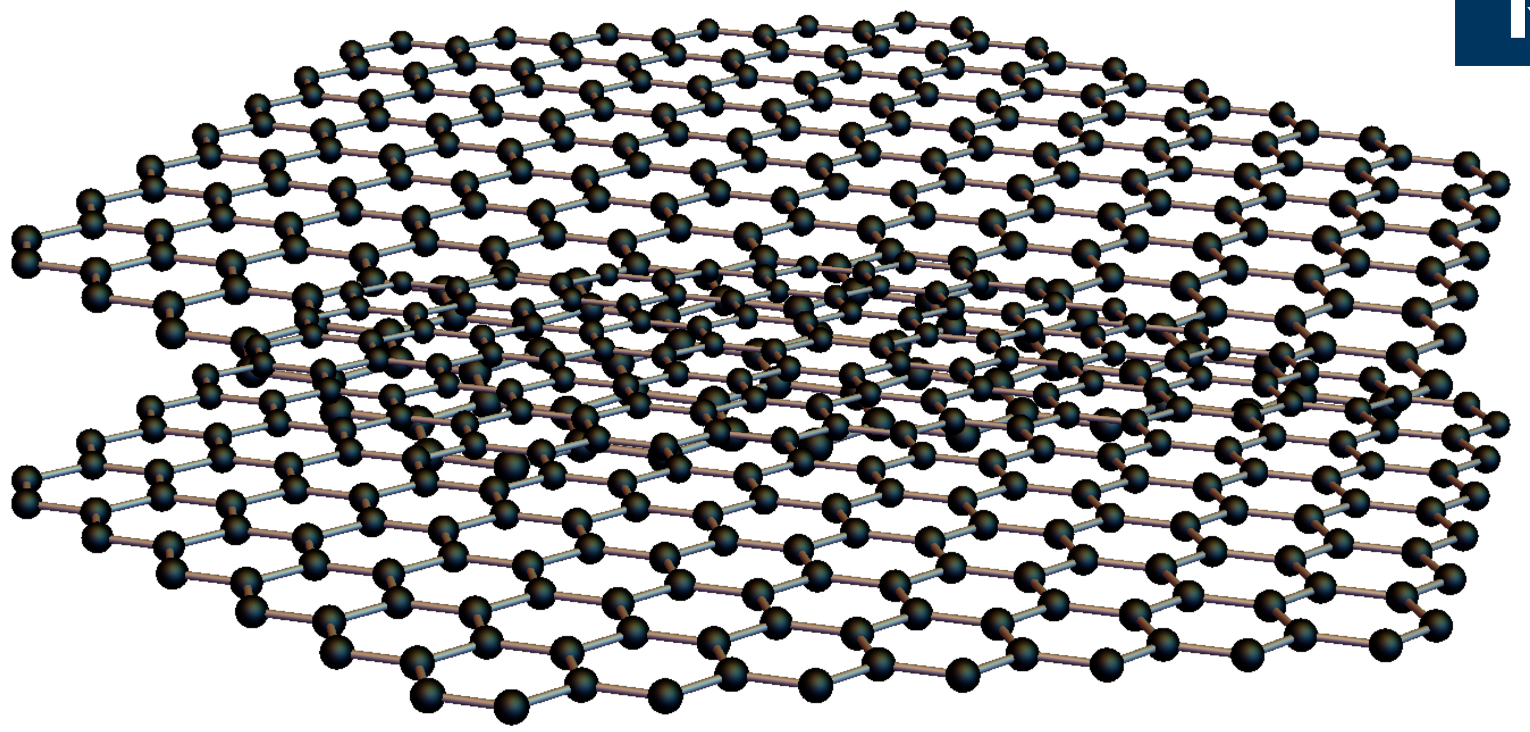

- **theoretical study** of strongly-correlated quantum materials
  - needs suitable **quantum many-body methods**

Quantum Monte Carlo (QMC)

Density-matrix renormalization group (DMRG)

Mean-field level approaches
- Hartree-Fock
- RPA
- *single-channel* resummations

Tensor networks

Dynamical mean-field theory (DMFT)

Functional renormalization group

...

Outline

RUB

- *Chapter I:* From 2D moiré materials to frustrated superlattice Hubbard models
- *Chapter II:* Interaction effects in hexagonal superlattice Hubbard models
- *Chapter III:* Functional renormalization group
- *Chapter IV:* Functional renormalization group for moiré materials
- *Chapter V:* Further developments and outlook

RUB

Chapter I: From 2D moiré materials to frustrated superlattice Hubbard models

- 2D materials and their heterostructures
- Geometric theory of 2D moiré patterns
- Band structure of transition metal dichalcogenides
- Moiré bands
- Effective moiré tight-binding models and Coulomb interactions
- Mini review of some theoretical and experimental results

Katsnelson, *Graphene* (2012)

Wu, Lovorn, Tutuc, MacDonald, PRL (2018)

Koshino *et al.*, PRX (2018)

2D materials LEGO® with a twist

RUB

- broader class of **2D materials** (semi-conductors, insulators,...)
- heterostructures from **stacking** and **twisting** 2D materials

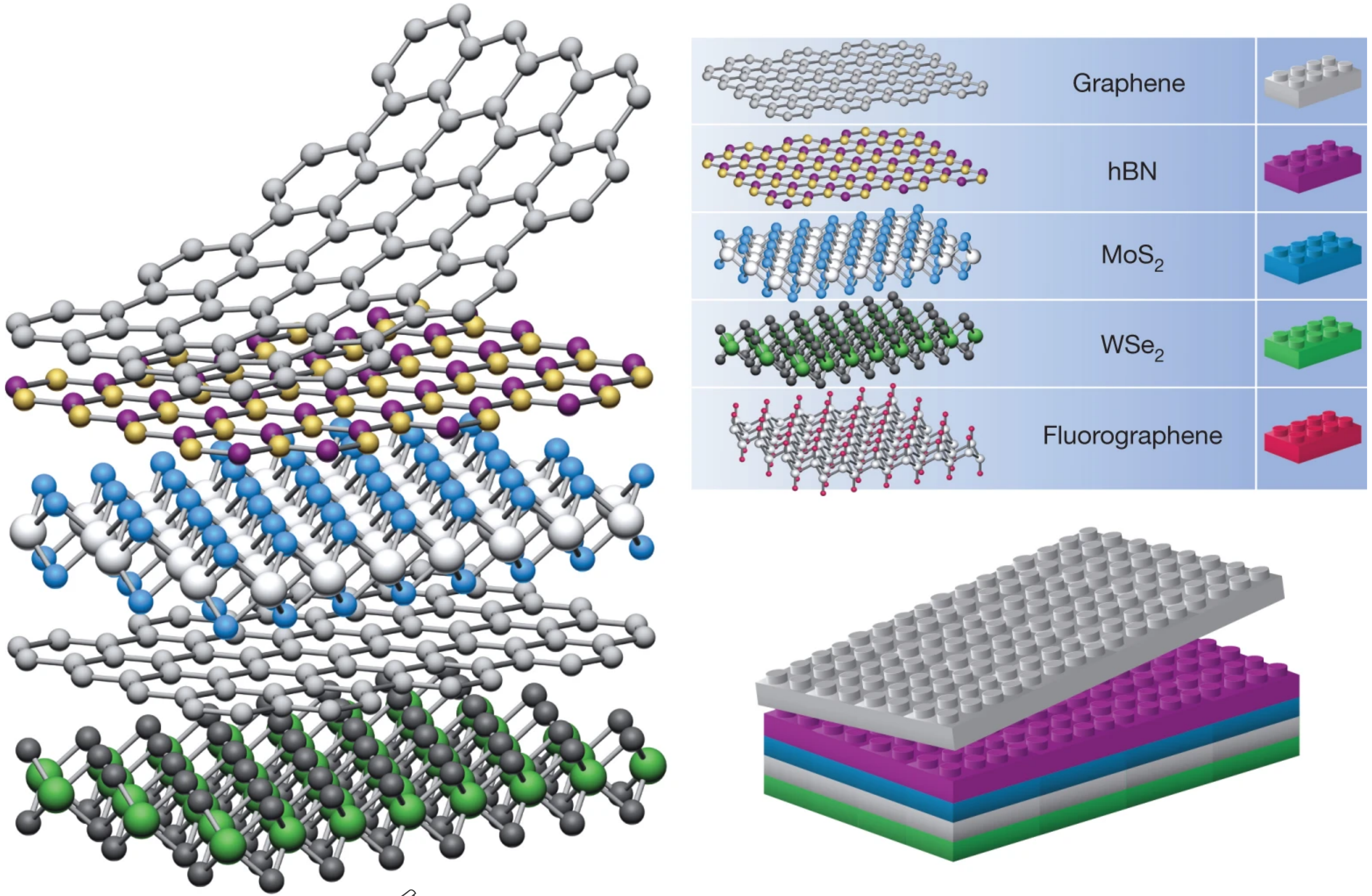

Geim & Grigorieva, Nature (2013)

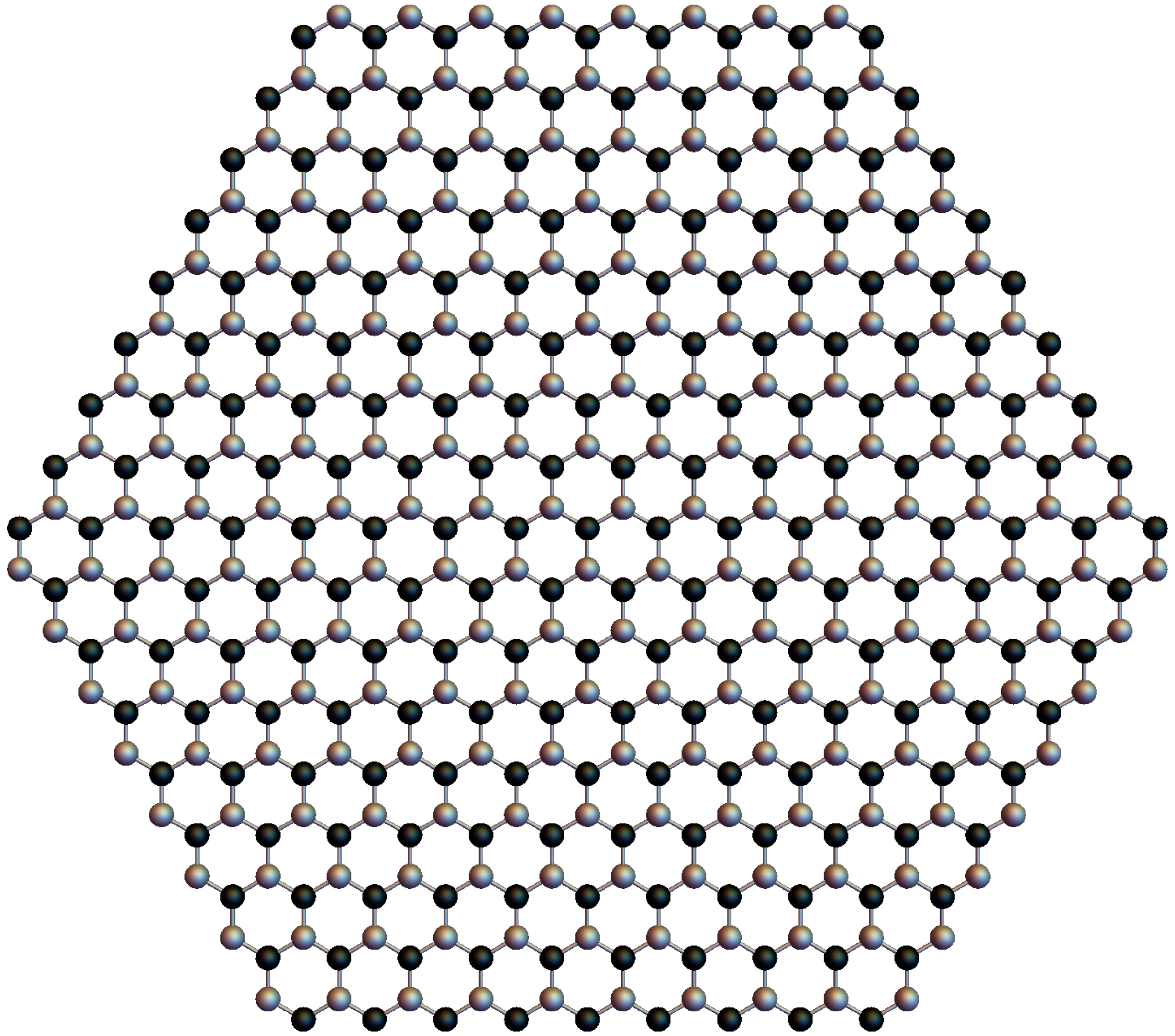

top view

→ *see also tutorial by M. Koshino!*

2D moiré materials

- AA stacking

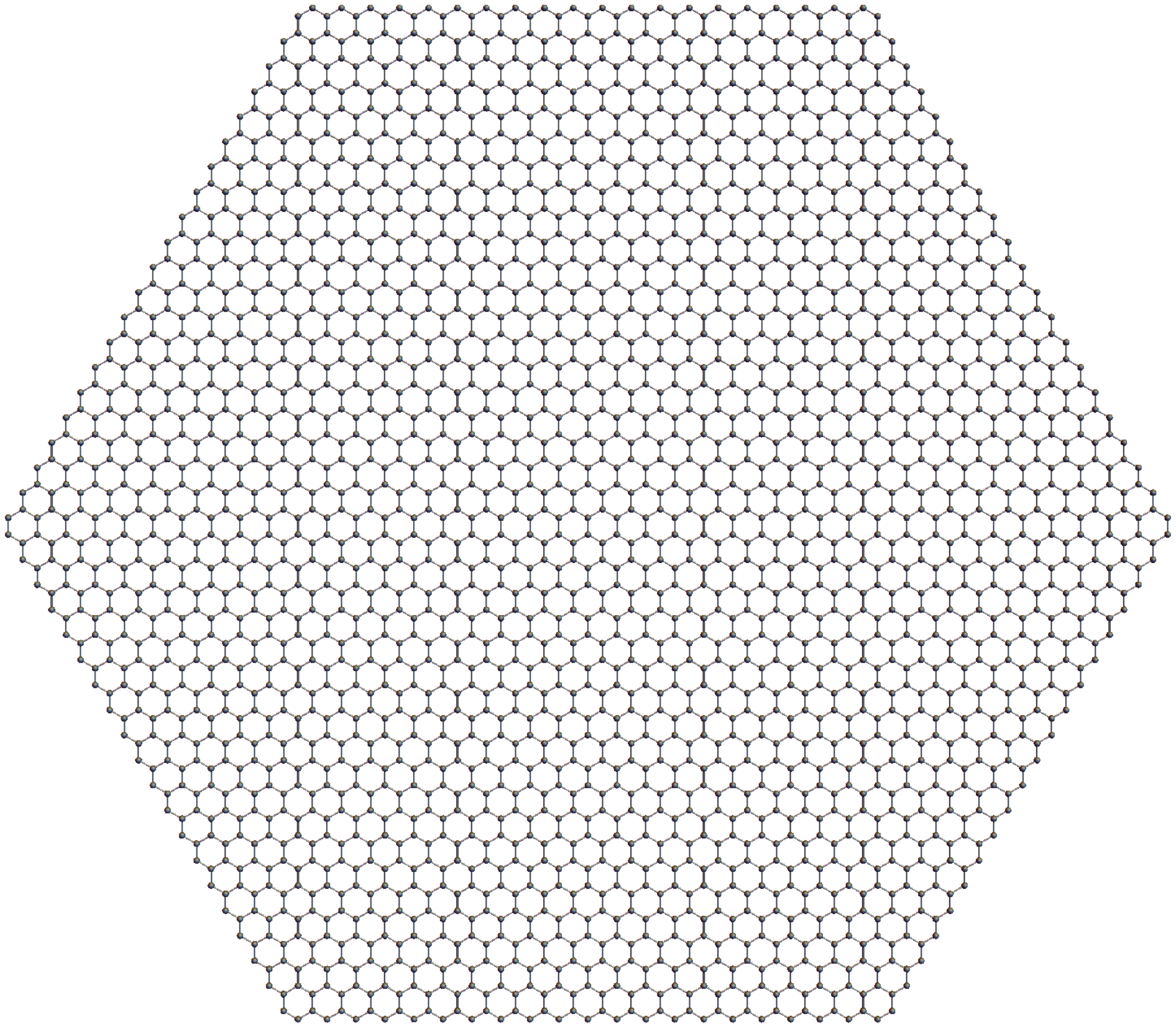

2D moiré materials

- rotation by $\theta = 30^{\circ}$

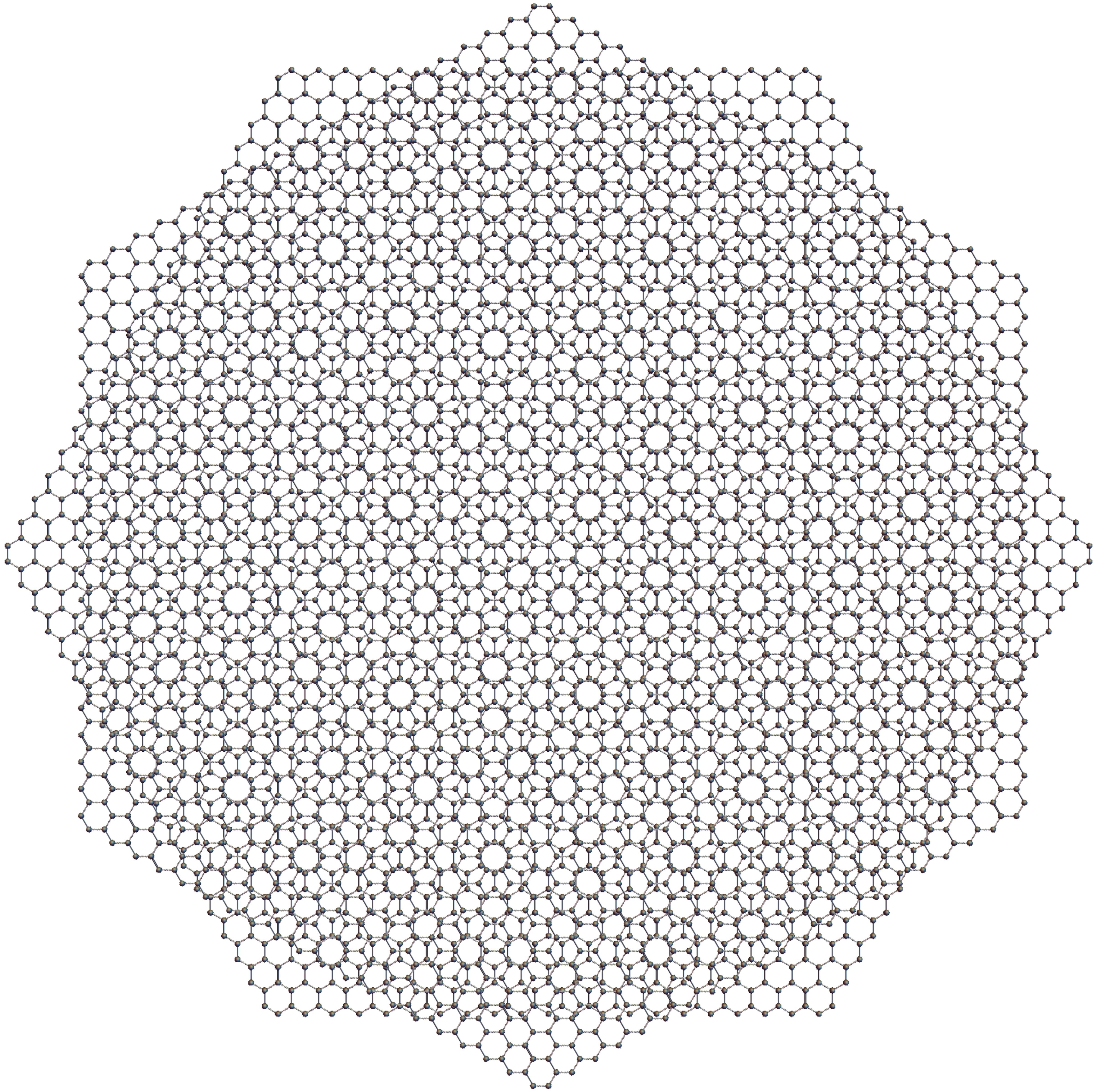

  - 12-fold rotationally symmetric lattice without any translational symmetry (quasicrystal)

2D moiré materials

- rotation by $\theta = 5^\circ$

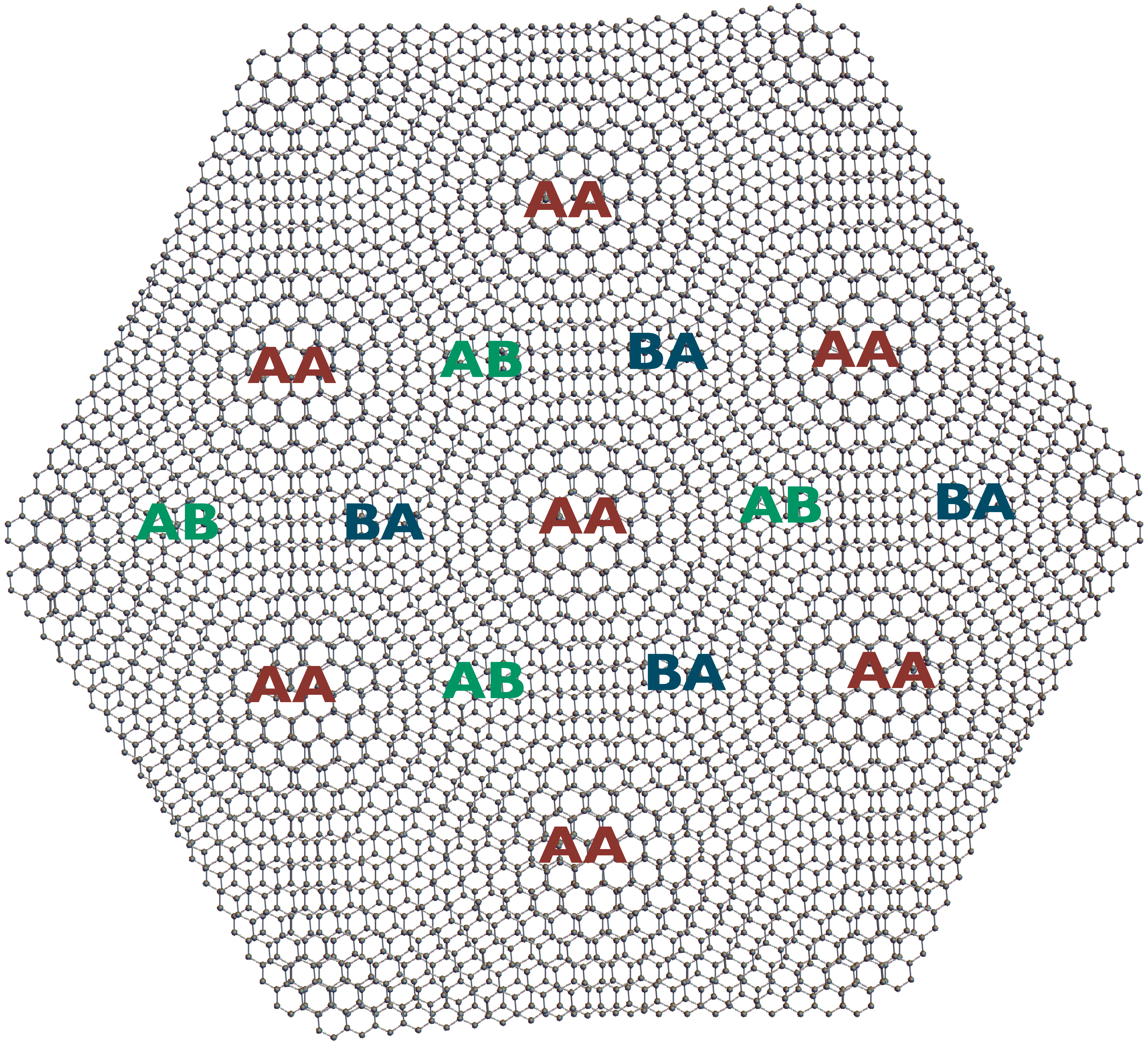

- small twist angle → interference effect → large-scale **moiré superlattice**

2D moiré materials

- generally: overlay of 2 periodic structures with slight mismatch → moiré interference pattern

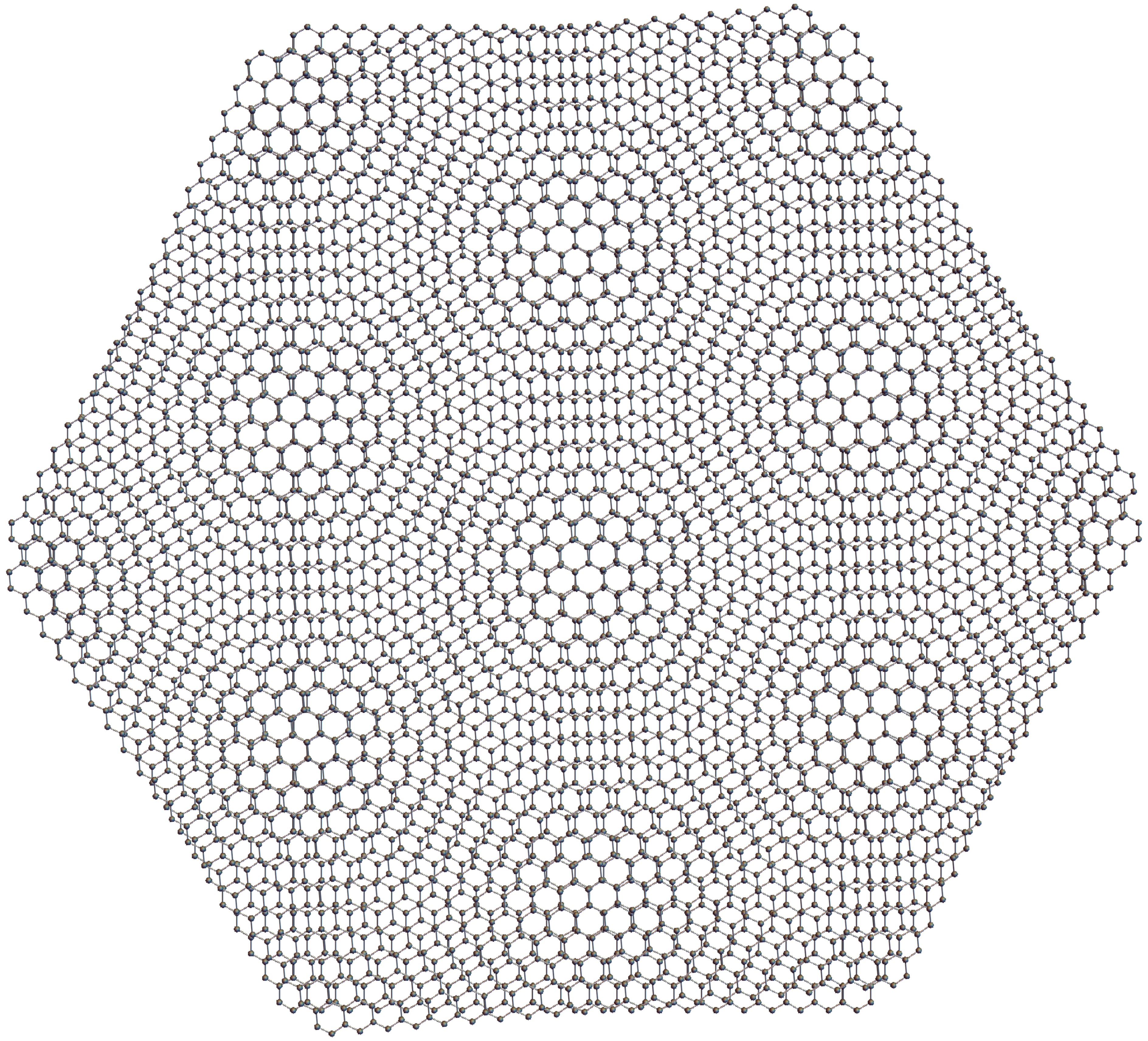

rotation by $\theta = 5^\circ$

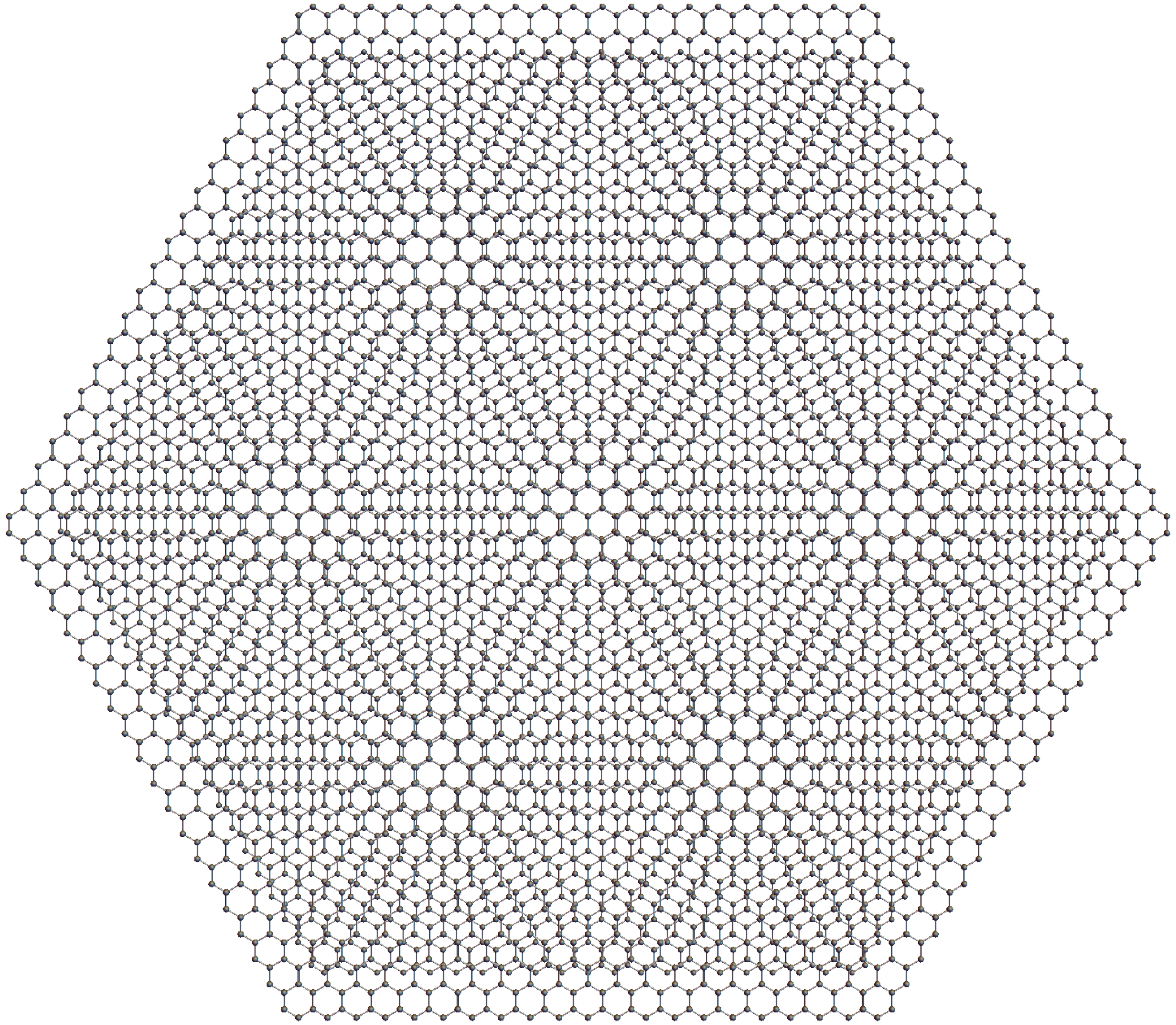

$\theta = 0^\circ$ but different lattice constants

Geometric theory of 2D moiré patterns

RUB

- start with 2 identical honeycomb lattices
  - rotate layers 1 and 2 around a pair of B sites by $\mp\theta/2$
  - Bravais lattice vectors of layer l after rotation:

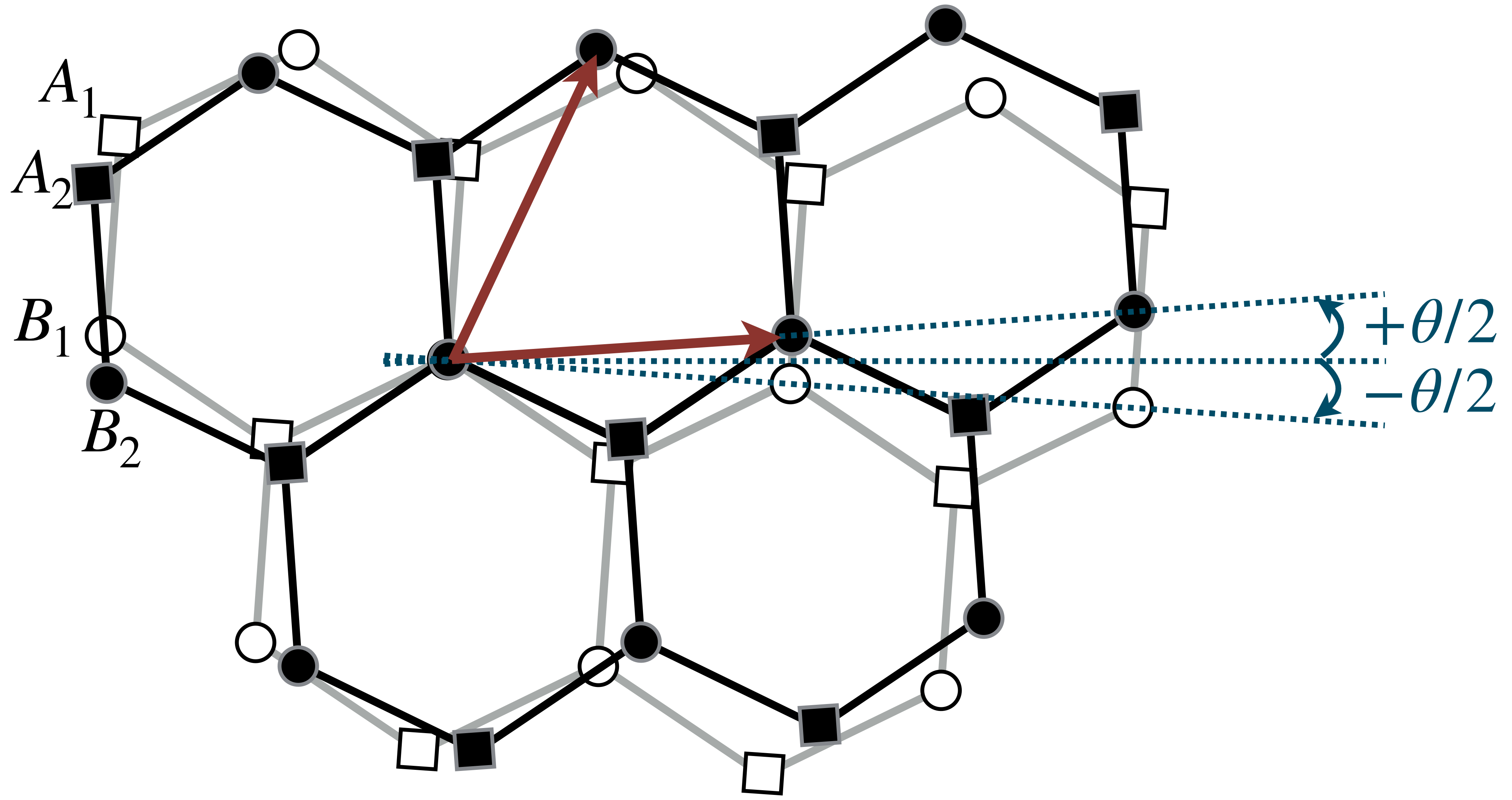

$$\vec{a}_i^{(l)} = R(\mp\theta/2)\vec{a}_i \text{ with } R(\varphi) = \begin{pmatrix} \cos\varphi & \sin\varphi \\ -\sin\varphi & \cos\varphi \end{pmatrix}$$

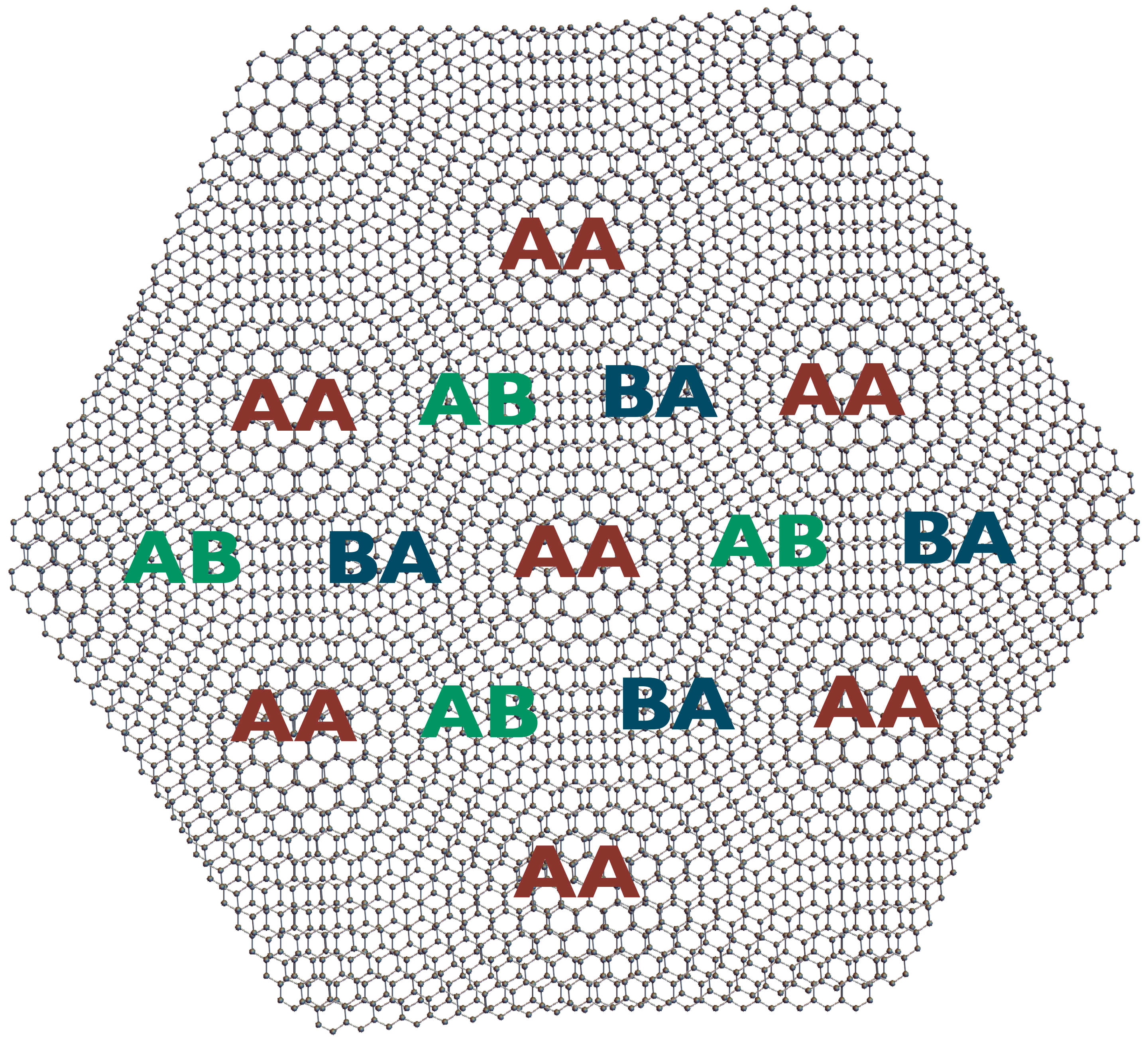

  - likewise the reciprocal lattice vectors become $\vec{a}_i^{*(l)} = R(\mp\theta/2)\vec{a}_i^*$
  - ions at lattice sites generate **(crystal) potential** for electrons

Geometric theory of 2D moiré patterns

RUB

- **crystal potential** $V(\vec{r})$ of bilayer structure → superposition of crystal potentials of both layers
  - sum of 2 Fourier series:

$$V(\vec{r}) = \sum_{mn} \left[u_{mn} e^{im\vec{a}_1^{*(1)}\cdot\vec{r} + in\vec{a}_2^{*(1)}\cdot\vec{r}} + w_{mn} e^{im\vec{a}_1^{*(2)}\cdot\vec{r} + in\vec{a}_2^{*(2)}\cdot\vec{r}} \right], \quad m, n \in \mathbb{Z}$$

$$= \sum_{mn} u_{mn} e^{im\vec{a}_1^{*(1)}\cdot\vec{r} + in\vec{a}_2^{*(1)}\cdot\vec{r}} \left[1 + \frac{w_{mn}}{u_{mn}} e^{im\vec{G}_1^M\cdot\vec{r} + in\vec{G}_2^M\cdot\vec{r}} \right]$$

modulation on scale of graphene lattice constant

(moiré) interference effect

  - here $\vec{G}_i^M = \vec{a}_i^{*(1)} - \vec{a}_i^{*(2)}$ can be seen as reciprocal lattice vectors of moiré superlattice

$$\vec{G}_i^M = \left[R(-\theta/2) - R(+\theta/2)\right] \vec{a}_i^* = \begin{pmatrix} 0 & 2\sin(\theta/2) \\ -2\sin(\theta/2) & 0 \end{pmatrix} \vec{a}_i^*, \quad i \in \{1,2\}$$

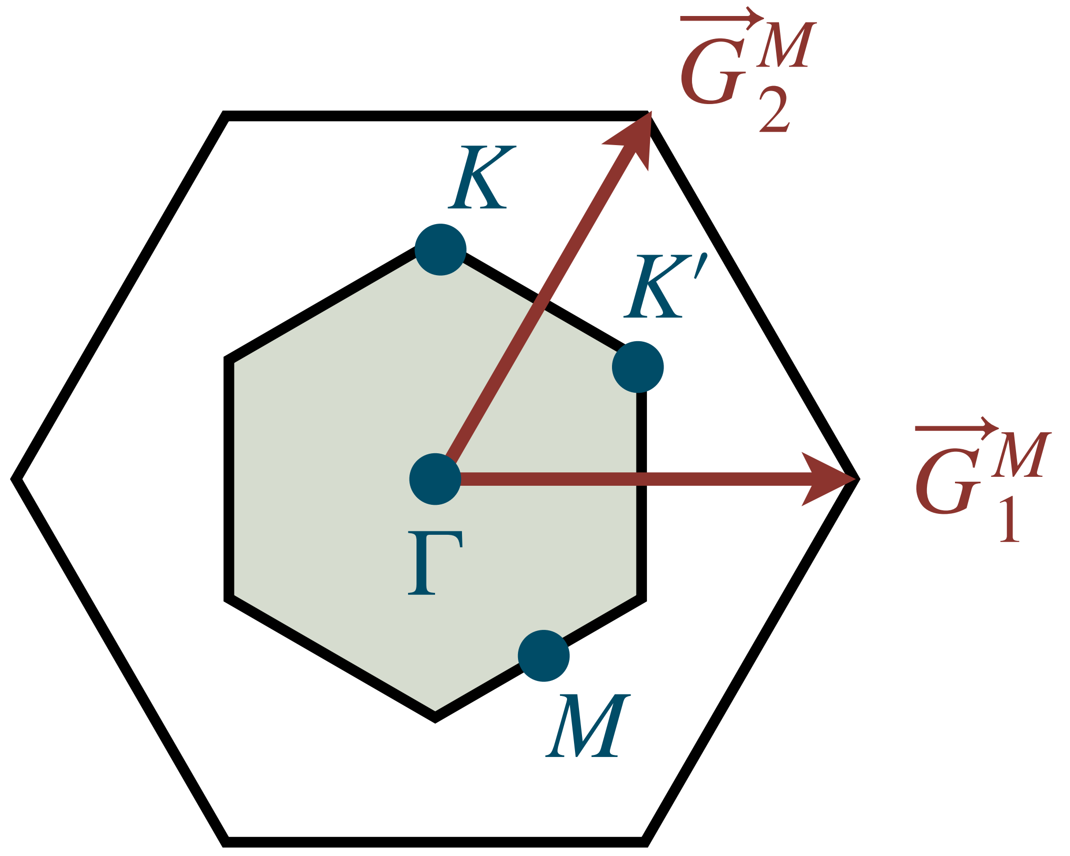

  - $\vec{G}_1^M, \vec{G}_2^M$ define the moiré Brillouin zone of the superlattice

Geometric theory of 2D moiré patterns

RUB

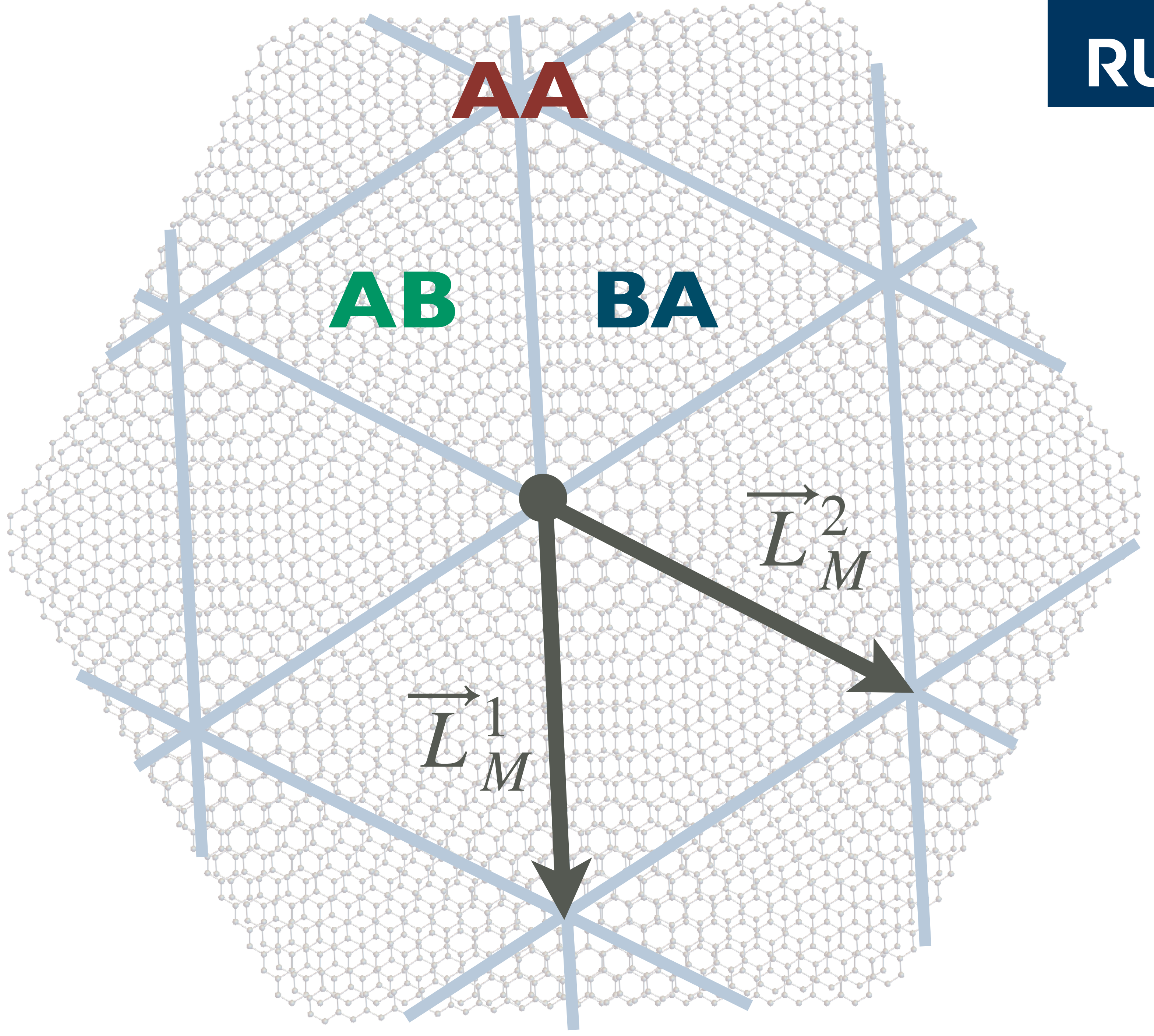

- real-space moiré lattice vectors $\vec{L}_j^M$
  - obtained from relation $\vec{G}_i^M \cdot \vec{L}_j^M = 2\pi\delta_{ij}$
  - length of moiré unit vectors: $a_M = |\vec{L}_j^M| = \dfrac{a_0}{2|\sin(\theta/2)|} \approx \dfrac{a_0}{|\theta|}$
  - for small θ : $a_M \approx a_0/|\theta| \gg a_0$
- include small mismatch δ in lattice constants → moiré lattice constant: $a_M \approx \dfrac{a_0}{\sqrt{\theta^2+\delta^2}}$
- note: generally moiré pattern is not periodic as periods of layers are incommensurate for general (θ, δ)
  - commensurability for special (θ, δ) → rigorously periodic pattern
  - but: moiré superlattice vectors can be defined for any (θ, δ) as above
  - for small (θ, δ) → incommensuration effects are small

2D group-VI transition metal dichalcogenides

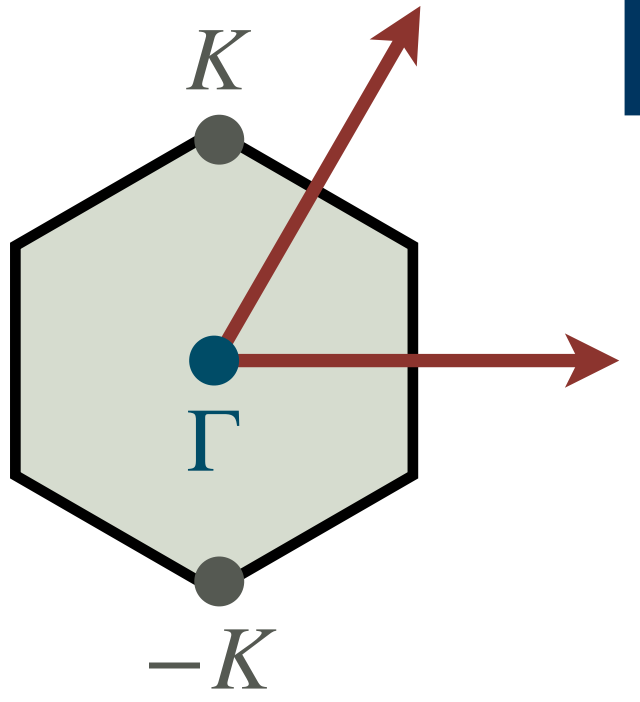

- schematic band structure of singlelayer WSe_2
  - band extrema at two inequivalent BZ corners K and K'

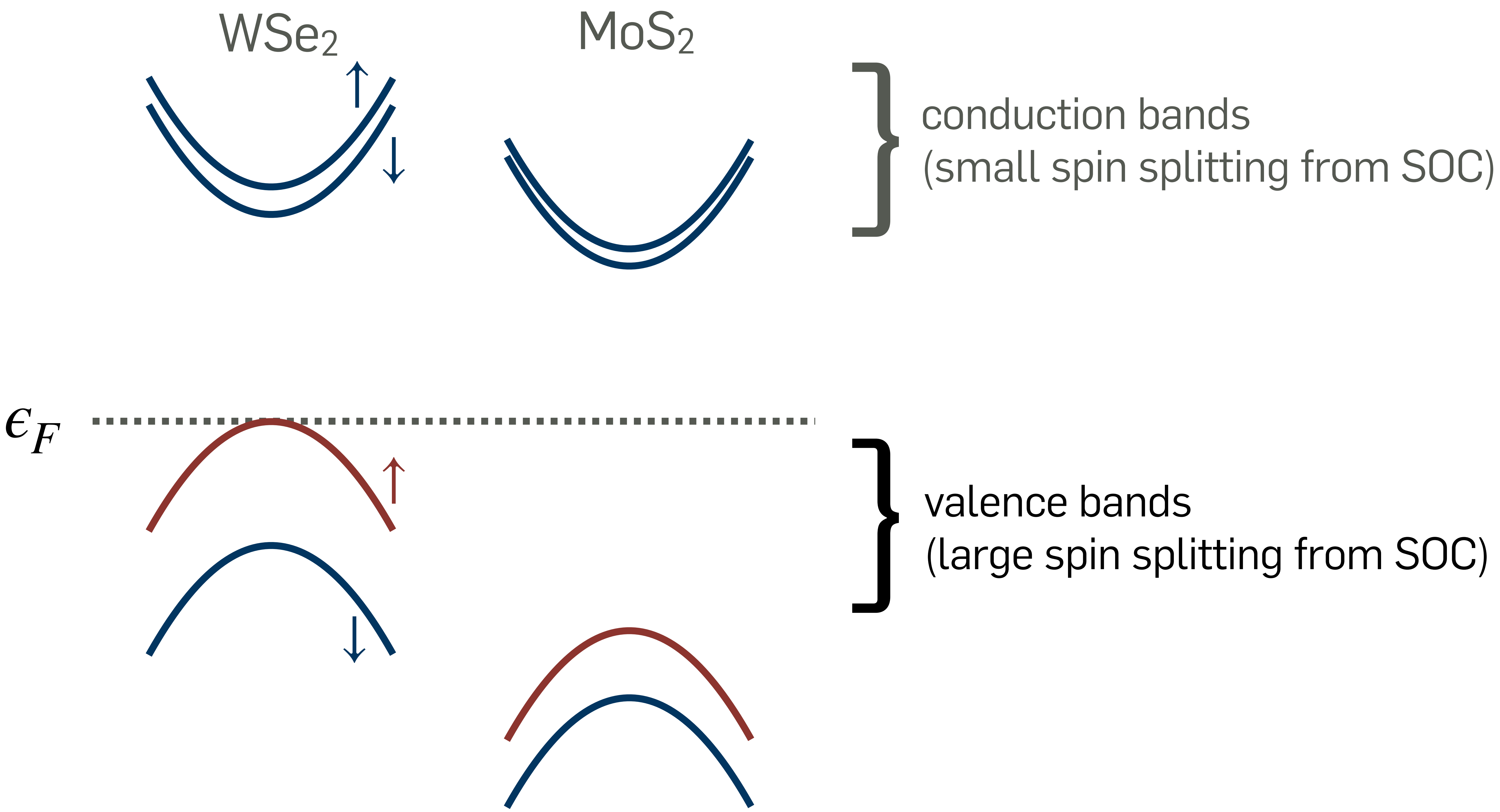

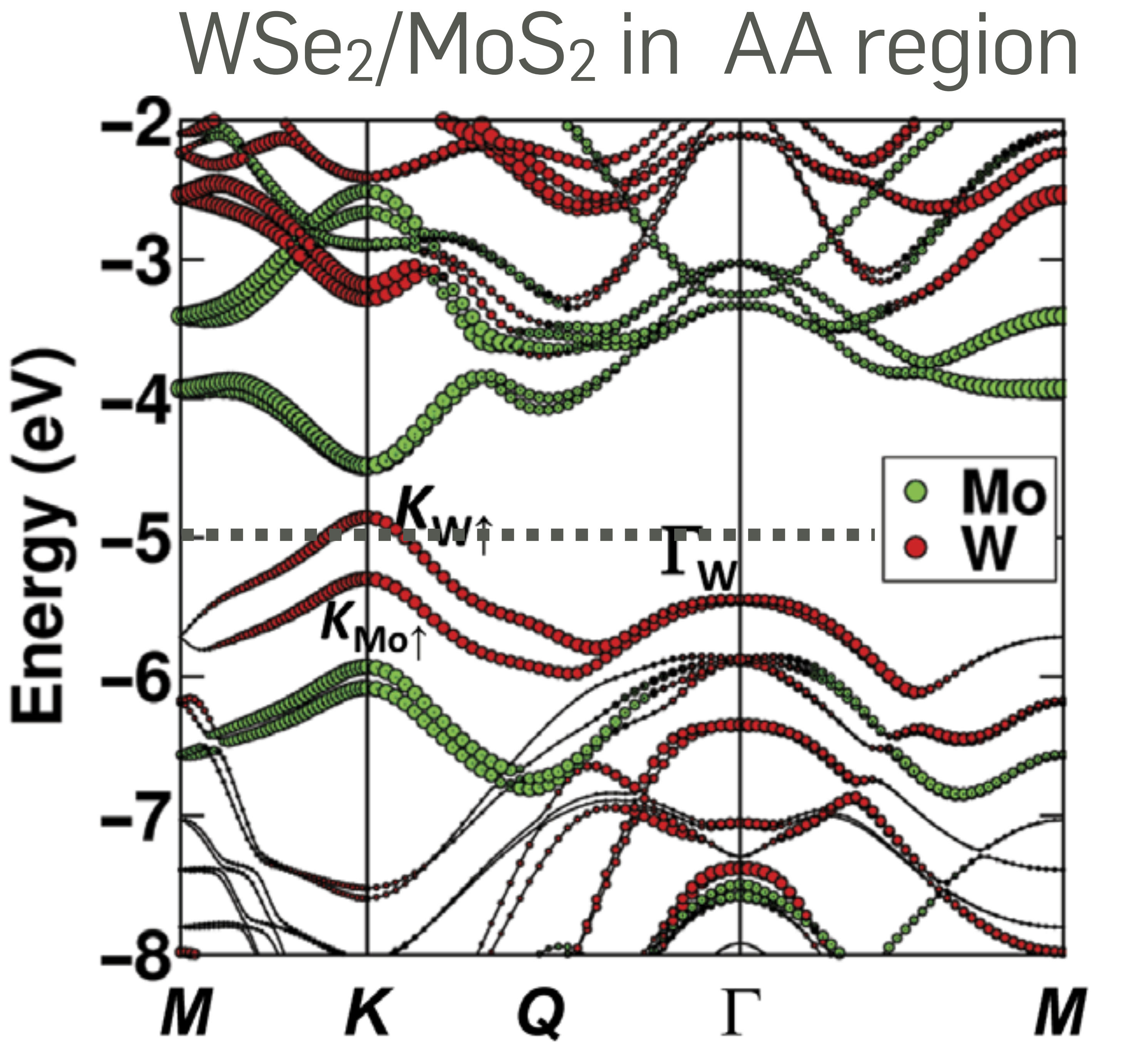

Zhang *et al.*, Sci. Adv. (2017)

- focus on energies/states near maximum of WSe_2 valence bands

WSe_2/MoS_2 heterobilayer at $\theta = 0°$

RUB

- WSe_2 lattice constant $a_0 \approx 3.32\,\text{Å}$
- MoS_2 lattice constant $a_0 \approx 3.19\,\text{Å}$

$$\delta = |a_0 - a_0'|/a_0 \approx 0.039 \quad \Rightarrow \quad a_M \approx \frac{a_0}{\sqrt{\theta^2 + \delta^2}} \approx 8.5\,\text{nm}$$

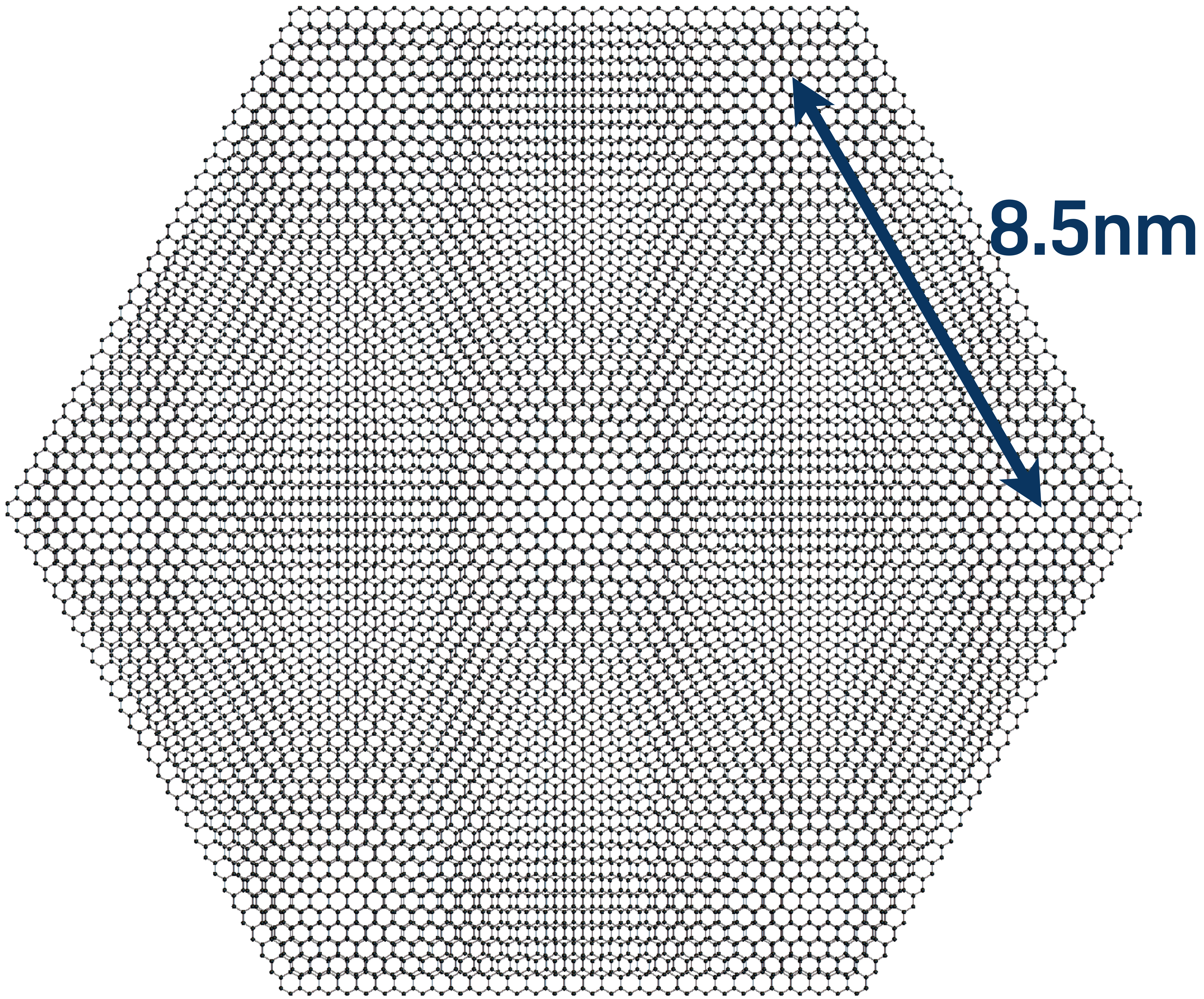

Moiré potential of WSe_2/MoS_2

RUB

- long-range moiré pattern of WSe_2/MoS_2 features different stacking regions
  - induces periodic potential for WSe_2 valence band states → **moiré potential $\Delta(\vec{r})$** with period a_M

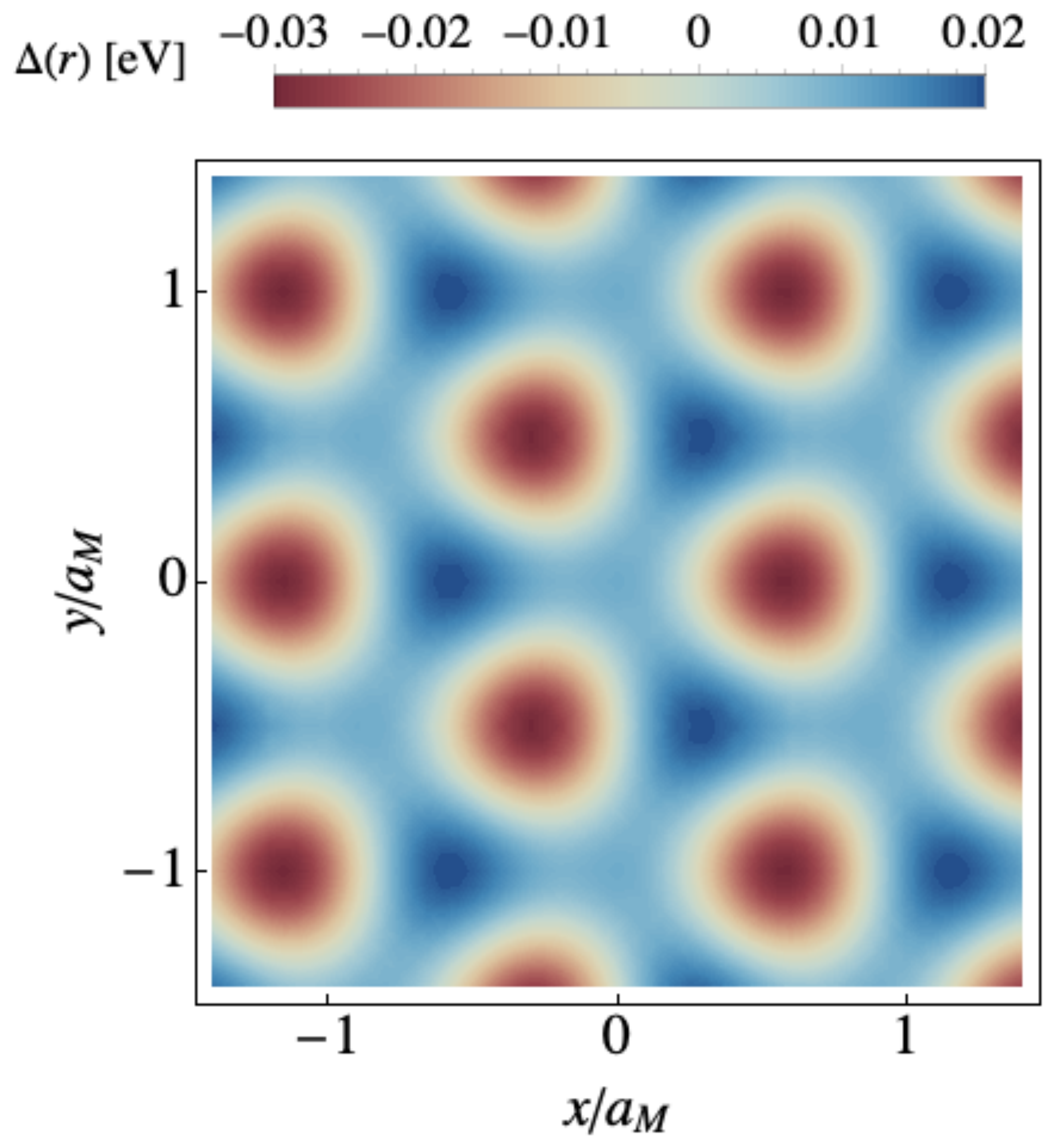

- $\Delta(\vec{r})$ can be approximated by Fourier series $\Delta(\vec{r}) = \sum_{\vec{G}} V(\vec{G})\, e^{i\vec{G}\cdot\vec{r}}$
  - sum over moiré reciprocal lattice vectors $\vec{G}$
  - sufficient to include 6 $\vec{G}$ in **first shell**
  - $\Delta(\vec{r}) \in \mathbb{R} \;\Rightarrow V(\vec{G}) = V^*(-\vec{G})$
  - C_3 symmetry $\;\Rightarrow V(R(2\pi/3)\vec{G}) = V(\vec{G})$

  ➡ all six $V(\vec{G})$ fixed by $V(\vec{G_1}) = Ve^{i\psi}$

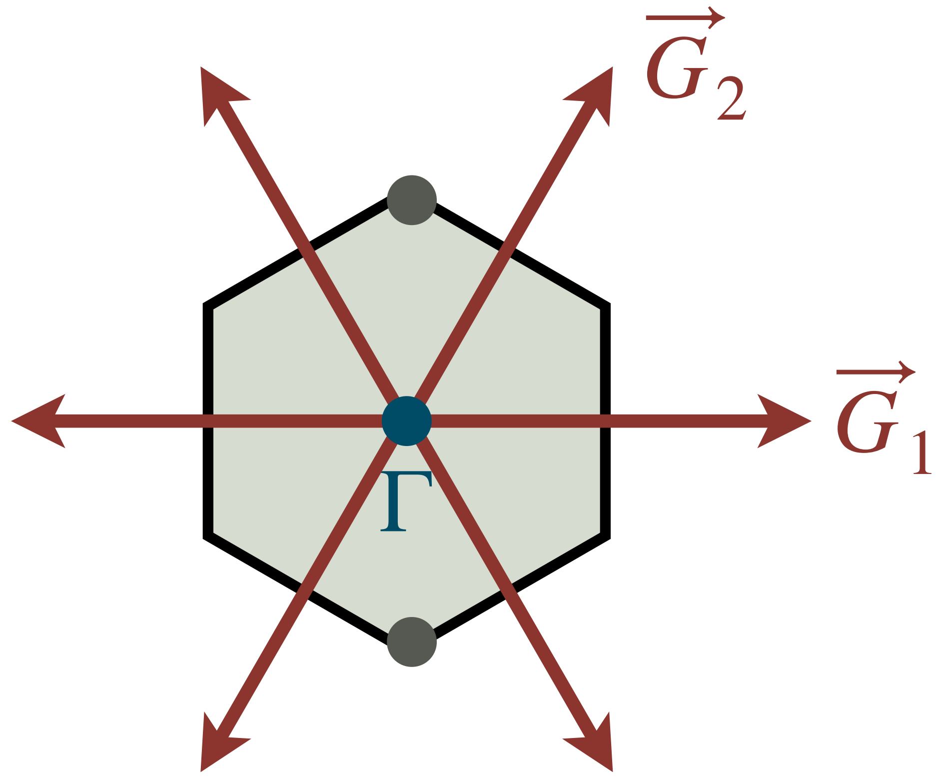

- moiré potential can be measured experimentally (STM) → **parameter fit**: $(V, \psi) \approx (5.1\,\mathrm{meV}, -71°)$
- interlayer coupling can be modified by external fields and pressure

Wu, Lovorn, Tutuc, MacDonald, PRL (2018)

Moiré band Hamiltonian of WSe_2/MoS_2

- focus on effect of moiré potential on states near maximum of WSe_2 valence band
  - effective mass approximation for maximum of WSe_2 band

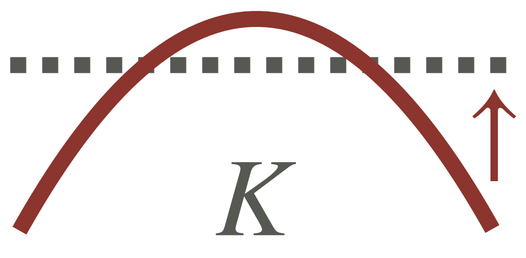

$$\mathscr{H}_{\text{kin}} = -\frac{\hbar^2 \vec{Q}^2}{2m^*} \quad \text{with} \quad m^* \approx 0.35 m_0$$

- **moiré band Hamiltonian** for WSe_2 valence band maximum states

$$\mathscr{H} = \mathscr{H}_{\text{kin}} + \Delta(\vec{r}) \quad \text{with} \quad \Delta(\vec{r}) = \sum_{i=1}^{6} V(\vec{G}_i)\, e^{i\vec{G}_i \cdot \vec{r}}$$

- dispersion from **moiré Bloch Hamiltonian** in plane wave representation

$$\langle \vec{k} + \vec{G} \,|\, \mathscr{H} \,|\, \vec{k} + \vec{G}' \rangle = -\frac{\hbar^2 |\vec{k} + \vec{G}|^2}{2m^*} \delta_{\vec{G},\vec{G}'} + \sum_{i=1}^{6} V(\vec{G}_i) \delta_{\vec{G}_i, \vec{G} - \vec{G}'}$$

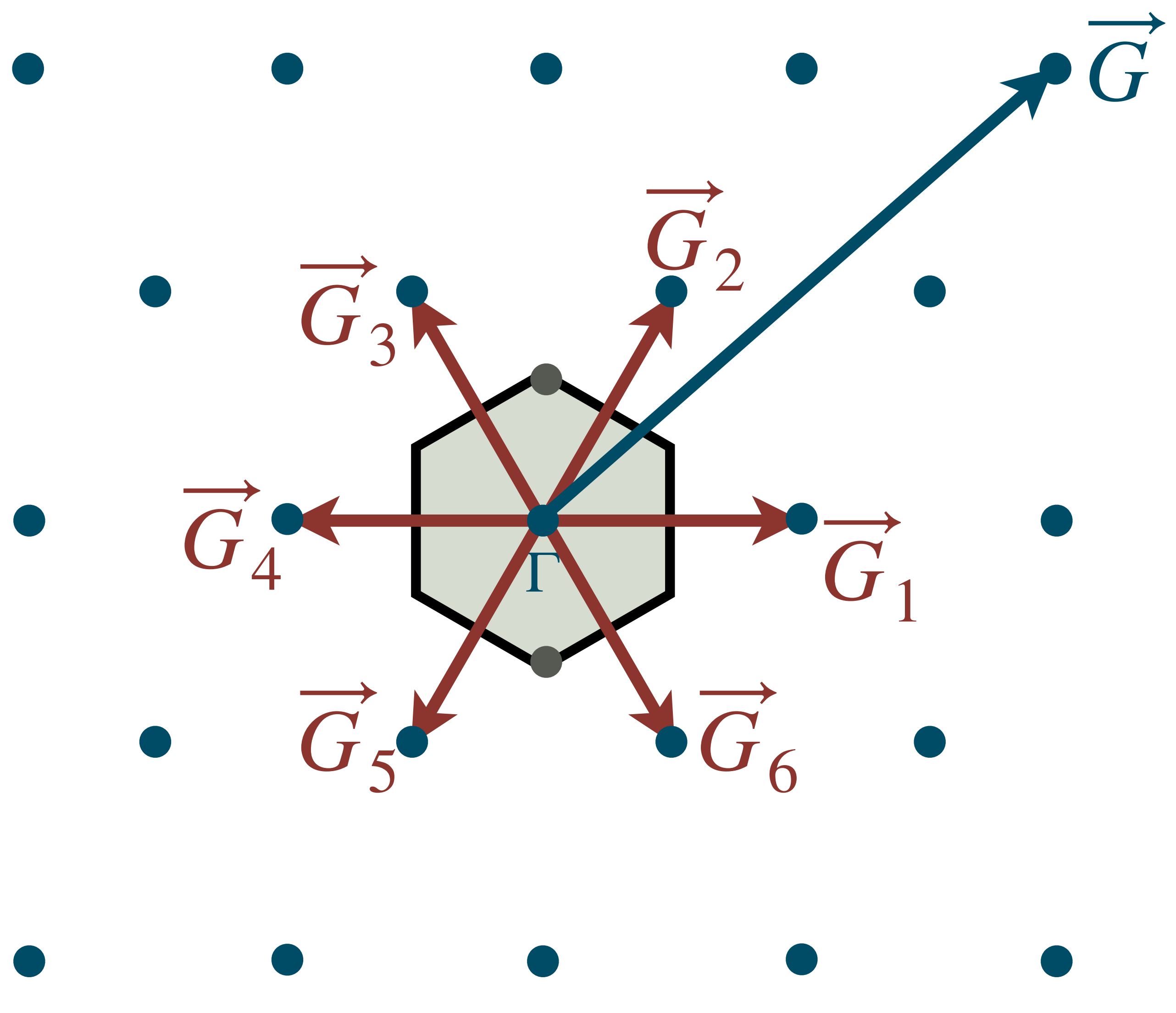

Moiré bands of WSe_2/MoS_2

- moiré bands from moiré potential

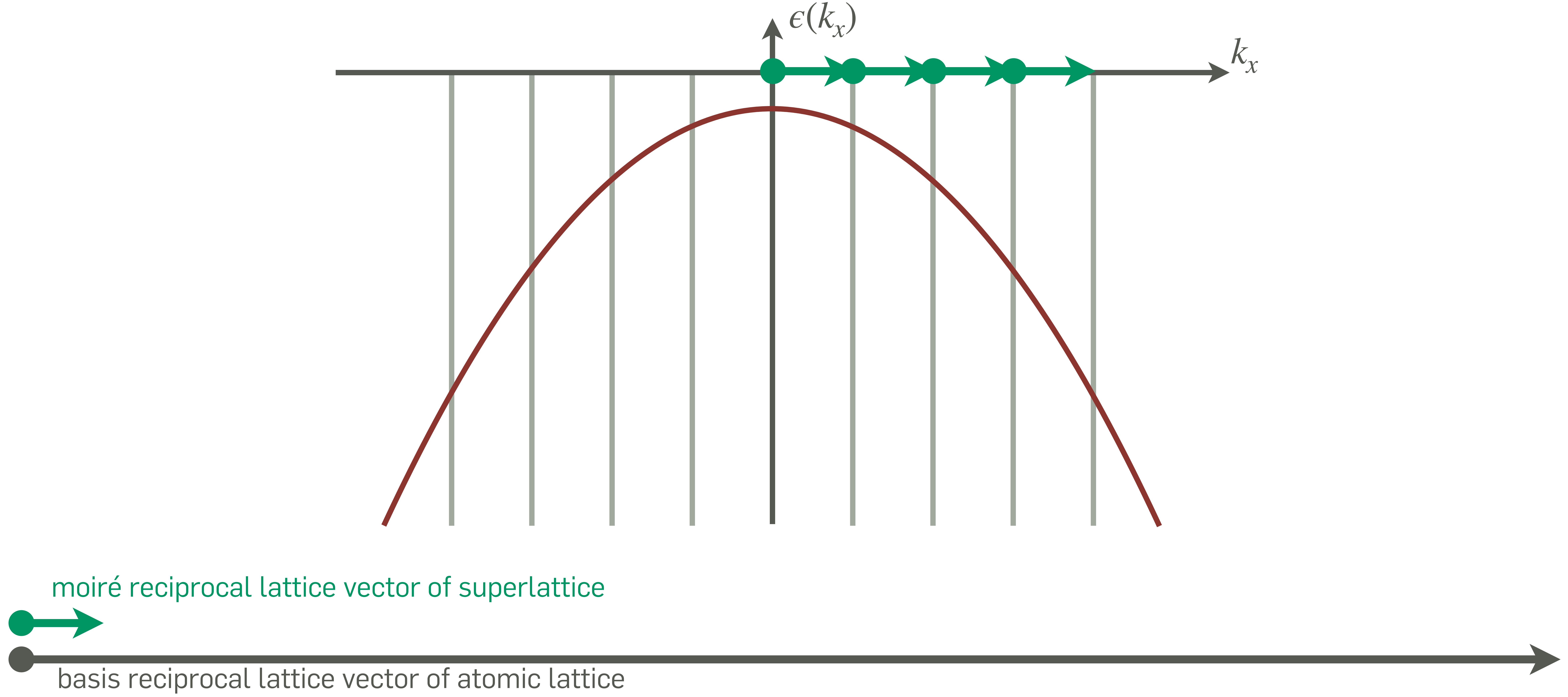

Moiré bands of WSe_2/MoS_2

- moiré bands from moiré potential

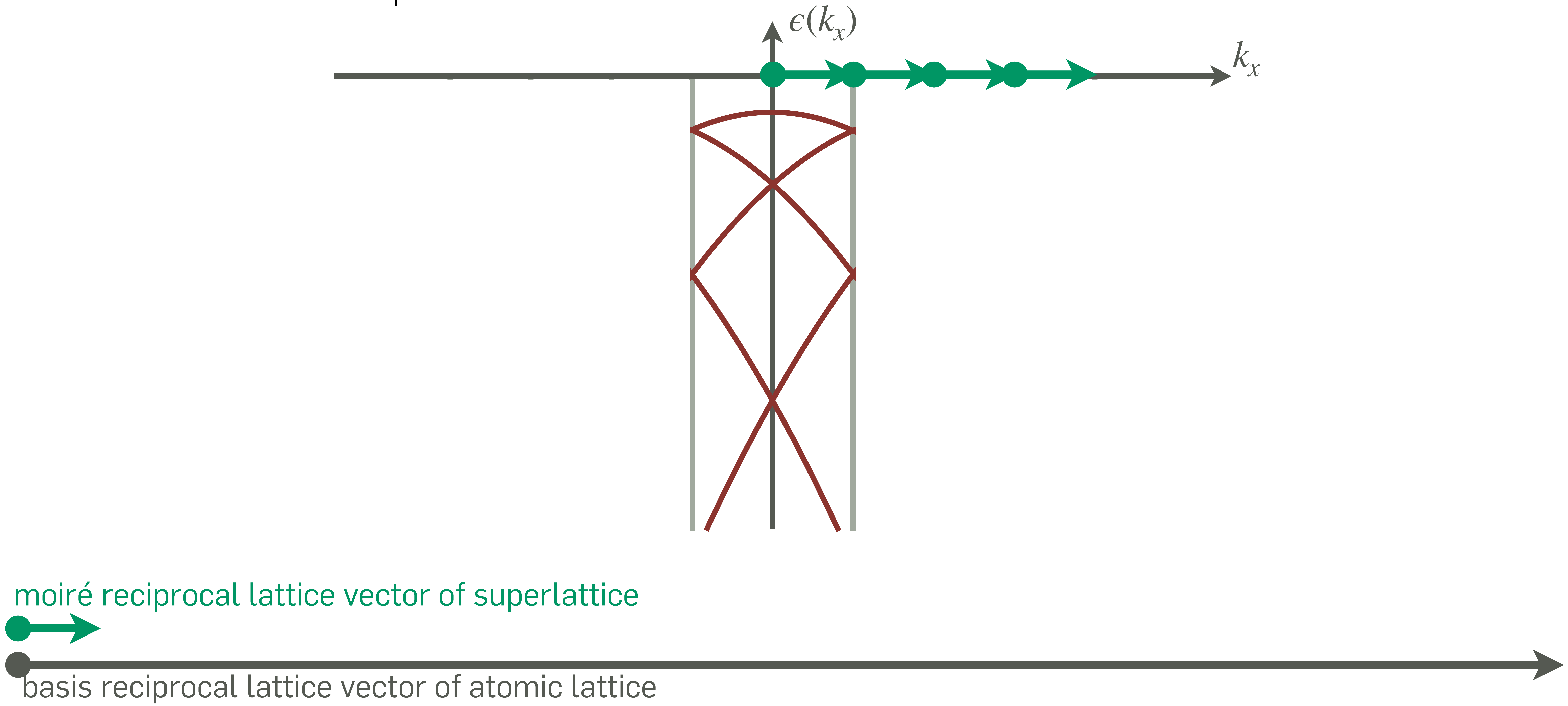

Moiré bands of WSe_2/MoS_2

- moiré bands from moiré potential

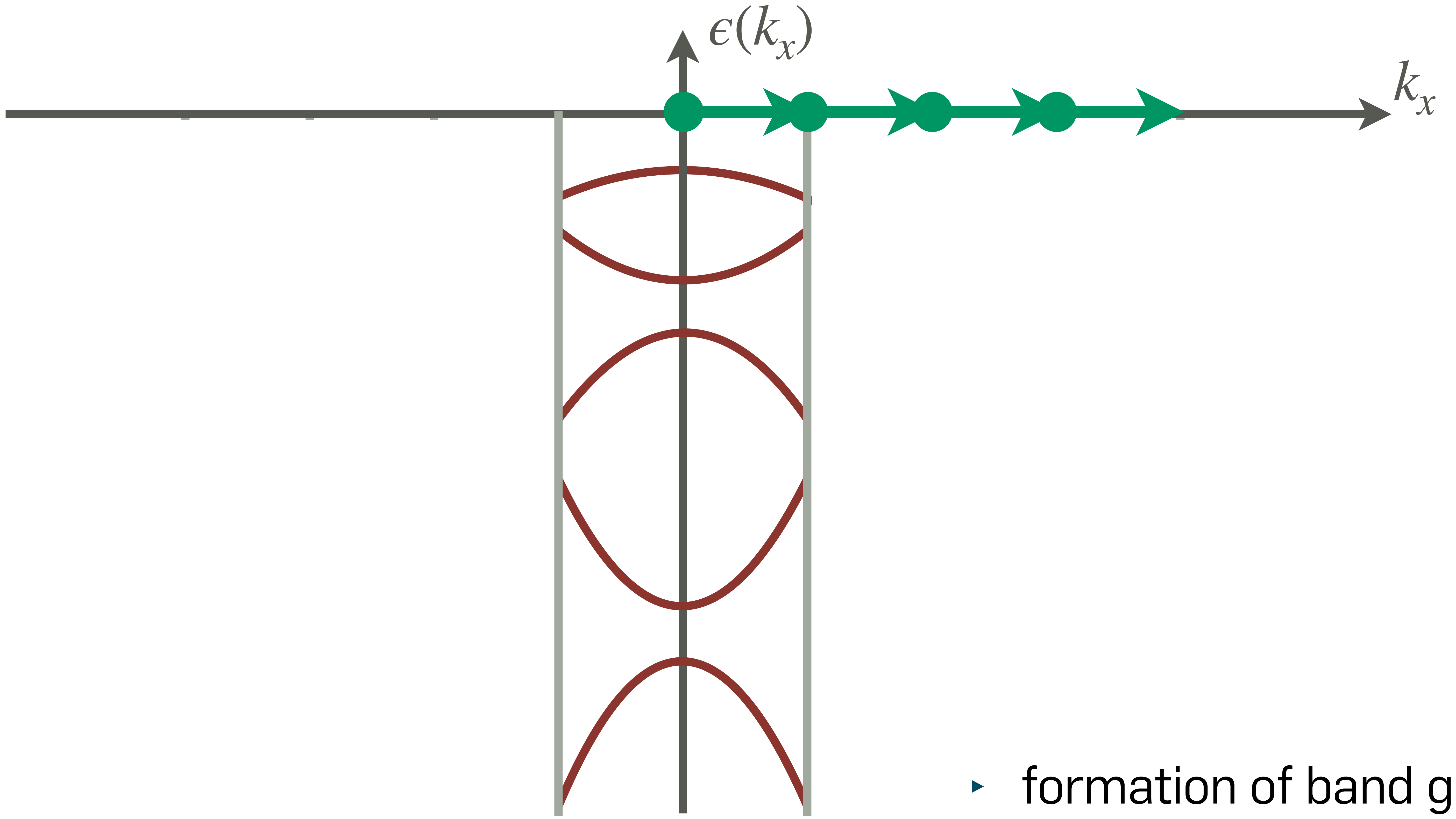

- formation of band gaps $\sim \Delta(r)$

Moiré bands of WSe_2/MoS_2 at $\theta = 0°$

RUB

- **diagonalization** of moiré Bloch Hamiltonian for $\vec{G}, \vec{G}'$ within cutoff circle of radius $4\,|\,\vec{G_1}\,|$

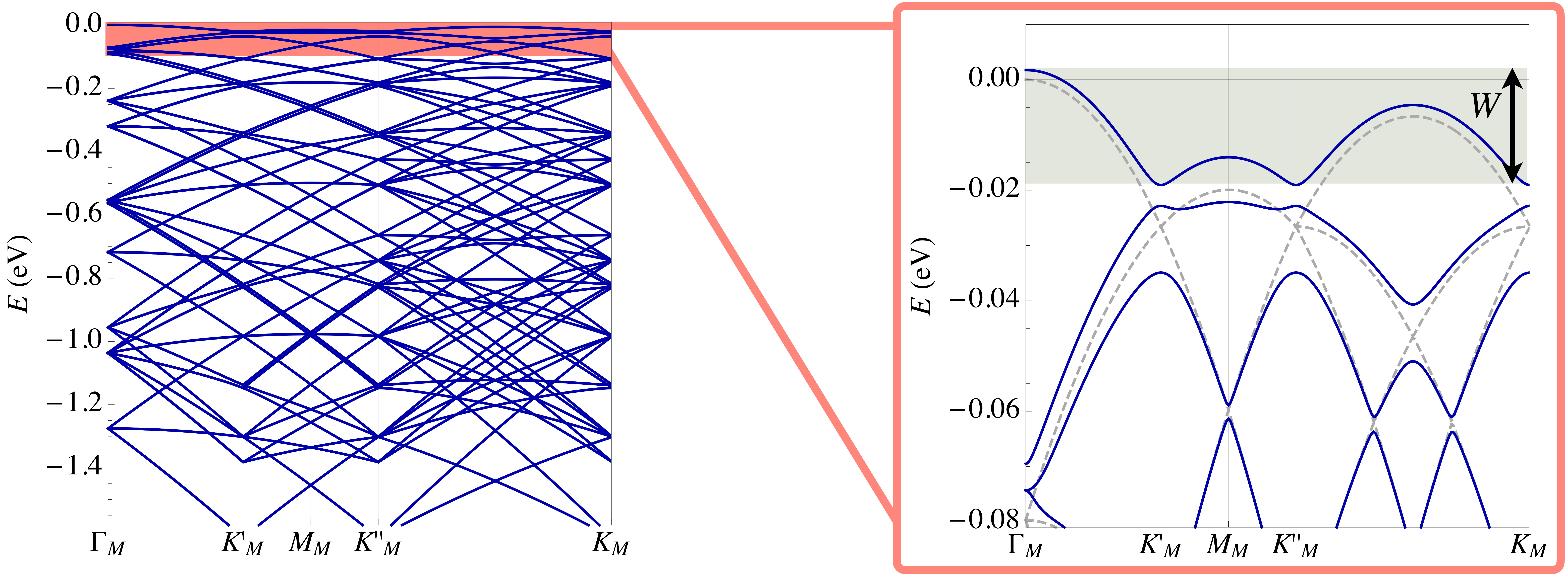

- highest valence moiré band is isolated by band gap and has small bandwidth $W \sim 20\,\mathrm{meV}$

Moiré tight-binding model

- isolated flat band can be described by **effective tight-binding model** $H_0 = \sum_{\nu=\pm} \sum_{\vec{R},\vec{R}'} t(\vec{R}' - \vec{R}) c^\dagger_{\vec{R},\nu} c_{\vec{R}',\nu}$

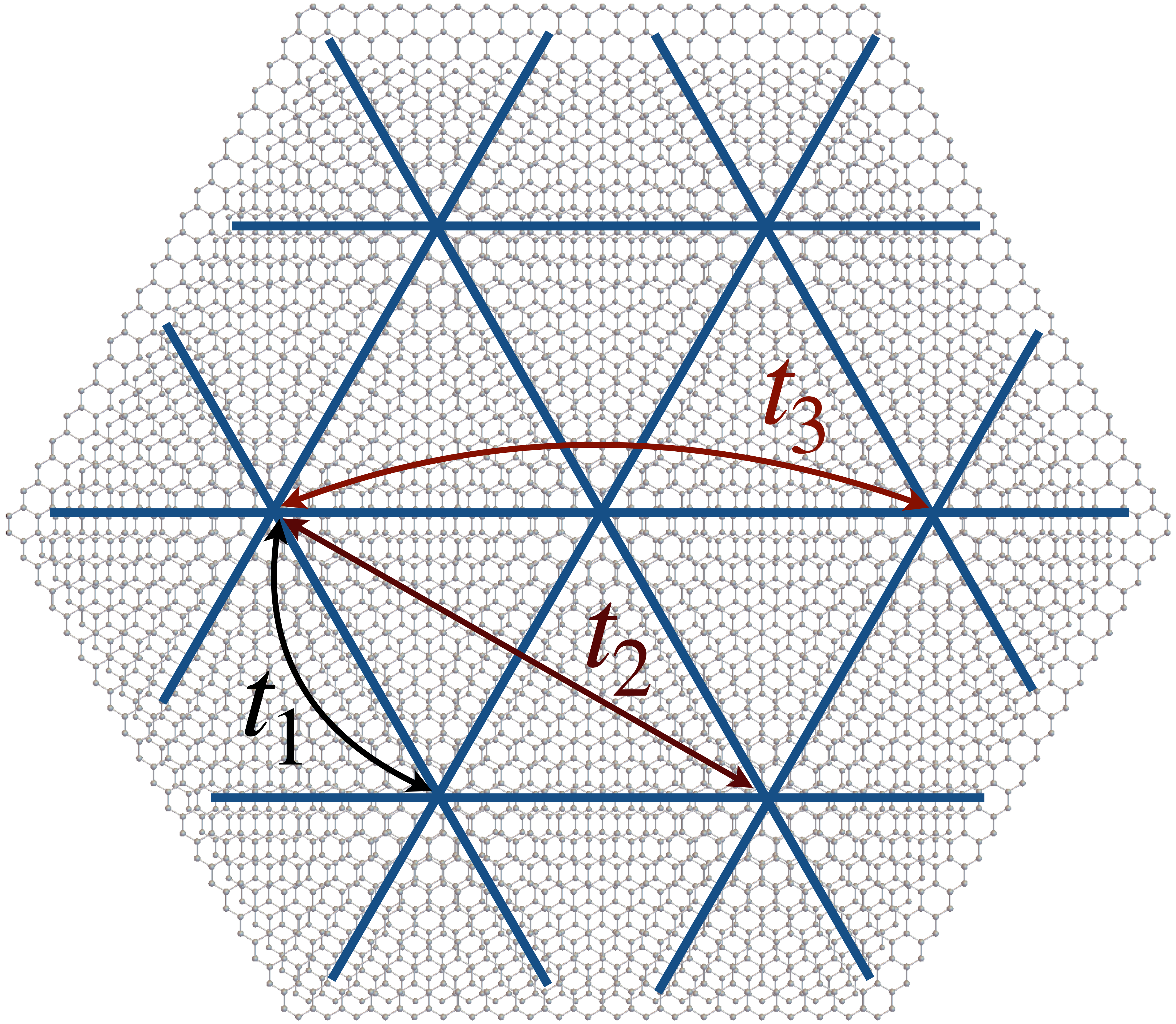

- $\vec{R}$ on sites of triangular moiré superlattice ($a = a_M$)
  - corresponding BZ is exactly the moiré BZ
- $\nu = \pm$ is valley index from K, K'
- accurate description of flat-band dispersion
  - **fit hopping parameters** t_1, t_2, t_3
  - for $\theta = 0°$:

$$t_1 \approx 2.5\,\text{meV}, \quad t_2 \approx 0.5\,\text{meV}, \quad t_3 \approx 0.25\,\text{meV}$$

- t_i **decrease exponentially with increasing** a_M

Moiré tight-binding model

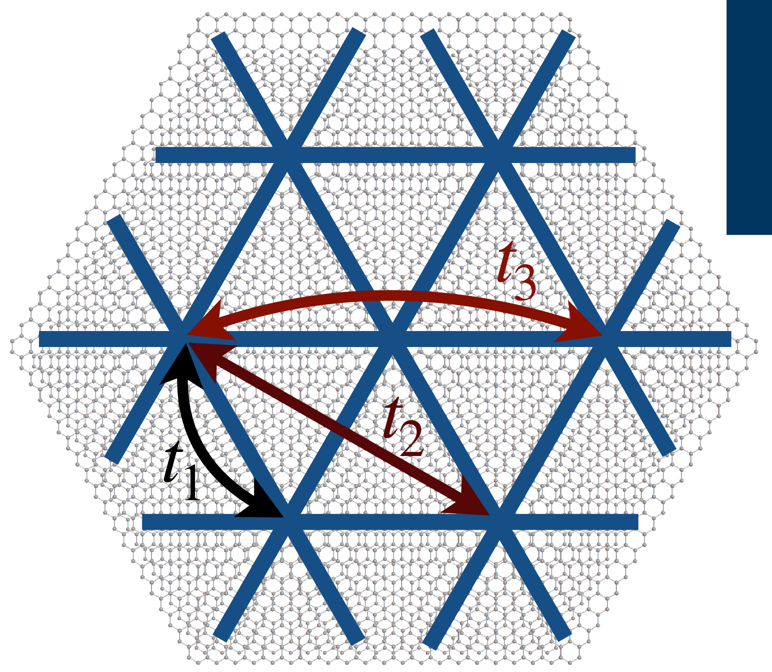

- isolated flat band can be described by **effective tight-binding model**

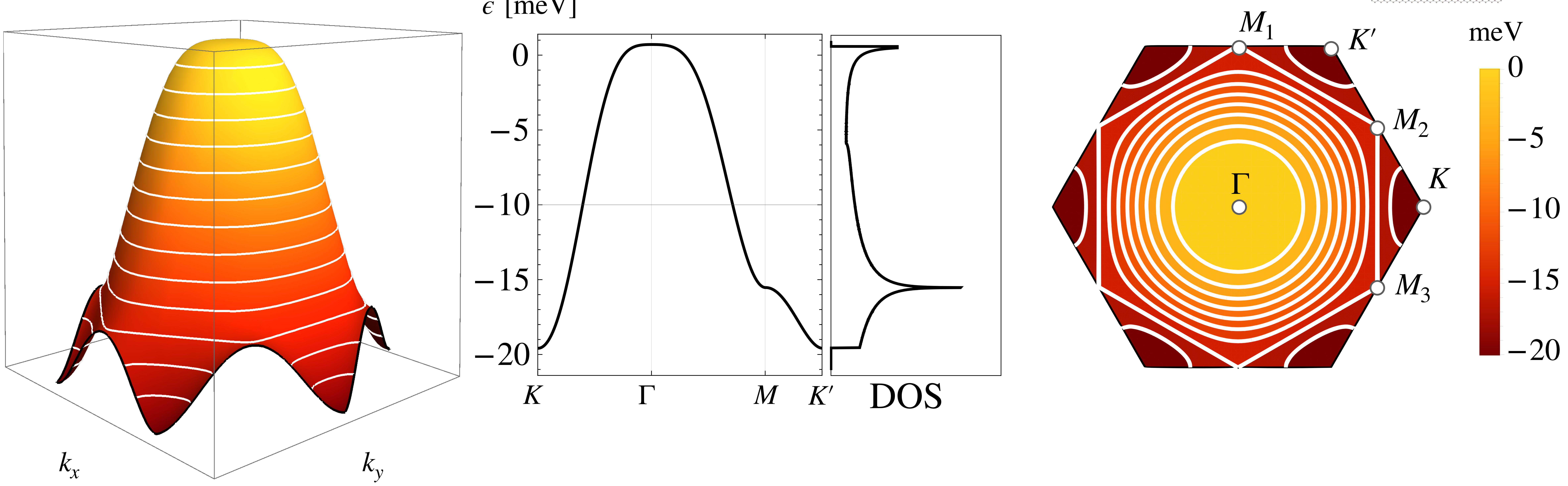

- isolated band is fully occupied at charge neutrality → becomes partially occupied upon hole doping
- full range of band fillings accessible by electrical gating
- **Fermi-surface nesting** and **van Hove singularity** at 3/4 hole doping

Wannier wave-function of isolated band

- can construct **localized Wannier functions** $w(\vec{r})$ for isolated band centered at moiré potential maxima
- spatial extent a_W of $w(\vec{r})$ increases with a_M as $a_W \propto \sqrt{a_M}$ (harmonic oscillator approximation)

➡ $a_W/a_M \propto 1/\sqrt{a_M}$

➡ **onsite repulsion** $U \sim e^2/(\epsilon a_W)$ decreases slowly as a_M increases

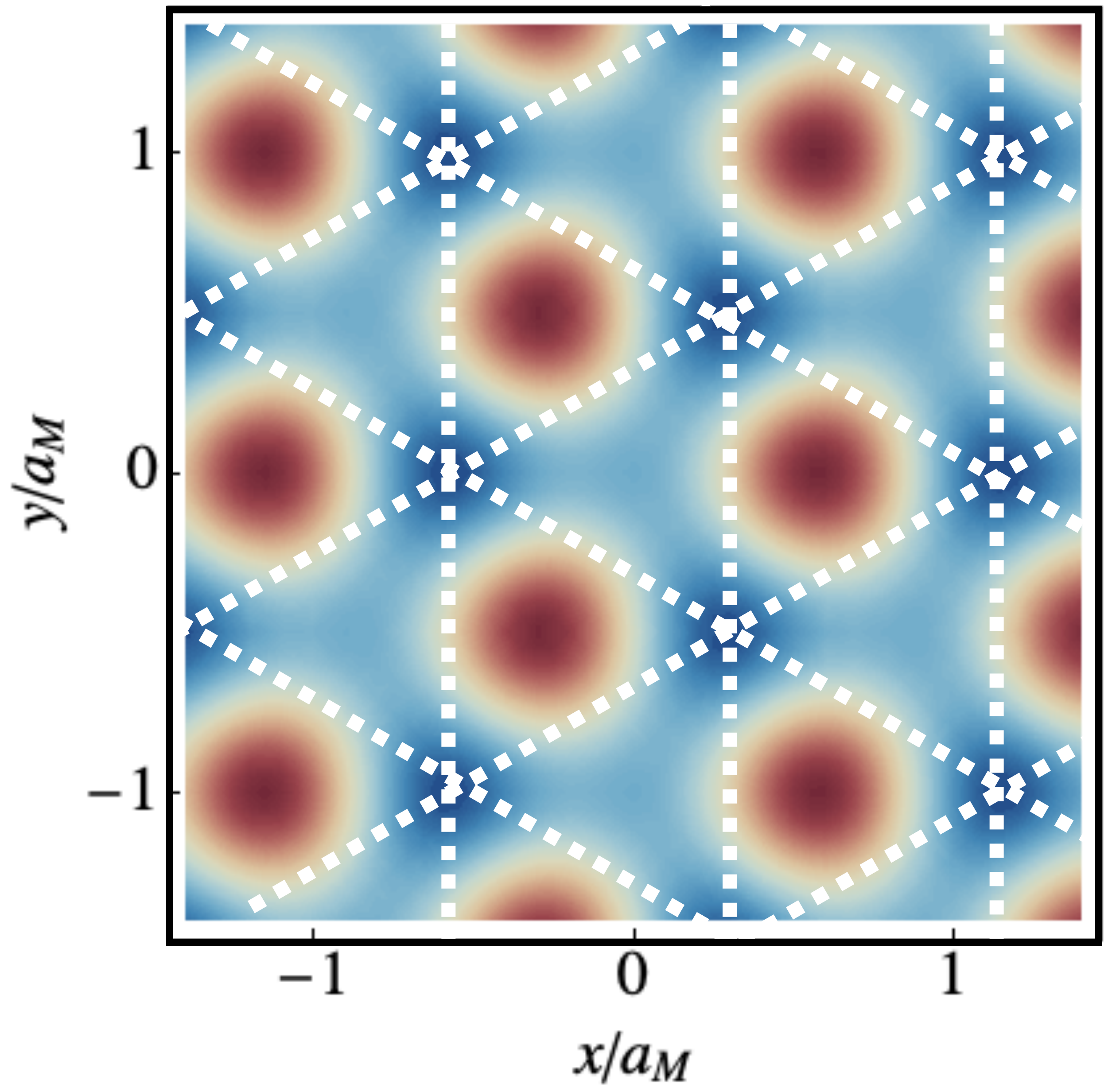

➡ ratio of interaction to bandwidth:

$$\frac{U}{W} \text{ increases quickly with } a_M \sim \frac{1}{\theta}$$

➡ supports formation of strongly correlated states!

Wu, Lovorn, Tutuc, MacDonald, PRL (2018)

Extended Hubbard interactions

- effective dielectric constant ϵ is sensitive to 3D dielectric environment
  - adding (metallic) screening layers at distance $d/2$
  - electron-electron interaction potential with screening

$$\tilde{U}(\vec{r}) = \frac{e^2}{\epsilon r} - \frac{e^2}{\epsilon\sqrt{r^2+d^2}}$$

background dielectric constant   vertical distance to screening layer

- use $\tilde{U}(\vec{r})$ to project onto isolated Wannier band states
  - extended Hubbard interaction

$$H_{\text{int}} = \frac{1}{2}\sum_{\nu,\nu'}\sum_{\vec{R},\vec{R}'} U(\vec{R}'-\vec{R})\, c^{\dagger}_{\vec{R}\nu} c^{\dagger}_{\vec{R}'\nu'} c_{\vec{R}'\nu'} c_{\vec{R}\nu}$$

$$= \sum_{\vec{R}} U_0 n_{\vec{R}\uparrow} n_{\vec{R}\downarrow} + \sum_{\langle \vec{R}\vec{R}'\rangle} U_1 n_{\vec{R}} n_{\vec{R}'} + \sum_{\langle\langle \vec{R}\vec{R}'\rangle\rangle} U_2 n_{\vec{R}} n_{\vec{R}'} + \ldots$$

  - strength and range of i.a. parameters can be adjusted by θ, d, and ϵ

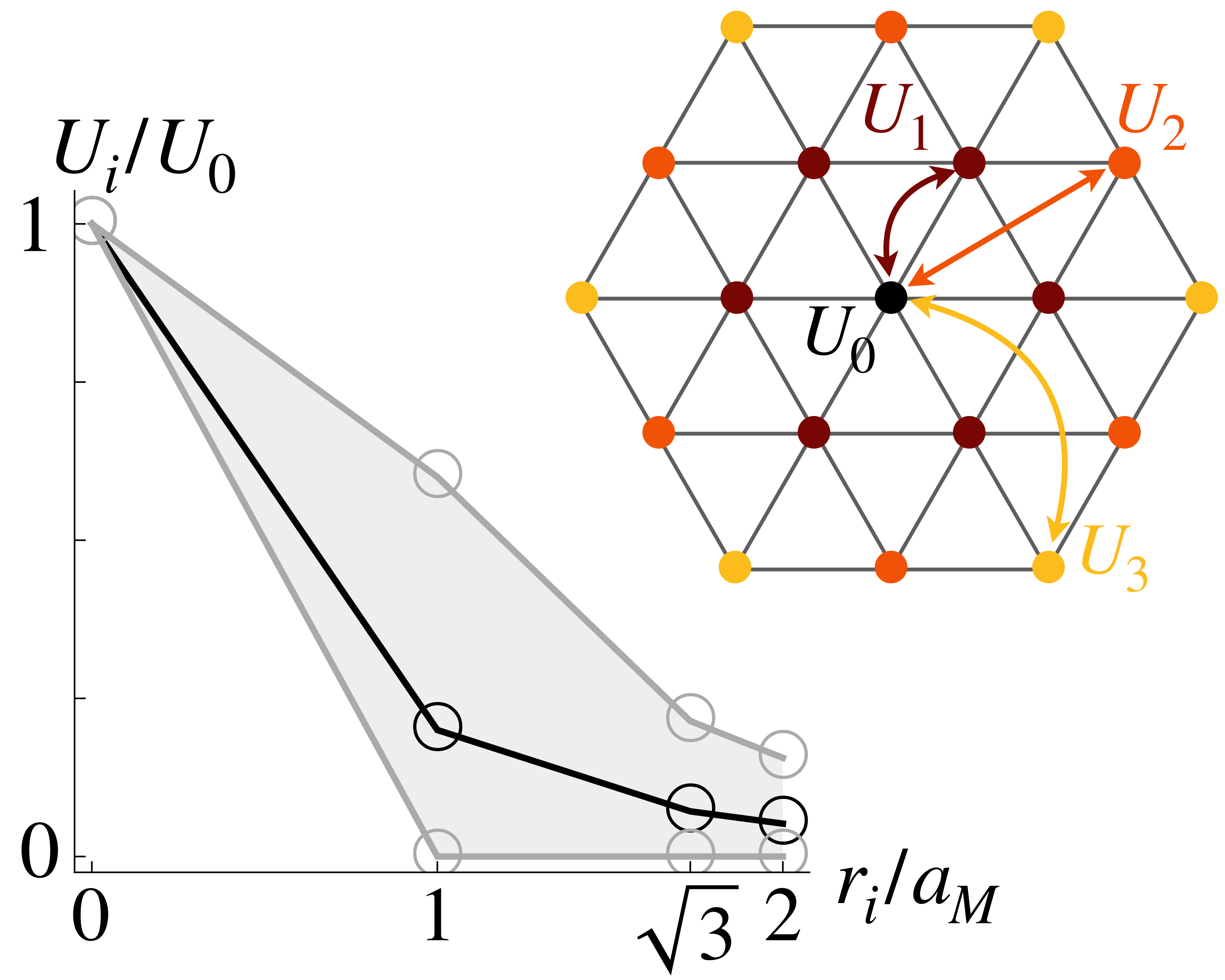

Extended Hubbard model on triangular lattice

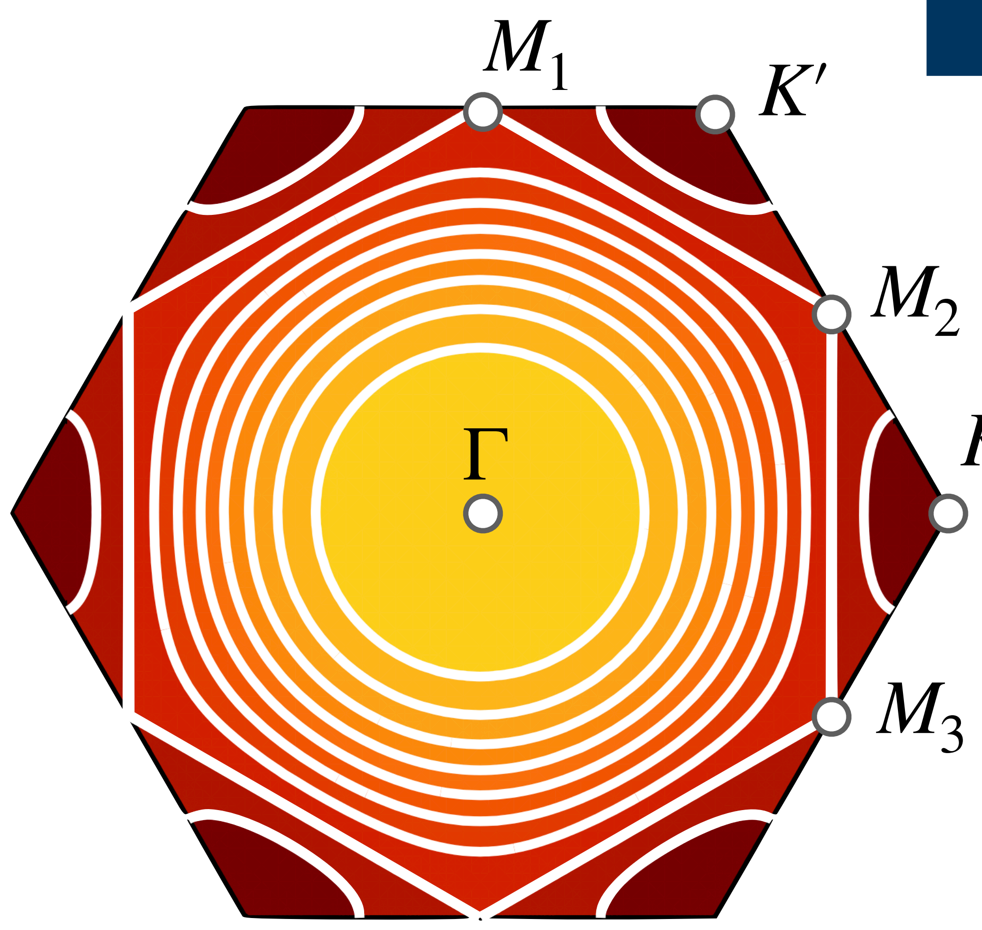

- summary of effective model:

$$H = \sum_{v=\pm} \sum_{\vec{R},\vec{R}'} t(\vec{R}' - \vec{R}) c^\dagger_{\vec{R},v} c_{\vec{R}',v} + \frac{1}{2} \sum_{v,v'} \sum_{\vec{R},\vec{R}'} U(\vec{R}' - \vec{R}) c^\dagger_{\vec{R}v} c^\dagger_{\vec{R}'v'} c_{\vec{R}'v'} c_{\vec{R}v}$$

  - *ab initio* w/ $\epsilon = 10$:

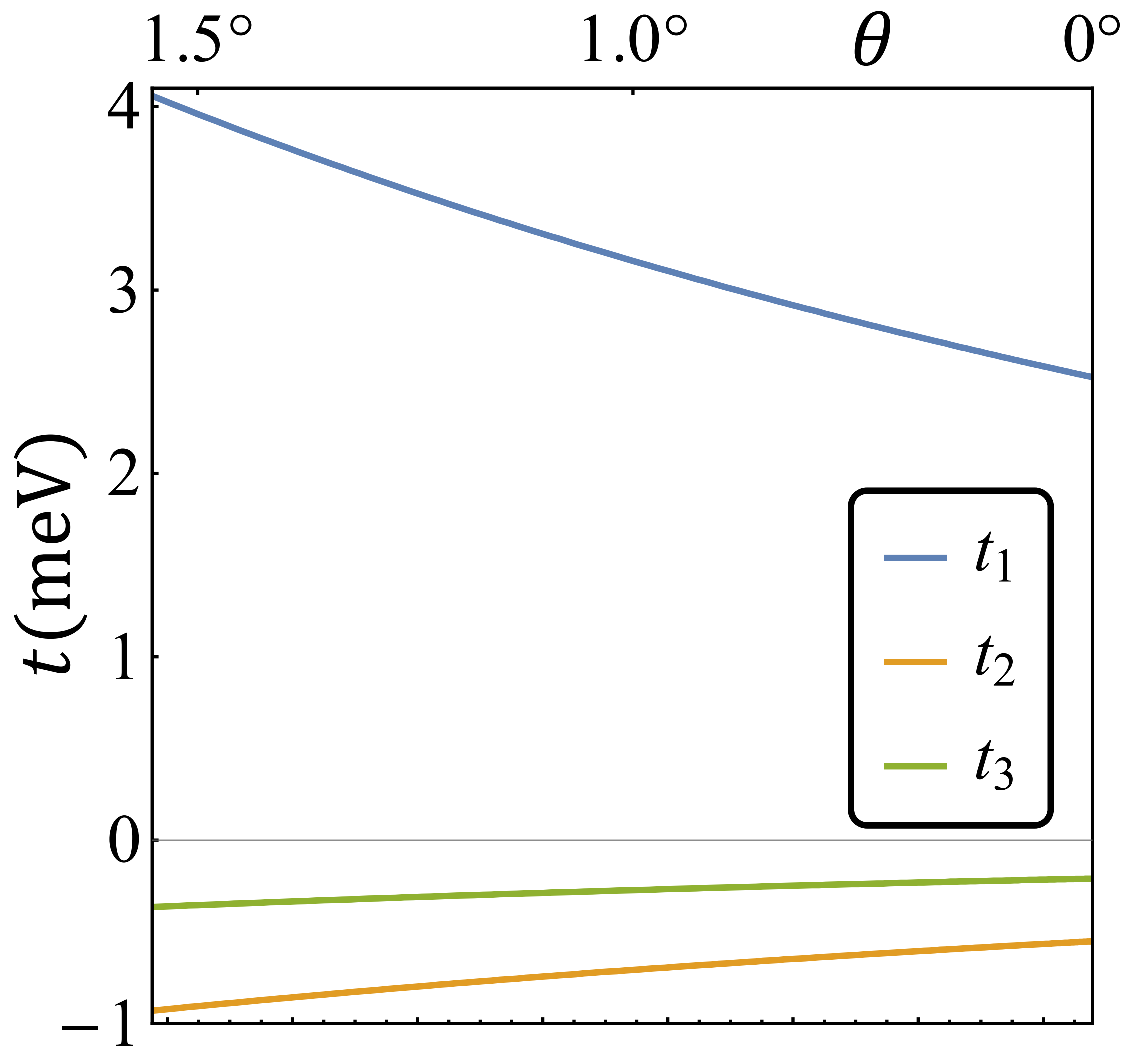

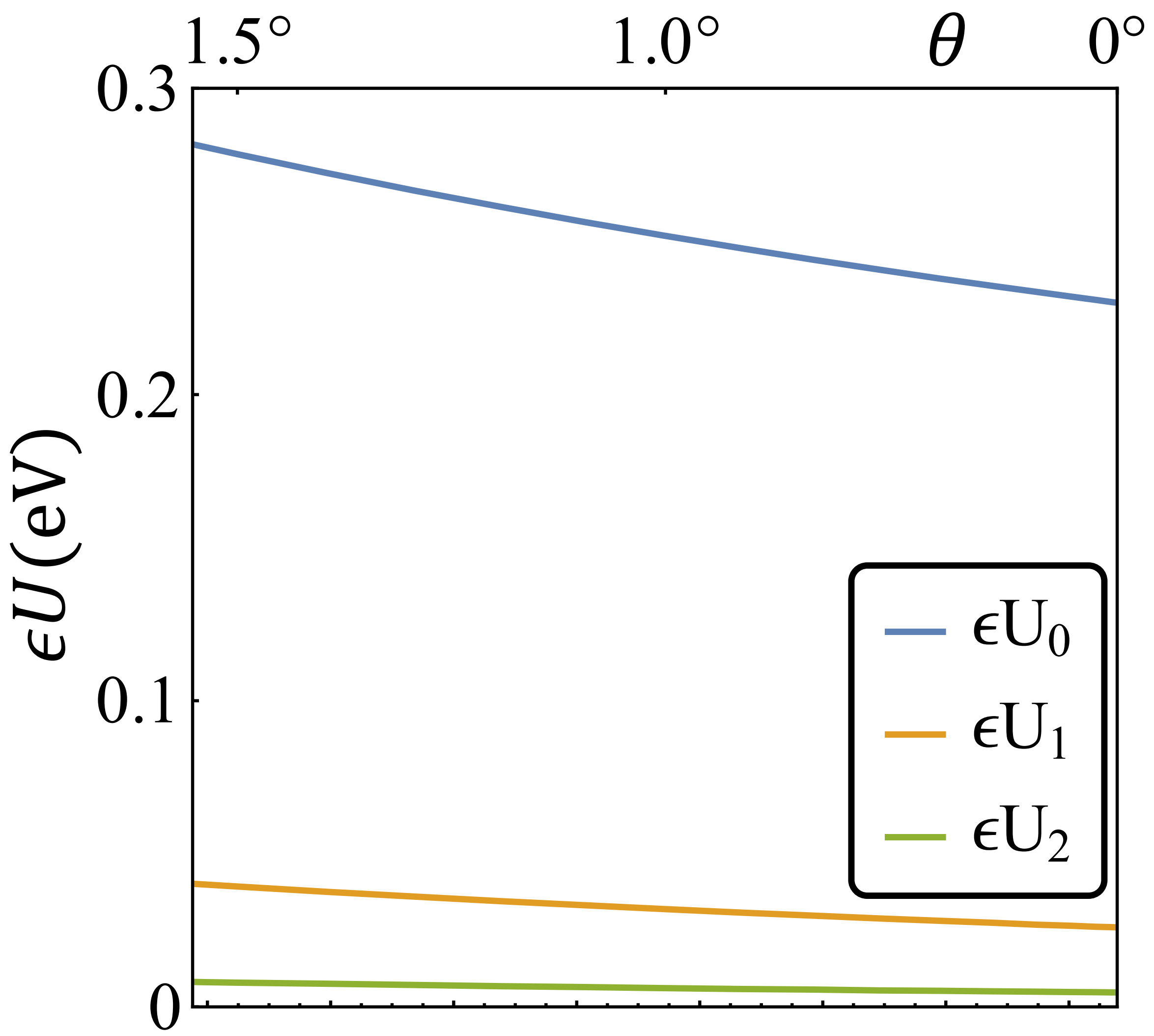

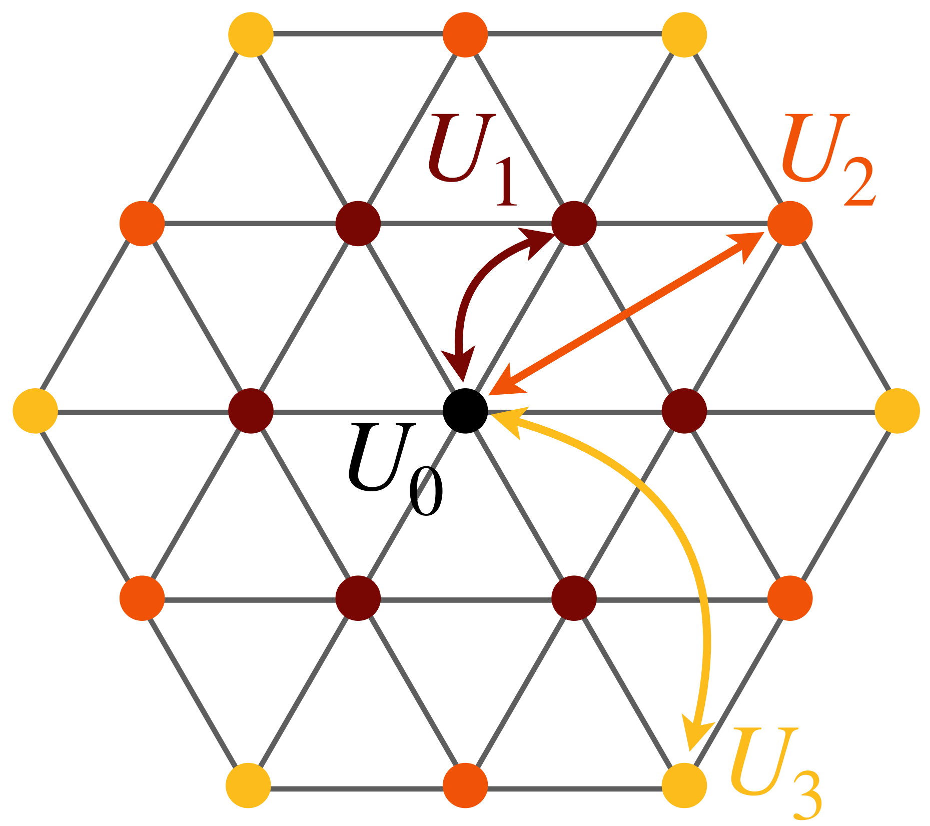

  - semiconductor background dielectric ϵ → can be tuned by choice of dielectric layer *($\epsilon \approx 5$ for hBN)*
  - example at $\theta = 0°$: $t_1 \approx 2.5\,\mathrm{meV},\ \epsilon U_0 \approx 0.22\,\mathrm{eV},\ \epsilon = 5\ \Rightarrow U_0/t_1 \approx 18$
  - example at $\theta = 1.5°$: $t_1 \approx 4.0\,\mathrm{meV},\ \epsilon U_0 \approx 0.28\,\mathrm{eV},\ \epsilon = 10\ \Rightarrow U_0/t_1 \approx 7$

Wu, Lovorn, Tutuc, MacDonald, PRL (2018)

Extended Hubbard model on triangular lattice

- summary of effective model:

$$H = \sum_{\nu=\pm} \sum_{\vec{R},\vec{R}'} t(\vec{R}' - \vec{R}) c^\dagger_{\vec{R},\nu} c_{\vec{R}',\nu} + \frac{1}{2} \sum_{\nu,\nu'} \sum_{\vec{R},\vec{R}'} U(\vec{R}' - \vec{R}) c^\dagger_{\vec{R}\nu} c^\dagger_{\vec{R}'\nu'} c_{\vec{R}'\nu'} c_{\vec{R}\nu}$$

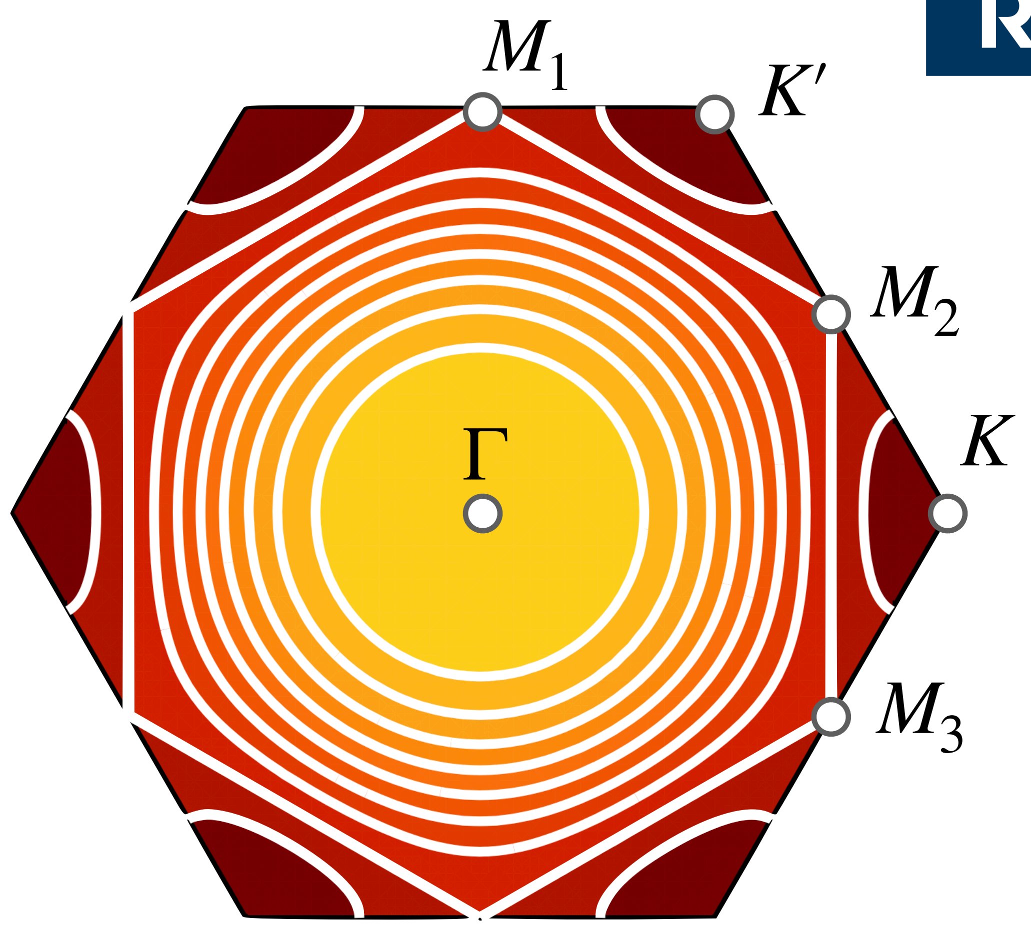

- triangular lattice → geometric frustration
- Fermi surface nesting and van Hove singularities in band structure
- flat bands with W ~ $\mathcal{O}$(10 meV) and band filling tunable by gating
- tunable strength and range of electron-electron interactions

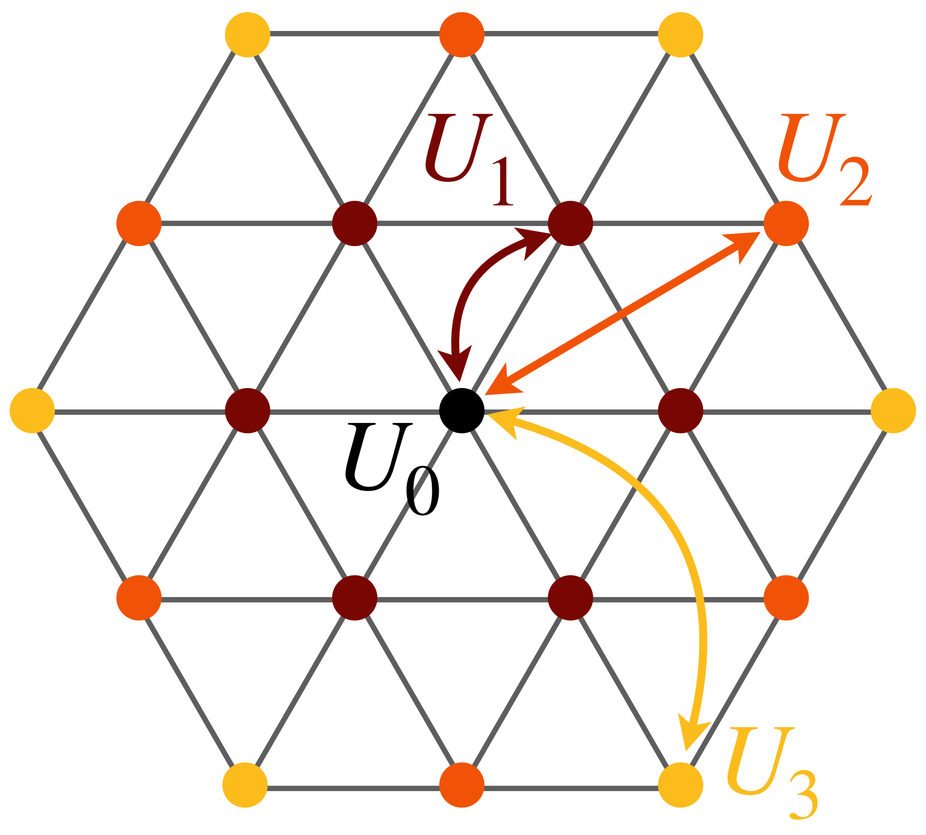

➡ complex **interplay** between **electronic interactions** and **geometric frustration**

- plethora of strongly-correlated phases expected (MIT, spin liquids, magnetism,…)

Half-filling and strong-coupling limit

- ratio between interaction & kinetic energy $\sim U_0/t$ can be tuned → **strong-coupling** $U_0 \gg t_1$ accessible
  - consider **half-filled** isolated band → strong repulsion suppresses double occupancy of moiré sites
  - Mott insulator ground state with localized spin/valley d.o.f.
  - perform strong-coupling limit → **spin/valley Heisenberg model**:
  - J_1, J_2, J_3 from t/U perturbation theory (e.g., $J_1 = 4t_1^2/U_0$)

$$H_s = \sum_{\vec{R},\vec{R}'} J(\vec{R}' - \vec{R}) \vec{S}_{\vec{R}} \cdot \vec{S}_{\vec{R}'}$$

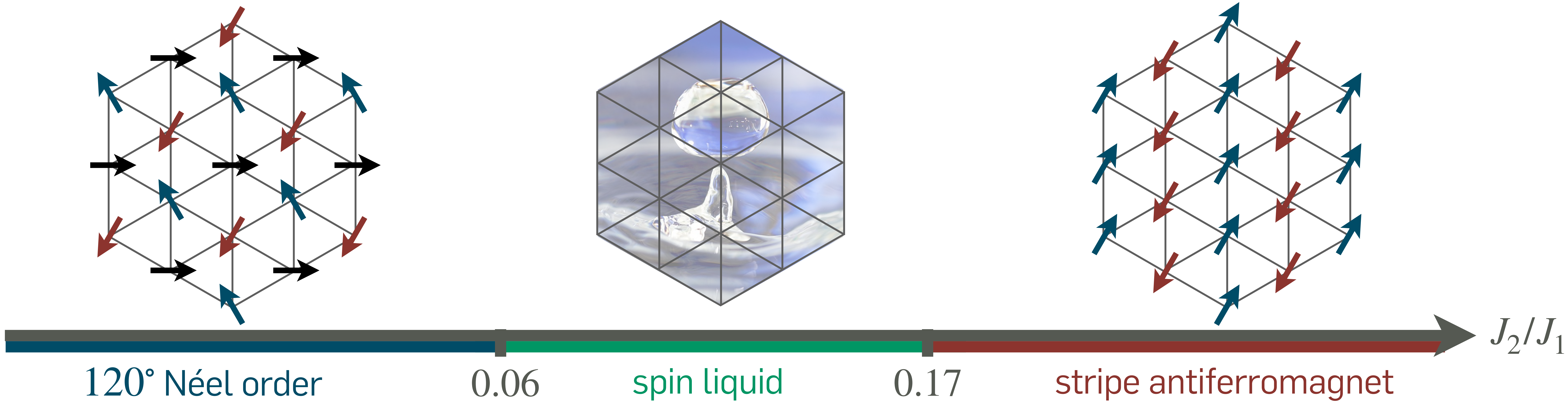

Zhu & White, PRB (2015), Hu, Gong, Zhu, Sheng, PRB (2015)

Half-filling from weak to strong coupling

- away from the effective spin model in the strong-coupling limit → charge fluctuations
  - need to study Hubbard model directly
  - focus of many current numerical efforts (DMRG/tensor-network methods, Monte Carlo methods,...)
  - schematic **phase diagram**:

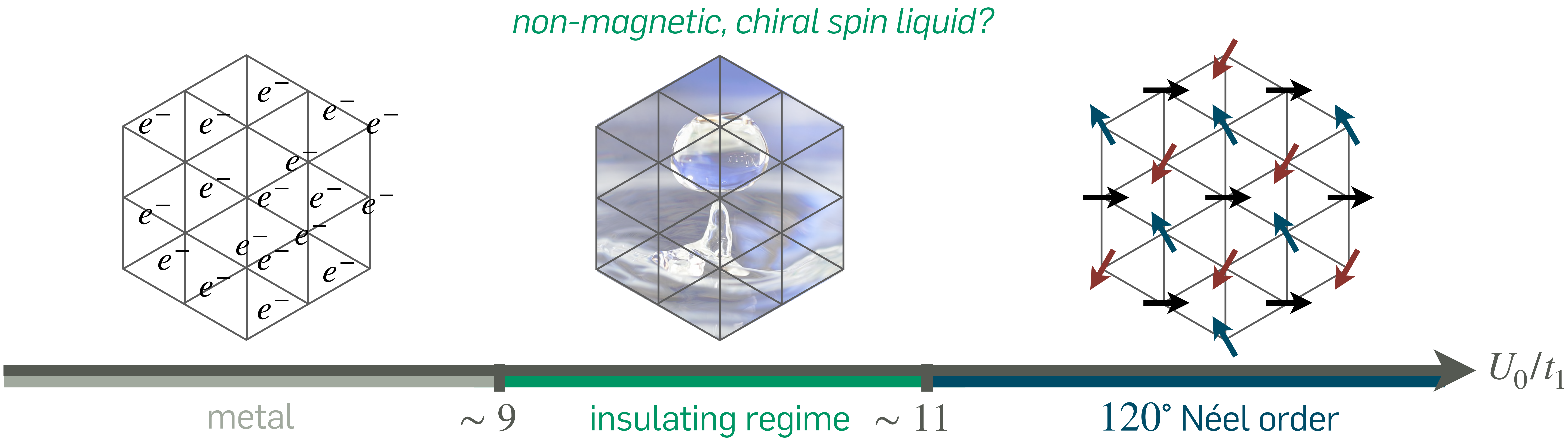

Wietek *et al.*, PRX (2021), Szasz *et al.*, PRX (2020), Chen *et al.*, arxiv:2102.05560 (2021),...

Away from half filling

- situation is less explored away from half filling
- at or near 3/4 filling → van Hove singularity & approximate nesting (depending on $t_1, t_2, t_3, \ldots$)
  - nesting supports spin/valley fluctuations → **magnetic/valley ordering tendencies**?
  - pairing glue and **superconductivity** from spin/valley fluctuations?

- how to find out? … appropriate many-body methods …
- which kind of superconductivity? … symmetry of pairing function, gap, …
- phenomenology of superconducting state? … excitation spectrum, edge states, …

Experimental status of moiré TMDs

RUB

- Mott physics at 1/2 filling & Wigner crystals or stripe phases at **fractional fillings**:

Mott and generalized Wigner crystal states in WSe_2/WS_2 moiré superlattices, Regan *et al.*, Nature 579 (2020)

Correlated insulating states at fractional fillings of moiré superlattices, Xu *et al.*, Nature 587 (2020)

Stripe phases in WSe_2/WS_2 moiré superlattices, Jin *et al.*, Nature Materials 20, 940 (2021)

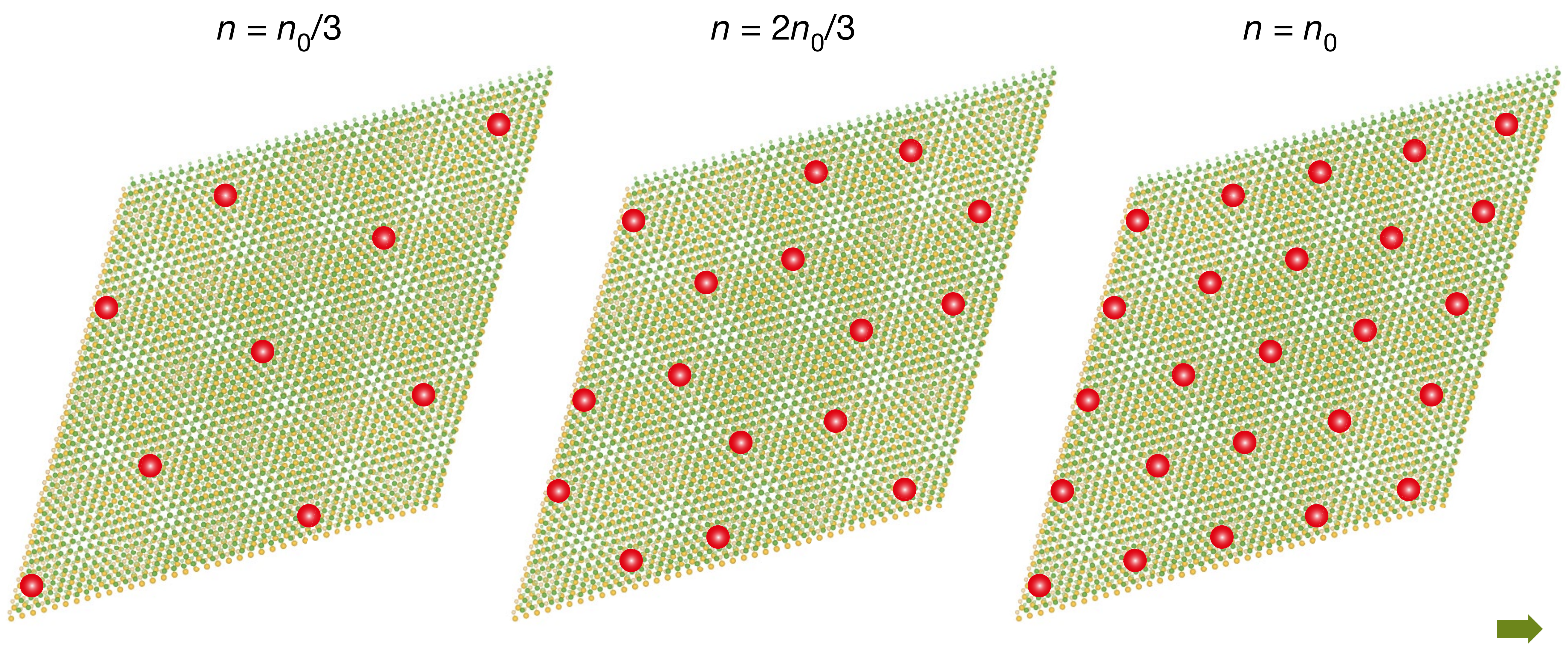

➡ Interactions of **extended range** important!

Superconductivity (?)

- Clear signs of superconductivity in graphene based heterostructures:
  - At magic angle in TBG and symmetric TTG
  - In rhombohedral trilayer graphene and Bernal bilayer graphene (with perpendicular electric field)
- Evidence of zero-resistance state in twisted bilayer WSe_2

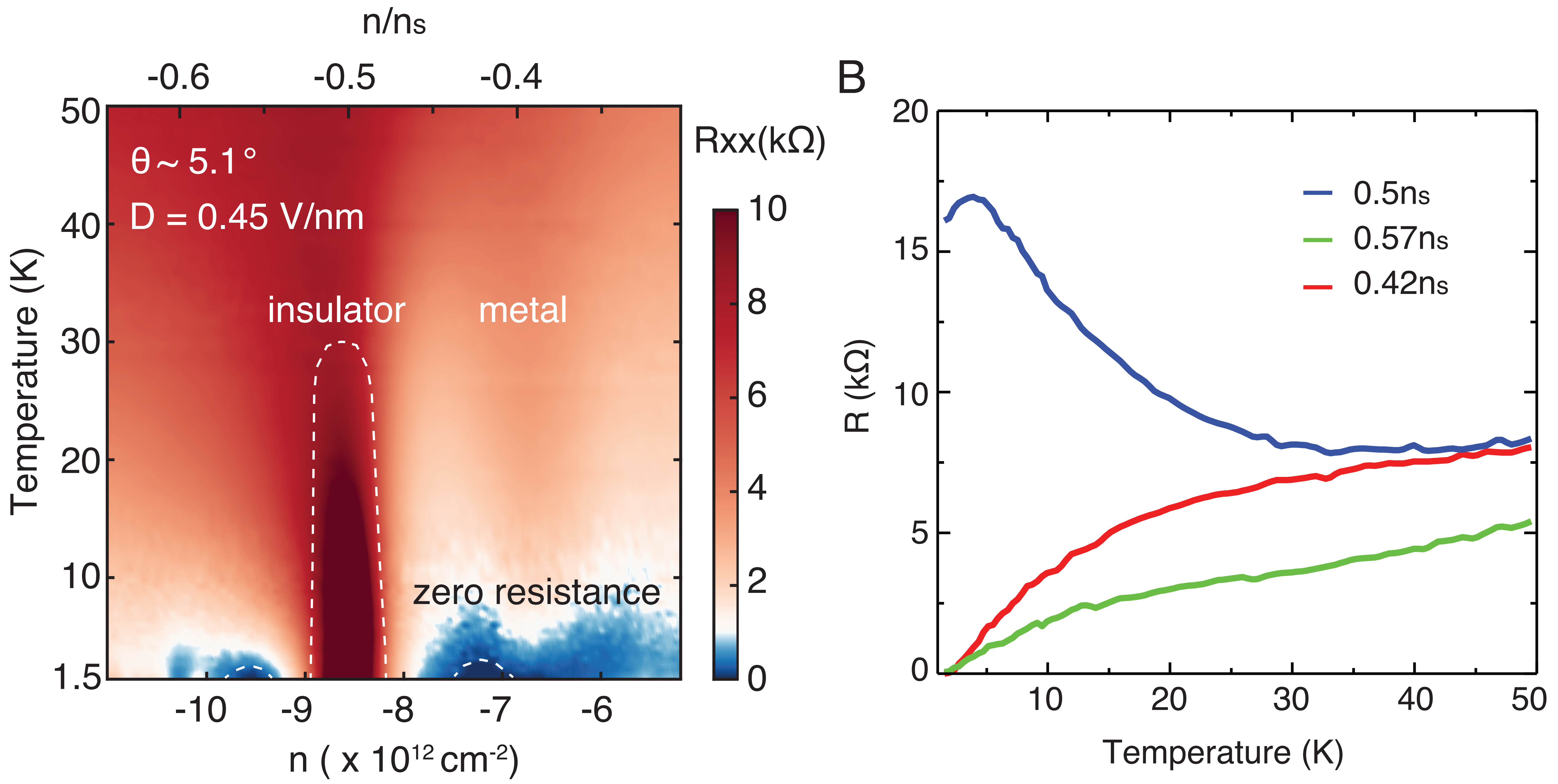

Wang *et al.*, Nature Materials (2020)

Open questions:

- **Superconductivity exclusive for graphene systems?**
- **Conventional or electronic mechanism?**

Outline

RUB

- *Chapter I:* From 2D moiré materials to frustrated superlattice Hubbard models
- *Chapter II:* Interaction effects in hexagonal superlattice Hubbard models
- *Chapter III:* Functional renormalization group
- *Chapter IV:* Functional renormalization group for moiré materials
- *Chapter V:* Further developments and outlook

RUB

Chapter II: Interaction effects in hexagonal superlattice Hubbard models

- Instabilities from amplified interactions
- Van-Hove scenario on the triangular lattice
- Particle-particle and particle-hole instabilities
- Competing interaction effects and unconventional superconductivity

Furukawa, Rice, Salmhofer, PRL (1998)
Nandkishore, Levitov, Chubukov, Nat. Phys. (2012)
Classen, Chubukov, Honerkamp, Scherer, PRB (2020)

Fermi-surface instabilities from amplified interactions

RUB

- Consider itinerant electron system:
  - density of states (DOS) ρ
  - interaction U (is it weak or strong?)

- Define dimensionless interaction = interaction x DOS: $\lambda \sim U \times \rho$
- Example: In 2D away from Van Hove points: $\rho \approx 1/W \;\Rightarrow \lambda \sim U/W$ ← $\frac{\text{interaction}}{\text{bandwidth}}$
- **Generally**: $\lambda \sim (U/W)\,\hat{\rho}(E)$

  dimensionless

- Increase λ through band restructuring:
  1. decrease W
  2. increase $\hat{\rho}$ (e.g. near Van-Hove singularity)
- Generalized Stoner criterium for Fermi-surface instability: $\lambda > 1$ ...

Van Hove scenario on the triangular lattice

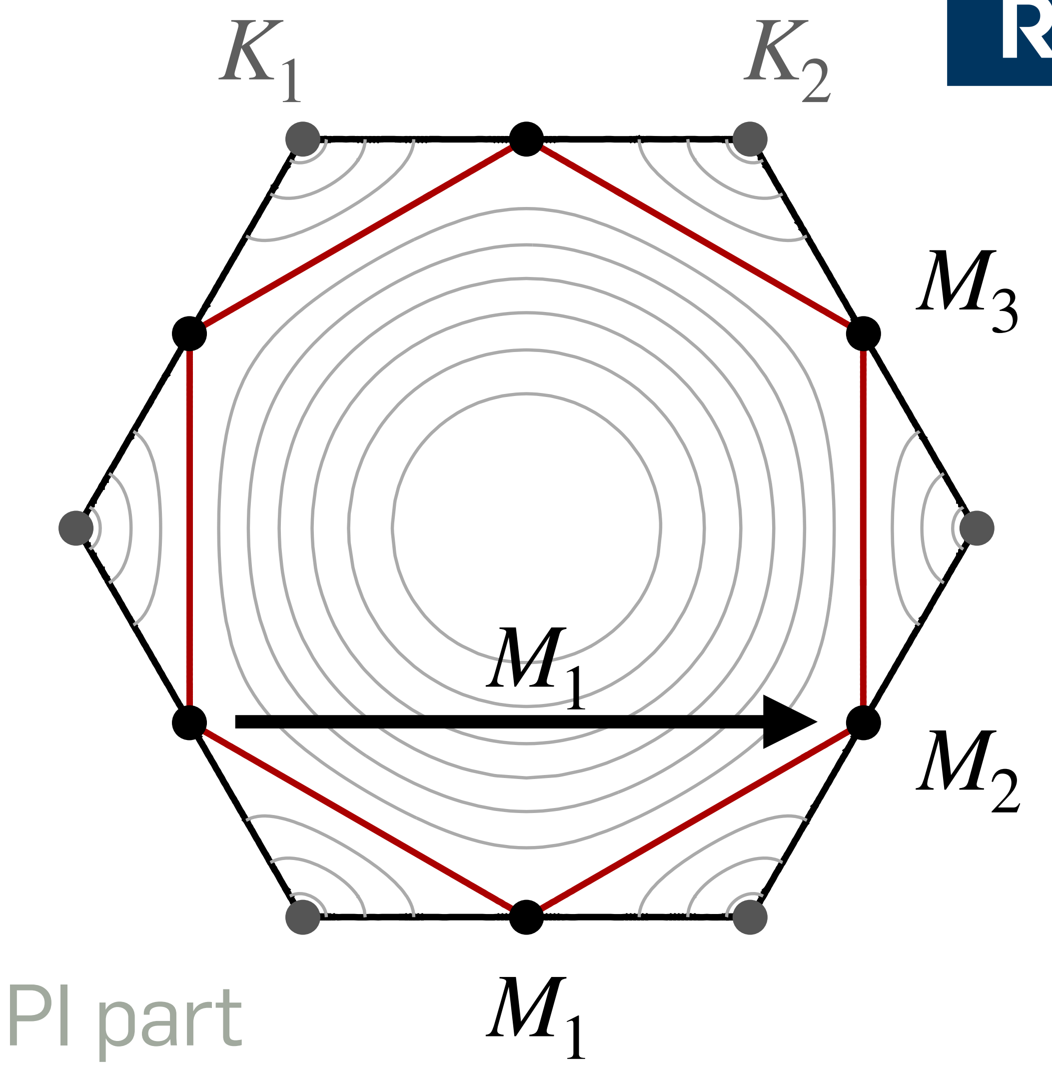

- Density of states at Van-Hove filling: $\rho(\epsilon) = \hat{\rho}_0 \ln(\epsilon/T)$
- Nested Fermi surface with nesting vectors M_1, M_2, M_3: $\epsilon(\vec{k} + M_i) \approx -\epsilon(\vec{k})$

1PI part

- Effective interaction from 2-particle correlation function $\langle c_1 c_2 \bar{c}_3 \bar{c}_4 \rangle \sim G_1 G_2 \Gamma^{(4)}_{1234} G_3 G_4$

- $\Gamma^{(4)} =$ 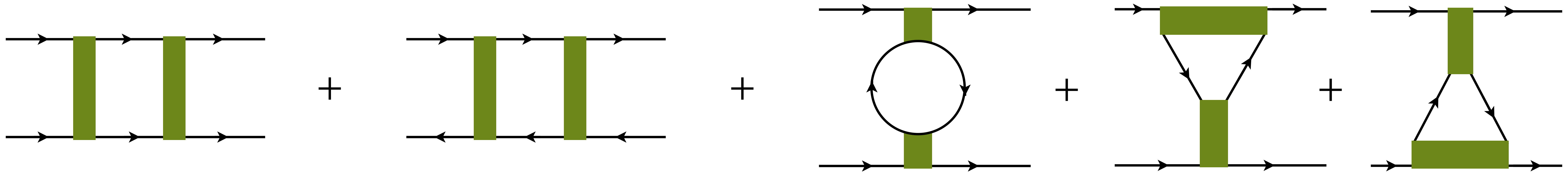 $+ \ldots$

particle-particle crossed particle-hole direct particle-hole

Fermi-surface instabilities from amplified interactions

RUB

- Density of states at Van-Hove filling: $\rho(\epsilon) = \hat{\rho}_0 \ln(\epsilon/T)$
- Nested Fermi surface with nesting vectors M_1, M_2, M_3: $\epsilon(\vec{k} + M_i) \approx -\epsilon(\vec{k})$

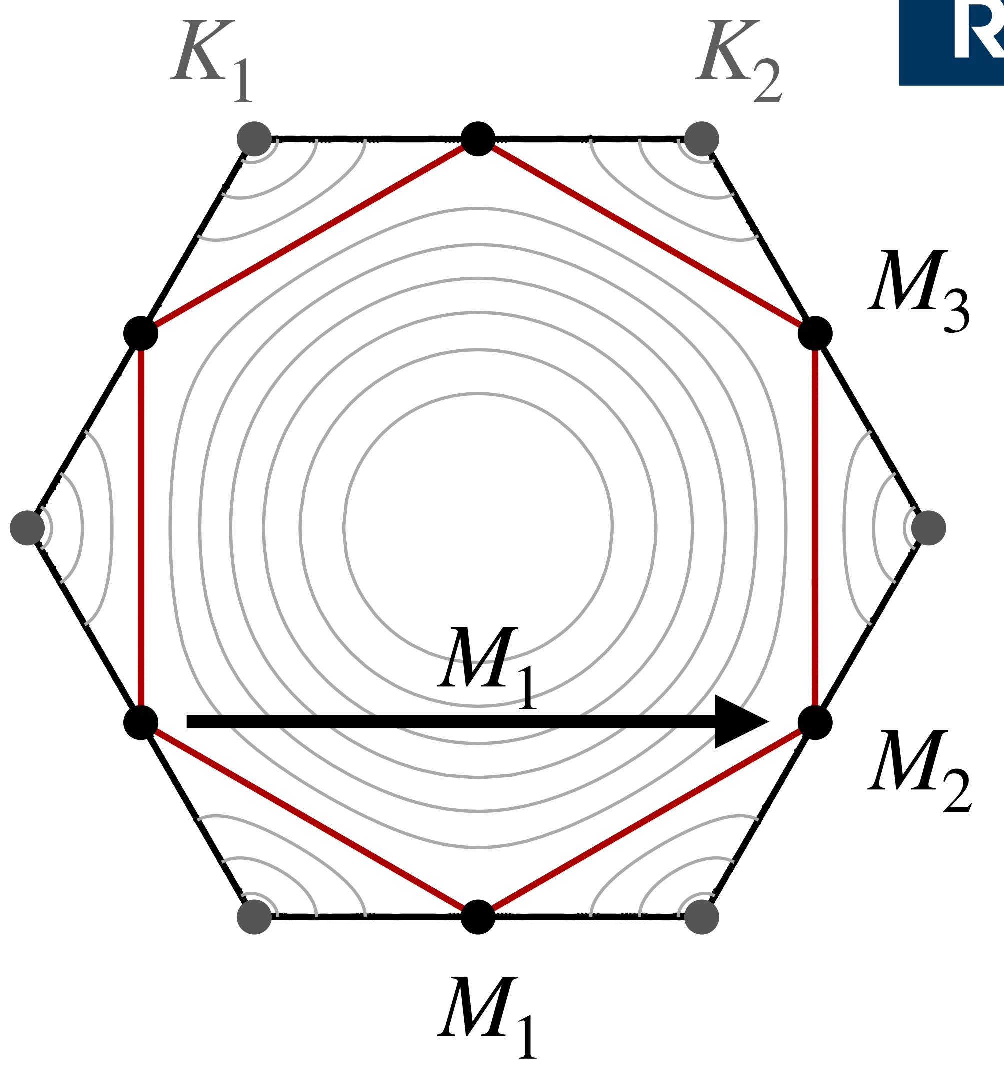

- Leading diagrams at E_{VH} with bare on-site interaction $U \sum_i c^\dagger_{i+} c^\dagger_{i-} c_{i-} c_{i+}$

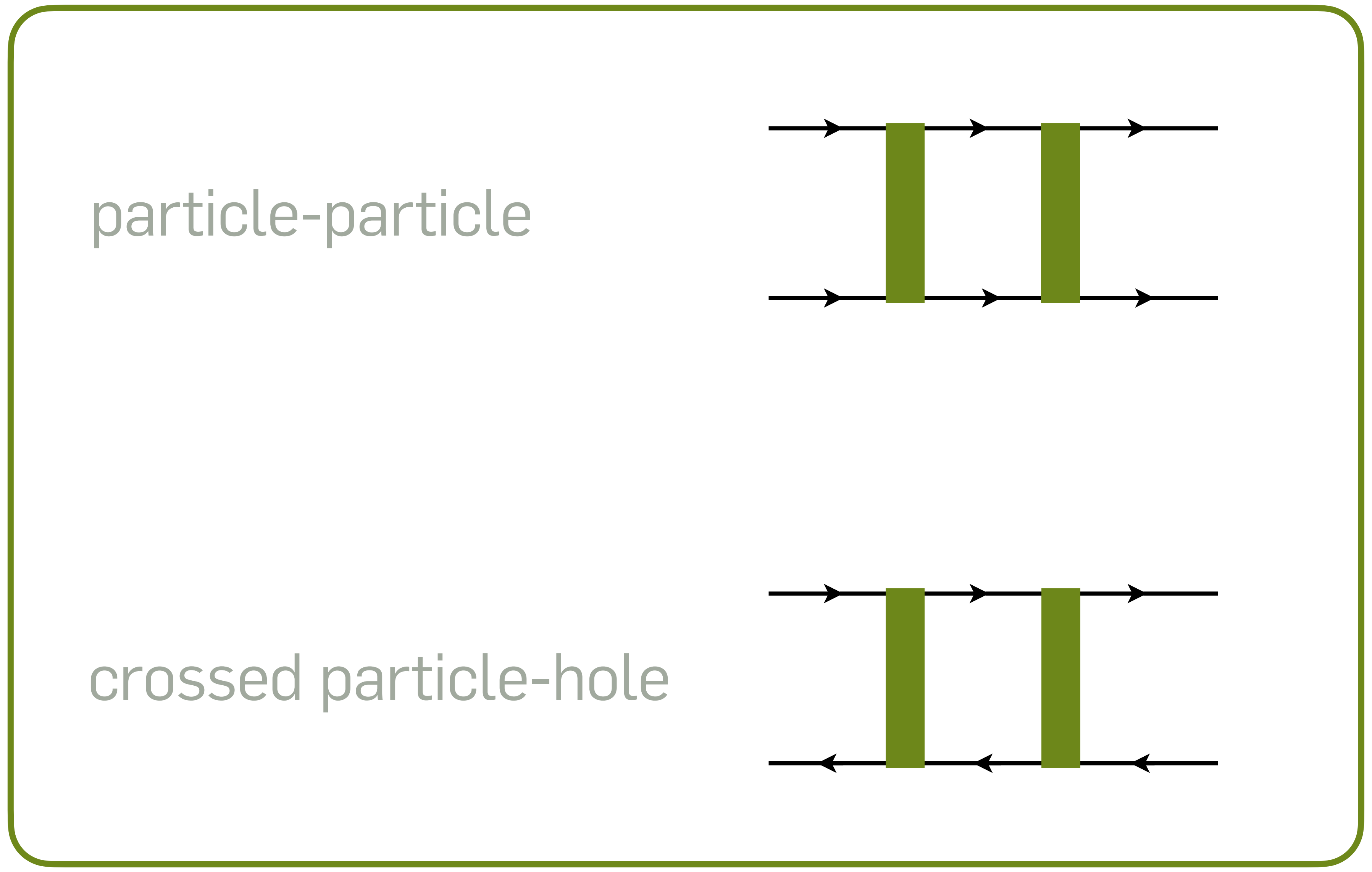

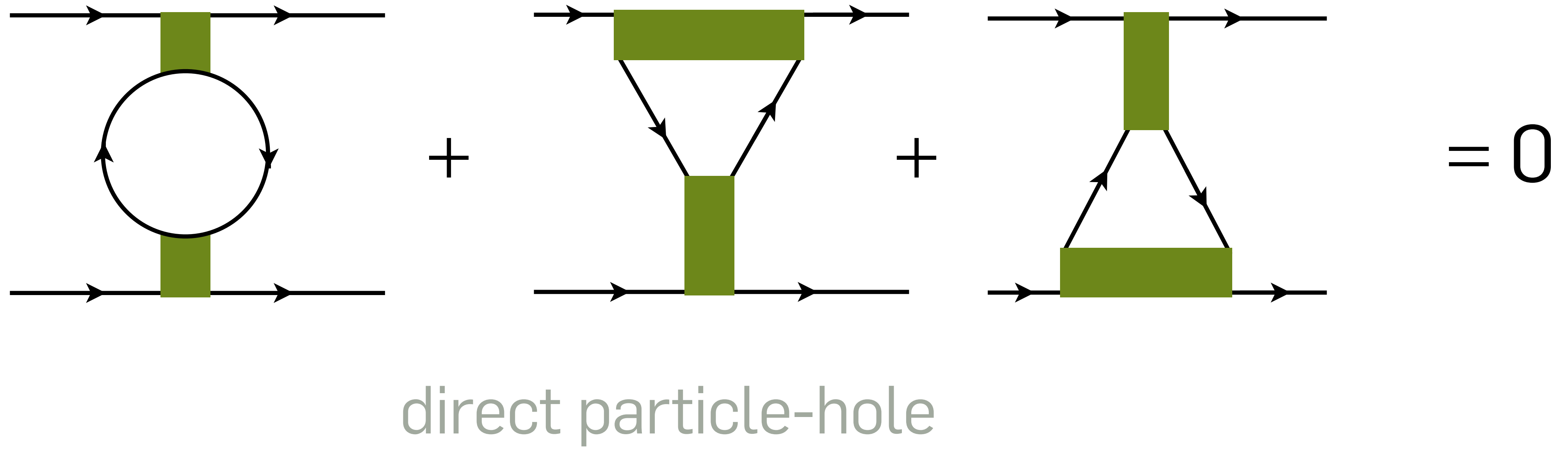

Fermi-surface instabilities from amplified interactions

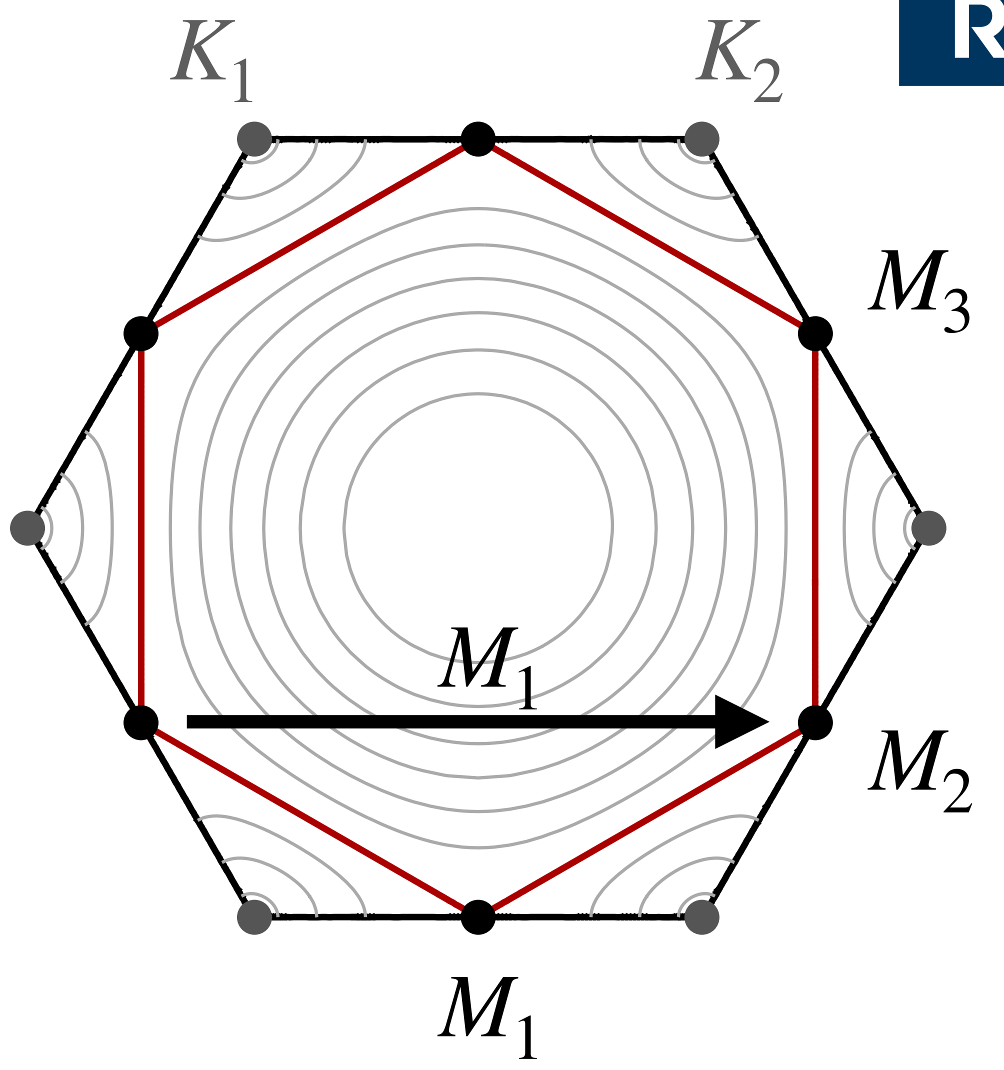

- Density of states at Van-Hove filling: $\rho(\epsilon) = \hat{\rho}_0 \ln(\epsilon/T)$
- Nested Fermi surface with nesting vectors M_1, M_2, M_3: $\epsilon(\vec{k} + M_i) \approx -\epsilon(\vec{k})$

particle-particle

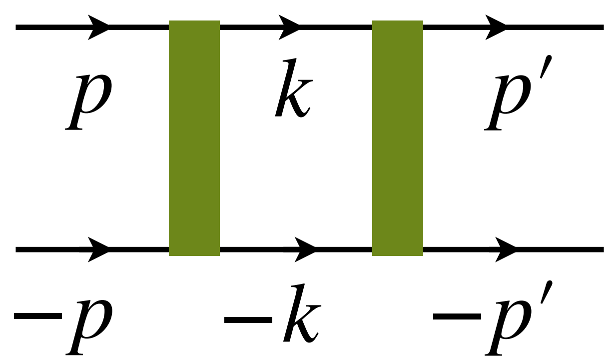

$$= U^2 \, T \sum_{i\omega} \int_{\vec{k}} G(i\omega, \vec{k}) G(-i\omega, -\vec{k})$$

$$= U^2 \int_{\vec{k}} \frac{1 - n_F(\epsilon_{\vec{k}}) - n_F(\epsilon_{-\vec{k}})}{\epsilon_{\vec{k}} + \epsilon_{-\vec{k}}} = U^2 \int_{\vec{k}} \frac{1 - n_F(\epsilon_{\vec{k}}) - n_F(\epsilon_{\vec{k}})}{2\epsilon_{\vec{k}}}$$

$$= U^2 \int d\epsilon \rho(\epsilon) \frac{1 - 2n_F(\epsilon)}{2\epsilon} = U^2 \frac{\hat{\rho}_0}{W} \int \ln\left(\frac{\epsilon}{T}\right) \frac{1 - 2n_F(\epsilon)}{2\epsilon} \sim \ln^2 \frac{W}{T}$$

- Sum particle-particle channel (pp ladder diagrams)

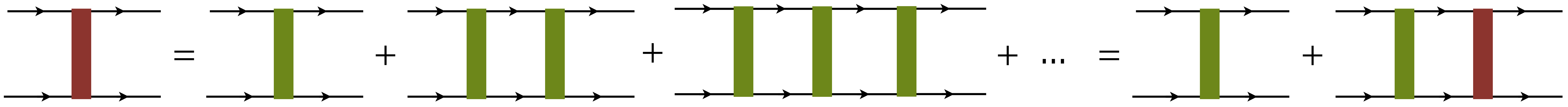

$$= \frac{U}{1 + \frac{U}{W} \hat{\rho}_0 \ln^2 \frac{W}{T}}$$

effective interaction in pp channel

Cooper instability!

Fermi-surface instabilities from amplified interactions

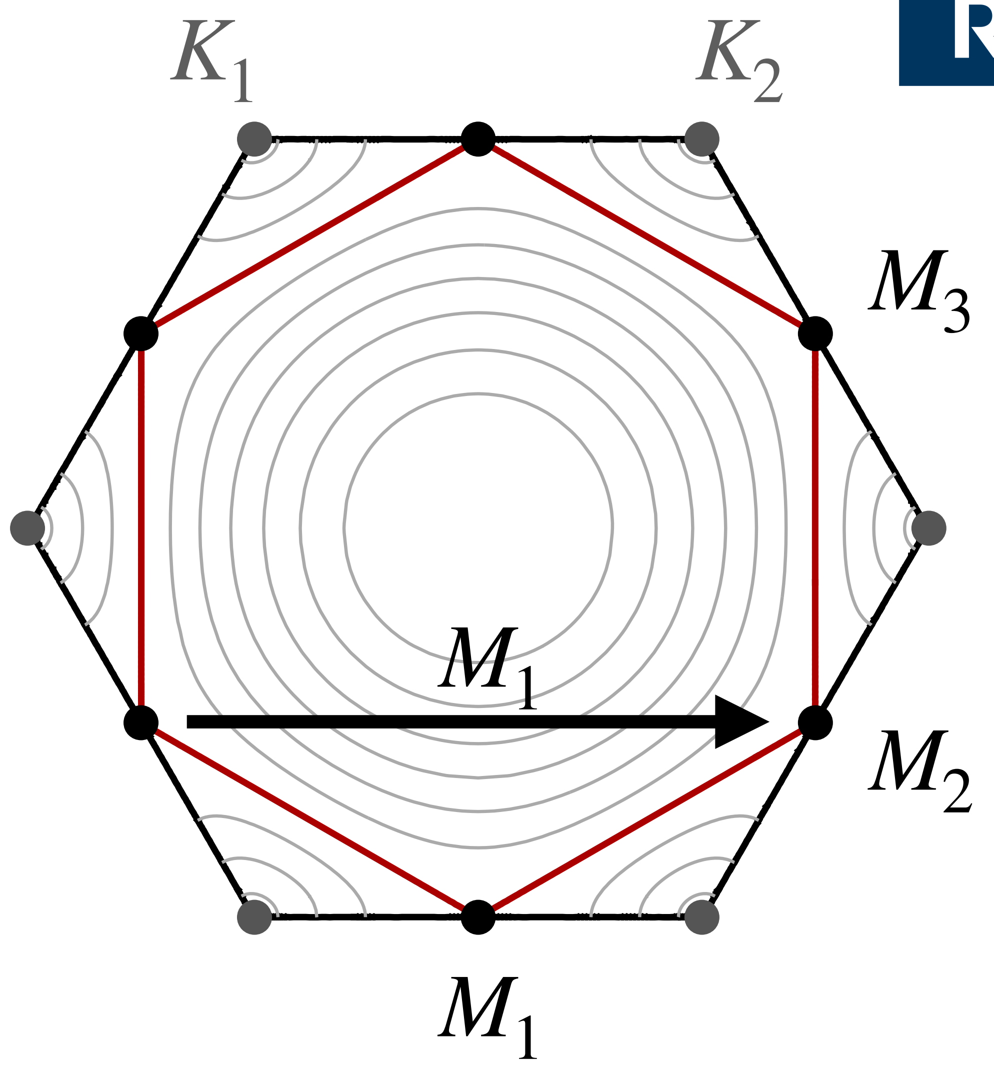

- Density of states at Van-Hove filling: $\rho(\epsilon) = \hat{\rho}_0 \ln(\epsilon/T)$
- Nested Fermi surface with nesting vectors M_1, M_2, M_3: $\epsilon(\vec{k} + M_i) \approx -\epsilon(\vec{k})$

particle-hole

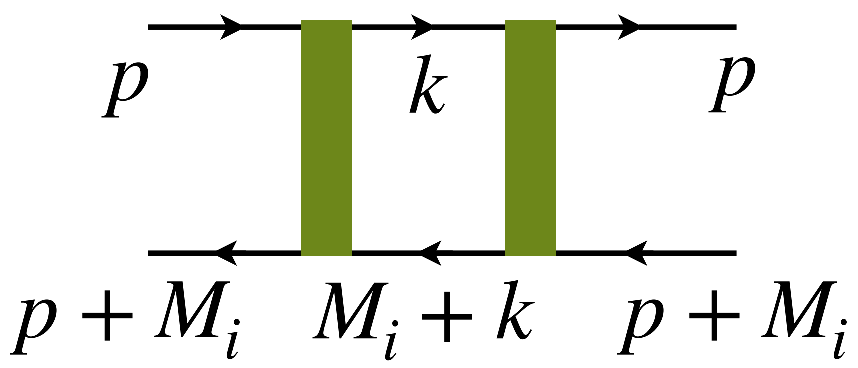

$$= U^2\, T \sum_{i\omega} \int_{\vec{k}} G(i\omega, \vec{k}) G(i\omega, \vec{k} + \vec{M}_i)$$

$$= U^2 \int_{\vec{k}} \frac{n_F(\epsilon_{\vec{k}}) - n_F(\epsilon_{\vec{k}+\vec{M}_i})}{\epsilon_{\vec{k}} - \epsilon_{\vec{k}+\vec{M}_i}} = U^2 \int_{\vec{k}} \frac{2 n_F(\epsilon_{\vec{k}}) - 1}{2\epsilon_{\vec{k}}}$$

$$\sim -\ln^2 \frac{W}{T}$$

- Sum particle-hole channel (analoguously to pp-ladder)

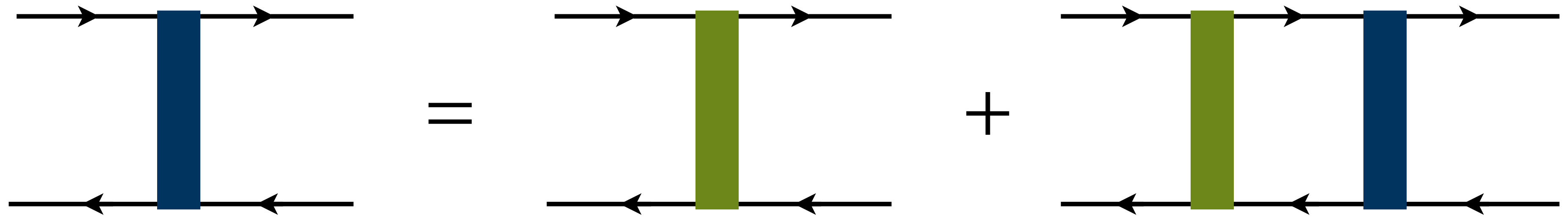

$$= \frac{U}{1 - \frac{U}{W} \hat{\rho}_0 \ln^2 \frac{W}{T}}$$

effective interaction in ph channel

(Generalized) Stoner instability!

Fermi-surface instabilities at van-Hove filling

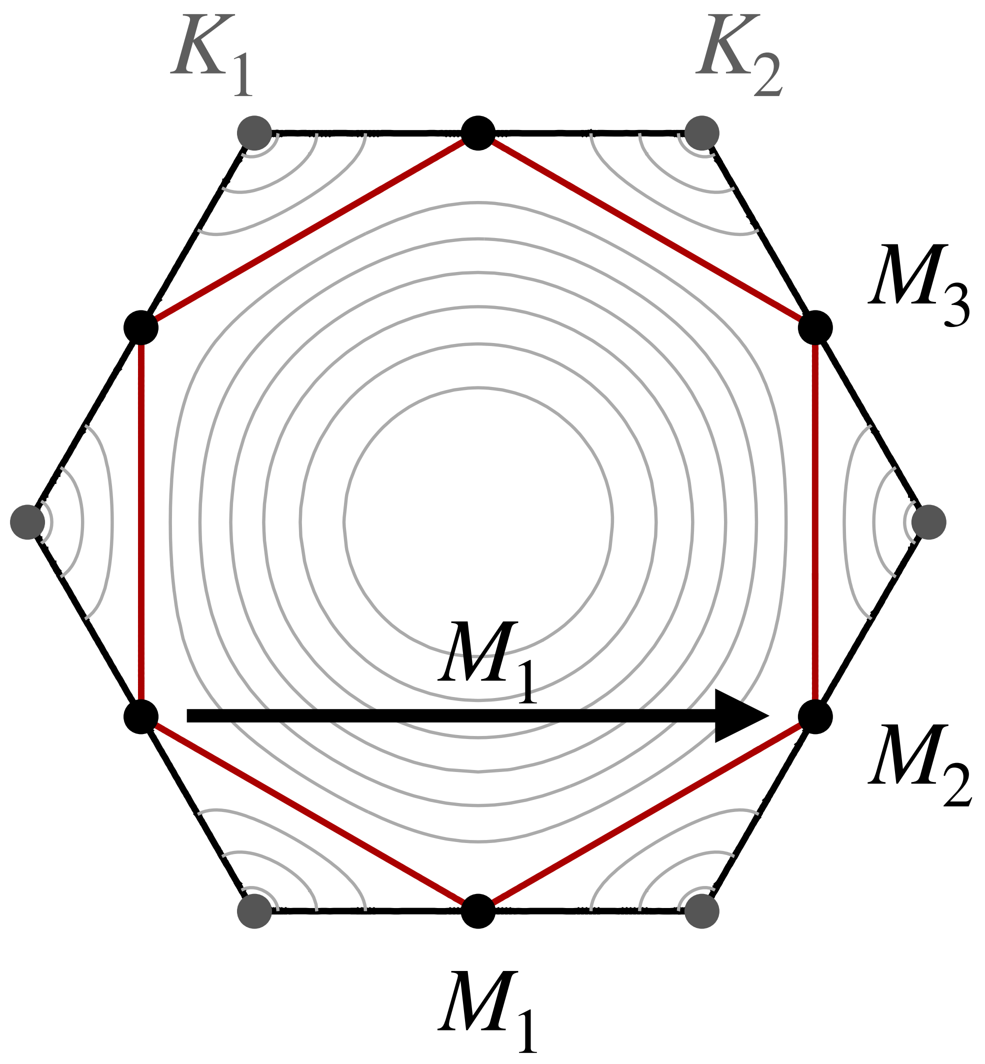

- Summary

particle-particle

particle-hole

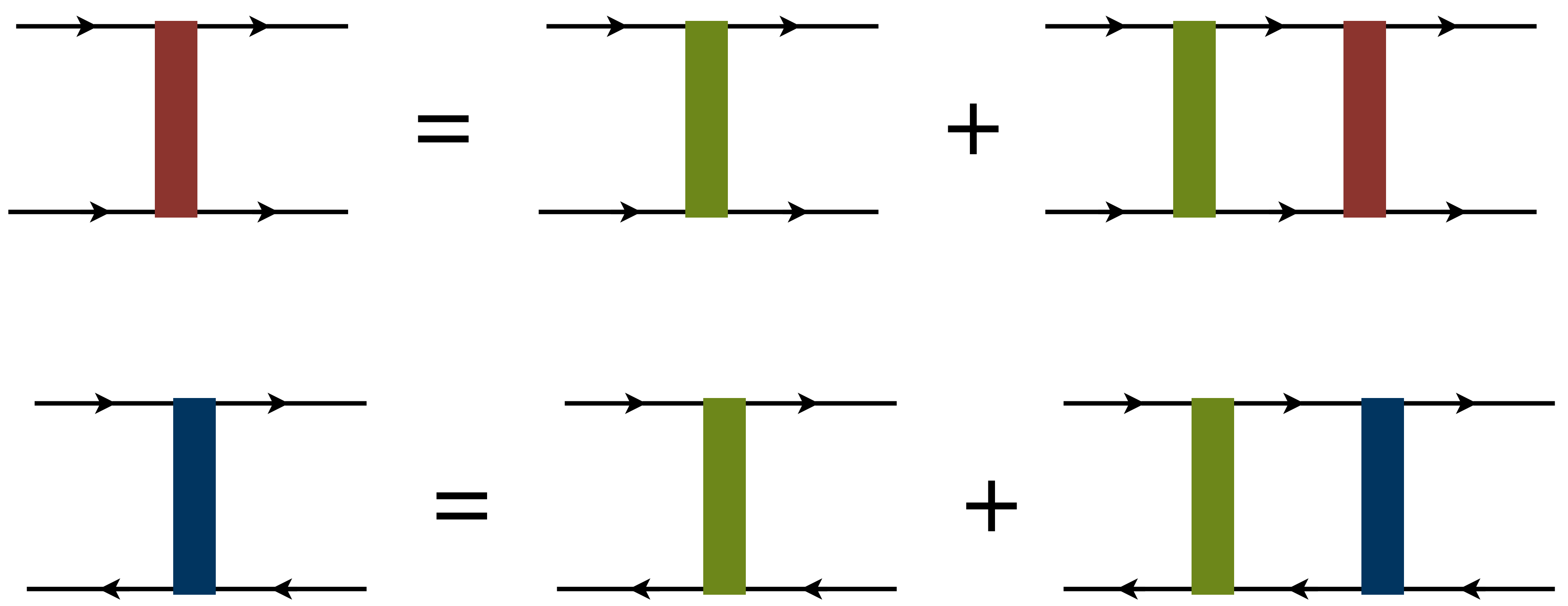

$$= \frac{U}{1 + \frac{U}{W}\hat{\rho}_0 \ln^2 \frac{W}{T}}$$

$$= \frac{U}{1 - \frac{U}{W}\hat{\rho}_0 \ln^2 \frac{W}{T}}$$

- Instabilities/singularities upon lowering temperature (! sign)

$$1 = \frac{|U|}{W}\hat{\rho}_0 \ln^2 \frac{W}{T} \quad \Rightarrow \quad T_c = W \exp\left[-\sqrt{\frac{W}{|U|\hat{\rho}_0}}\right]$$

- Correlations grow strong at T_c $\rightarrow$ signature for spontaneous symmetry breaking / ordering transition
  - U<0: superconductivity
  - U>0: density wave with wave vector $\vec{M}_i$

Fermi-surface instabilities from amplified interactions

RUB

- Instabilities appear in several channels: **competing instabilities/orders**
- Cannot be considered separately
- For example: **unconventional pairing mechanism**
  1. start with repulsive interaction
  2. ph fluctuations grow strong → tendency to density wave instability
  3. at the same time: ph fluctuations mediate attraction in pairing channel
  4. pp fluctuations can overcome ph channel → tendency to superconductivity
- **Who wins at the end?**

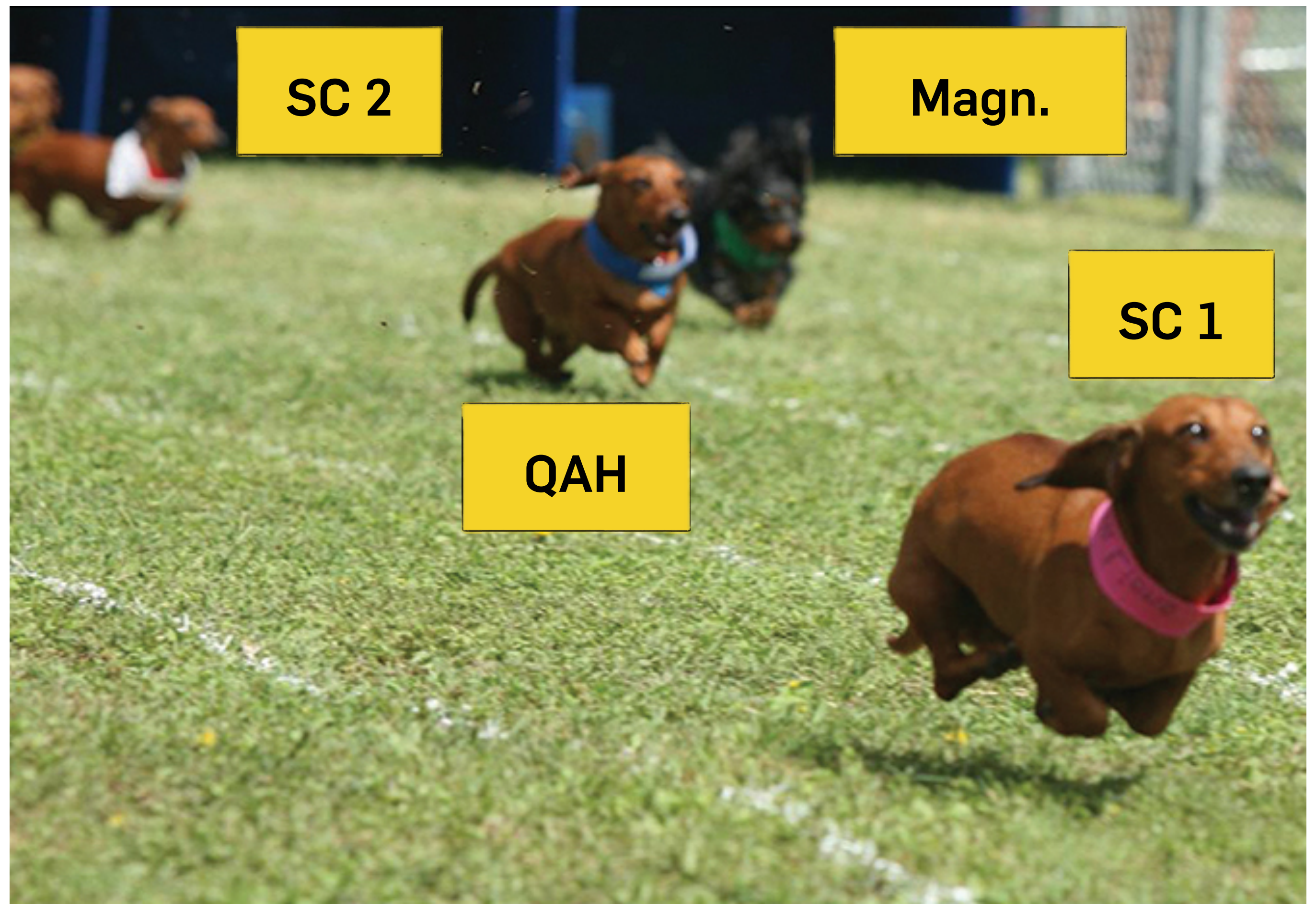

Outline

RUB

- *Chapter I:* **From 2D moiré materials to frustrated superlattice Hubbard models**
- *Chapter II:* **Interaction effects in hexagonal superlattice Hubbard models**
- *Chapter III:* **Functional renormalization group**
- *Chapter IV:* **Functional renormalization group for moiré materials**
- *Chapter V:* **Further developments and outlook**

Chapter III: Functional renormalization group

- Physics of scales and renormalization group concept
- Functional renormalization for correlated fermions
- Truncations and approximations
- Implementation

Wetterich, Phys. Lett. B (1992)
Metzner et al., RMP (2012)
Platt, Hanke, Thomale, Adv. Phys. (2013)

Quantum fields and renormalization

RUB

- quantum field theory:

  framework for systems with a large number of coupled degrees of freedom

- renormalization group (RG):

  mathematical procedure to study changes of a physical system when viewed at different scales ***k*** *(T)*

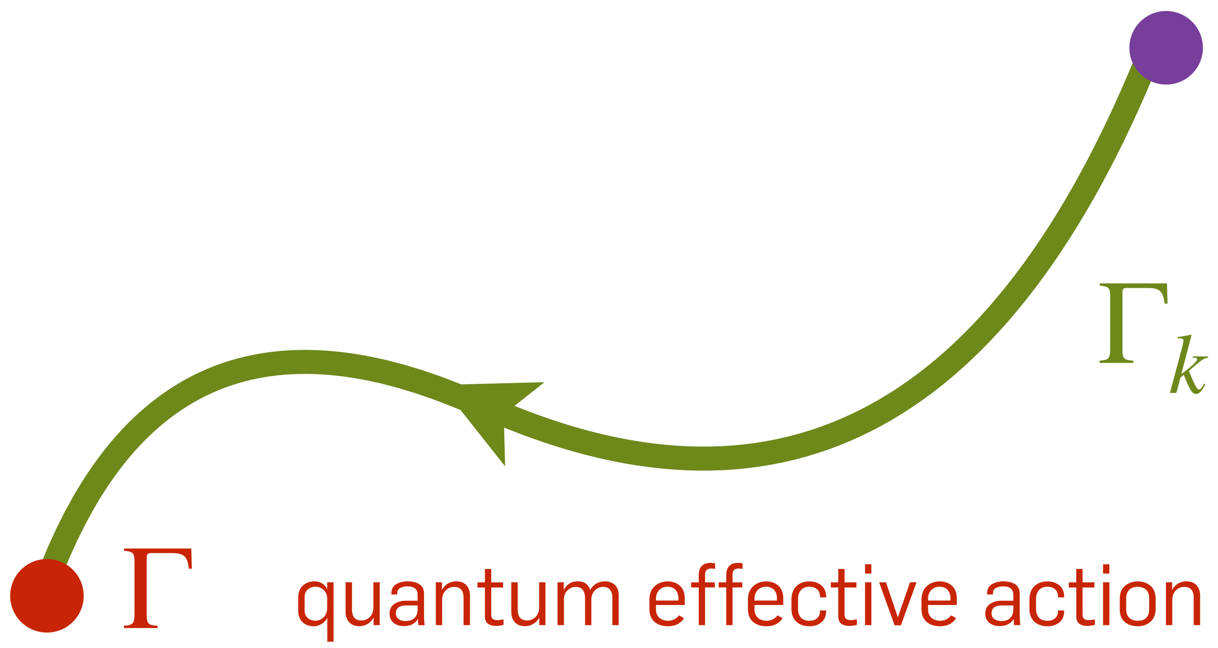

- exact functional RG flow equation $$k\partial_k \Gamma_k[\Phi] = \frac{1}{2}\mathrm{STr}\left(\frac{k\partial_k R_k}{\Gamma_k^{(2)}[\Phi] + R_k}\right)$$ Wetterich (1992)

- allows for non-perturbative truncations and/or systematic approximations…
  - dynamical generation of mass gaps
  - unbiased detection of ordering tendencies
  - (quantum) critical exponents, …

Functional renormalization group for correlated electrons

- Preliminary consideration:
  - ladders can also be expressed as differential equations

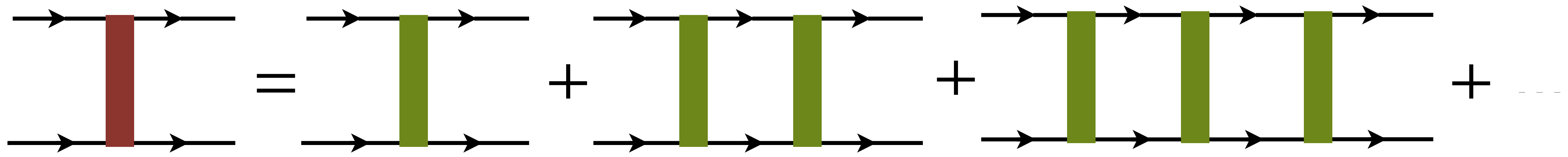

  - define $y = \frac{\hat{\rho}_0}{W} \ln^2 \frac{W}{T}$
  - then write for an **effective interaction** V: $\frac{d}{dy} V = \pm V^2 \quad \Rightarrow \quad V = \mp \frac{1}{y + c}$
  - with $V(T = W) = U$: $V = \frac{U}{1 \mp \frac{U}{W} \hat{\rho}_0 \ln^2 \frac{W}{T}}$

- Diff. eq. can be derived from Wilson RG → integrate out fast modes in momentum shell

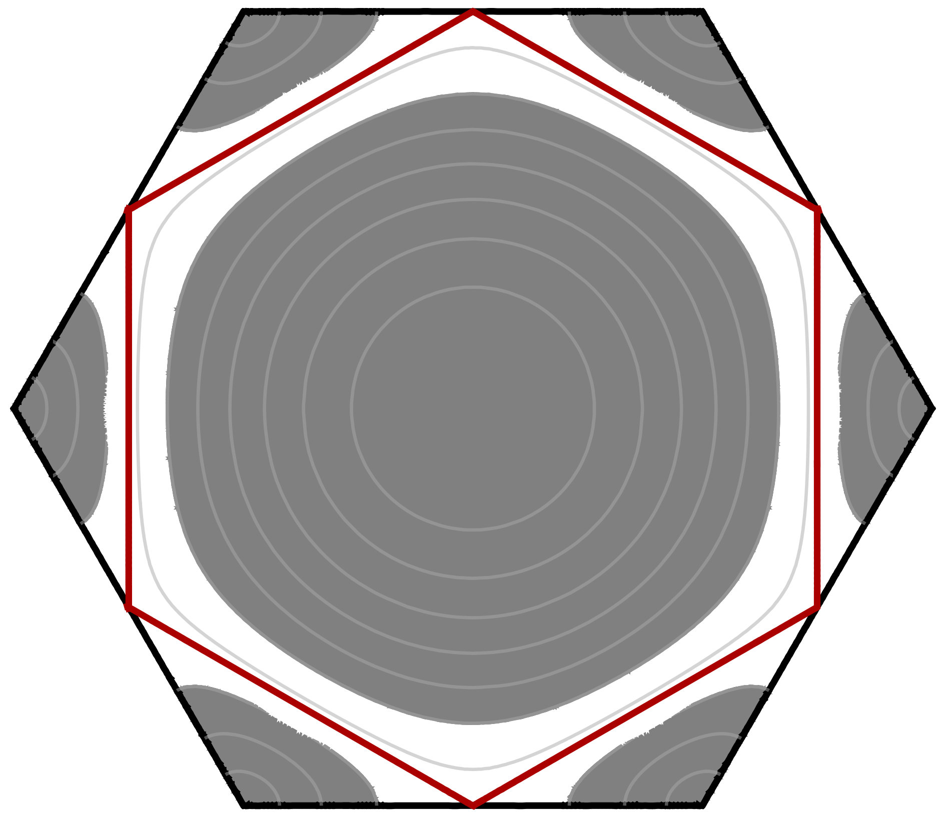

- Also possible to account for coupling of different channels in this way
- FRG provides formalism and generalization…

Functional renormalization group for correlated electrons

RUB

- system of interacting fermions: $\mathcal{S}[\psi,\bar\psi] = -(\bar\psi, G_0^{-1}\psi) + V[\psi,\bar\psi]$
- bare propagator: $G_0(k_0,\mathbf{k}) = \dfrac{1}{ik_0 - \xi_{\mathbf{k}}}, \quad \xi_{\mathbf{k}} = \epsilon_{\mathbf{k}} - \mu$
- generating functional (connected Green fcts): $\mathcal{G}[\eta,\bar\eta] = -\ln \int \mathcal{D}\psi\mathcal{D}\bar\psi\, e^{\mathcal{S}[\psi,\bar\psi]} e^{(\bar\eta,\psi)+(\bar\psi,\eta)}$
- effective action (generates 1PI correlators): $\Gamma[\phi,\bar\phi] = (\bar\eta,\phi) + (\bar\phi,\eta) + \mathcal{G}[\eta,\bar\eta], \quad \phi = -\dfrac{\partial\mathcal{G}}{\partial\bar\eta}$
- modify bare propagator by IR cutoff $G_0^\Lambda(k_0,\mathbf{k}) = \dfrac{\Theta_\epsilon(|\xi_{\mathbf{k}}| - \Lambda)}{ik_0 - \xi_{\mathbf{k}}}$
- define above quantities with modified propagator → variation w.r.t to scale

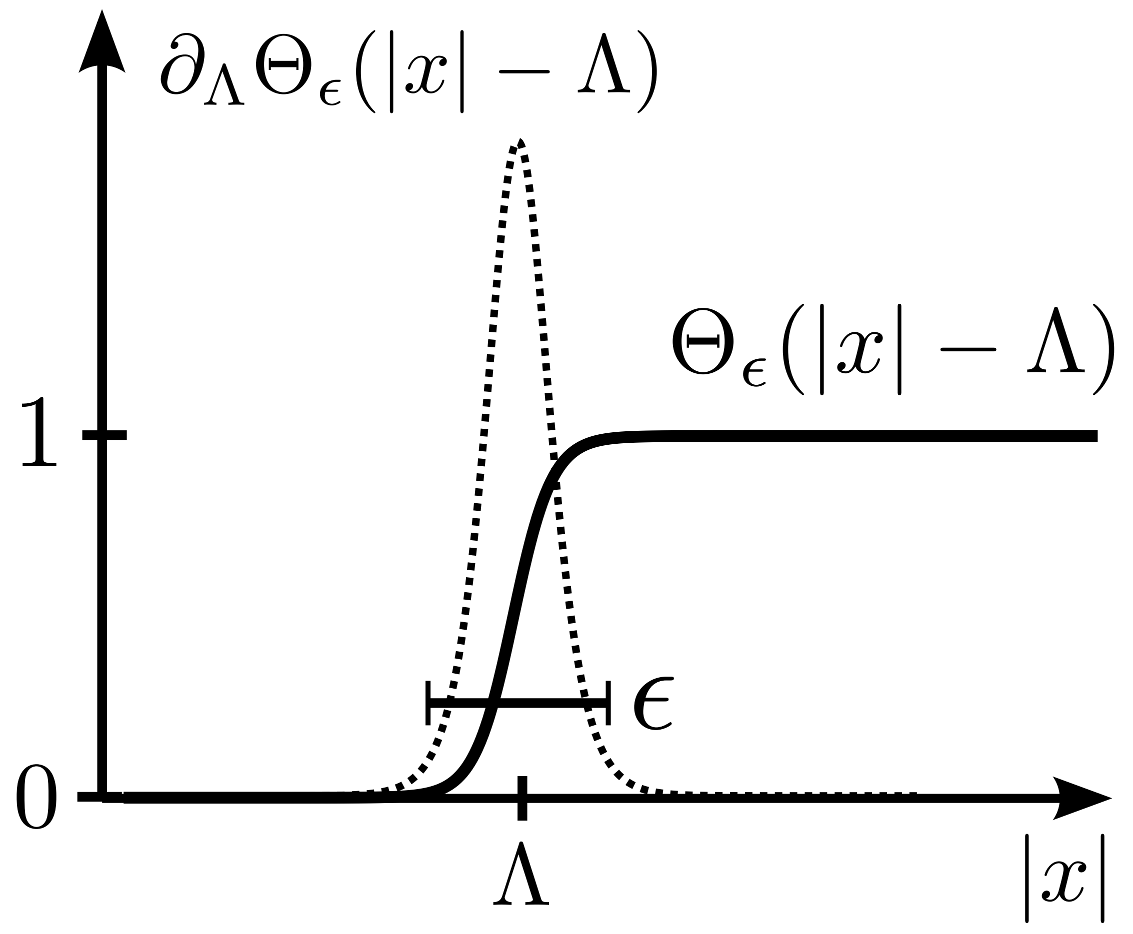

Functional renormalization group for correlated electrons

- exact RG equation

$$\frac{\partial}{\partial\Lambda}\Gamma^\Lambda[\phi,\bar\phi] = \mathrm{Tr}\left[G_0^\Lambda \frac{\partial (G_0^\Lambda)^{-1}}{\partial\Lambda}\right] - \mathrm{Tr}\left[\left(\frac{\delta^2\Gamma^\Lambda[\phi,\bar\phi]}{\delta\phi\delta\bar\phi} + (G_0^\Lambda)^{-1}\right)^{-1} \frac{\partial (G_0^\Lambda)^{-1}}{\partial\Lambda}\right]$$

- exact RG equation has one-loop structure
- removing cutoff ($\Lambda \to 0$) yields the full effective action
- lowering cutoff corresponds to momentum-shell integration
- cannot be solved exactly!

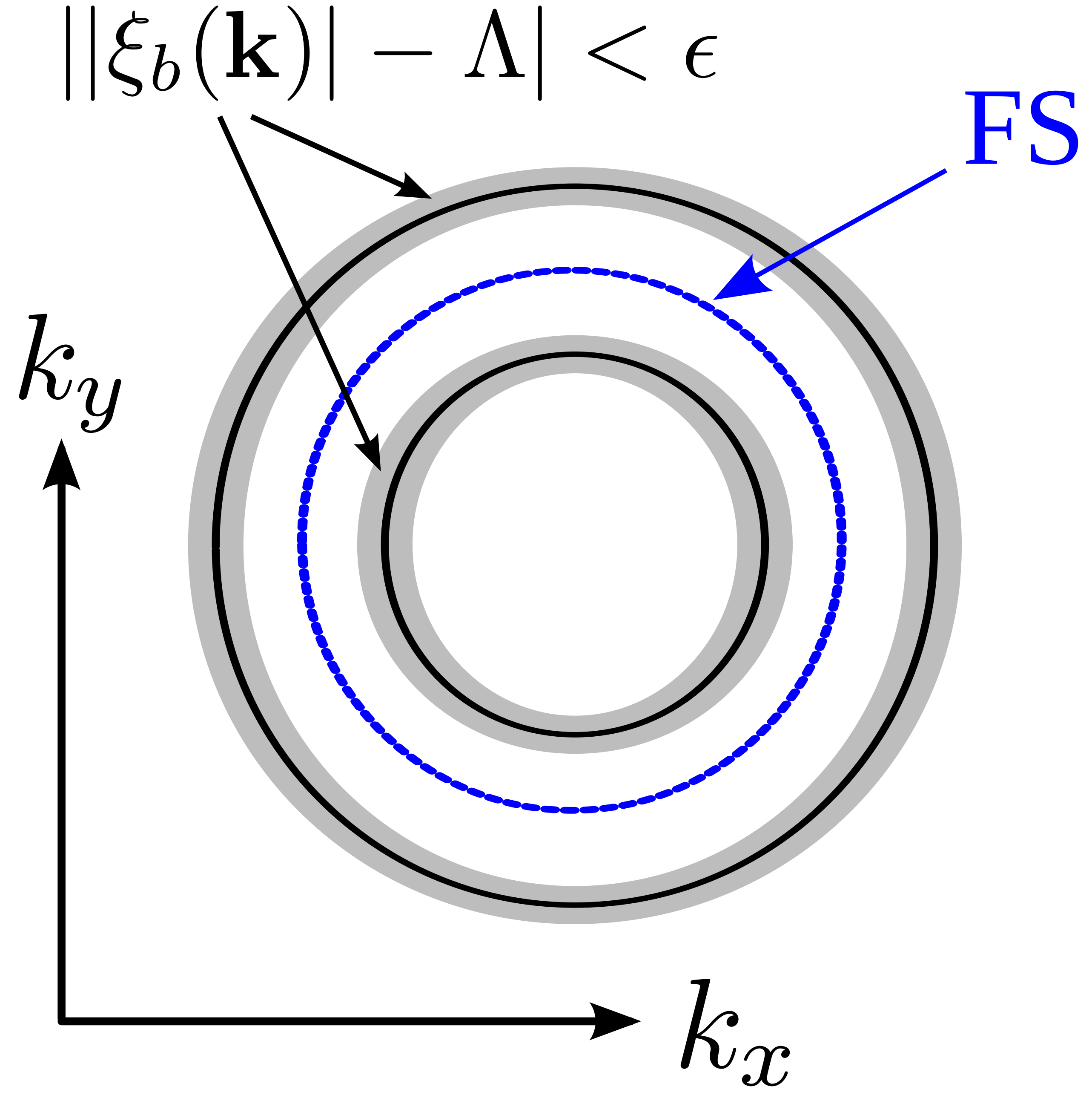

Platt, Hanke, Thomale (2013)

Functional renormalization group for correlated electrons

- exact RG equation
$$\frac{\partial}{\partial\Lambda}\Gamma^{\Lambda}[\phi,\bar{\phi}] = \mathrm{Tr}\left[G_0^{\Lambda}\frac{\partial (G_0^{\Lambda})^{-1}}{\partial\Lambda}\right] - \mathrm{Tr}\left[\left(\frac{\delta^2\Gamma^{\Lambda}[\phi,\bar{\phi}]}{\delta\phi\delta\bar{\phi}} + (G_0^{\Lambda})^{-1}\right)^{-1}\frac{\partial (G_0^{\Lambda})^{-1}}{\partial\Lambda}\right]$$
  - starting point for systematic approximations (vertex expansion)

$$\Gamma^{\Lambda}[\psi,\bar{\psi}] = \sum_{i=0}^{\infty}\frac{(-1)^i}{(i!)^2}\sum_{\substack{K_1,\dots,K_i\\K_1',\dots,K_i'}}\Gamma^{(2i)\Lambda}(K_1',\dots,K_i',K_1,\dots,K_i)\;\bar{\psi}(K_1')\dots\bar{\psi}(K_i')\psi(K_i)\dots\psi(K_1)$$

exact RG equation

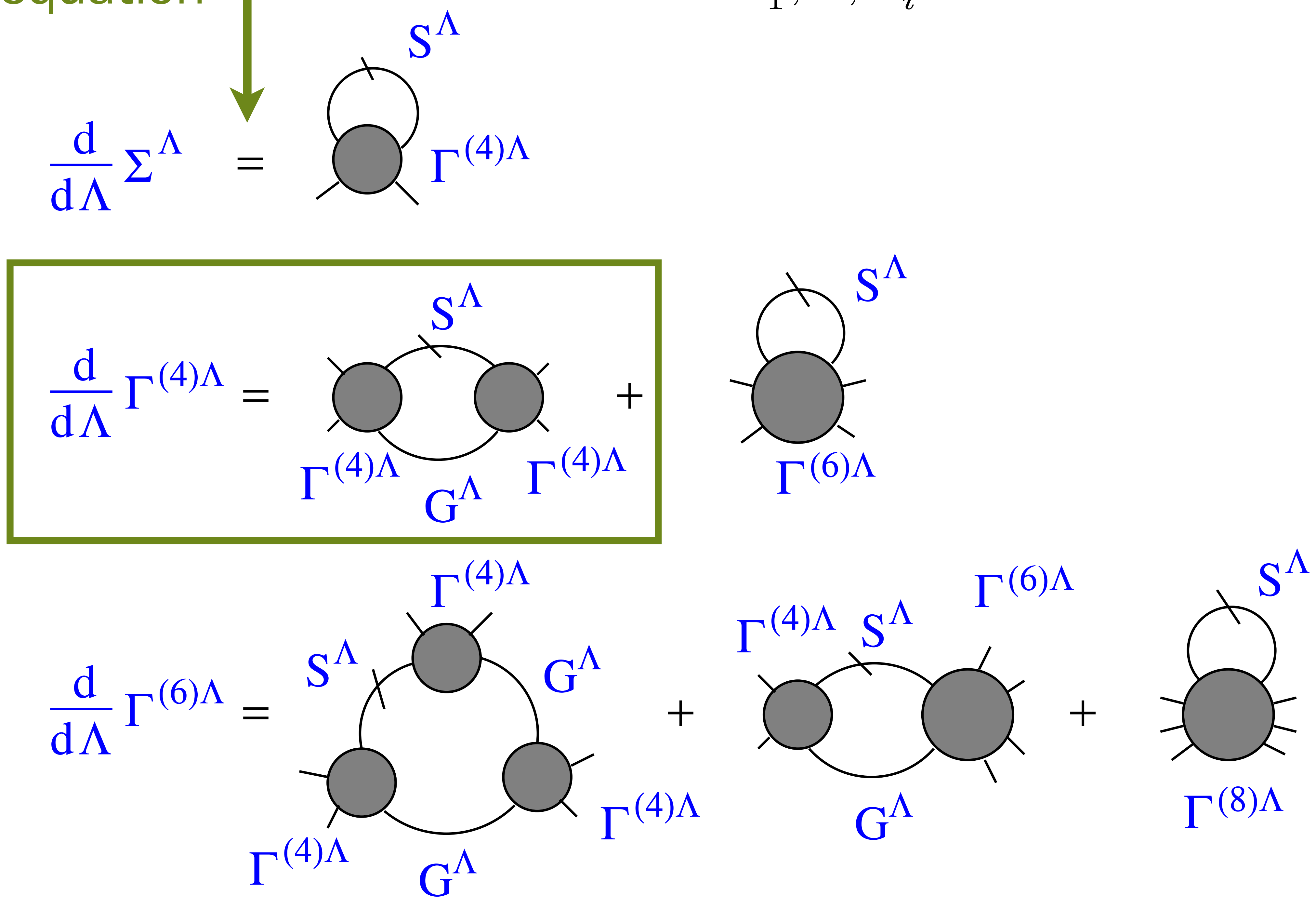

- neglect 6-point and higher vertices
- neglect self-energy feedback

Salmhofer & Honerkamp (2001)

... infinite hierarchy of flow equations!

Functional renormalization group for correlated electrons

- system with **spin-rotational invariance**

- General 4-point function: $\Gamma^{(4)\Lambda}_{\sigma_1,\sigma_2,\sigma_3,\sigma_4} = V^\Lambda \delta_{\sigma_1\sigma_3}\delta_{\sigma_2\sigma_4} - V^\Lambda \delta_{\sigma_1\sigma_4}\delta_{\sigma_2\sigma_3}$

  - simplified flow of **spin-independent interaction vertex** V^Λ:

$$\frac{d}{d\Lambda}V^\Lambda(K_1,K_2;K_3,K_4) = \int dK\, V^\Lambda(K_1,K_2,K)\; L^\Lambda(K,-K+K_1+K_2)\, V^\Lambda(K,-K+K_1+K_2,K_3)\ ,$$

$$+ \int dK \Big[-2V^\Lambda(K_1,K,K_3)\, L^\Lambda(K,K+K_1-K_3)\, V^\Lambda(K+K_1-K_3,K_2,K)$$

$$+V^\Lambda(K_1,K,K+K_1-K_3)\, L^\Lambda(K,K+K_1-K_3)\, V^\Lambda(K+K_1-K_3,K_2,K)$$

$$+V^\Lambda(K_1,K,K_3)\, L^\Lambda(K,K+K_1-K_3)\, V^\Lambda(K_2,K+K_1-K_3,K)\Big]\ ,$$

$$+ \int dK\, V^\Lambda(K_1,K+K_2-K_3,K)\, L^\Lambda(K,K+K_2-K_3)\, V^\Lambda(K,K_2,K_3)\ .$$

with $L^\Lambda(K,K') = \frac{d}{d\Lambda}[G_0^\Lambda(K)G_0^\Lambda(K')]$

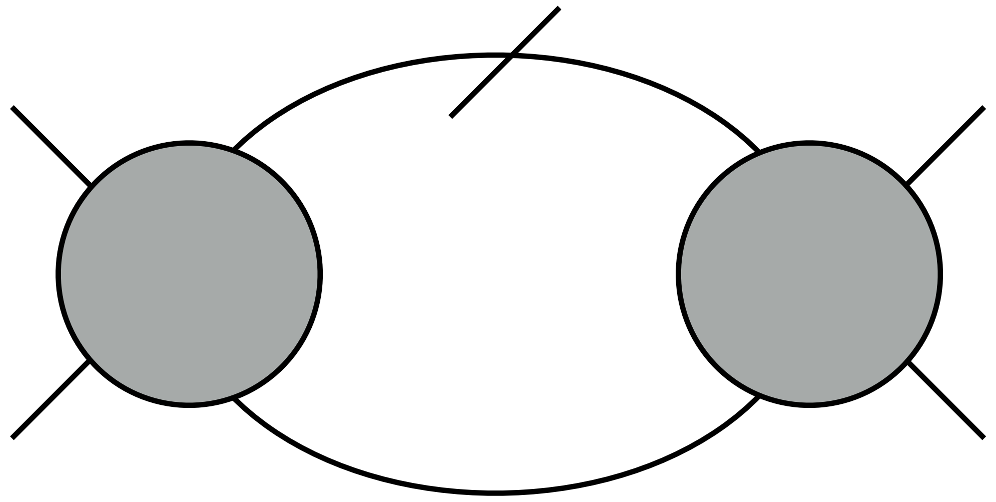

Functional renormalization group for correlated electrons

RUB

- system with **spin-rotational invariance**
- General 4-point function: $\Gamma^{(4)\Lambda}_{\sigma_1,\sigma_2,\sigma_3,\sigma_4} = V^{\Lambda}\delta_{\sigma_1\sigma_3}\delta_{\sigma_2\sigma_4} - V^{\Lambda}\delta_{\sigma_1\sigma_4}\delta_{\sigma_2\sigma_3}$
  - simplified flow of **spin-independent interaction vertex** V^{Λ}:

$$\frac{d}{d\Lambda}V^{\Lambda}(K_1, K_2; K_3, K_4) =$$

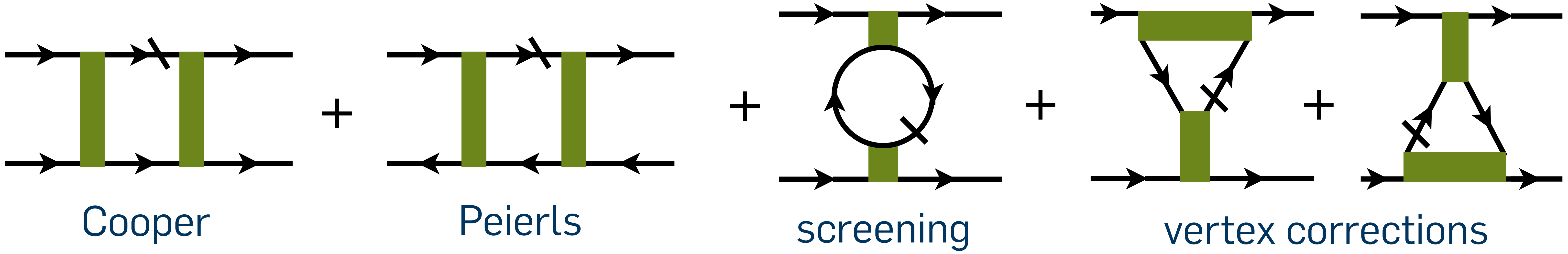

  - corresponds to infinite order summation of one-loop pp and ph terms (ladder summations)
  - takes into account competition between various interaction channels
  - flow to strong coupling ($V^{\Lambda} \gg W$ for $T \to T_c > 0$) indicates ordering transition -- but which one?

Functional renormalization group for correlated electrons

RUB

- Interaction vertex:

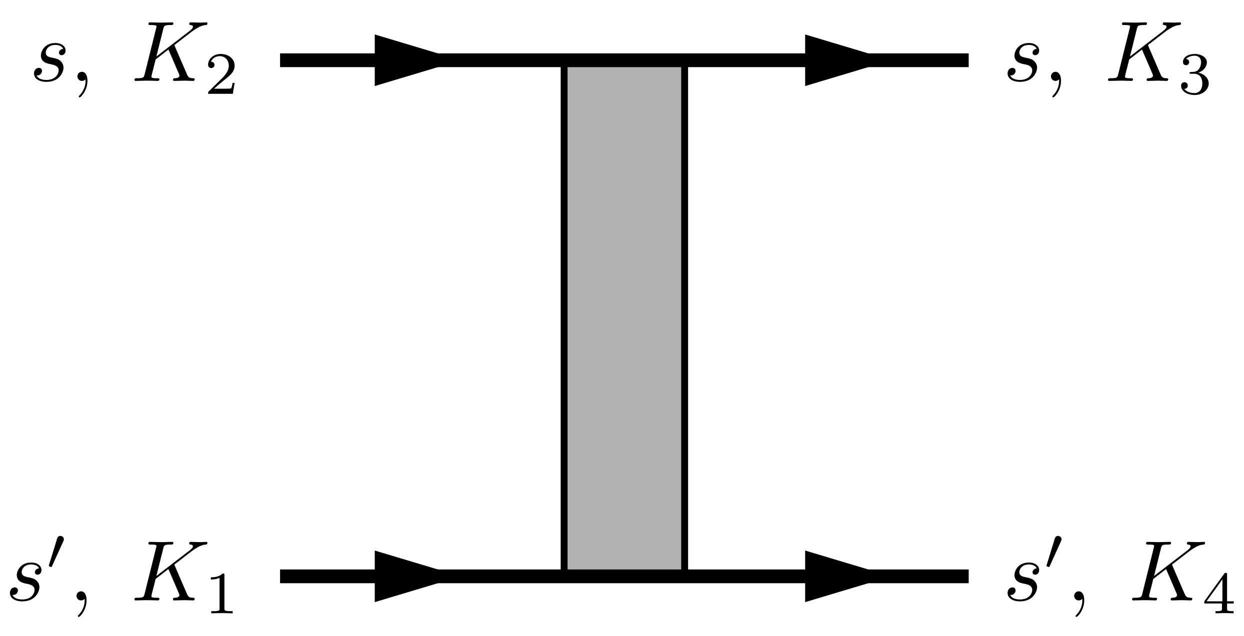

$$V_\Lambda(k_1, k_2, k_3, k_4)$$

- momentum arguments include frequency, wavevector and orbital/band indices

- ground-state properties:

  set external frequencies to zero (neglect frequency dependence)

Functional renormalization group for correlated electrons

- Interaction vertex:

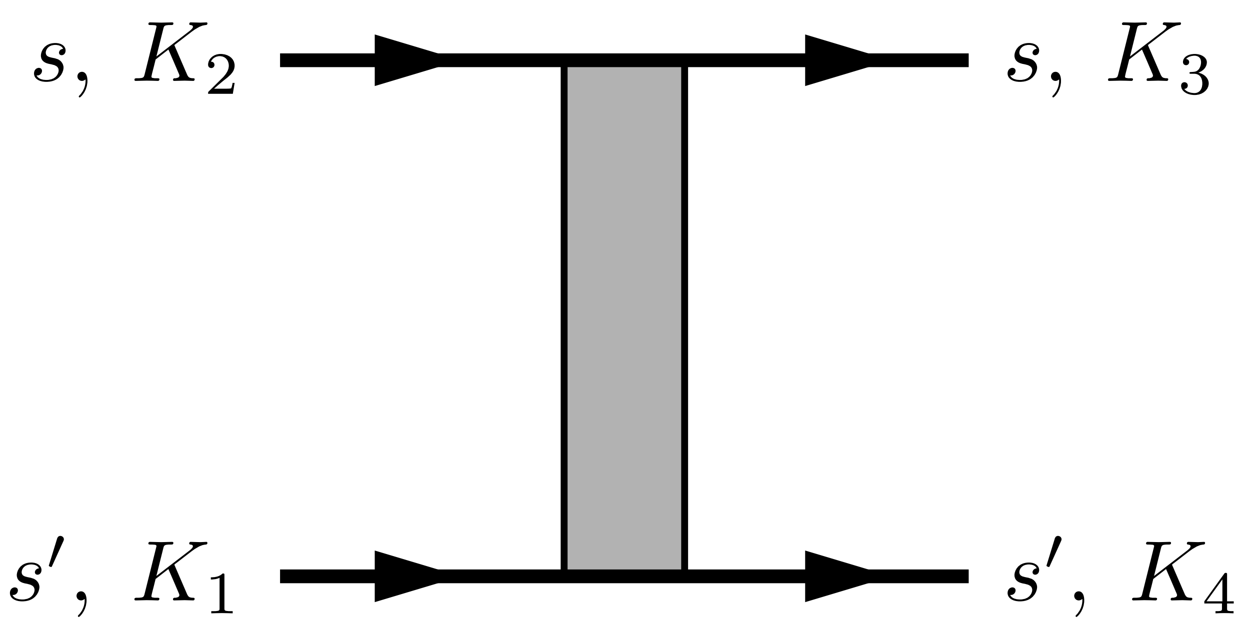

$$V_\Lambda(k_1, k_2, k_3, k_4)$$

- wavevector dependence from discretization of BZ in ***N* patches:**

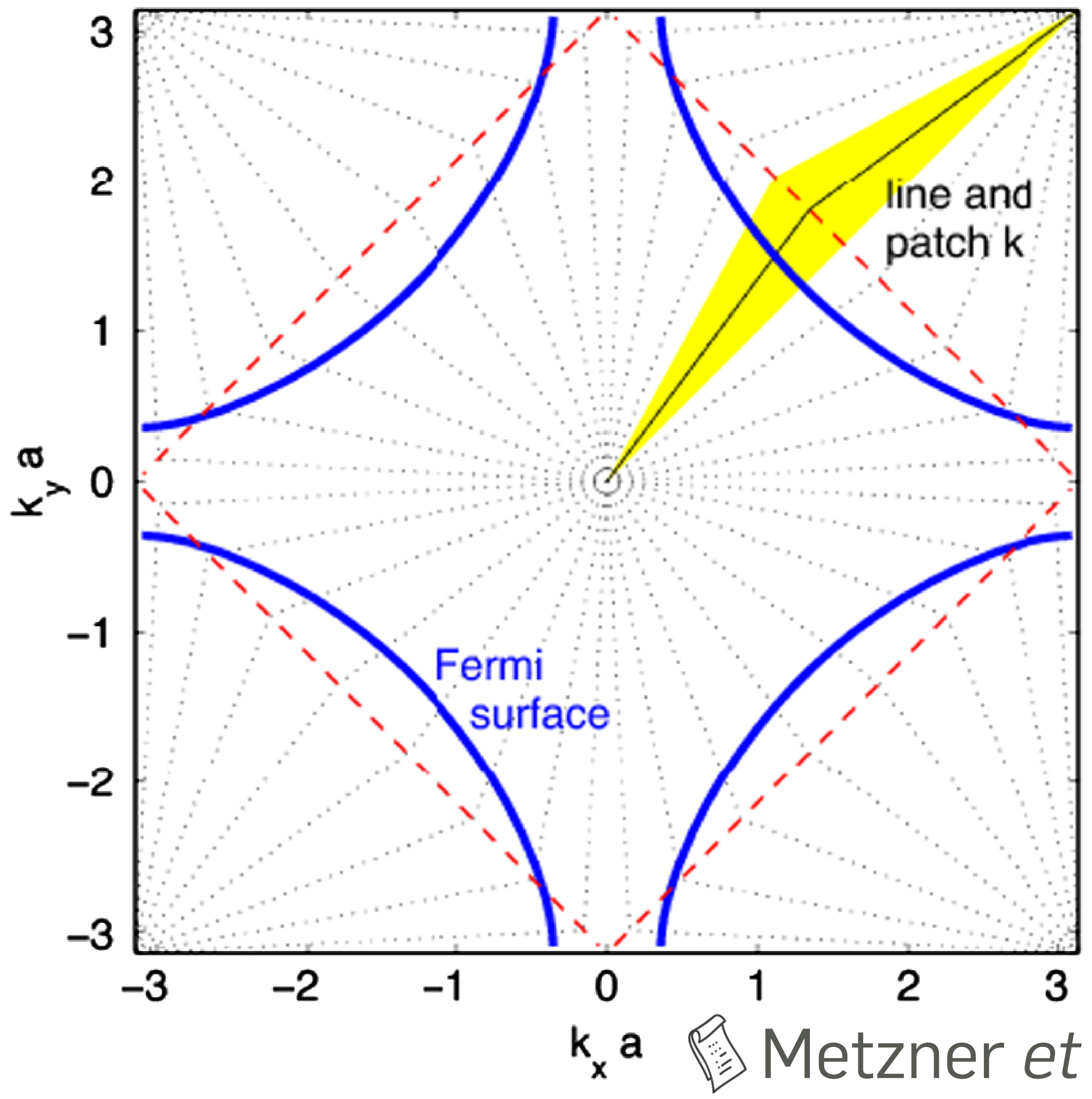

Metzner *et al.*, RMP (2012)

- interaction constant within one patch
- finite set of coupled flow equations for components of *V*^
- *V*^ has $N_b^4 N^3$ components
- largest contribution due to external momenta on Fermi surface
- Exclusively resolve momentum dependence on **Fermi surface!**
- facilitates efficient numerical implementation!

Functional renormalization group for correlated electrons

- Case of hexagonal Brillouin zone with nesting

- introduce patches with magnitude on FS and describe angular dependence

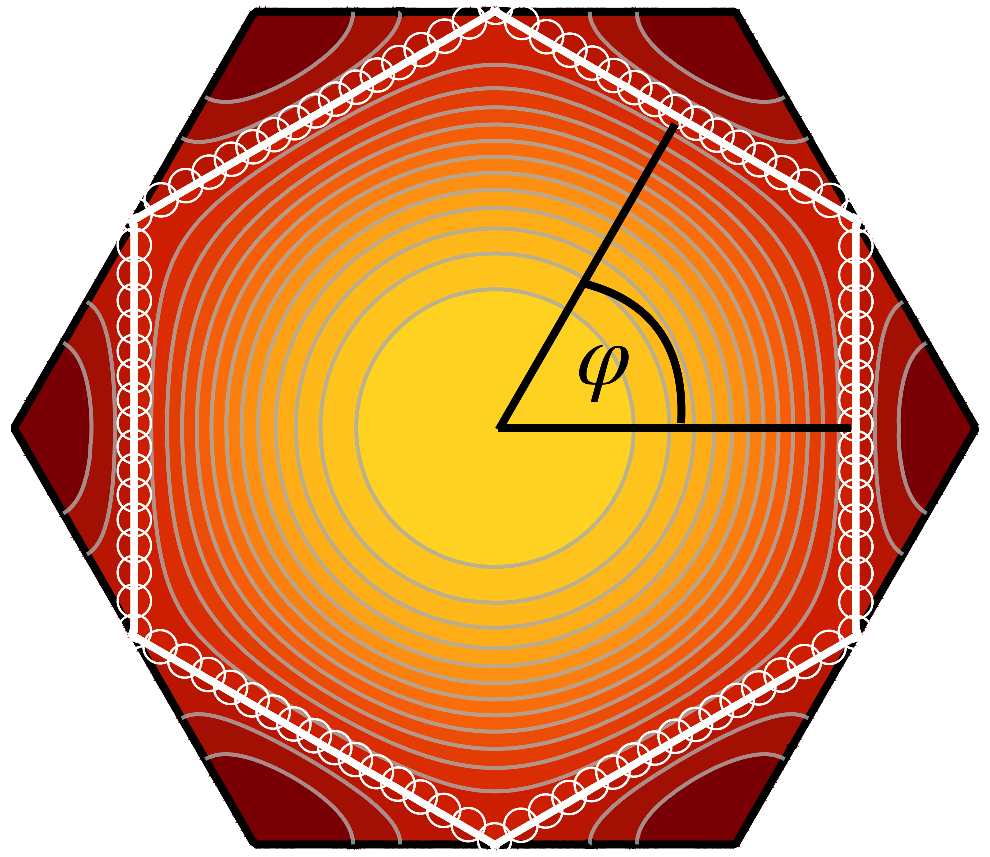

$$\vec{k} = k_F^{\varphi}(\cos\varphi, \sin\varphi)$$

- Solve flow equation for effective interaction $V^{\Lambda}(\varphi_1, \varphi_2, \varphi_3)$

  (=1PI part of 2-particle correlation function)

- **Fermi-surface instability**:

  correlations grow + sharp structures develop for certain momentum combinations

  $\rightarrow$ long-ranged correlations in real space

- Extract type of correlations, e.g., SC or (spin) density wave

Functional renormalization group for correlated electrons

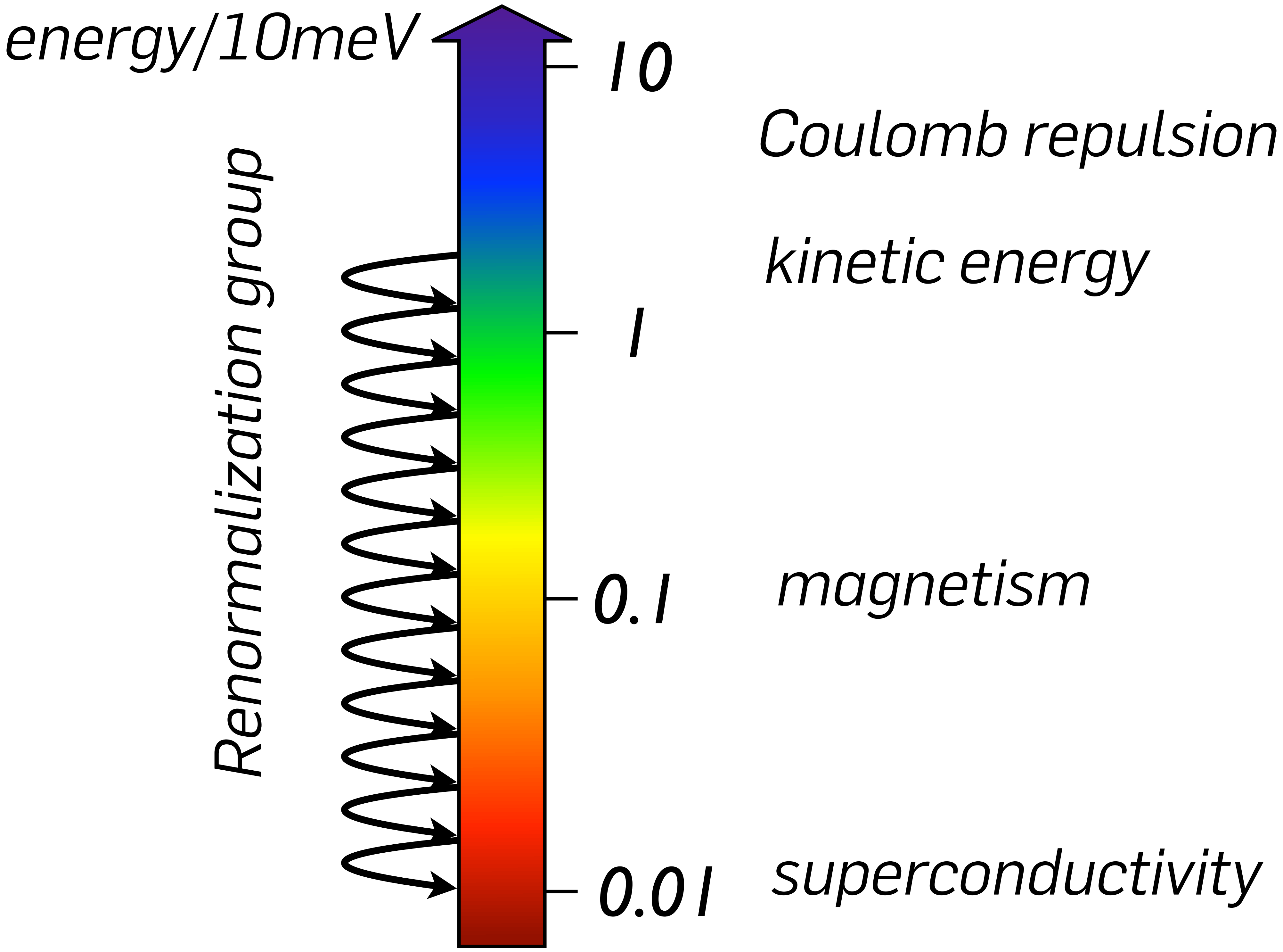

microscopic model

$$H_{\text{bare}} = \text{band structure} + \text{interactions } V_{\text{bare}}$$

$$\frac{d}{dk} V_k =$$

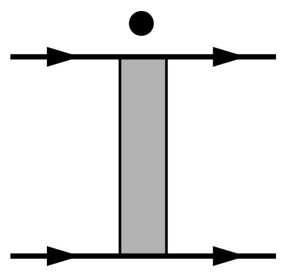

$$V_{\text{eff}}(p, p', q)$$

Functional renormalization group for correlated electrons

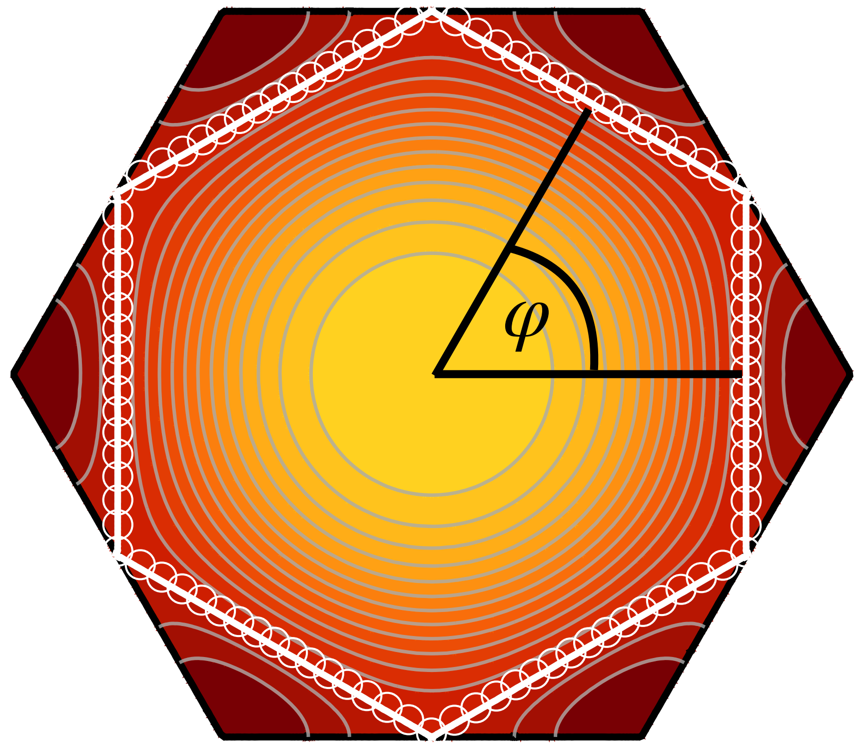

- **example** for RG evolution of V^Λ

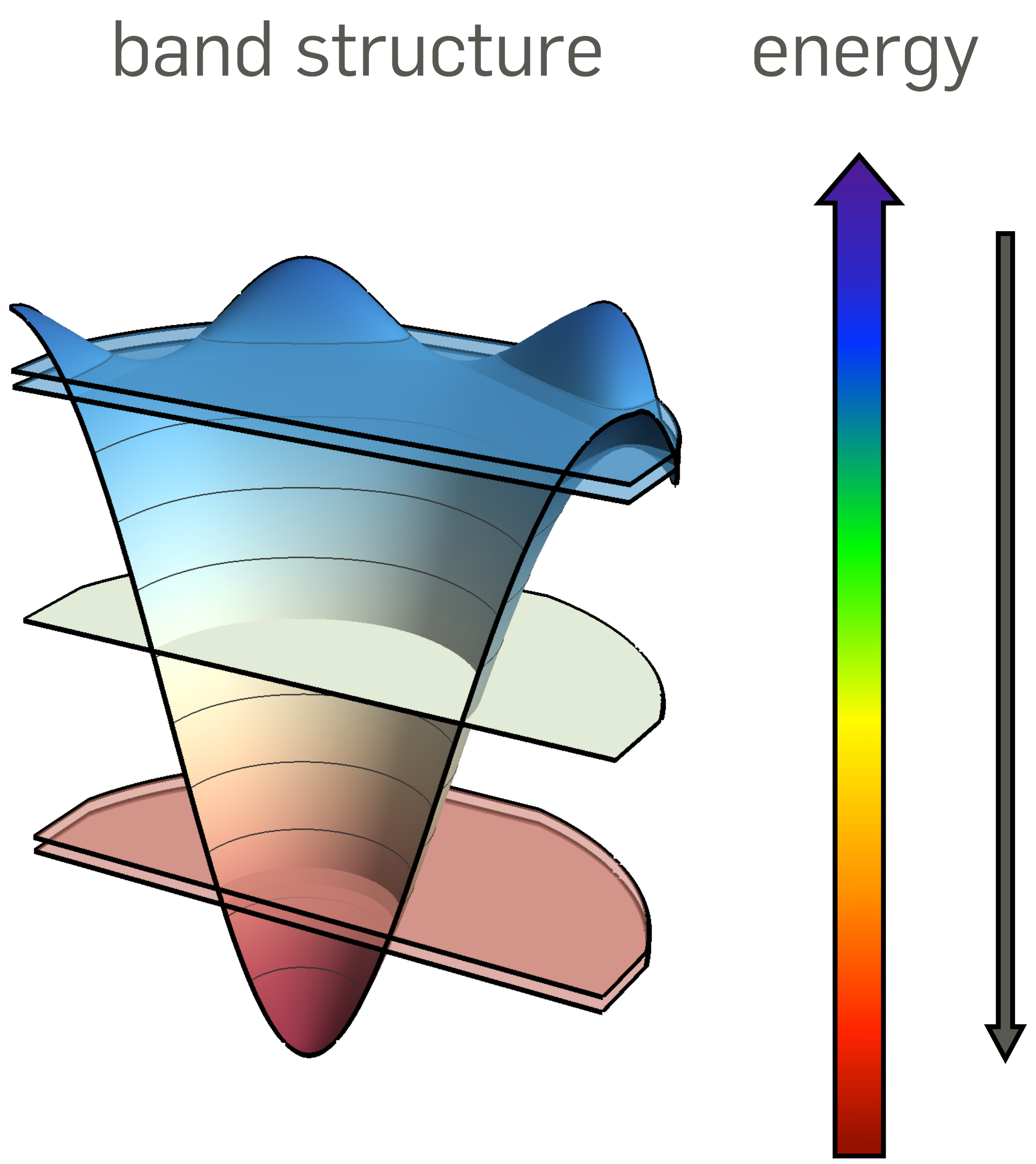

$$H_{\rm int} = U \sum_i \left(\sum_{\alpha=1}^{4} n_{i\alpha} \right)^2 + \dots$$

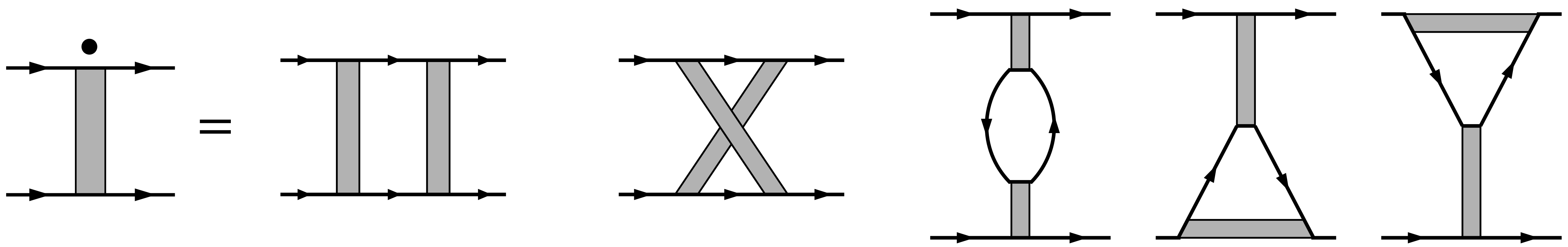

$$H_{\rm eff} = \frac{1}{2} \sum_{\vec{p},\vec{p}',\vec{q},s,s'} V(\vec{p},\vec{p}',\vec{p}+\vec{q}) c^\dagger_{\vec{p}+\vec{q},s} c^\dagger_{\vec{p}'-\vec{q},s'} c_{\vec{p}',s'} c_{\vec{p},s}$$

Functional renormalization group for correlated electrons

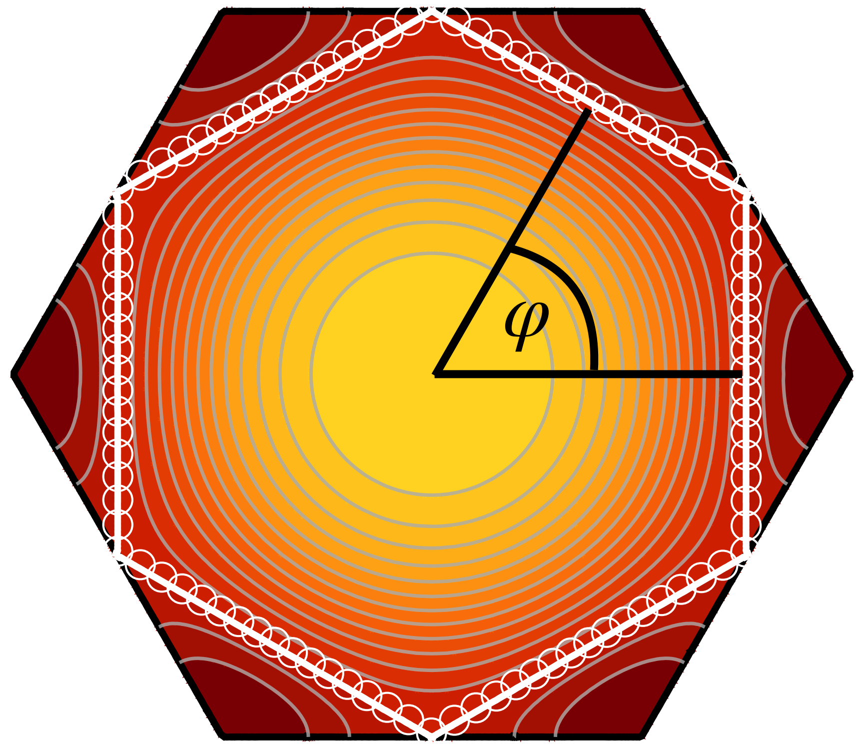

- **example** for RG evolution of V^{Λ}

band structure energy

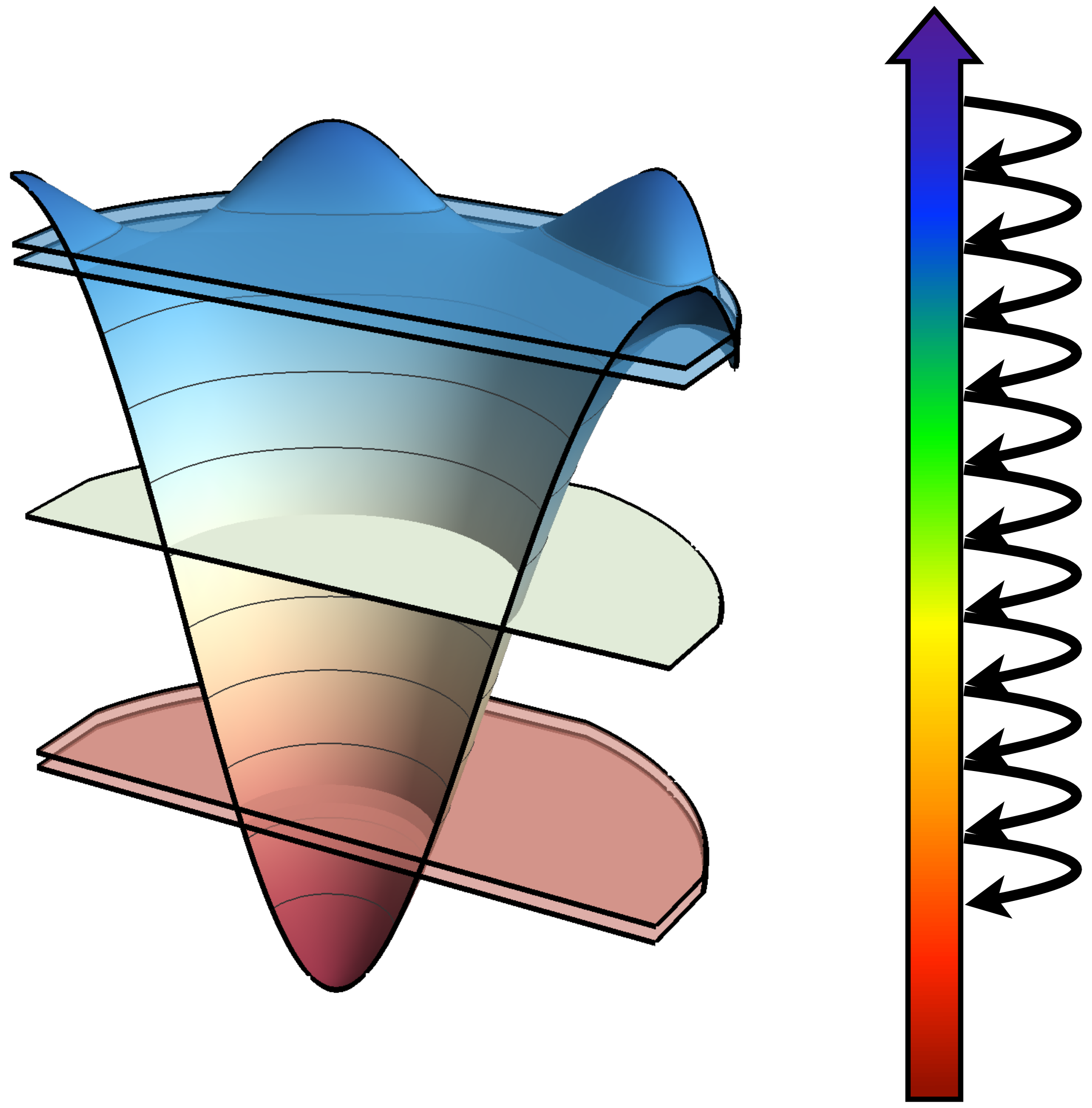

$$H_{\text{int}} = U \sum_i \left(\sum_{\alpha=1}^{4} n_{i\alpha} \right)^2 + \dots$$

$$V^{\Lambda} =$$

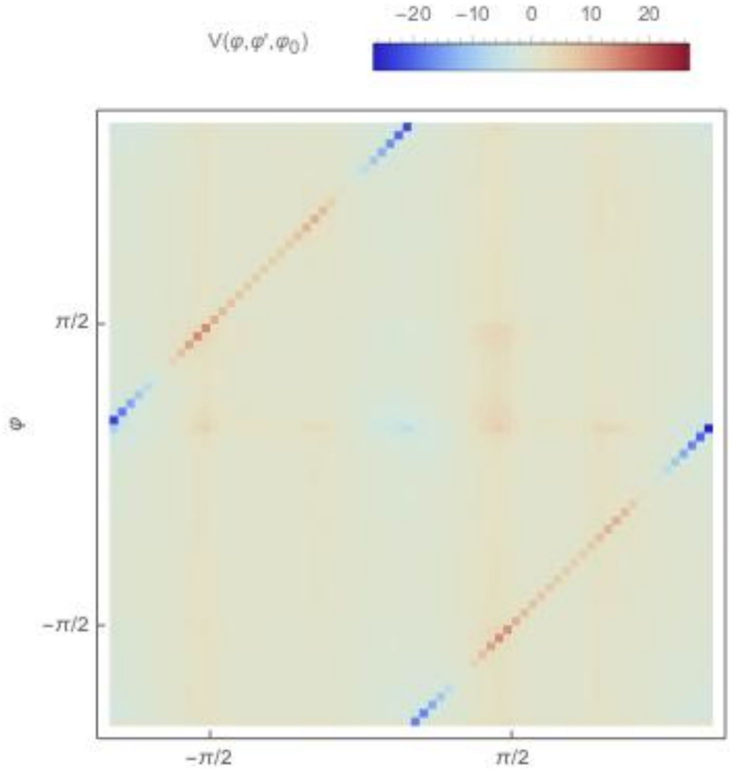

φ_1

φ_2

$$H_{\text{eff}} = \frac{1}{2} \sum_{\vec{p},\vec{p}',\vec{q},s,s'} V(\vec{p},\vec{p}',\vec{p}+\vec{q}) c^{\dagger}_{\vec{p}+\vec{q},s} c^{\dagger}_{\vec{p}'-\vec{q},s'} c_{\vec{p}',s'} c_{\vec{p},s}$$

Functional renormalization group for correlated electrons

- **example** for RG evolution of V^Λ

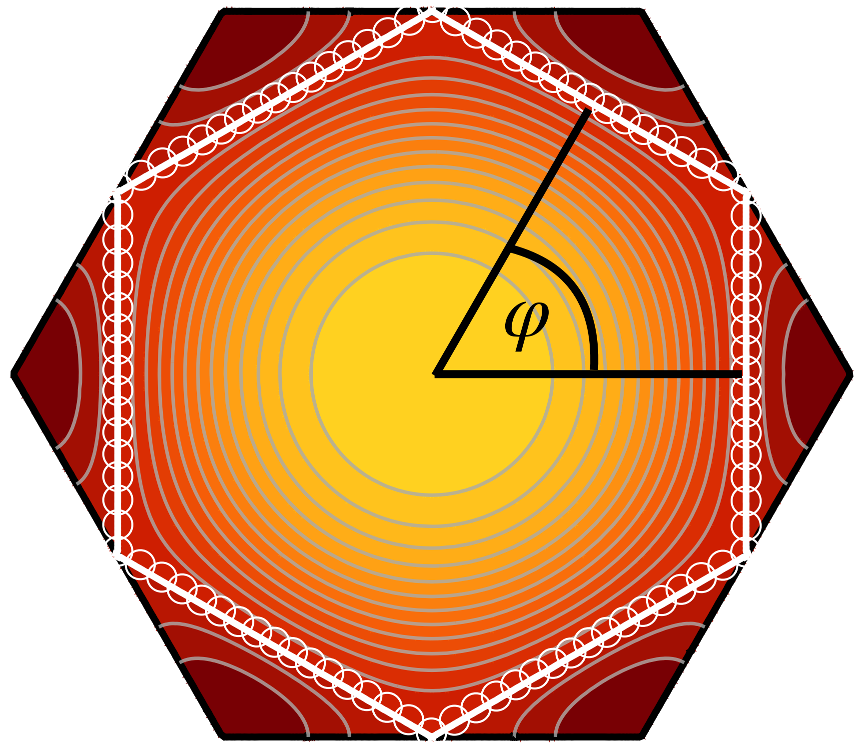

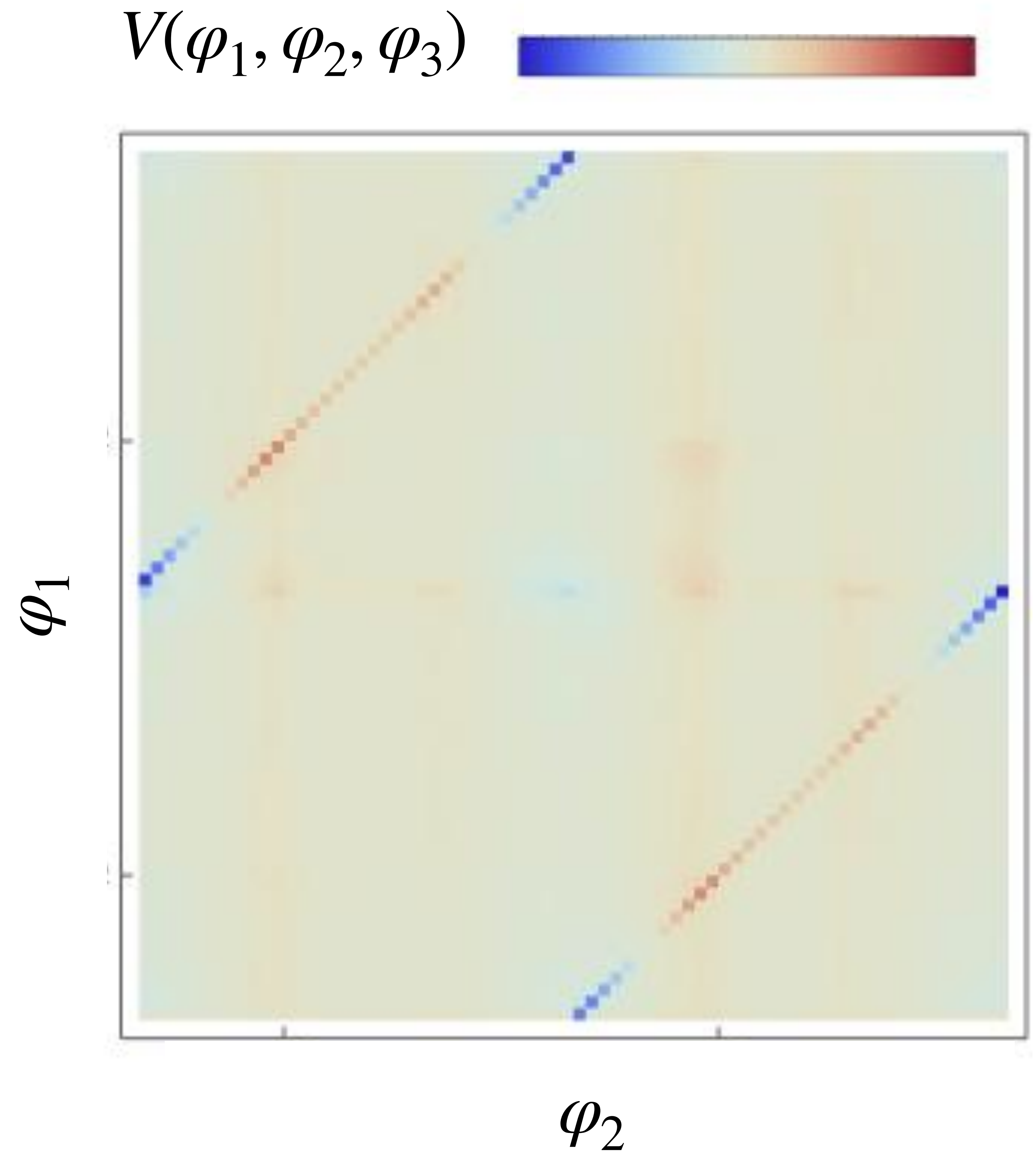

- sharp diagonal features
  - indicate large effective interaction for incoming momenta that lie on opposite sides of the Fermi surface!
  - pronounced pairing interaction with $\vec{k}$ and $-\vec{k}$
  - indicates superconducting instability
  - additional modulation on diagonal features: unconventional SC!

Outline

RUB

- *Chapter I:* From 2D moiré materials to frustrated superlattice Hubbard models
- *Chapter II:* Interaction effects in hexagonal superlattice Hubbard models
- *Chapter III:* Functional renormalization group
- *Chapter IV:* Functional renormalization group for moiré materials
- *Chapter V:* Further developments and outlook

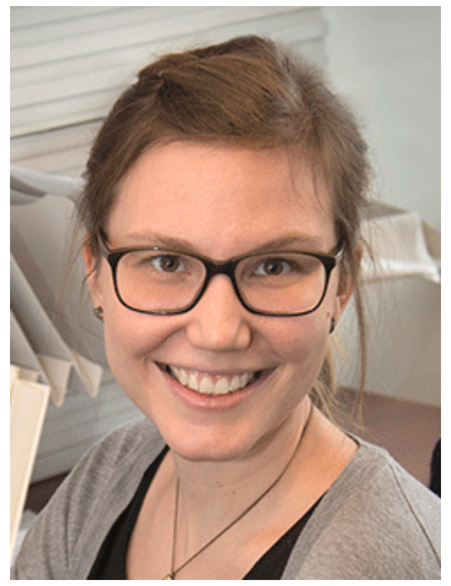

Laura Classen
MPI-FKF Stuttgart

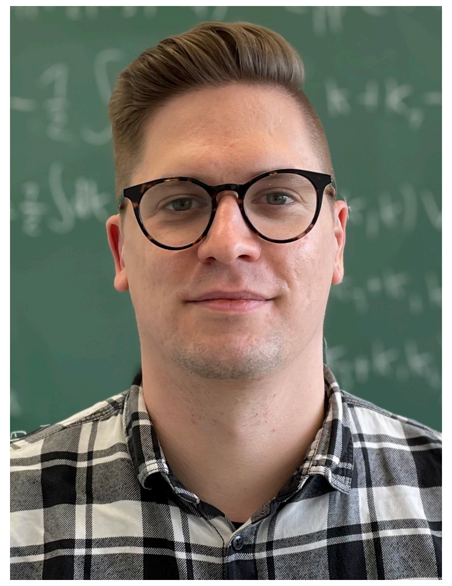

Nico Gneist
Uni Bochum

Dante M. Kennes
RWTH Aachen

Chapter IV: Functional renormalization group for moiré WSe_2/MoS_2

- Functional renormalization group for extended Hubbard model on the triangular lattice
- Functional RG instabilities for WSe2/MoS2 model
- Pairing symmetry and topological superconductivity

Scherer, Kennes, Classen, npj Quant. Mat. (2022)
Gneist, Classen, Scherer, PRB (2022)

Extended Hubbard model on triangular lattice for moiré WSe_2/MoS_2

RUB

$$H = \sum_{\nu=\pm} \sum_{\vec{R},\vec{R}'} t(\vec{R}' - \vec{R}) c^\dagger_{\vec{R},\nu} c_{\vec{R}',\nu} + \frac{1}{2} \sum_{\nu,\nu'} \sum_{\vec{R},\vec{R}'} U(\vec{R}' - \vec{R}) c^\dagger_{\vec{R}\nu} c^\dagger_{\vec{R}'\nu'} c_{\vec{R}'\nu'} c_{\vec{R}\nu}$$

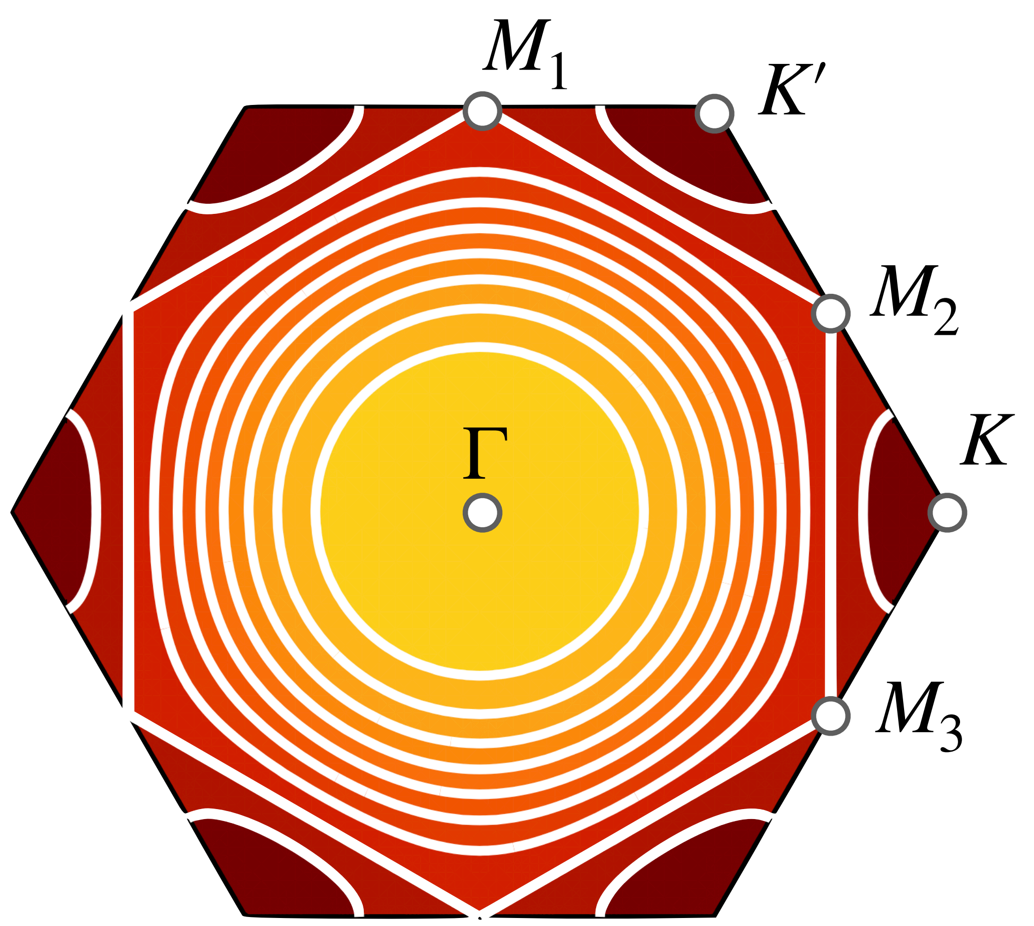

- full range of band fillings accessible by electrical gating
- van Hove singularities at 3/4 hole doping
- tunable strength & range of e⁻-e⁻ interactions → sizable non-local terms

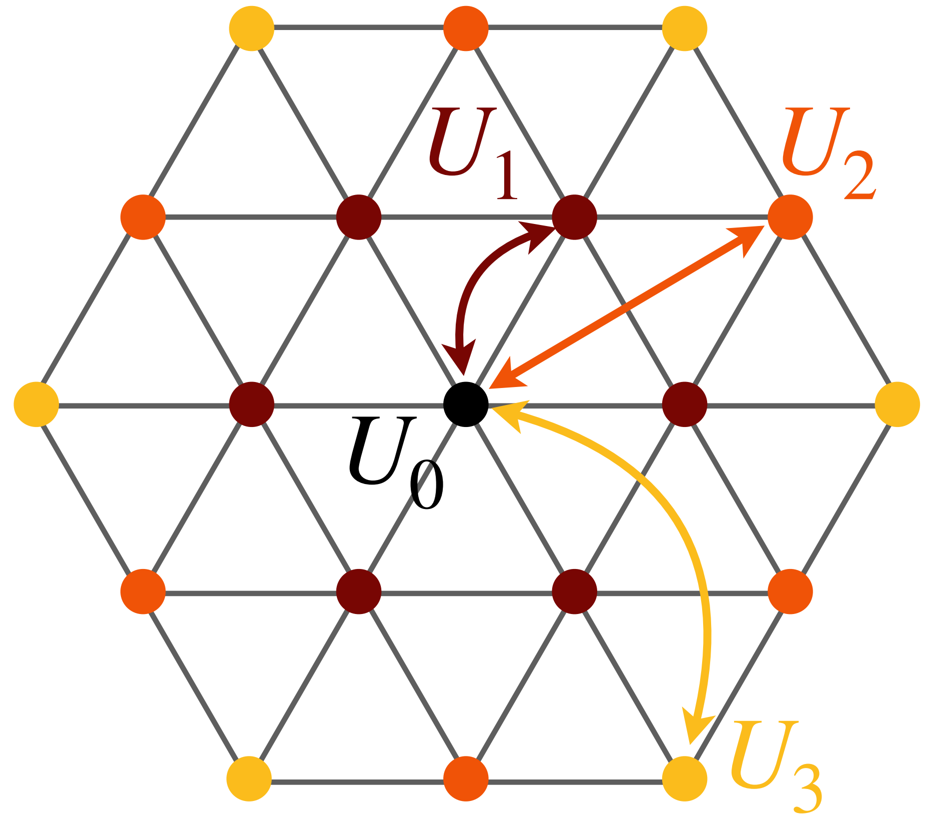

➡ complex interplay between electronic interactions and geometric frustration

➡ strongly-correlated phases (MIT, spin liquids, magnetism,… e.g. @ half filling)

Wietek *et al.*, PRX (2021)
Szasz *et al.*, PRX (2020)
Chen *et al.*, arxiv:2102.05560
Zhu & White, PRB (2015)
Hu, Gong, Zhu, Sheng, PRB (2015)
…

Van Hove filling in moiré WSe_2/MoS_2

- Extended Hubbard model on triangular lattice with accurate hoppings t_1, t_2, t_3

$$H = \sum_{v=\pm} \sum_{\vec{R},\vec{R}'} t(\vec{R}' - \vec{R}) c^{\dagger}_{\vec{R},v} c_{\vec{R}',v} + \frac{1}{2} \sum_{v,v'} \sum_{\vec{R},\vec{R}'} U(\vec{R}' - \vec{R}) c^{\dagger}_{\vec{R}v} c^{\dagger}_{\vec{R}'v'} c_{\vec{R}'v'} c_{\vec{R}v}$$

$$t_1 \approx -2.5\,\mathrm{meV}, \quad t_2 \approx 0.5\,\mathrm{meV}, \quad t_3 \approx 0.25\,\mathrm{meV}, \quad U/|t_1| = 3{,}4{,}5, \quad V_2/V_1 \approx 0.36, \quad V_3/V_1 \approx 0.26$$

- Consider Van Hove filling

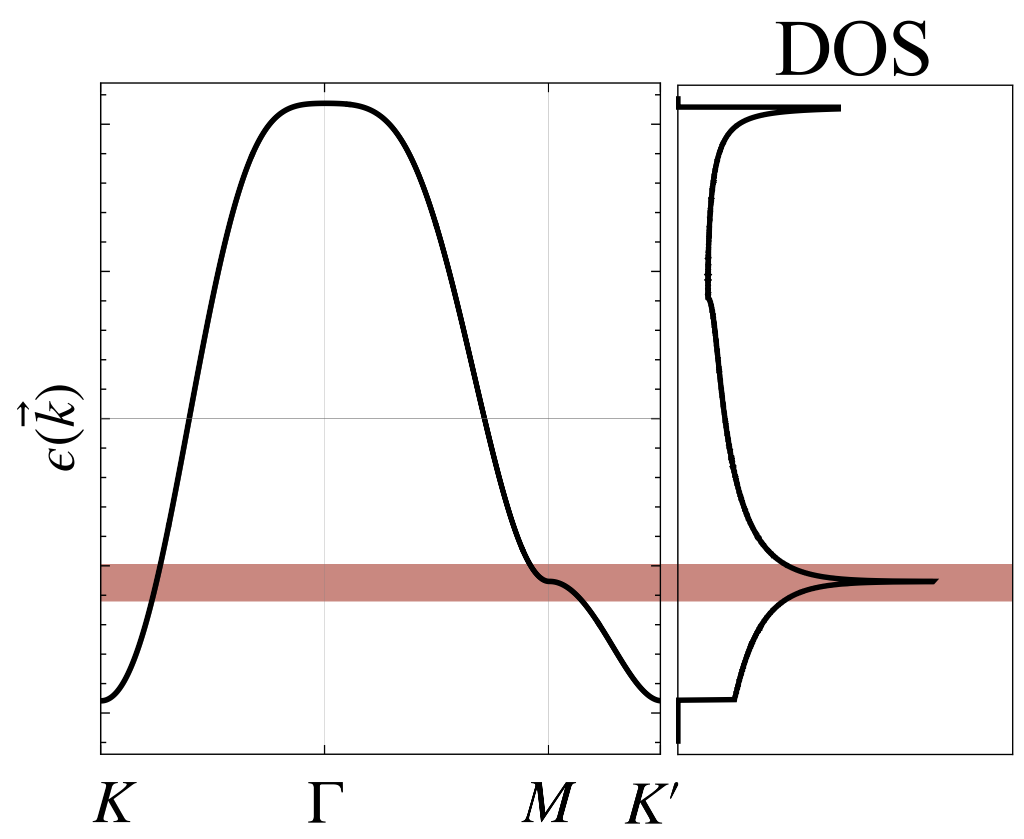

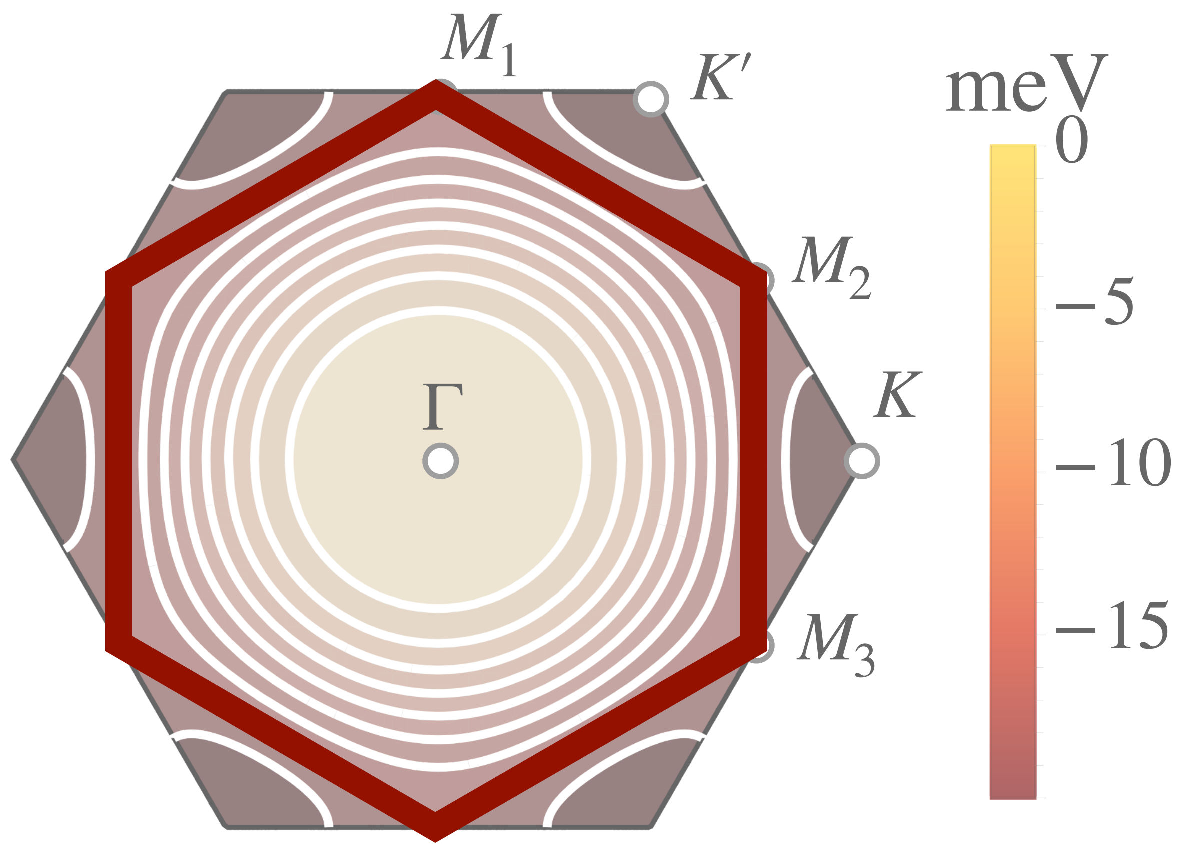

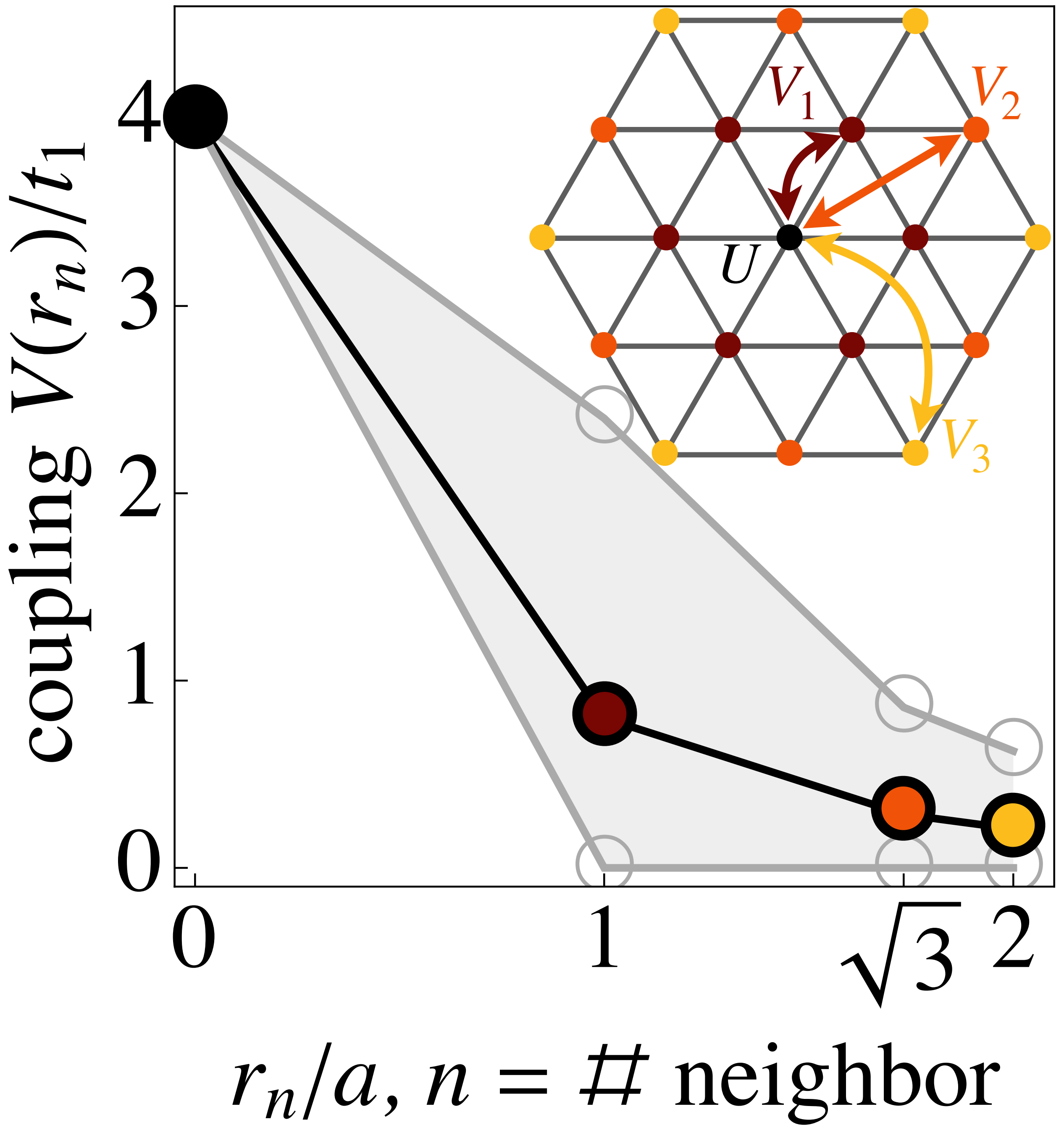

- Interactions up to V_3 sizable!

Wu, Lovorn, Tutuc, MacDonald, PRL (2018)

- What is their effect on Van Hove scenario & in particular superconductivity?

FRG phase diagram for moiré TMDs — *overview*

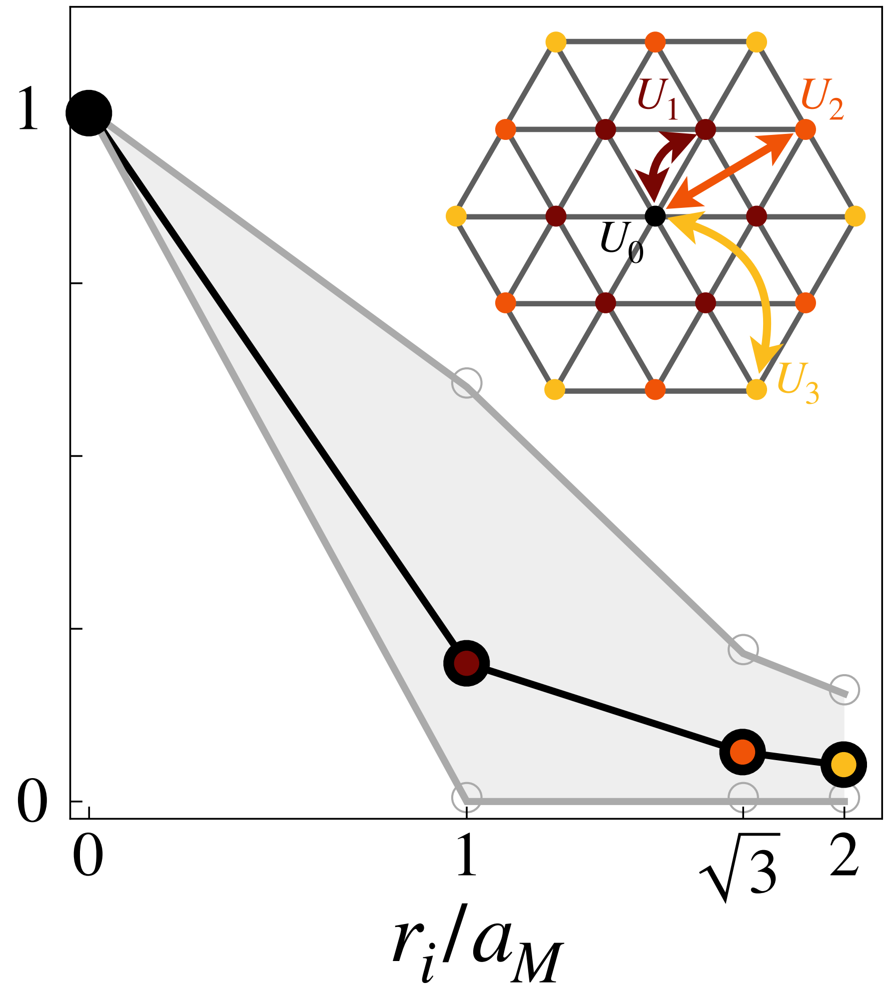

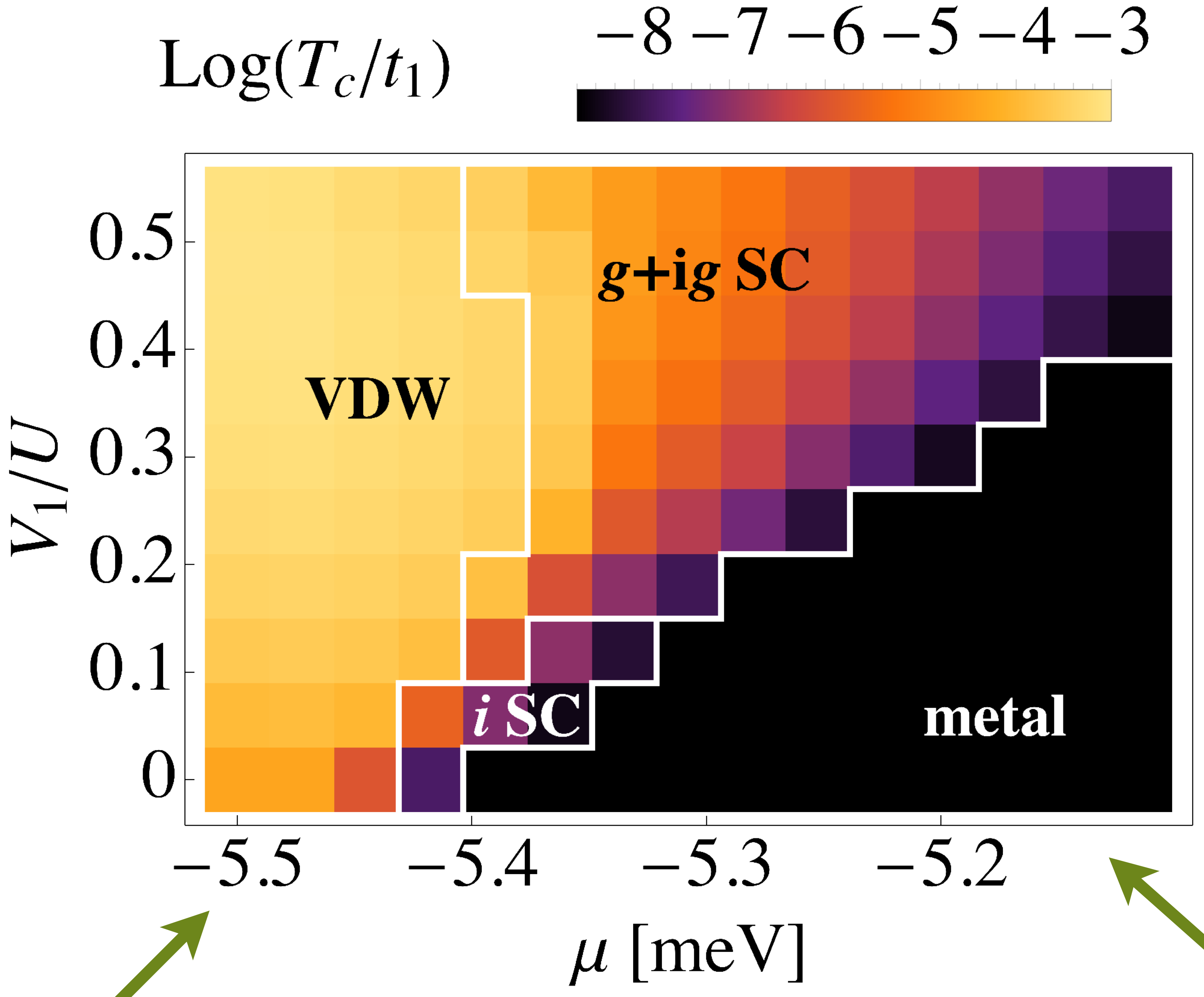

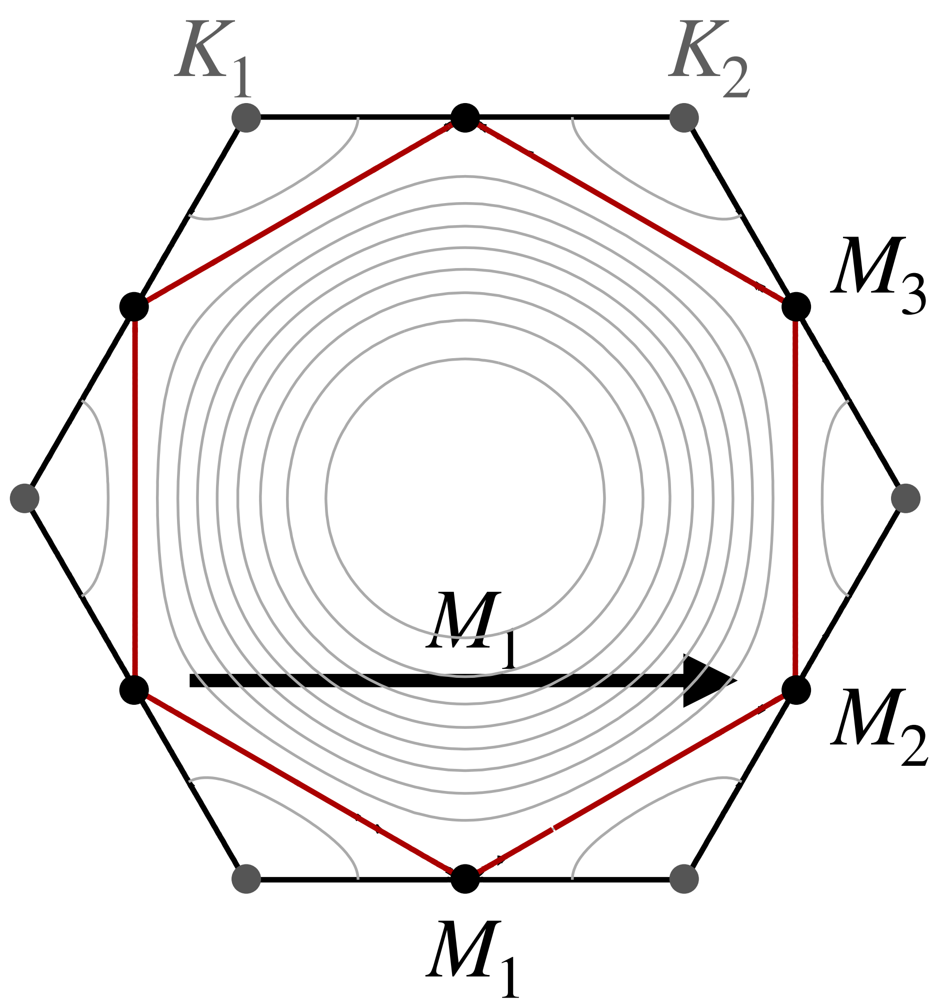

Van-Hove filling

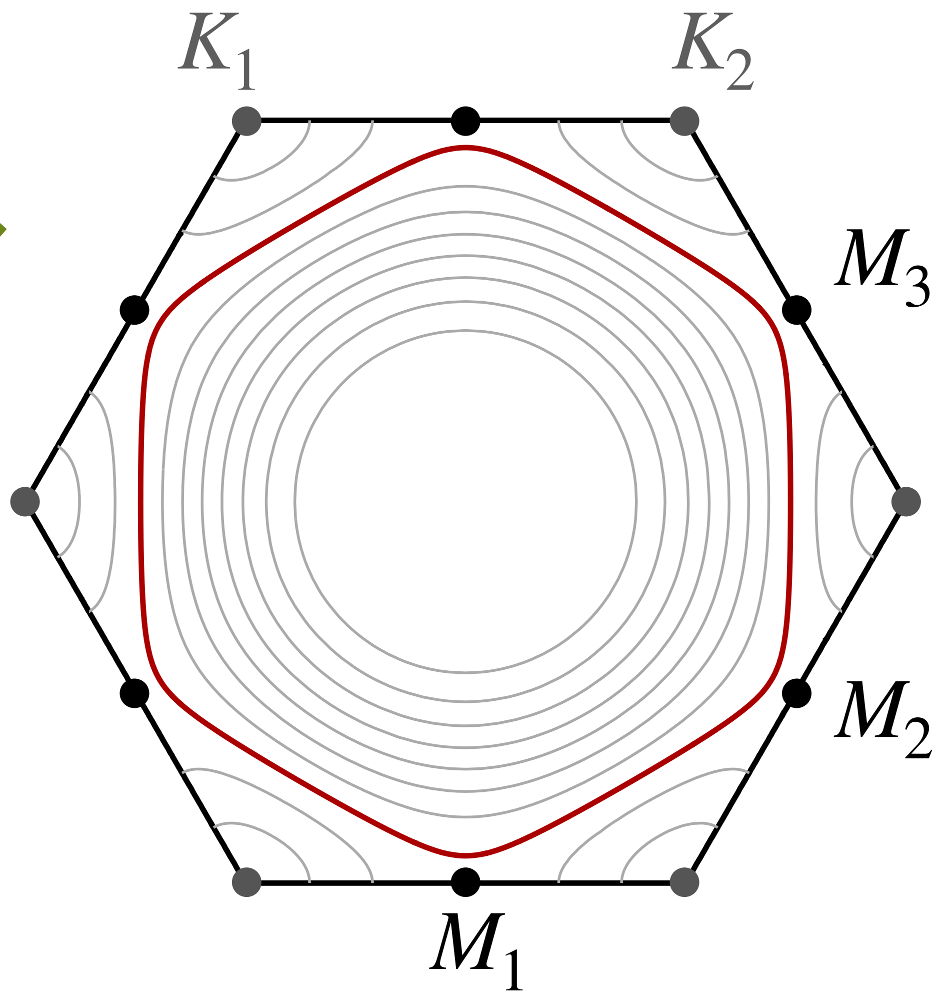

FRG phase diagram for moiré TMDs — *only onsite U*

RUB

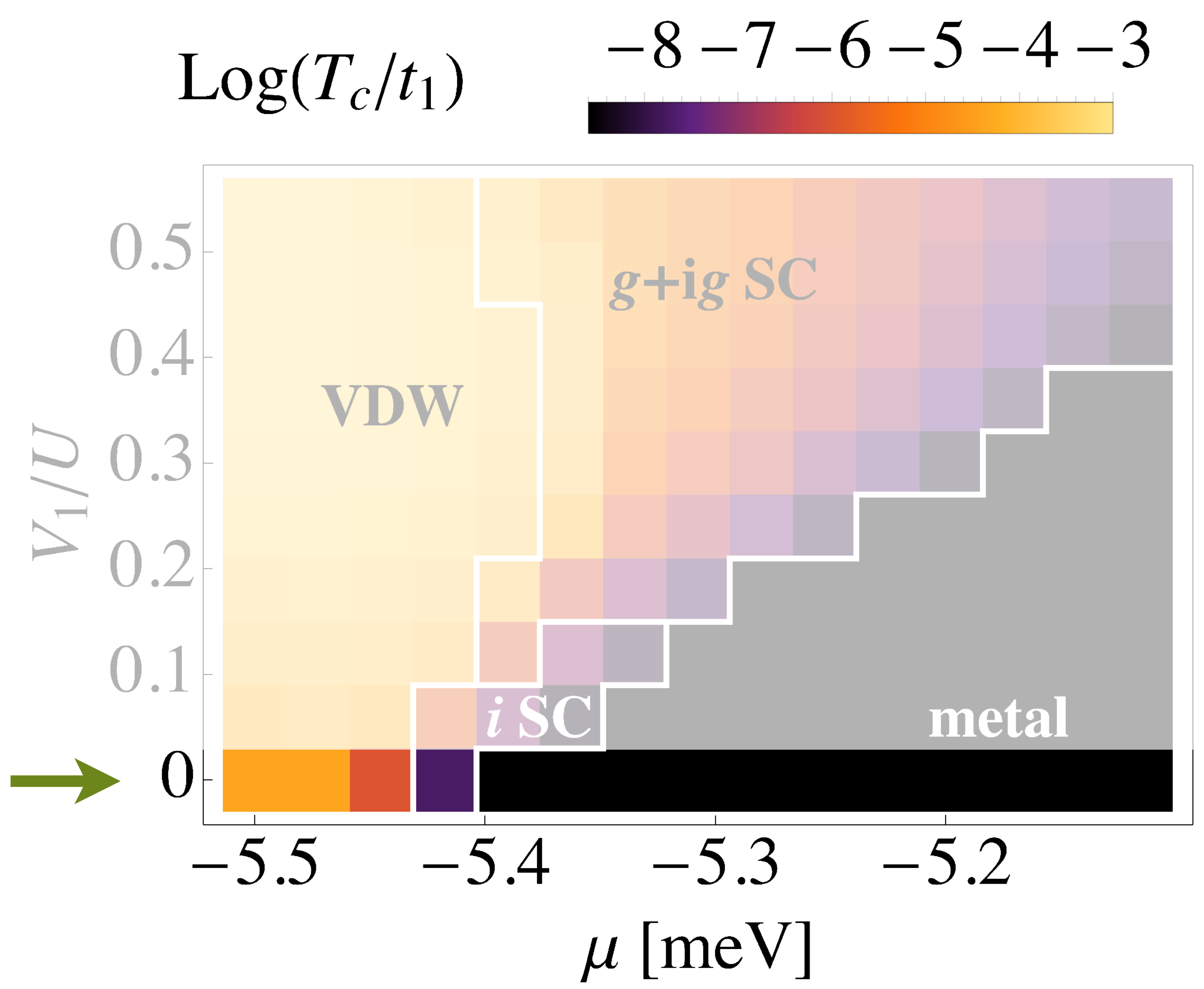

- at Van-Hove filling → peaks at nesting momenta
  - valley density wave: $H_{VDW} = V_{VDW} \sum_i \vec{T}_{M_i} \cdot \vec{T}_{-M_i}$ with $\vec{T}_q = \sum_k c^\dagger_{k\alpha} \vec{\tau}_{\alpha\beta} c_{k+M\beta}$ (analogue of SDW)
- in vicinity: **fragile** *i*-wave pairing

FRG phase diagram for moiré TMDs — *inclusion of V_1, V_2, V_3*

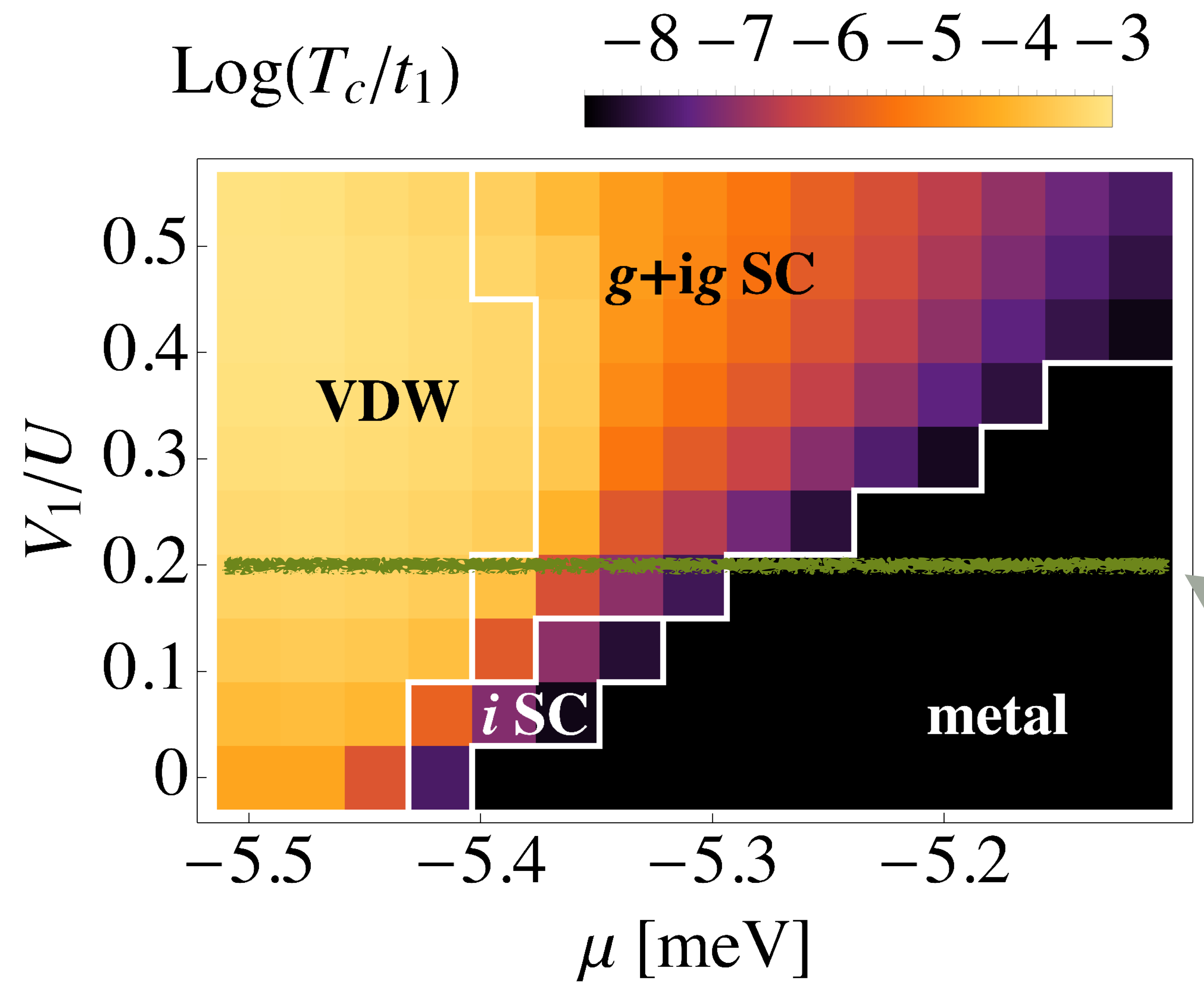

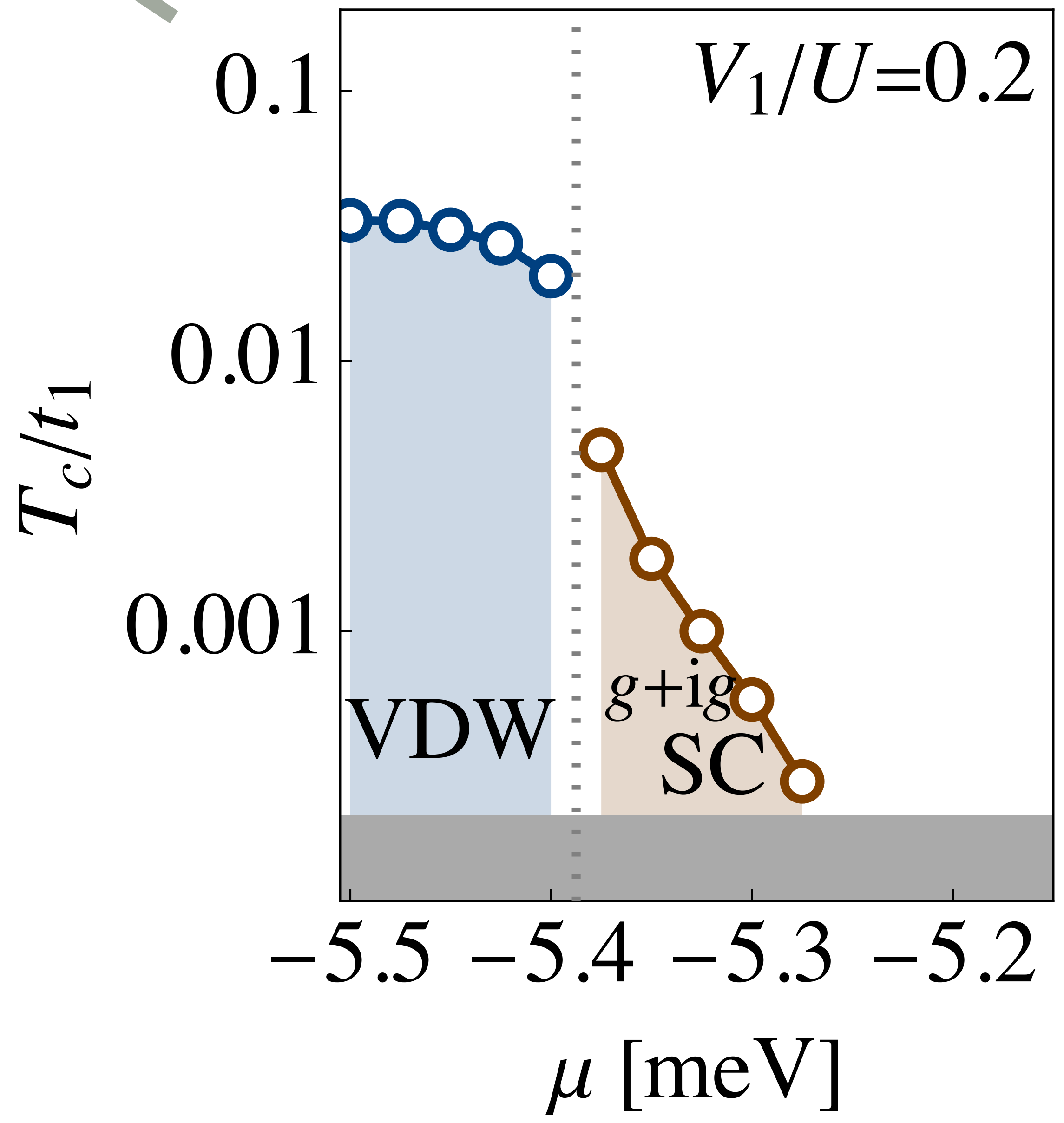

- no strong effect on VDW
- change of pairing symmetry: **robust** *g*+*ig* regime
- fluctuations of VDW mediate attraction in **singlet pairing** channel

FRG phase diagram for moiré TMDs — *inclusion of V_1, V_2, V_3*

RUB

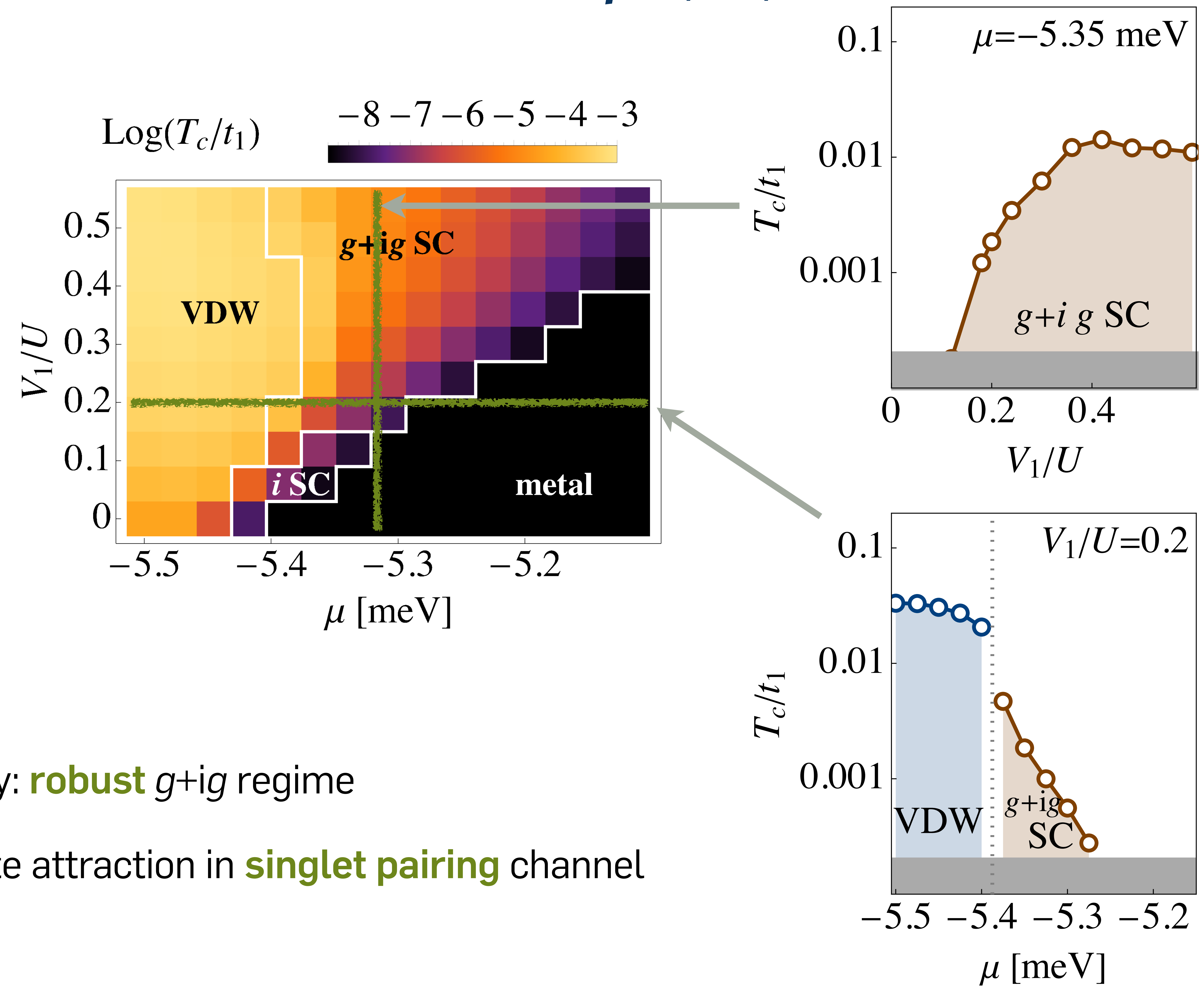

- no strong effect on VDW
- change of pairing symmetry: **robust** *g*+*ig* regime
- fluctuations of VDW mediate attraction in **singlet pairing** channel
- *g*-wave supported by V_i

Pairing symmetry

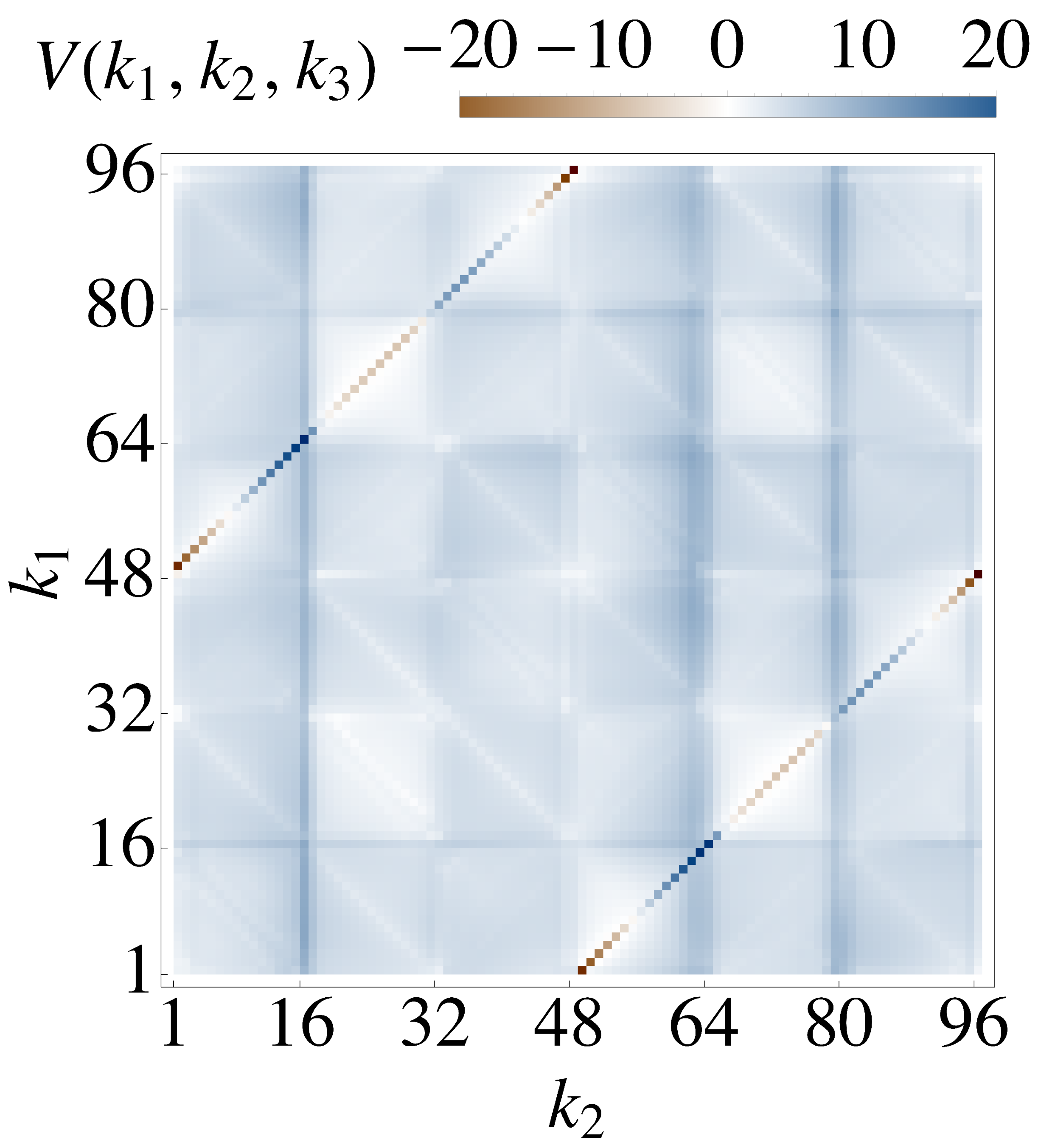

- generalized BCS theory:
  - determine eigensystem of pairing i.a. $V(\vec{k}, -\vec{k}, \vec{k}', -\vec{k}')$
  - largest T_c from largest eigenvalue $T_c \sim \exp(-\sqrt{W/\lambda\hat{\rho}_0})$
- extract pairing symmetry → fit lattice harmonics to eigenfunctions

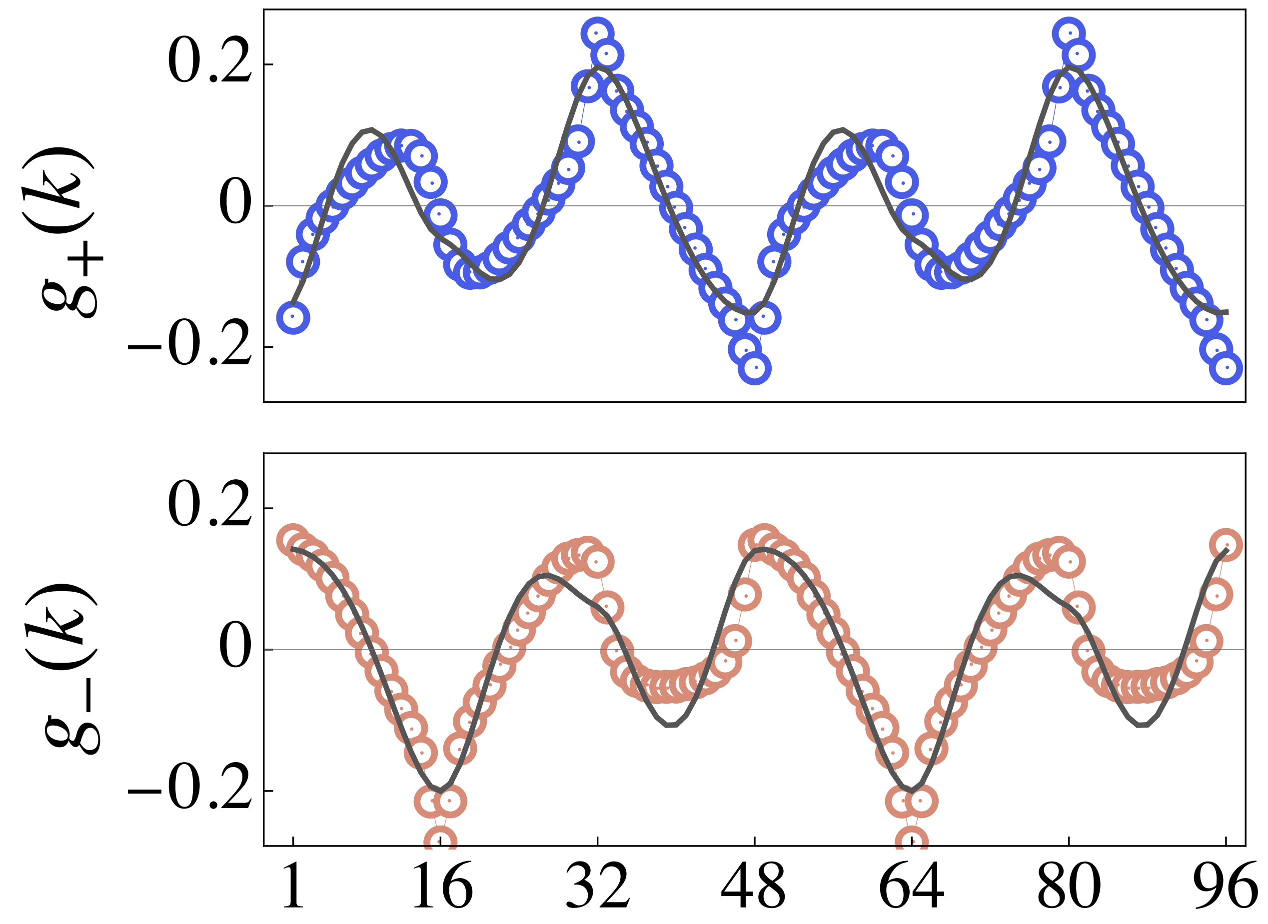

- *here:* largest eigenvalue **2-fold degenerate**
- fitted well by 2nd-nearest-neighbor lattice harmonics

$$g_1(\vec{k}) = 8/9[-\cos(3k_x/2)\cos(\sqrt{3}k_y/2) + \cos(\sqrt{3}k_y)]$$
$$g_2(\vec{k}) = 8/(3\sqrt{3})\sin(3k_x/2)\sin(\sqrt{3}k_y/2)$$

Pairing symmetry

- symmetry classified with irreducible representations of point group C_{6v}
- within irrep → lattice harmonics with different angular momentum can mix

C_{6v}	A1	A2	B1	B2	E1	E2
"orbital"	*s*-wave	*i*-wave	*f*-wave	*f*-wave	*p*-wave	*d*-wave *g*-wave

encode behavior under sym ops

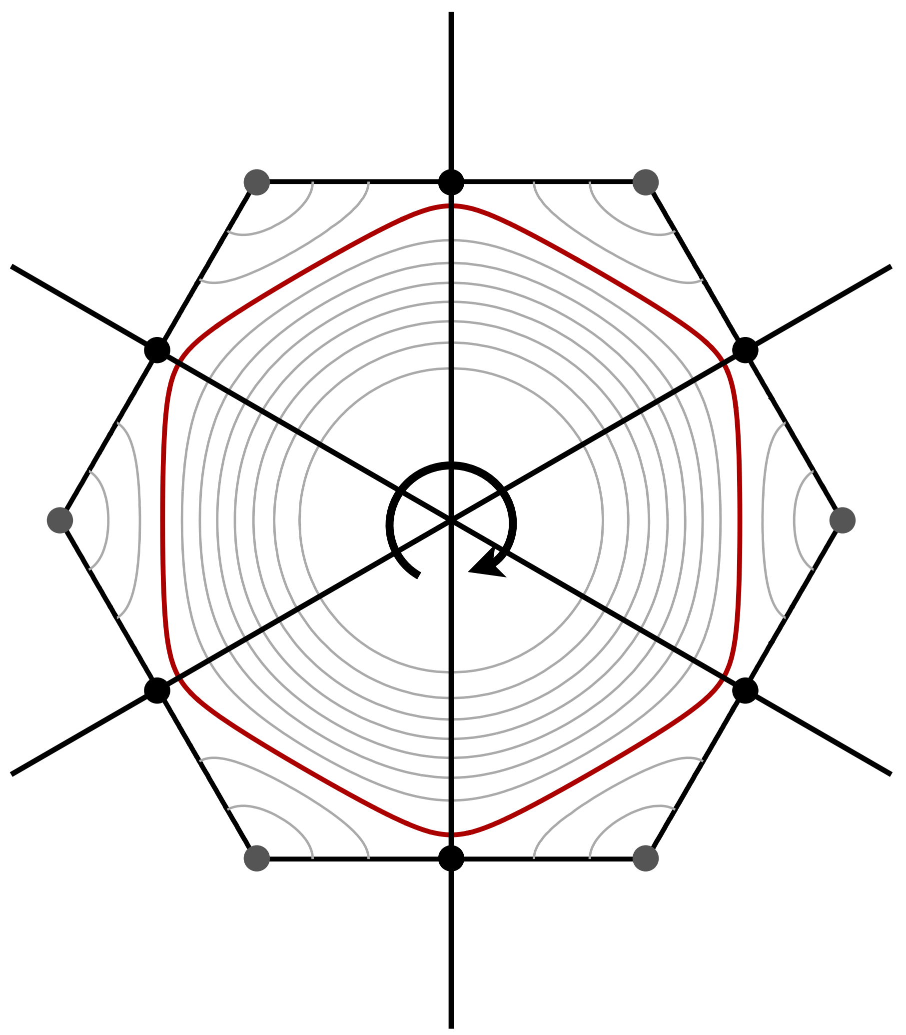

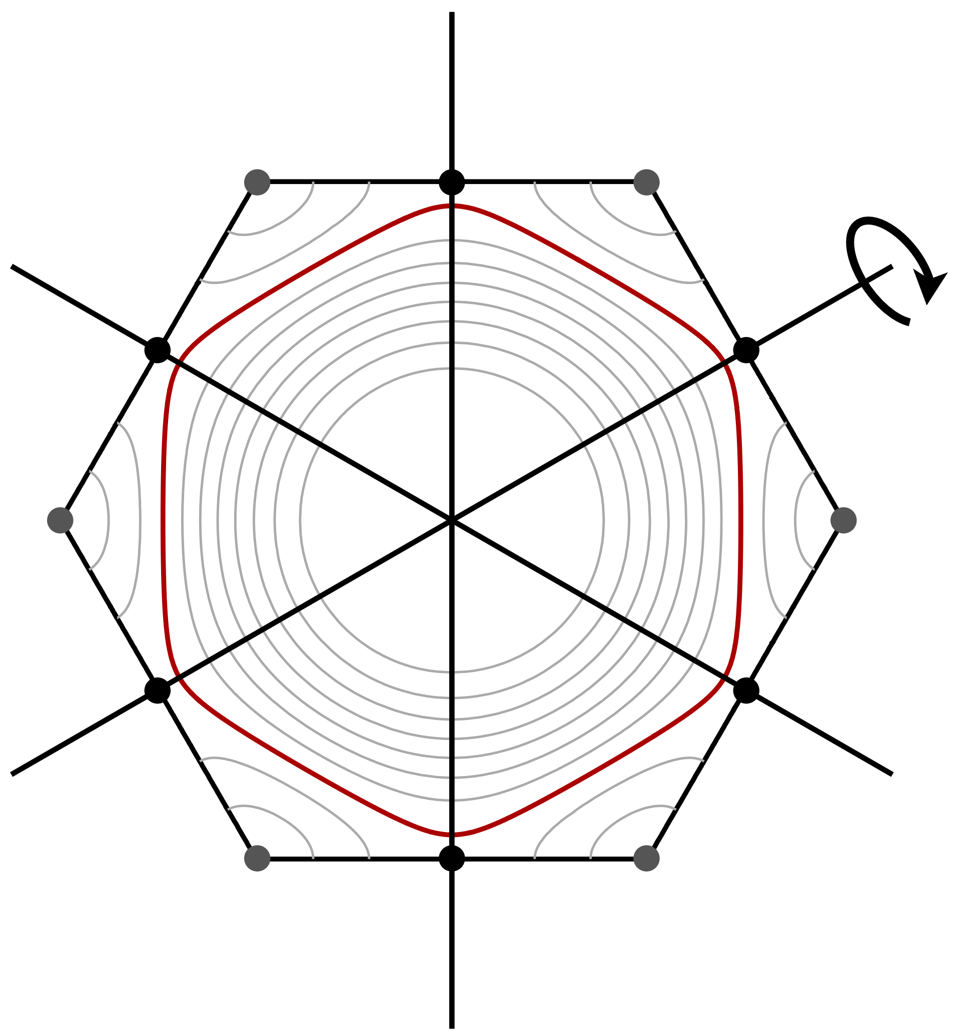

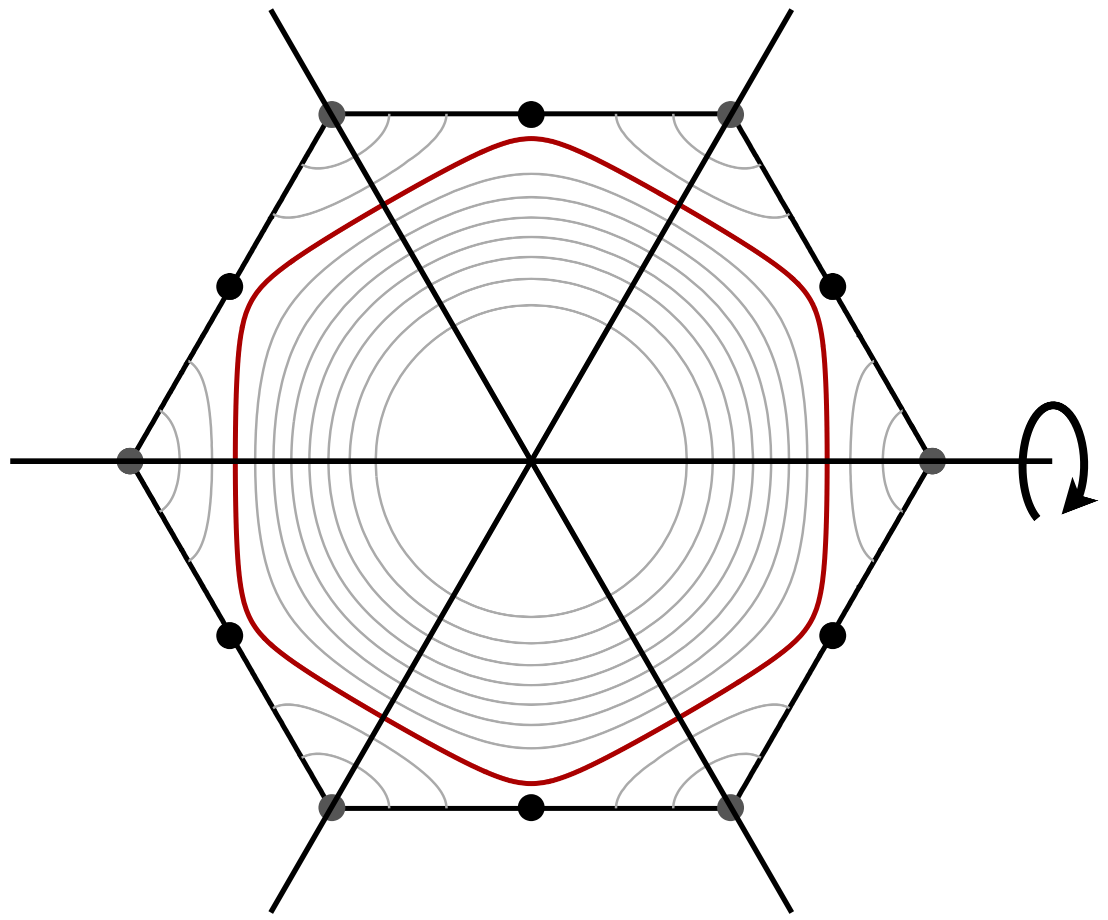

Pairing symmetry

- 2^{nd}-nn harmonics g_1, g_2 belong to 2D irrep E_2
- same symmetry properties under C_{6v} as 1^{st}-nn E_2 harmonics
- why 2^{nd} nn (and not 1^{st})?
  - overcome longer-ranged repulsion V_i
  - pairing pushed outwards

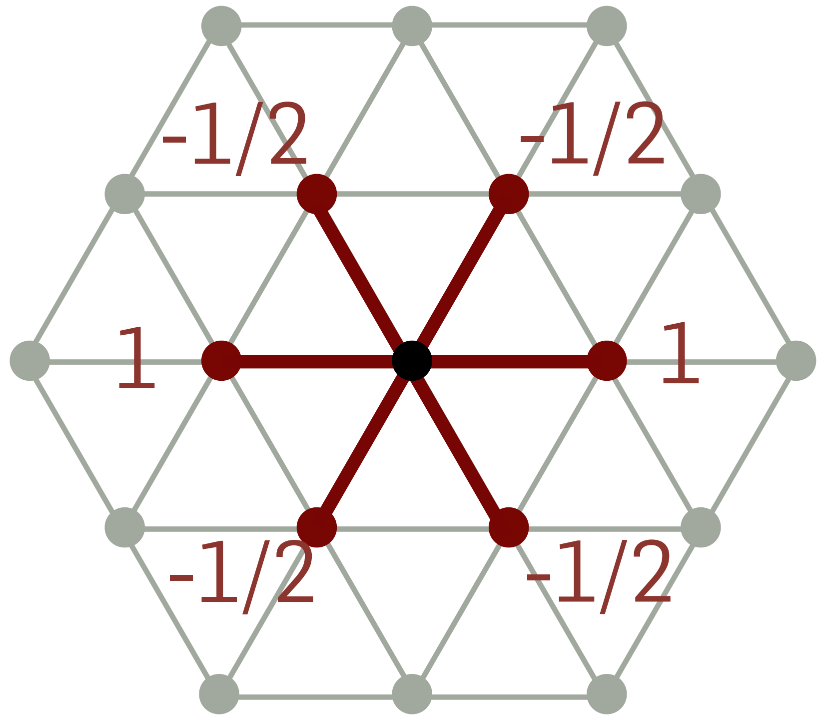

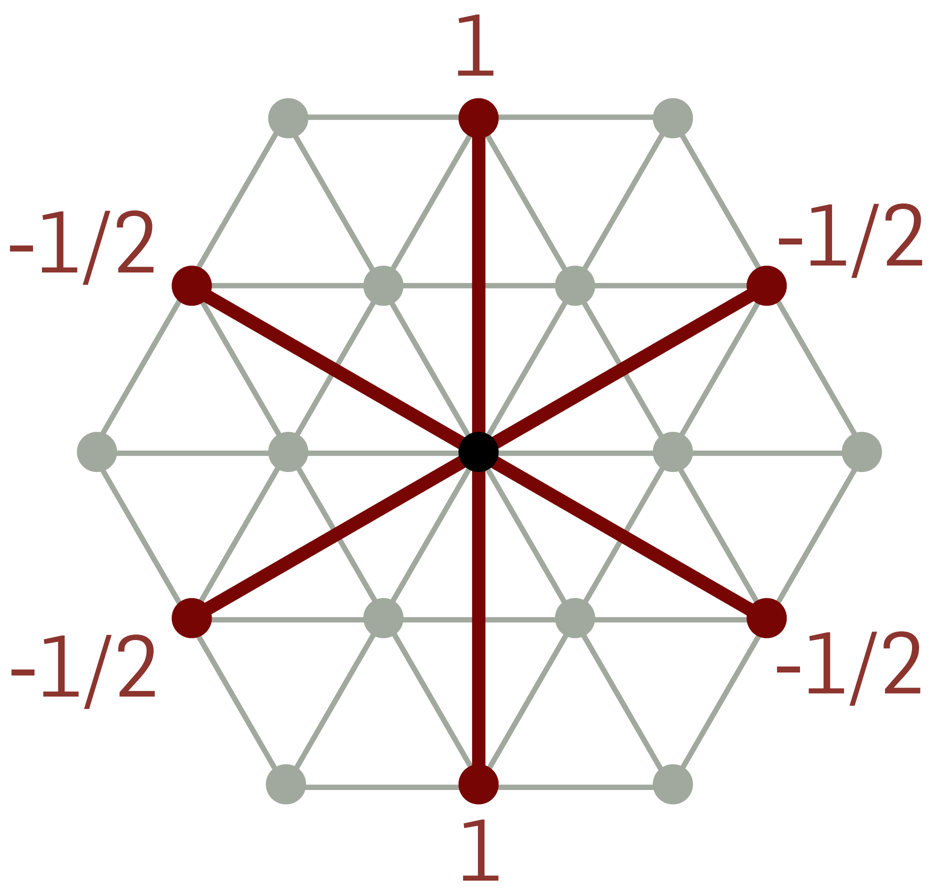

A_1	$x^2 + y^2$	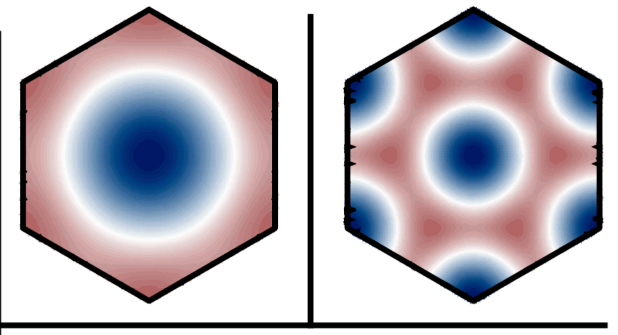
A_2	$xy(x^2 - 3y^2)(y^2 - 3x^2)$	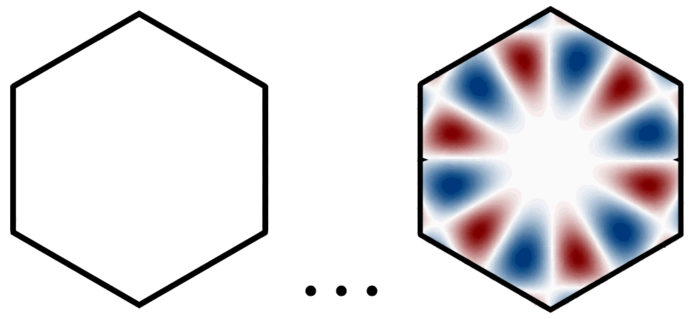 …
B_1	$x(x^2 - 3y^2)$	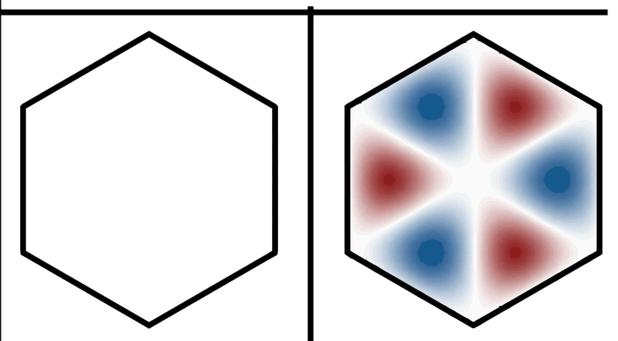
B_2	$y(y^2 - 3x^2)$	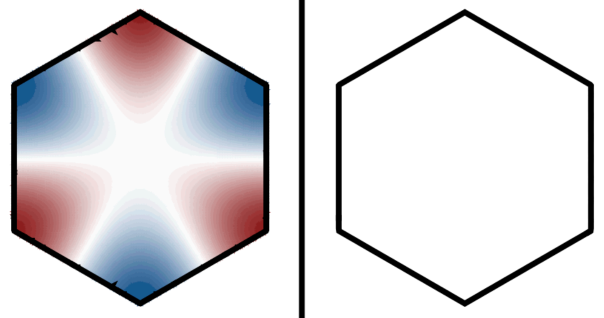
E_1	x	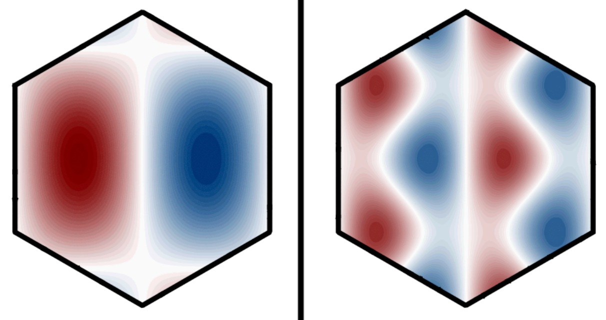
	y	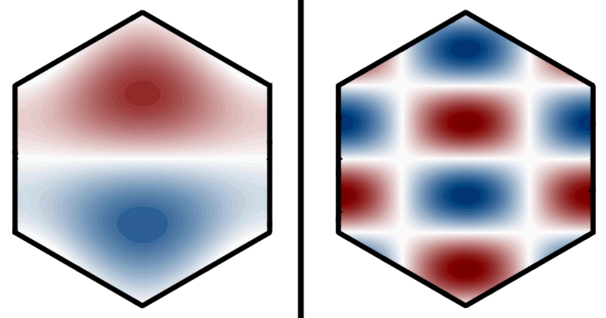
E_2	$x^2 - y^2$	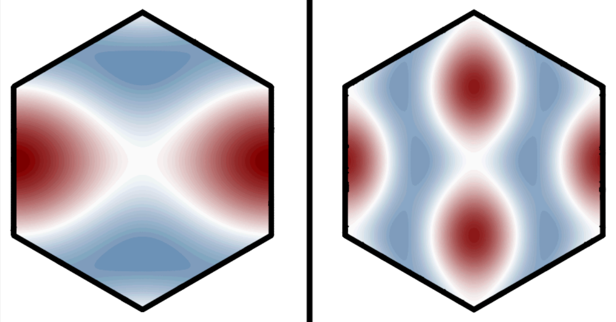
	xy	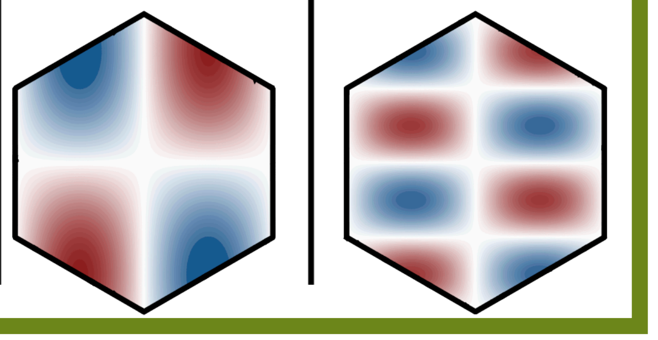

Pairing symmetry

- can we distinguish d_1, d_2 vs g_1, g_2 if symmetries are the same?
- number of nodes different!

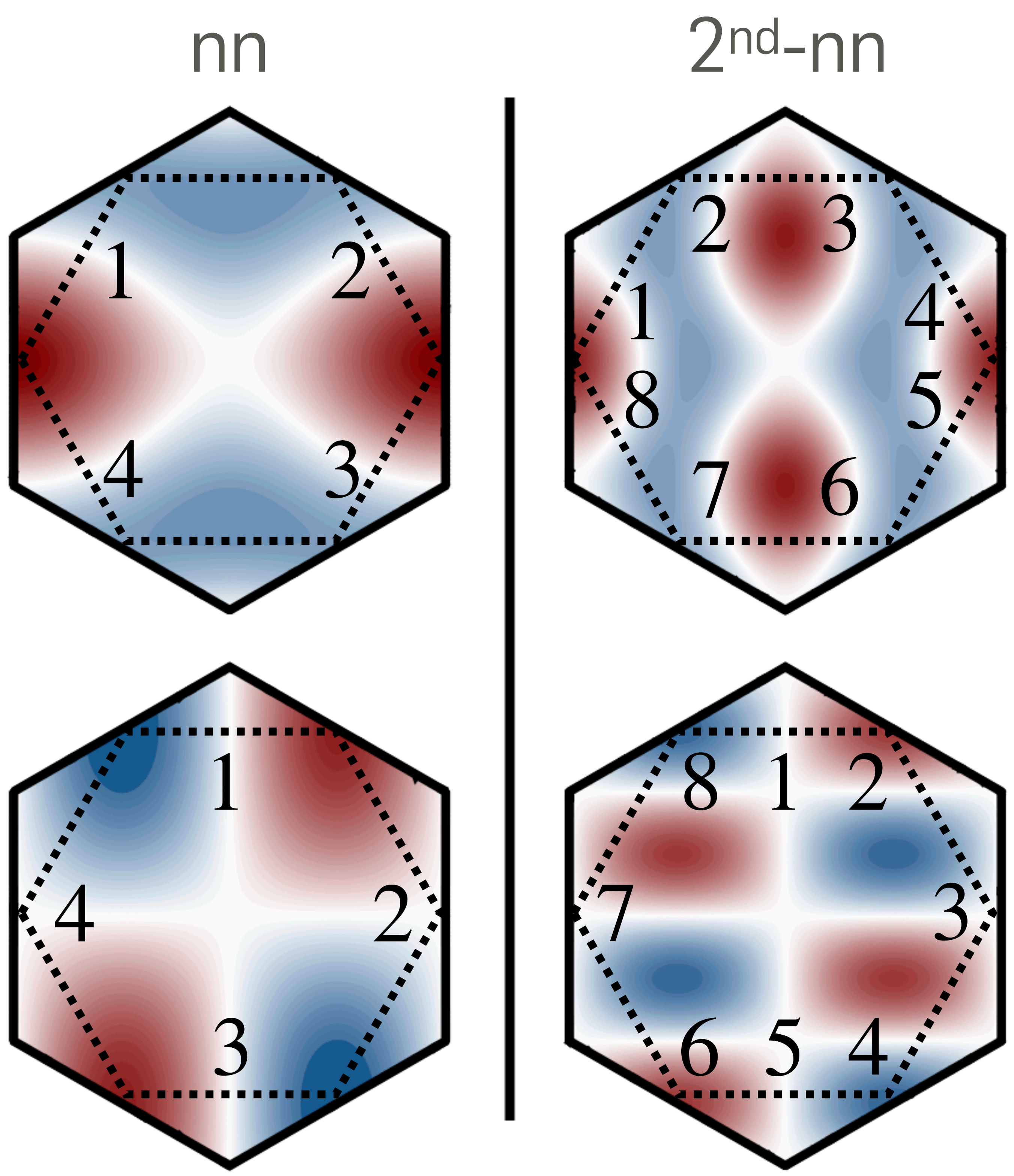

- effect on properties of superconducting phase?

FRG post-processing: superconducting gap Δ

RUB

- 2 degenerate pairing solutions $\rightarrow$ $\Delta(\vec{k}) = \Delta_1\, g_1(\vec{k}) + \Delta_2\, g_2(\vec{k})$
  - ground state is generally a linear combination
  - minimize Landau functional

$$\mathscr{L} = \alpha(|\Delta_1|^2 + |\Delta_2|^2) + \beta(|\Delta_1|^2 + |\Delta_2|^2)^2 + \gamma|\Delta_1^2 + \Delta_2^2|^2$$

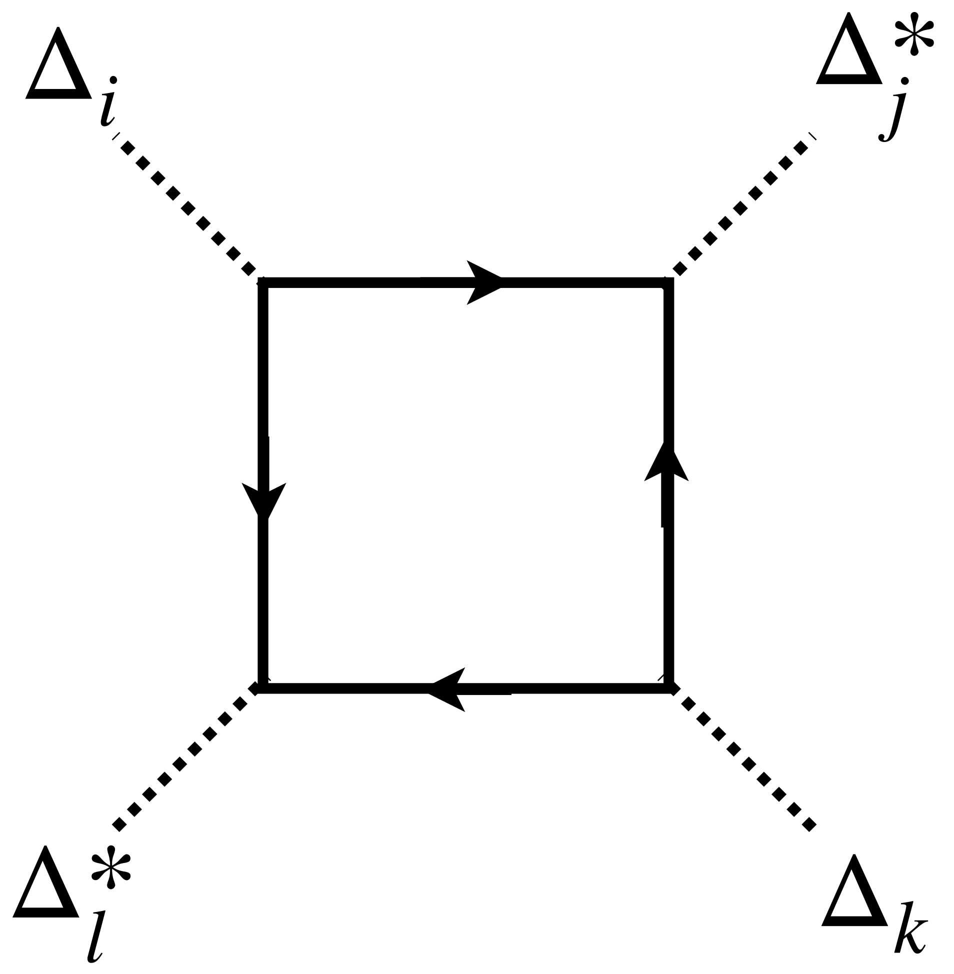

  - get α, β, γ by integrating out fermions with FRG data

$$\Rightarrow \gamma > 0$$

$$\Rightarrow \ \Delta_2 = \pm\, i\Delta_1 \text{ minimizes } \mathscr{L}$$

$$\Rightarrow \Delta(\vec{k}) = \hat{\Delta}\,[g_1(\vec{k}) \pm i g_2(\vec{k})]$$

  - $|\Delta(\vec{k})|$ has no nodes
  - $\arg\Delta(\vec{k})$ winds 4 times around FS

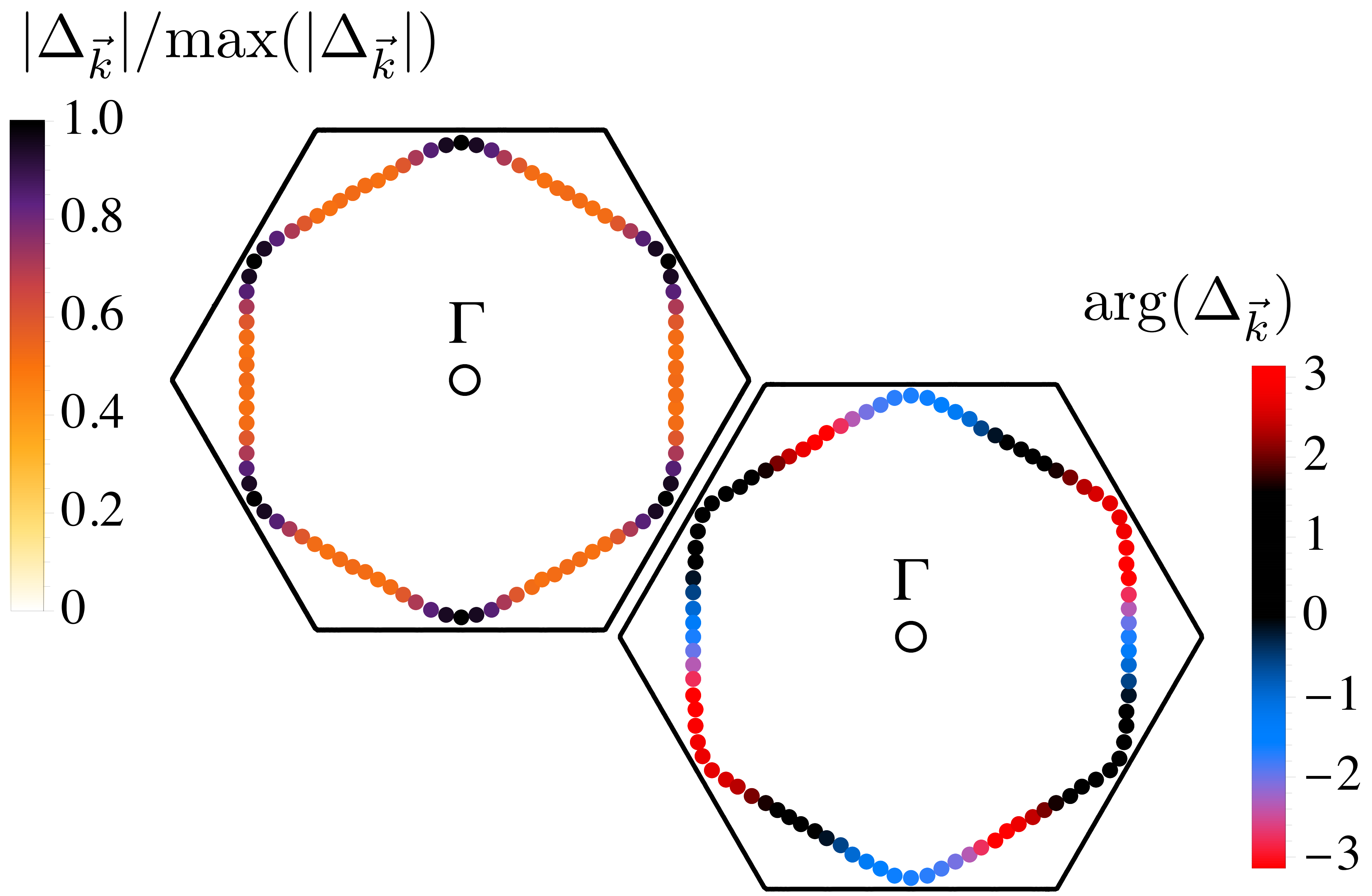

Properties of *g+ig* superconductivity

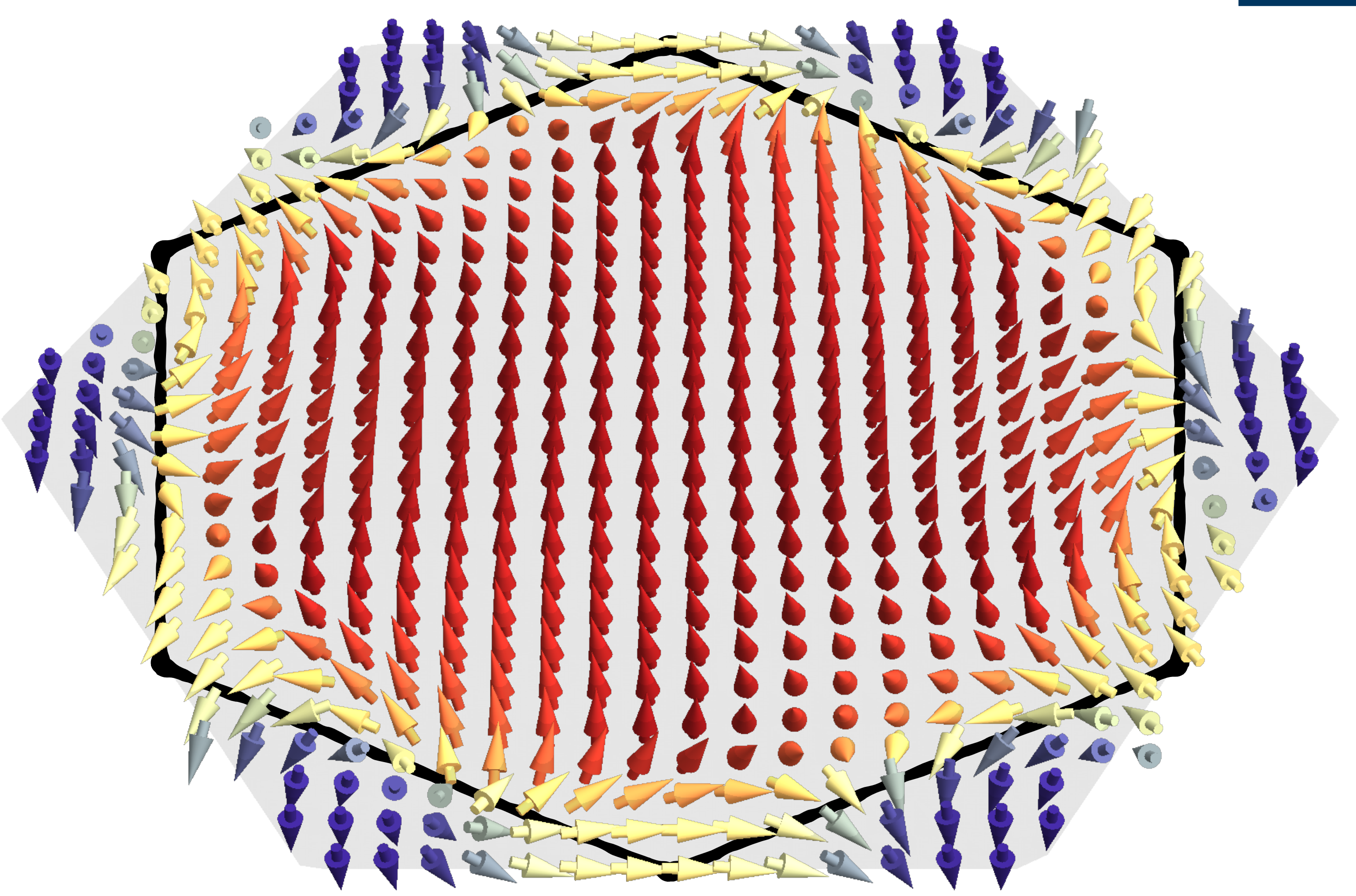

- spontaneous breaking of TRS: $g_1 + ig_2$ vs. $g_1 - ig_2$
  - define "pseudo-spin" $$\vec{m} = \frac{1}{\sqrt{(\epsilon_{\vec{k}} - \mu)^2 + \Delta_{\vec{k}}^2}} \begin{pmatrix} \mathrm{Re}\Delta_{\vec{k}} \\ \mathrm{Im}\Delta_{\vec{k}} \\ \epsilon_{\vec{k}} - \mu \end{pmatrix}$$
  - topological invariant → winding number $$\mathcal{N} = \frac{1}{4\pi} \int_{\mathrm{BZ}} d^2k \, \vec{m} \cdot \left(\frac{\partial \vec{m}}{\partial k_x} \times \frac{\partial \vec{m}}{\partial k_y} \right)$$
  - *g+ig*: $\mathcal{N} = \pm 4$
  - *d+id*: $\mathcal{N} = \pm 2$

  } same symmetries under C_{6v} but **different topological states**!
- $\mathcal{N}$ chiral edge modes → **enhanced quantized Hall responses!**
  - spin Hall conductance $\sigma_{xy}^s = \mathcal{N} \hbar / (8\pi)$
  - thermal Hall conductance $\kappa = \mathcal{N} \pi k_B^2 / (6\hbar)$

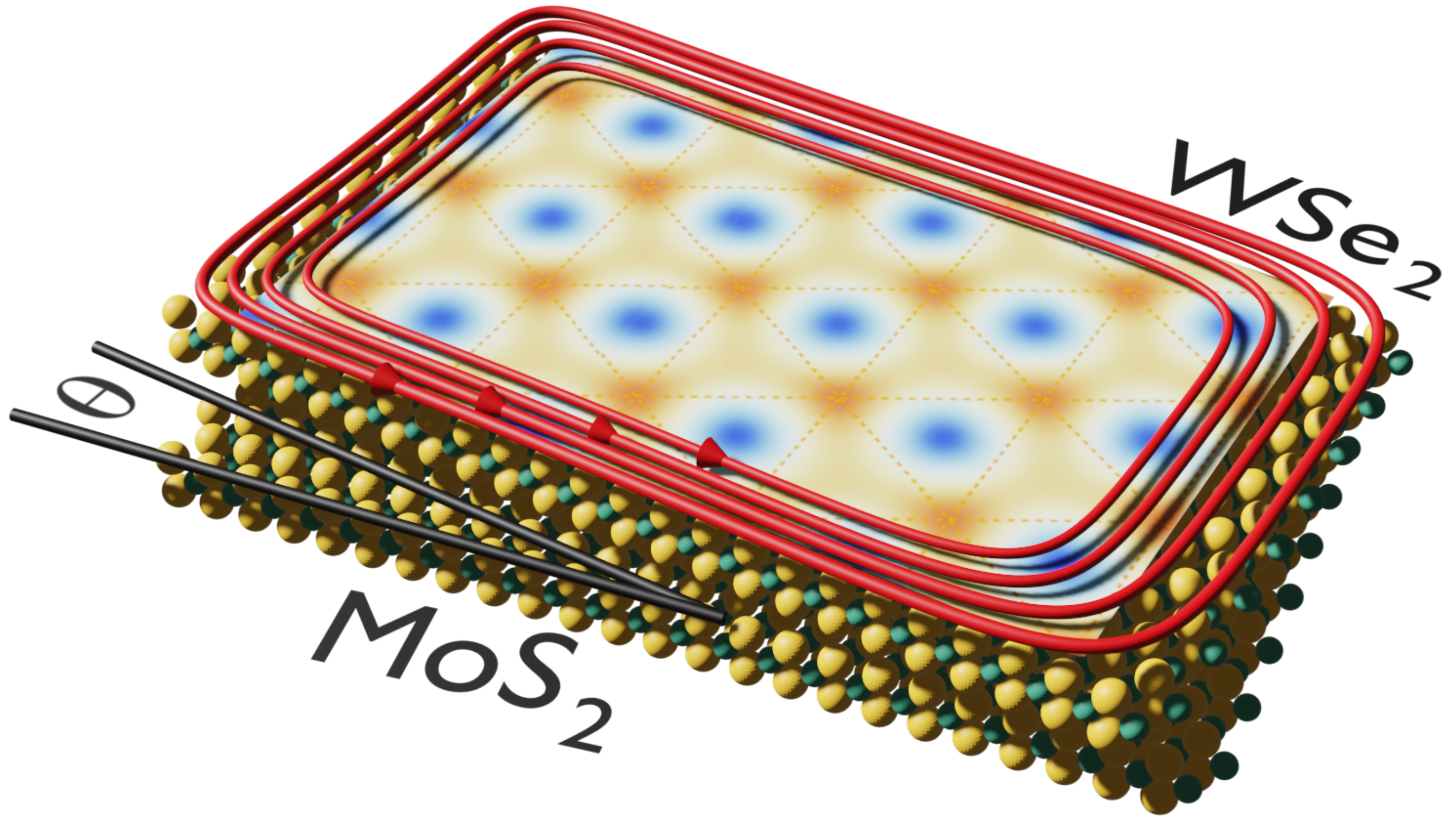

Robustness of *g+ig* state

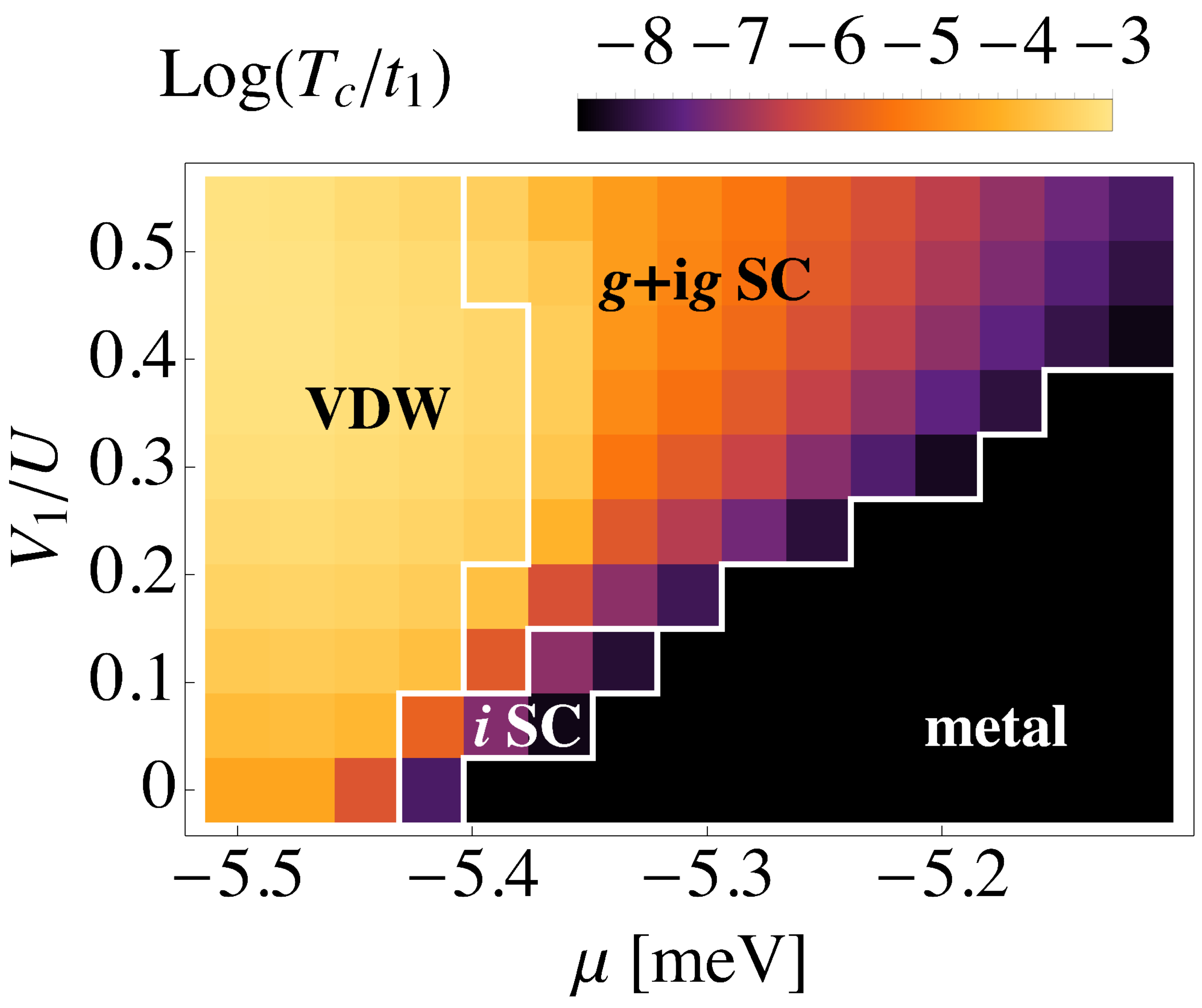

- *g+ig* SC occupies **extended region in phase diagram**
  - checked for $U/t = 3,4,5$ ✓

- model stronger coupling → include superexchange $J \sum_{\langle i,j \rangle} \vec{S}_i \cdot \vec{S}_j$
  - **g+ig dominant for small J/U**
  - for intermediate J/U *d+id*-wave contributes
  - topological transition when attraction from J overcomes repulsion V_i

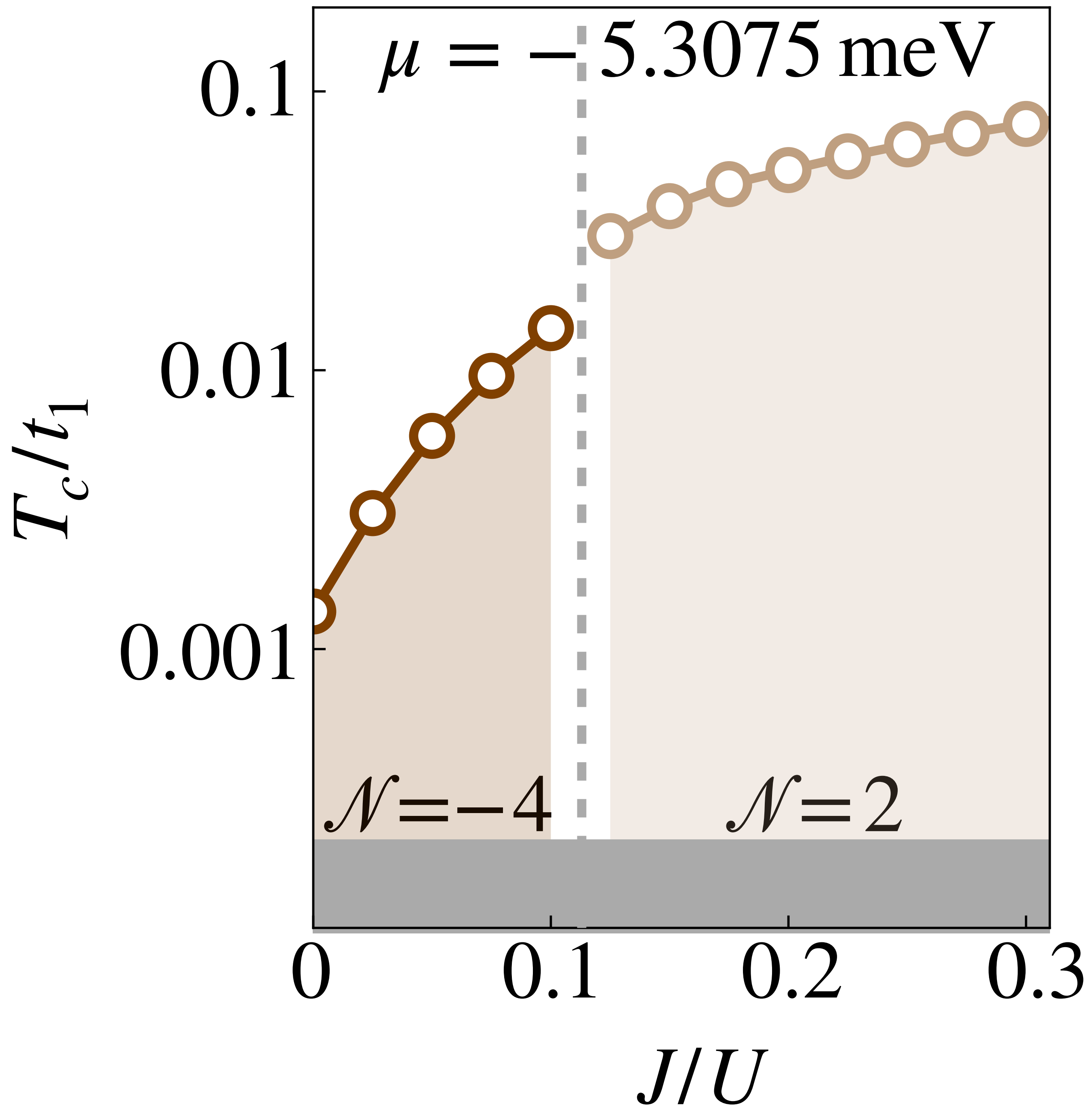

Outline

- *Chapter I:* From 2D moiré materials to frustrated superlattice Hubbard models
- *Chapter II:* Interaction effects in hexagonal superlattice Hubbard models
- *Chapter III:* Functional renormalization group
- *Chapter IV:* Functional renormalization group for moiré materials
- *Chapter V:* Further developments and outlook

Chapter V: Further developments and outlook

- Improvement of the FRG method
- Applications to related (moiré) materials

Gneist, Classen, Scherer, PRB (2022)

Klebl *et al.*, arxiv:2204.00648 (2021)

High-momentum resolution with truncated-unity FRG

- channel decomposition $V^{\Lambda} =$ 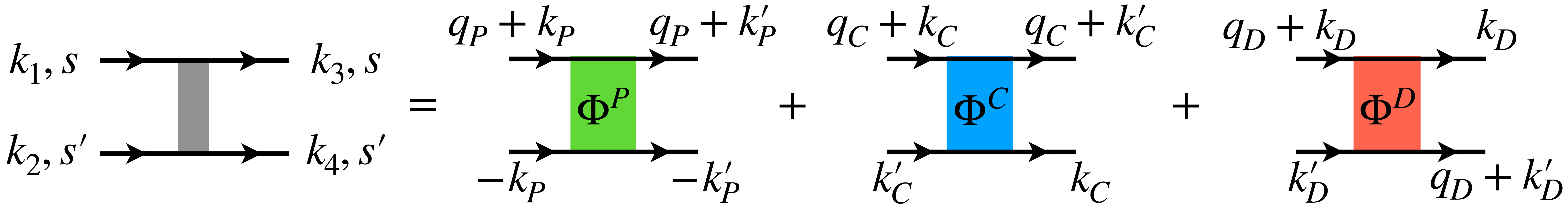

  - transfer momentum & form-factor expansion

$$\Phi^X(\boldsymbol{q}, \boldsymbol{k}, \boldsymbol{k}') = \sum_{l,l'} X^{l,l'}(\boldsymbol{q}) f_l(\boldsymbol{k}) f^*_{l'}(\boldsymbol{k}')$$

Channel X	P	C	D
Interaction type	Pairing	Magnetic	Density
Transfer momentum q_X	$\boldsymbol{k}_1 + \boldsymbol{k}_2$	$\boldsymbol{k}_1 - \boldsymbol{k}_4$	$\boldsymbol{k}_1 - \boldsymbol{k}_3$
Momentum k_X	$-\boldsymbol{k}_2$	$\boldsymbol{k}_4$	$\boldsymbol{k}_3$
Momentum k'_X	$-\boldsymbol{k}_4$	$\boldsymbol{k}_2$	$\boldsymbol{k}_2$

  - obtain flow equations for $X^{l,l'}(\mathbf{q})$

  - choose momentum mesh 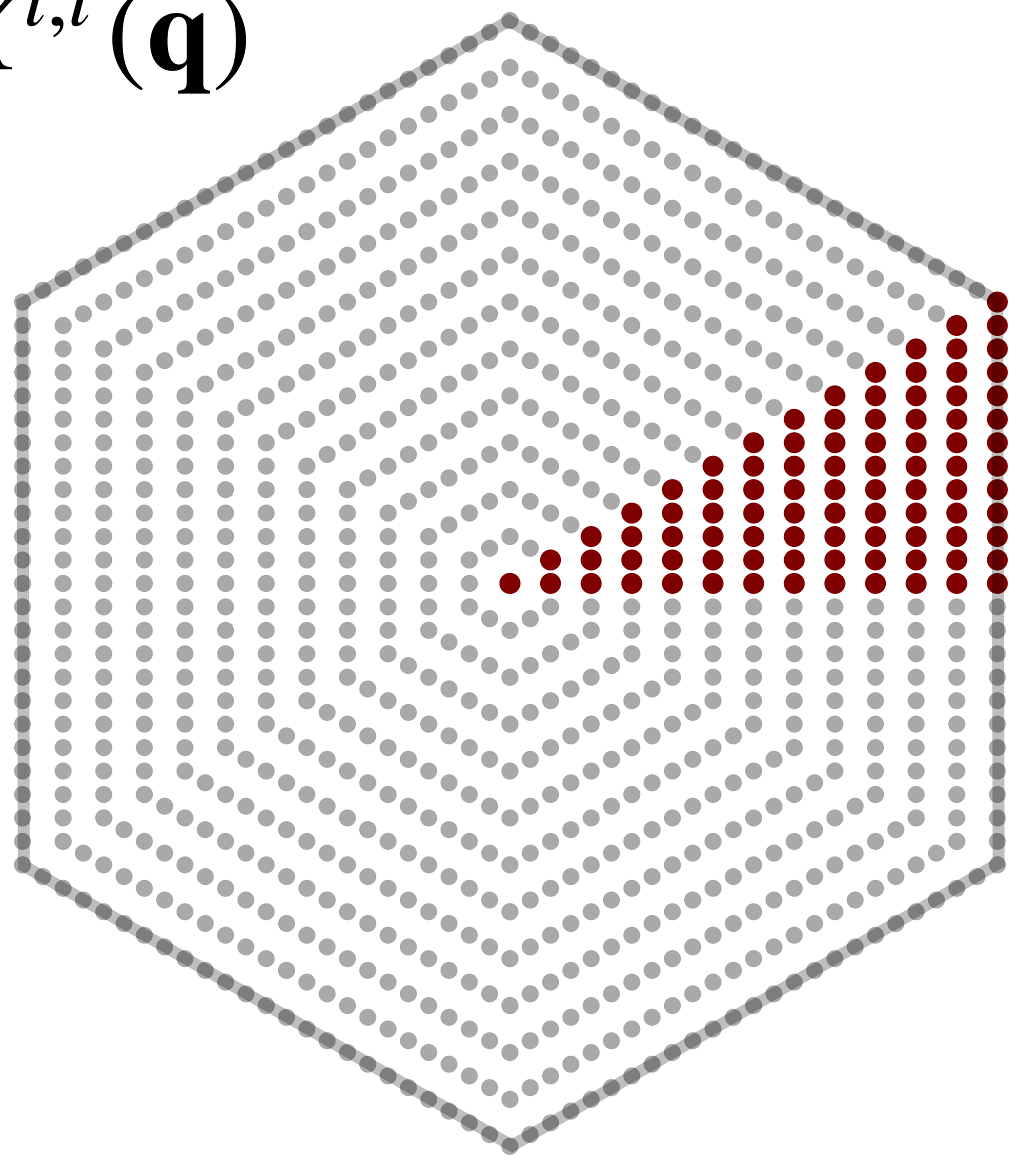 and form-factors $f_l(\mathbf{k}) = e^{i\mathbf{k}\cdot\mathbf{R}_l}$ 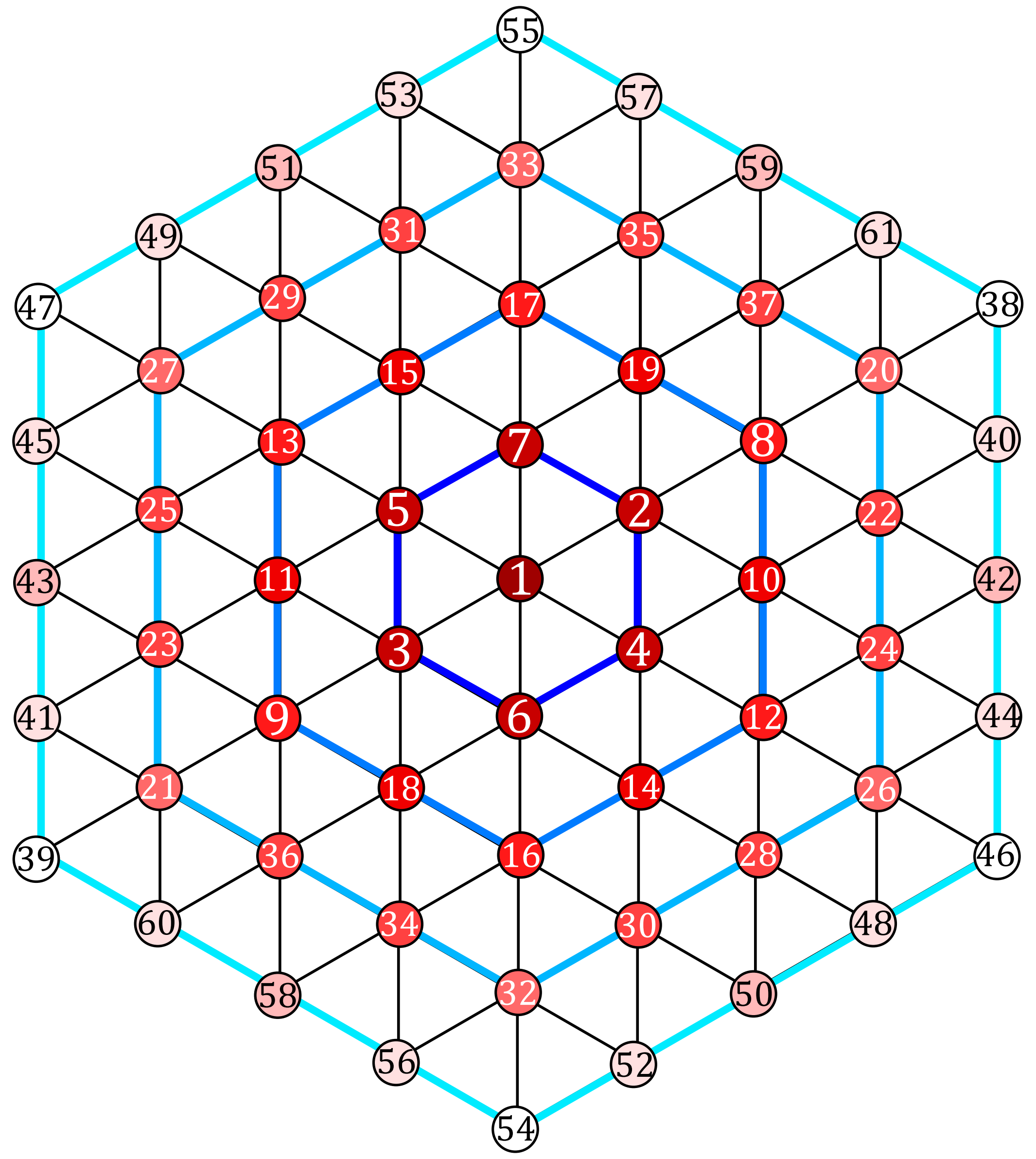

High-momentum resolution with truncated-unity FRG

$t_1 \approx -2.5\,\mathrm{meV}, \quad t_2 \approx 0.5\,\mathrm{meV}, \quad t_3 \approx 0.25\,\mathrm{meV}, \quad U/|t_1| = 4, \quad V_2/V_1 \approx 0.36, \quad V_3/V_1 \approx 0.26$ Zhou, Sheng, Kim, PRL (2022)

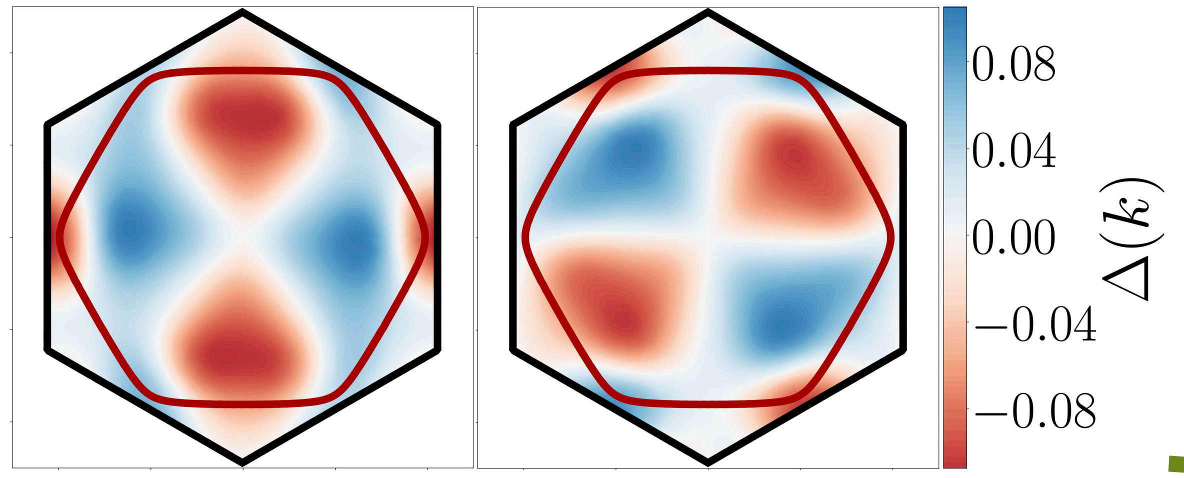

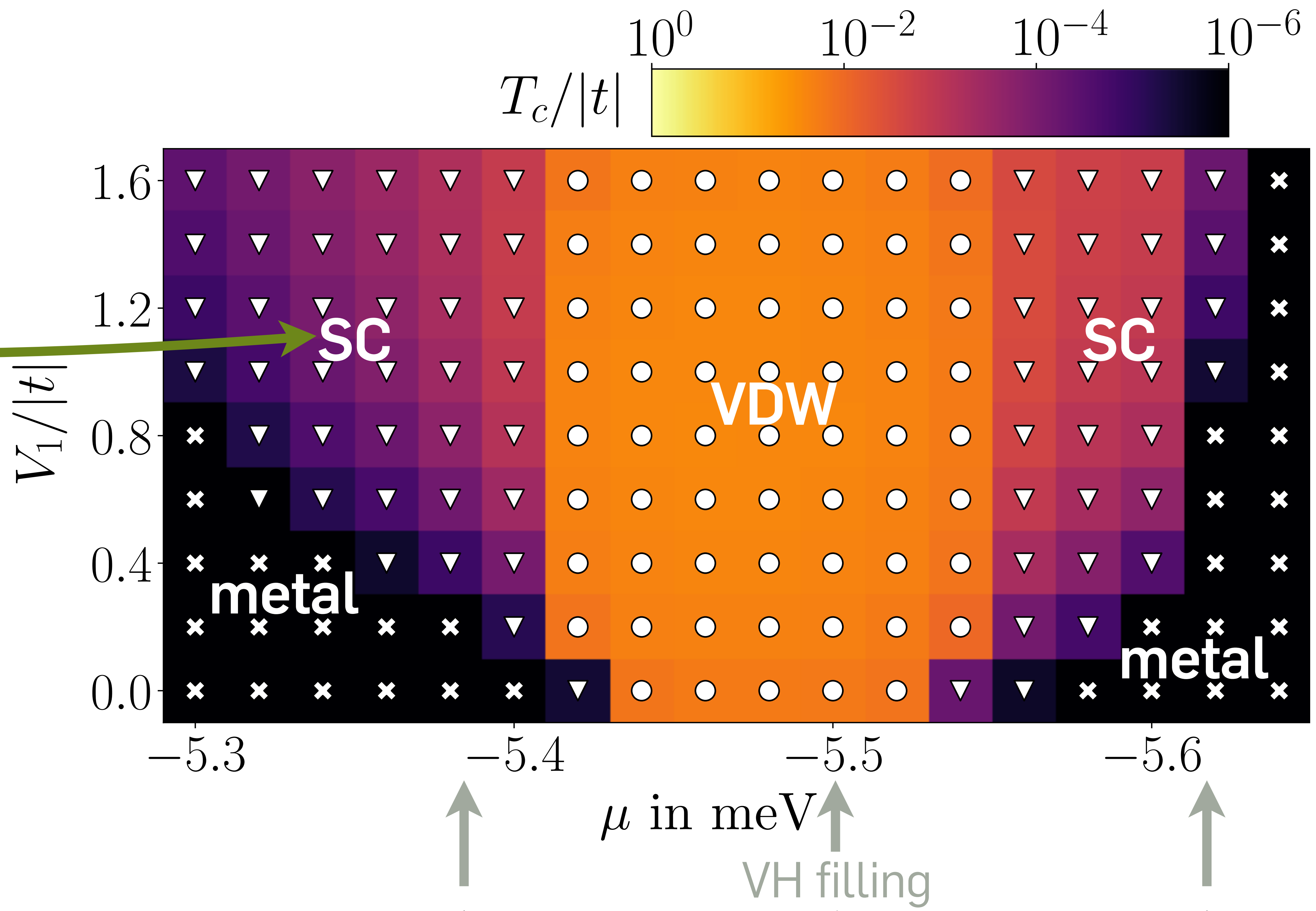

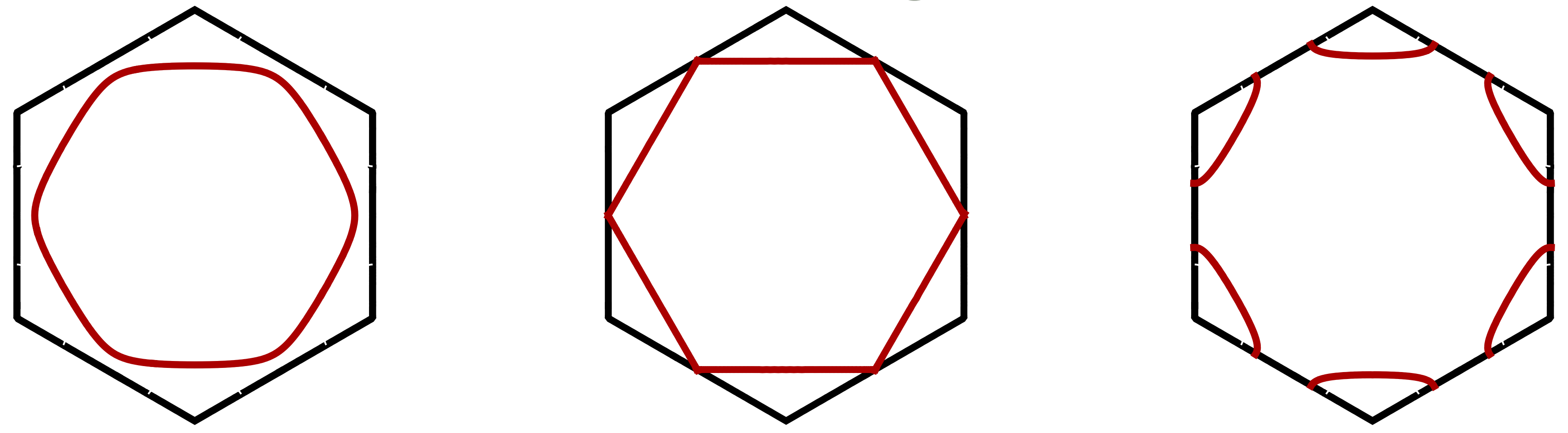

High-momentum resolution with truncated-unity FRG

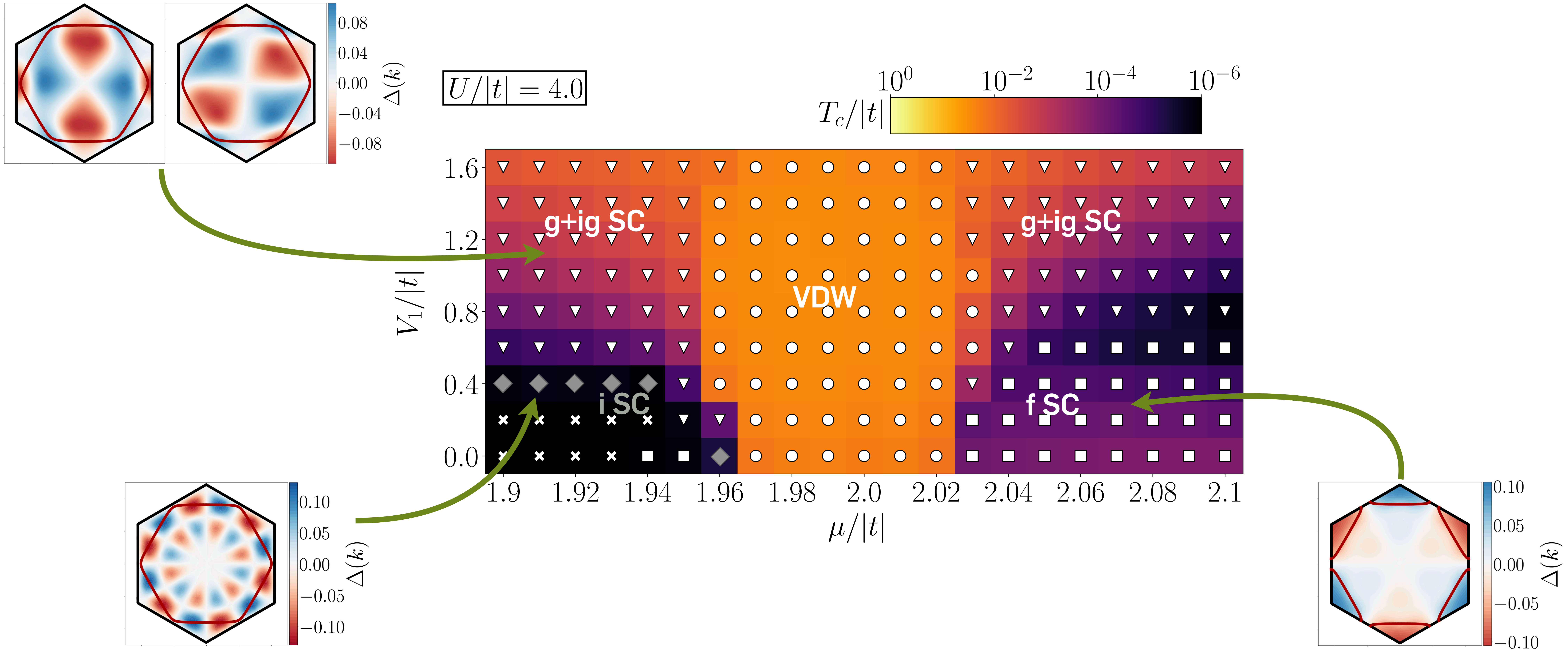

Twisted homobilayer WSe_2

- triangular lattice with a large moiré unit cell and corresponding moiré Brillouin zone
  - strong spin-momentum locking of layers
  - spin up (down) near moiré K point predominantly from top (bottom) layer
  - broken inversion symmetry of individual layers
    - inversion symmetry breaking in moiré system
    - retained C_3 three-fold rotation symmetry
  - Application of transverse displacement field (*D*)
    - $D =$ interlayer potential difference tuned by top/bottom gate voltages
    - splits up spin up/down Fermi surfaces

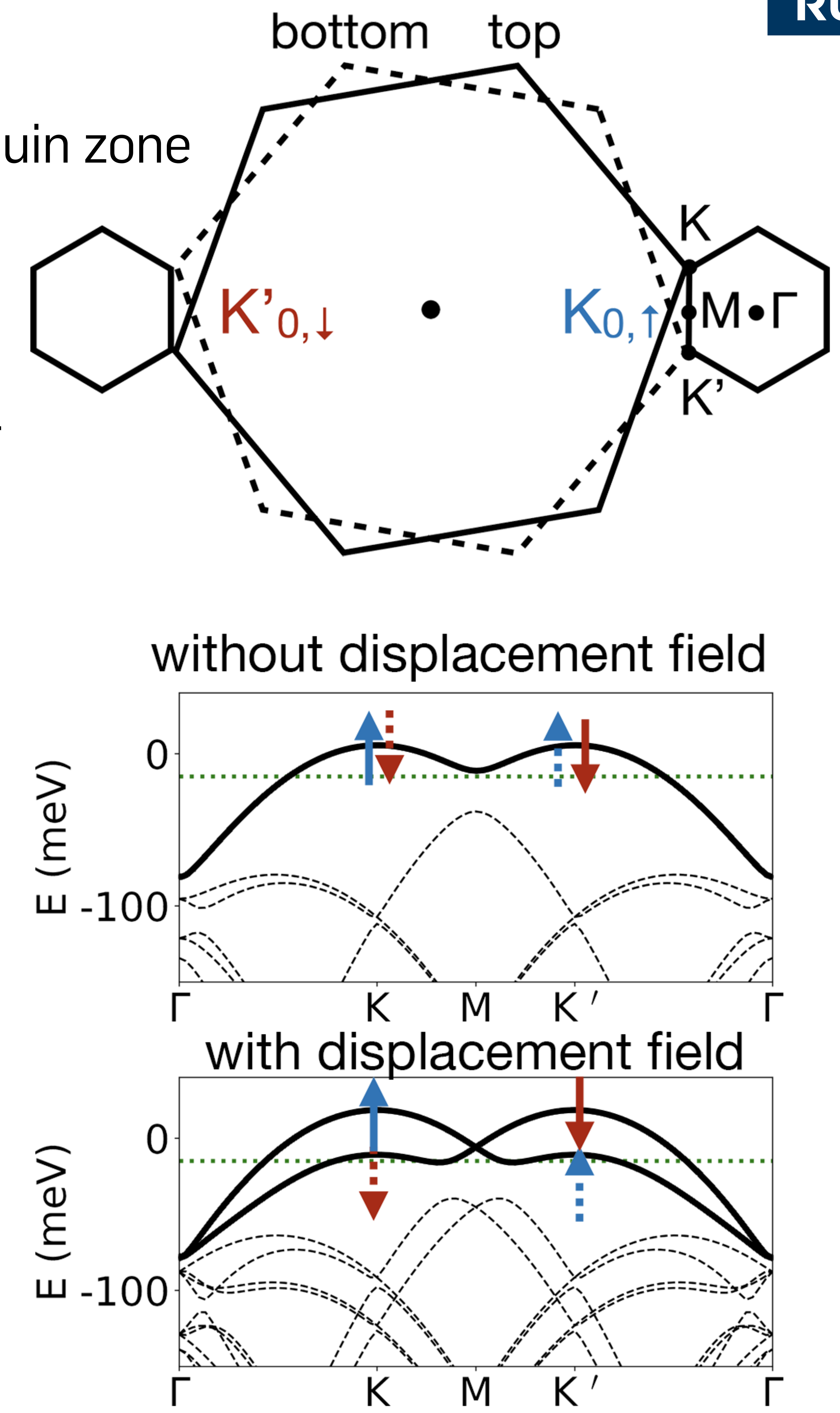

Zang, Wang, Cano, Millis, PRB (2021)

Twisted homobilayer WSe_2

RUB

- effective moiré tight-binding Hamiltonian $$H = -\sum_{\substack{\vec{k},\vec{a}_m,\\ \sigma=\pm}} 2|t|\cos(\vec{k}\cdot\vec{a}_m + \sigma\phi)c^\dagger_{\vec{k},\sigma}c_{\vec{k},\sigma}$$
  - effect of displacement field modeled by changing phase ϕ and $\sigma = \pm$
  - Examples for Fermi surface configurations:

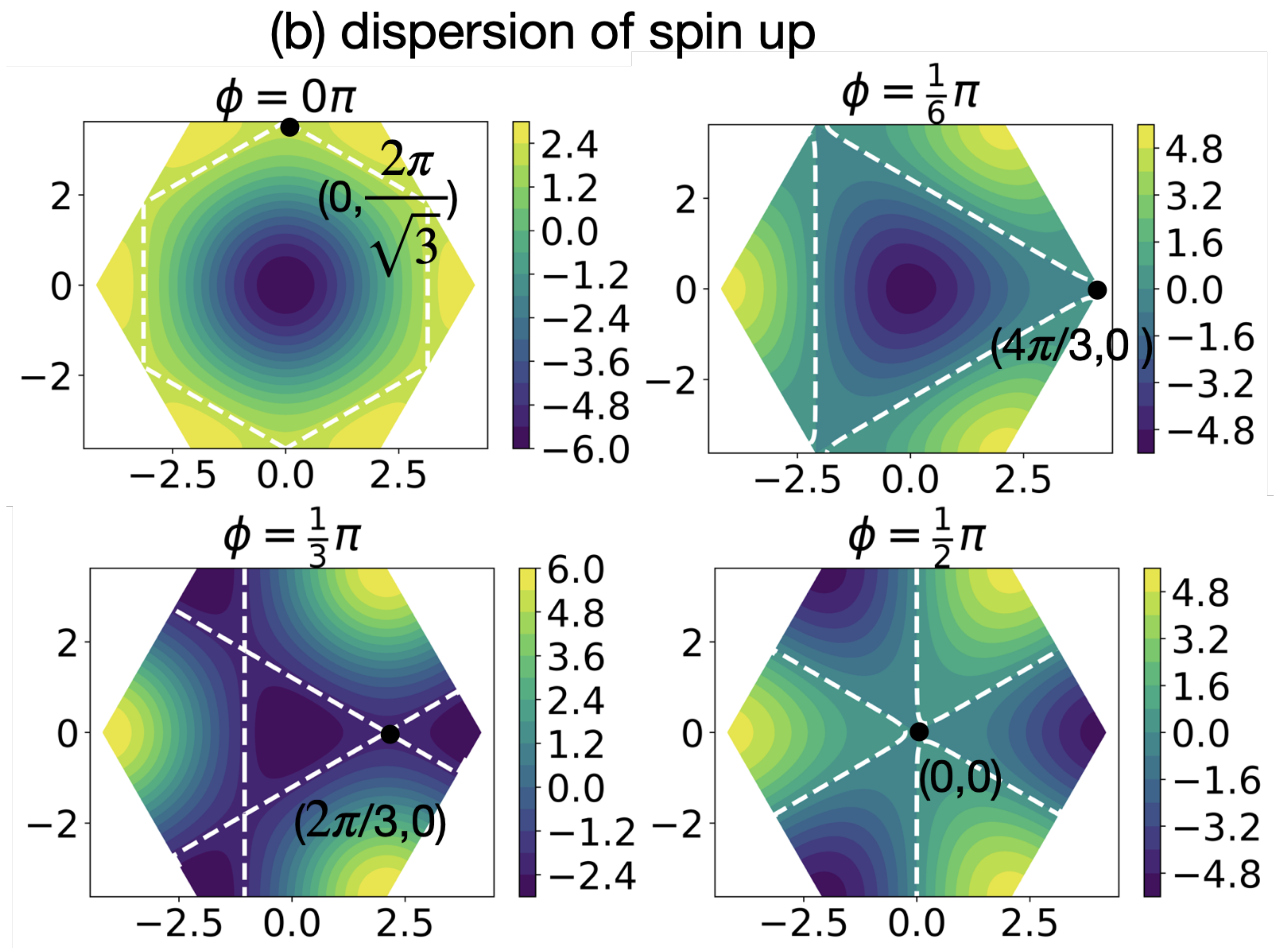

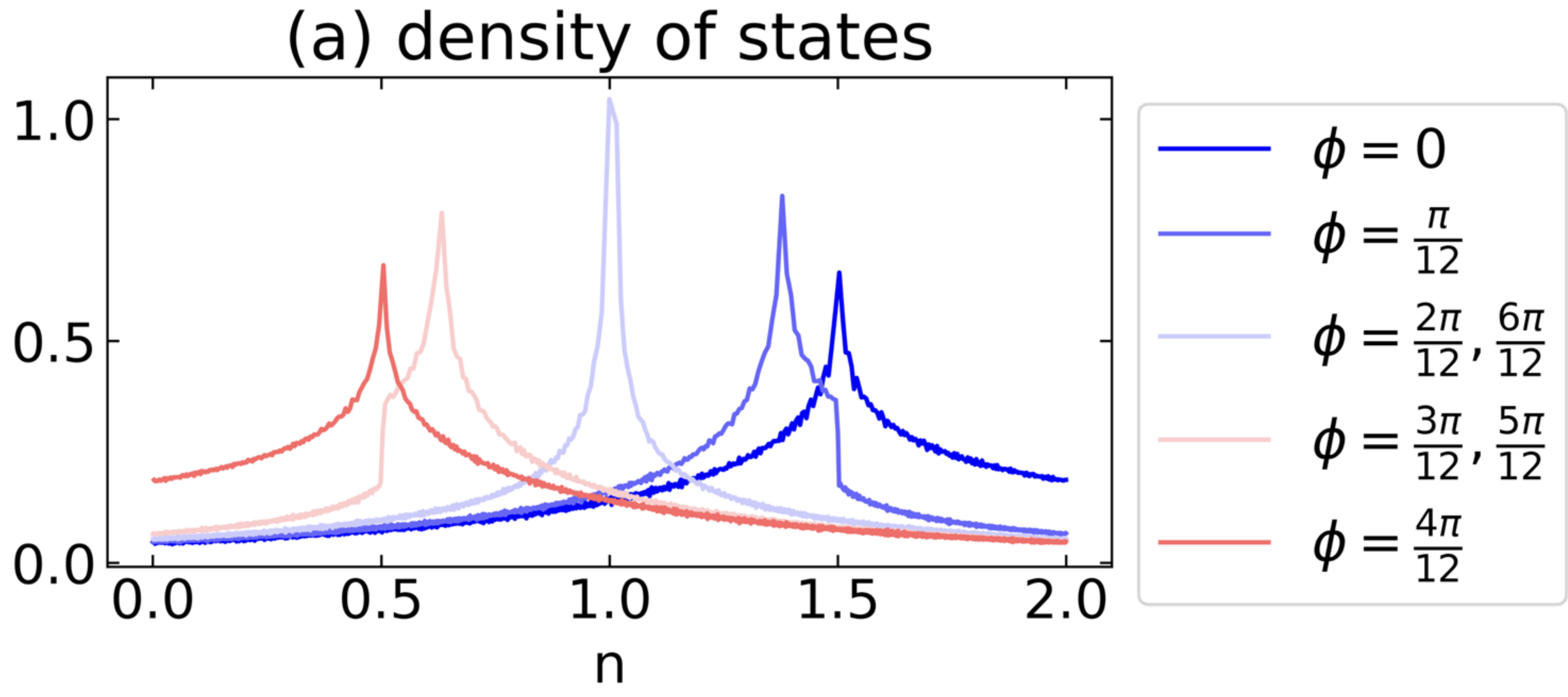

- Van-Hove singularities present in band dispersion!

Zang, Wang, Cano, Millis, PRB (2021)

Twisted homobilayer WSe_2

RUB

- effective moiré tight-binding Hamiltonian $$H = -\sum_{\substack{\vec{k},\vec{a}_m,\\ \sigma=\pm}} 2|t|\cos(\vec{k}\cdot\vec{a}_m + \sigma\phi)c^\dagger_{\vec{k},\sigma}c_{\vec{k},\sigma}$$
  - effect of displacement field modeled by changing phase ϕ and $\sigma = \pm$
  - Examples for Fermi surface configurations:

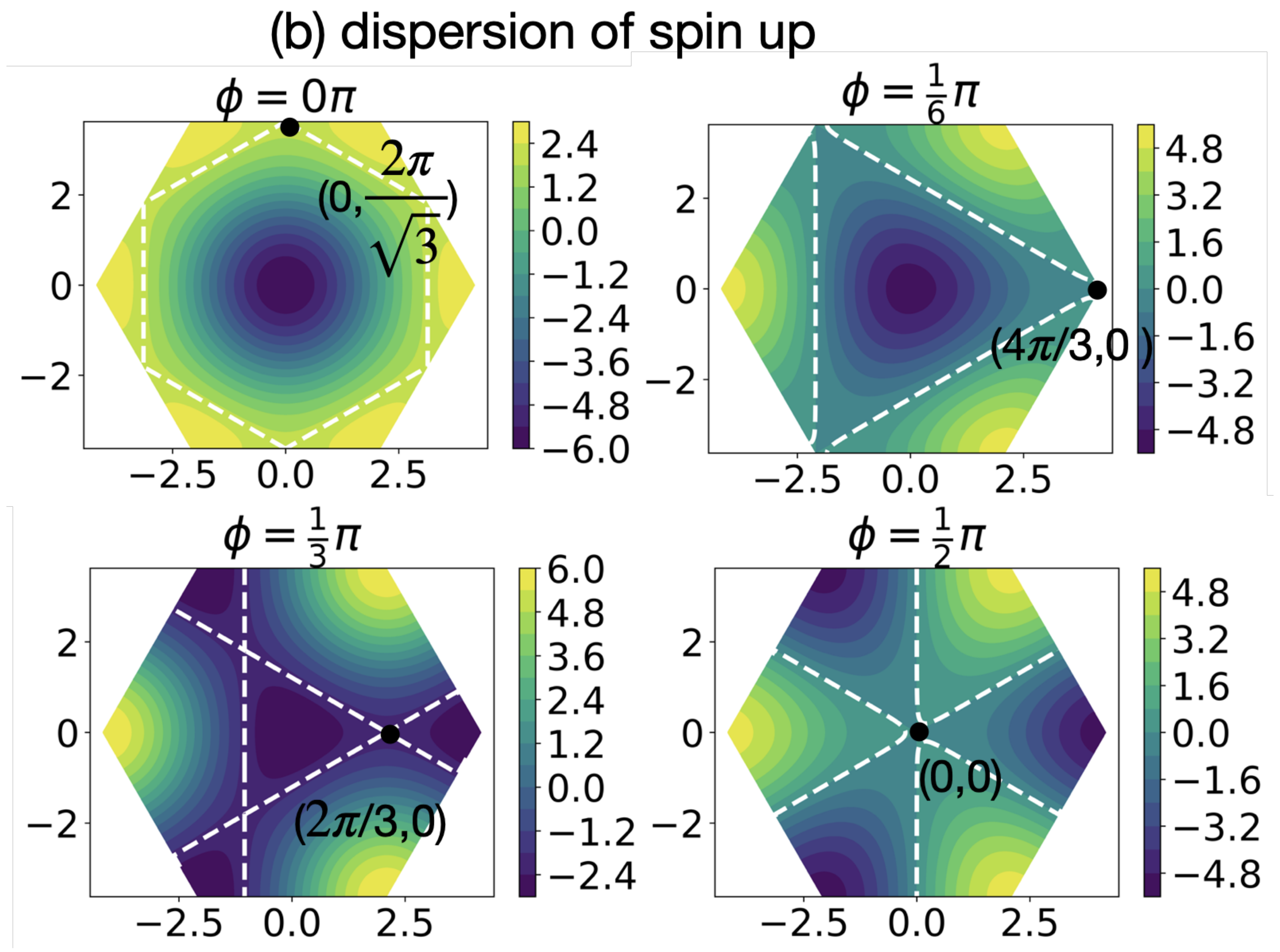

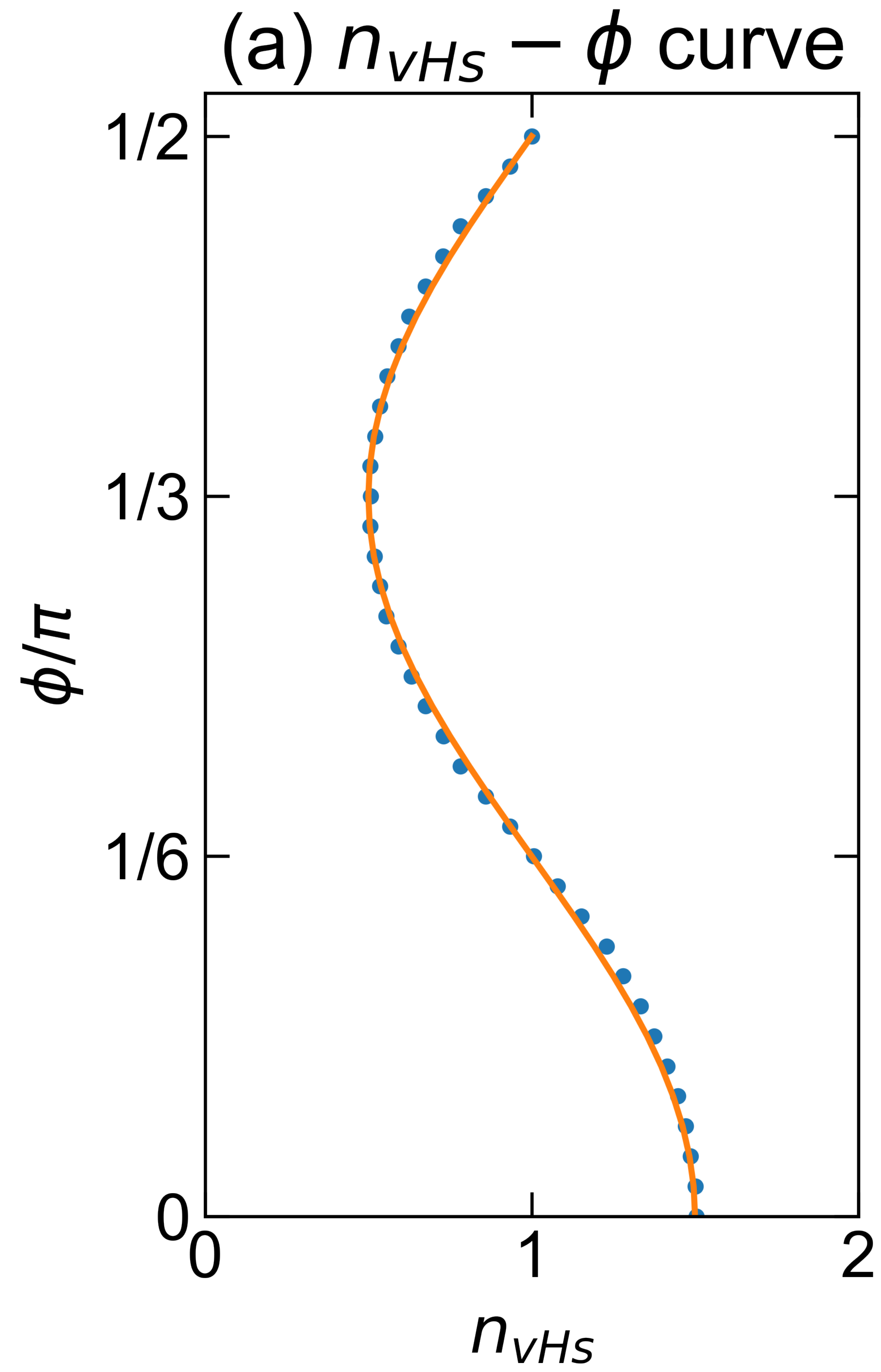

- Van-Hove singularities present in band dispersion!

Zang, Wang, Cano, Millis, PRB (2021)

Twisted homobilayer WSe_2

- effective moiré tight-binding Hamiltonian $$H = -\sum_{\substack{\vec{k},\vec{a}_m,\\ \sigma=\pm}} 2|t|\cos(\vec{k}\cdot\vec{a}_m + \sigma\phi)c^\dagger_{\vec{k},\sigma}c_{\vec{k},\sigma}$$
  - effect of displacement field modeled by changing phase ϕ and $\sigma = \pm$
  - Examples for Fermi surface configurations:

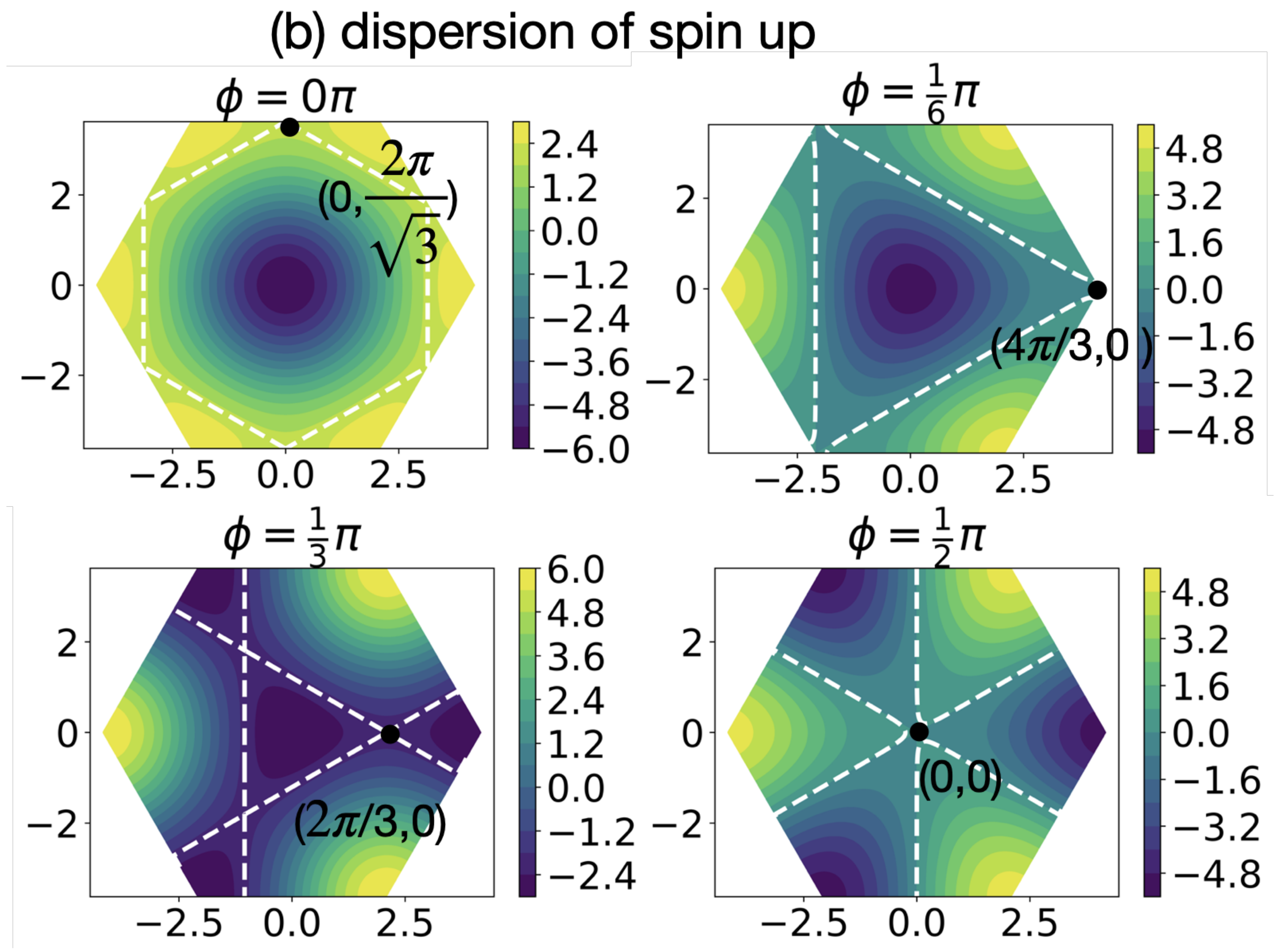

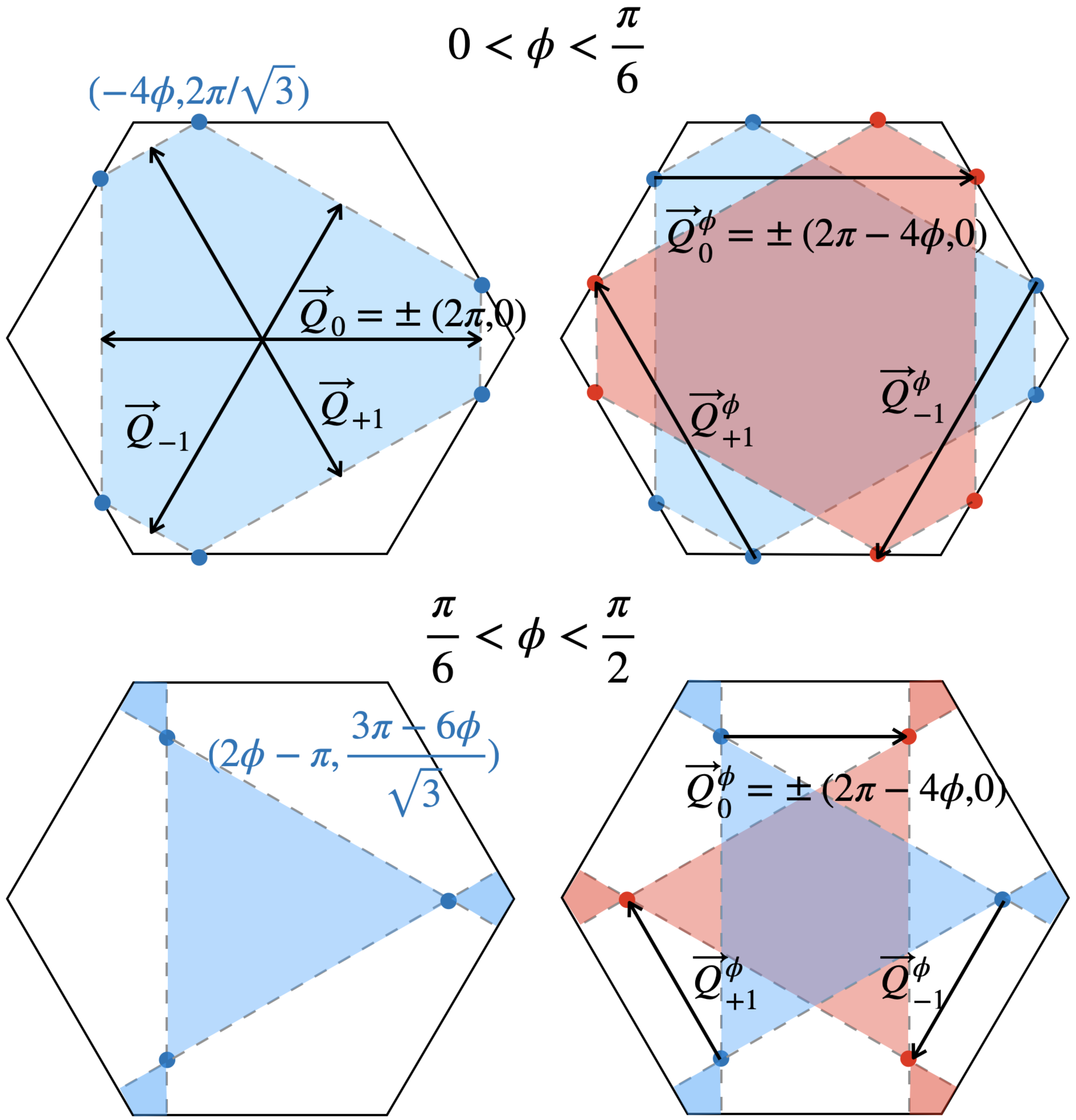

Zang, Wang, Cano, Millis, PRB (2021)

Hartree-Fock study of twisted homobilayer WSe_2

RUB

- effective moiré Hubbard Hamiltonian

$$H = -\sum_{\substack{\vec{k},\vec{a}_m,\\ \sigma=\pm}} 2|t|\cos(\vec{k}\cdot\vec{a}_m + \sigma\phi)c^\dagger_{\vec{k},\sigma}c_{\vec{k},\sigma} + U\sum_i n_{i\uparrow}n_{i\downarrow}$$

  - Hartree-Fock correlated phase diagram
  - general fillings and $U/t = 3{,}10$
  - Hartree-Fock approach
    - single-channel resummation of ph diagrams
    - ✓ finds plethora of (commensurate) magnetic orders!
    - \- misses inter-channel feedback
    - \- misses pp diagrams
    - ➡ no superconductivity!

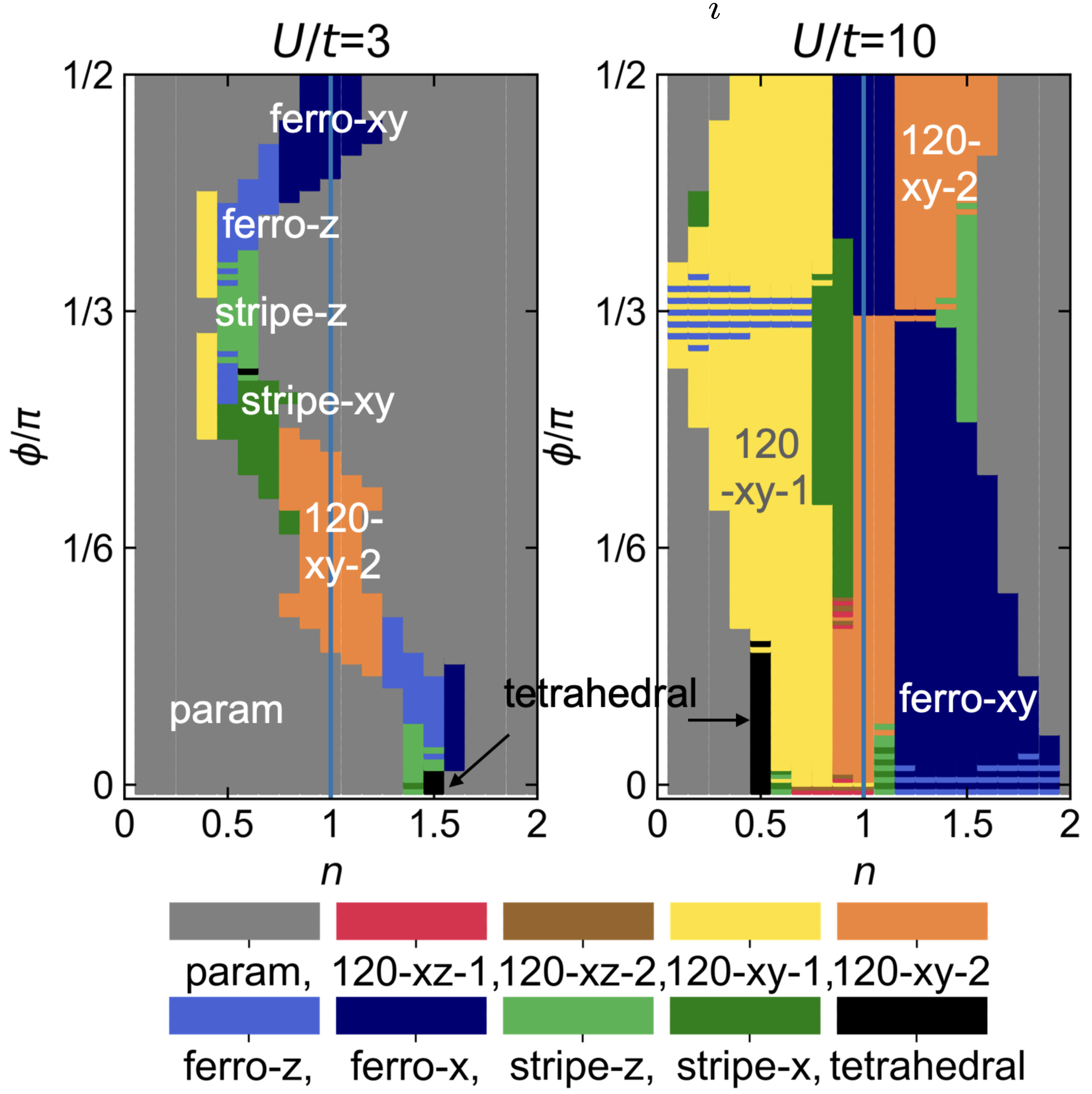

Zang, Wang, Cano, Millis, PRB (2021)

FRG study of twisted homobilayer WSe_2 - sanity check

RUB

- effective moiré Hubbard Hamiltonian

$$H = -\sum_{\substack{\vec{k},\vec{a}_m,\\ \sigma=\pm}} 2|t|\cos(\vec{k}\cdot\vec{a}_m + \sigma\phi) c^\dagger_{\vec{k},\sigma} c_{\vec{k},\sigma} + U\sum_i n_{i\uparrow}n_{i\downarrow}$$

  - FRG correlated phase diagram
  - general fillings and $U = 6t \simeq 0.7W$
  - numerically expensive FRG implementation
    - full resolution of BZ
  - ✓ finds (incommensurate) magnetic orders!
  - ✓ ph susceptibilities compatible w/ HF study

$$\chi^{ij}(\boldsymbol{q}) = \sum_{\sigma_1\ldots\sigma_4} \sigma_i^{\sigma_1\sigma_4}\, \chi^D_{\sigma_1\sigma_2\sigma_3\sigma_4}(\boldsymbol{q})\sigma_j^{\sigma_3\sigma_2}$$

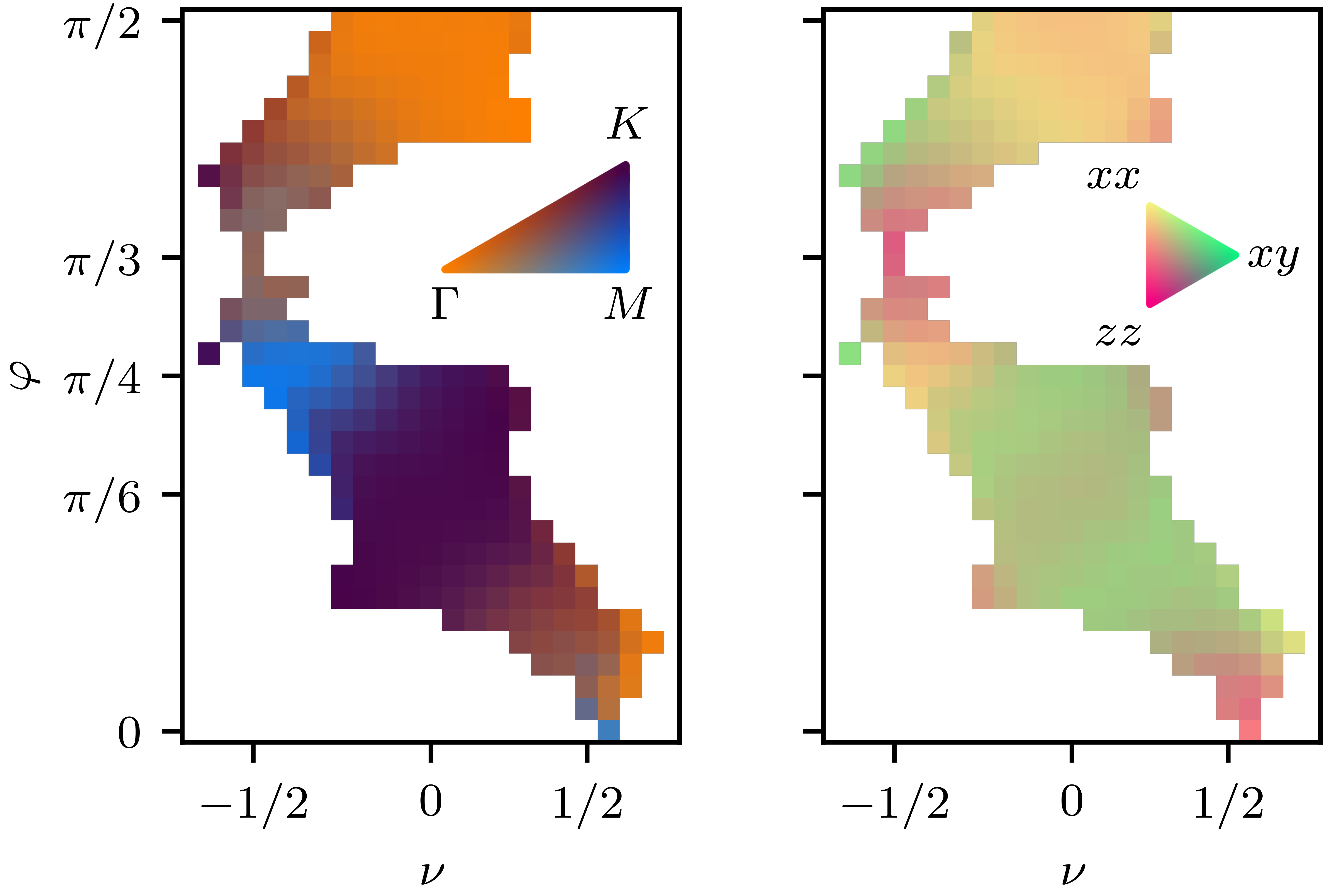

Klebl, Fischer, Classen, Scherer, Kennes, arxiv:2204.00648 (2021)

FRG study of twisted homobilayer WSe_2

RUB

- effective moiré Hubbard Hamiltonian $$H = -\sum_{\substack{\vec{k},\vec{a}_m,\\ \sigma=\pm}} 2|t|\cos(\vec{k}\cdot\vec{a}_m + \sigma\phi)c^\dagger_{\vec{k},\sigma}c_{\vec{k},\sigma} + U\sum_i n_{i\uparrow}n_{i\downarrow}$$
  - FRG correlated phase diagram
  - general fillings and $U = 6t \simeq 0.7W$
  - numerically expensive FRG implementation
    - full resolution of BZ
    - ✓ finds (incommensurate) magnetic orders!
    - includes inter-channel feedback
    - includes pp diagrams
    - ➡ unconventional superconductivity!

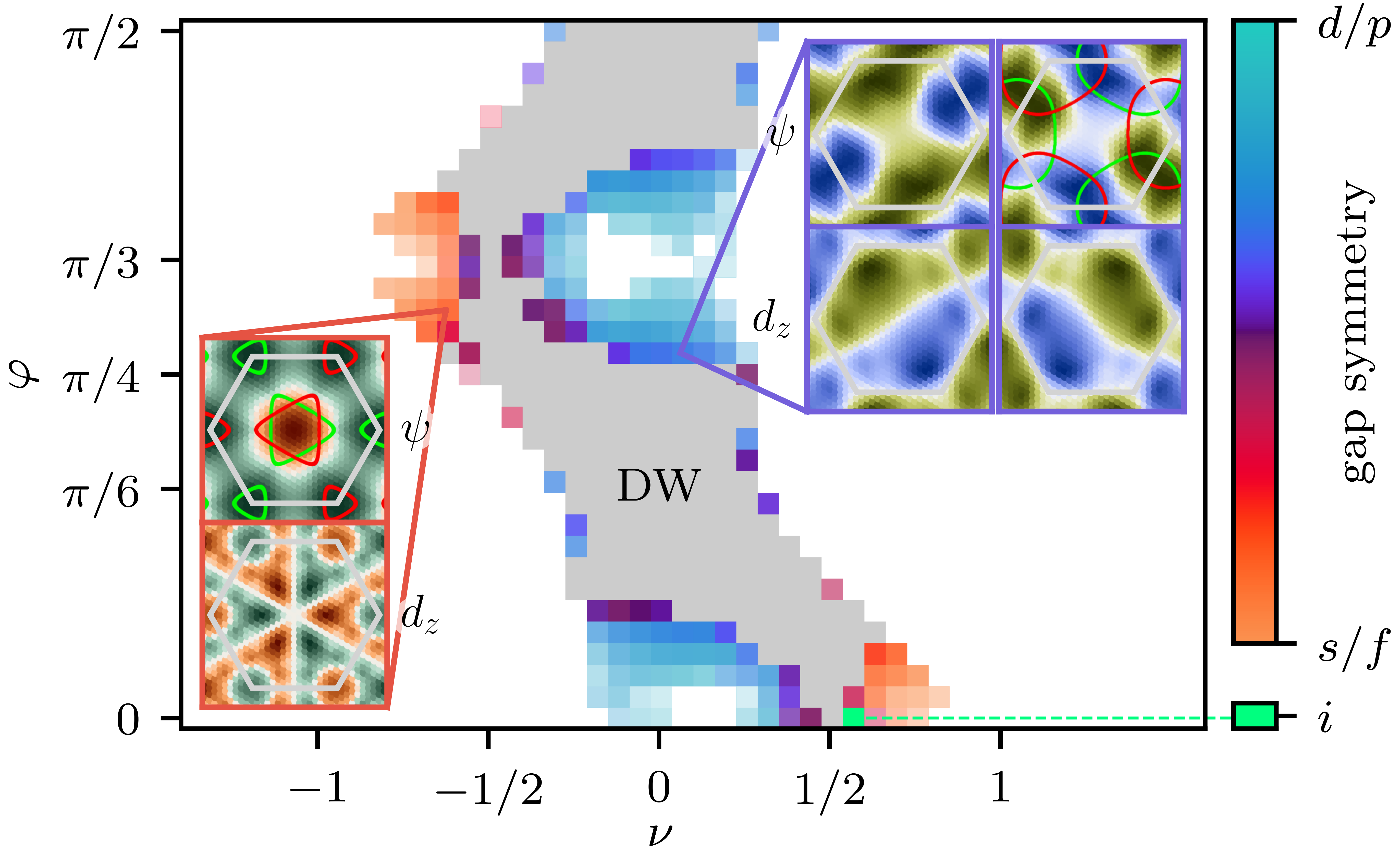

Klebl, Fischer, Classen, Scherer, Kennes, arxiv:2204.00648 (2021)

FRG study of twisted homobilayer WSe_2

- effective moiré Hubbard Hamiltonian $$H = -\sum_{\substack{\vec{k},\vec{a}_m,\\ \sigma=\pm}} 2|t|\cos(\vec{k}\cdot\vec{a}_m + \sigma\phi)c^\dagger_{\vec{k},\sigma}c_{\vec{k},\sigma} + U\sum_i n_{i\uparrow}n_{i\downarrow}$$
  - FRG correlated phase diagram

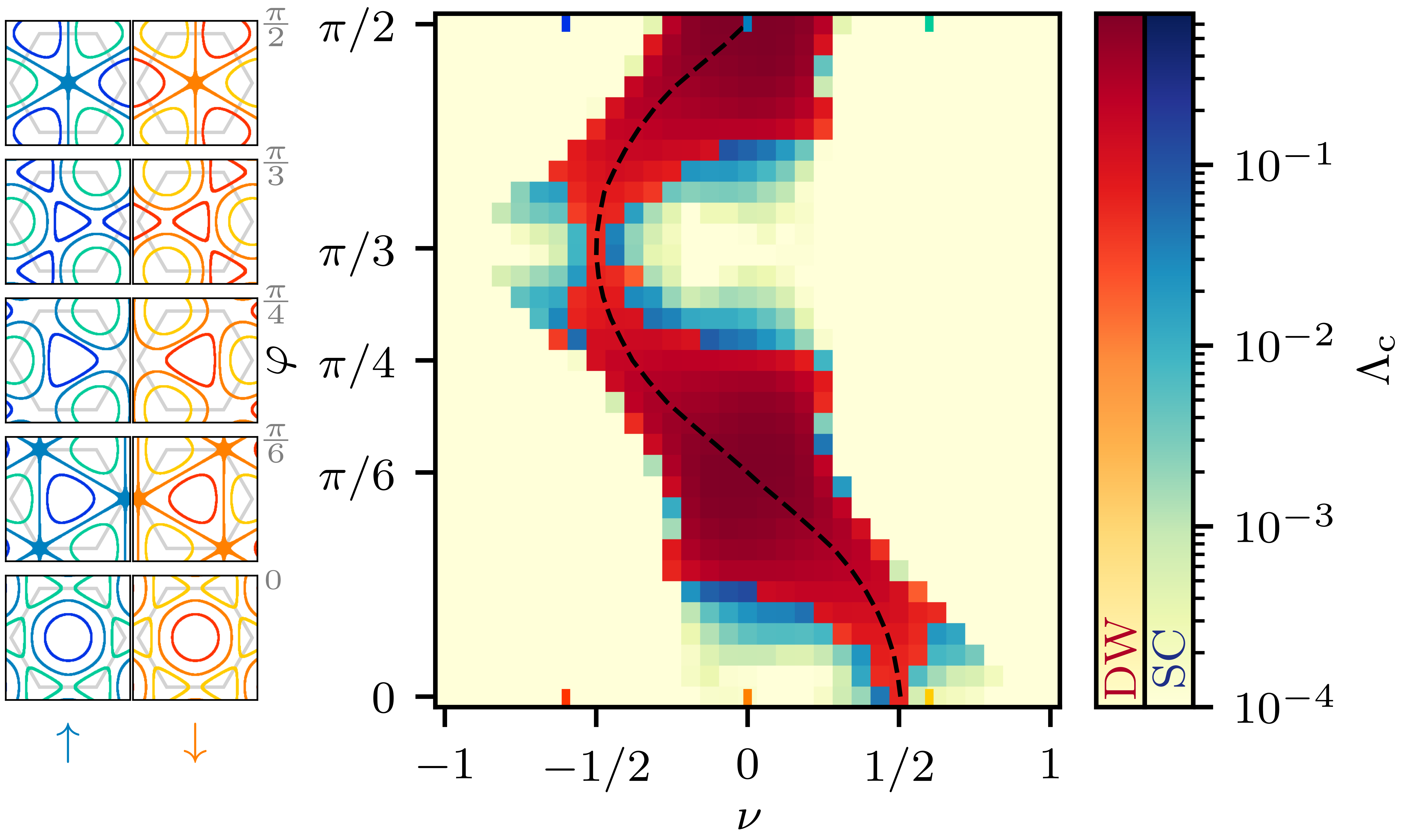

Klebl, Fischer, Classen, Scherer, Kennes, arxiv:2204.00648 (2021)

Summary I

RUB

- moiré TMDs as quantum simulators for Hubbard model and other strongly-correlated electrons systems
  - triangular lattice → geometric frustration
  - band filling tunable by gating
  - tunable strength and range of electron-electron interactions

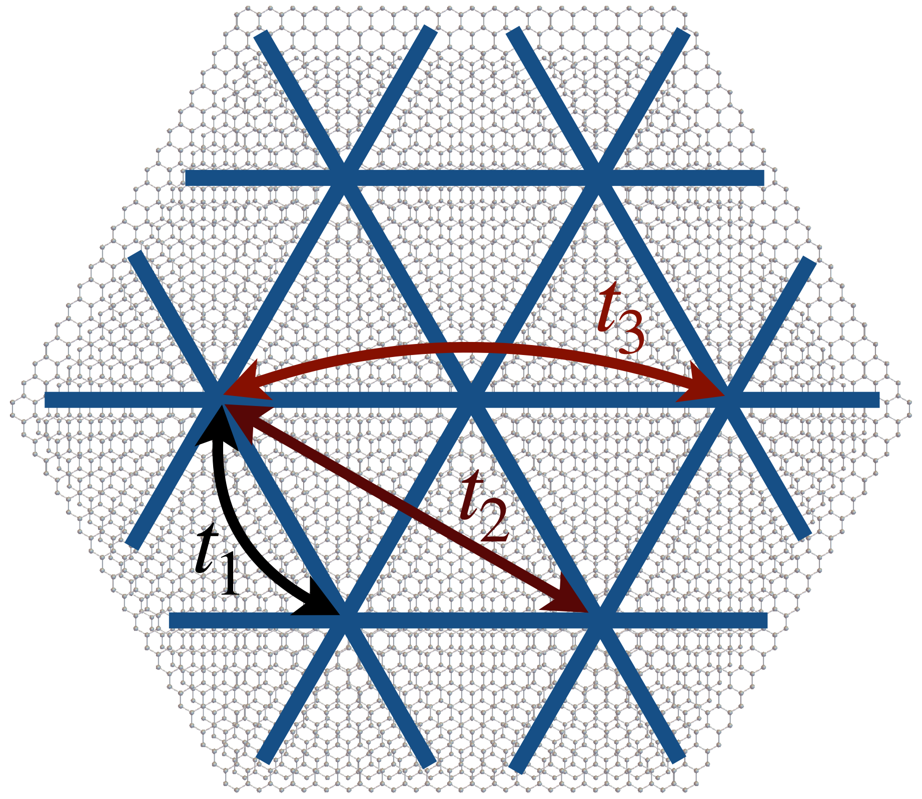

➡ complex **interplay** between **electronic interactions** and **geometric frustration**

  - plethora of strongly-correlated phases suggested (MIT, spin liquids, magnetism,...)
  - recent experiments → confirmation of relevance of many-body interactions
  - what about superconductivity...?

Summary II

RUB

- simulate **extended Hubbard model on triangular lattice** w/ moiré TMDs
- sizeable non-local Coulomb interactions
- Van-Hove filling accessible
- resolve competing orders with FRG
  - valley-density wave
  - **chiral (*g*+*ig*)-wave superconductivity**
    - breaks time-reversal
    - fully gapped Fermi surface
    - **topological** with Chern number $|\mathcal{N}| = 4$
- applications to related moiré materials, e.g., *t*WSe_2

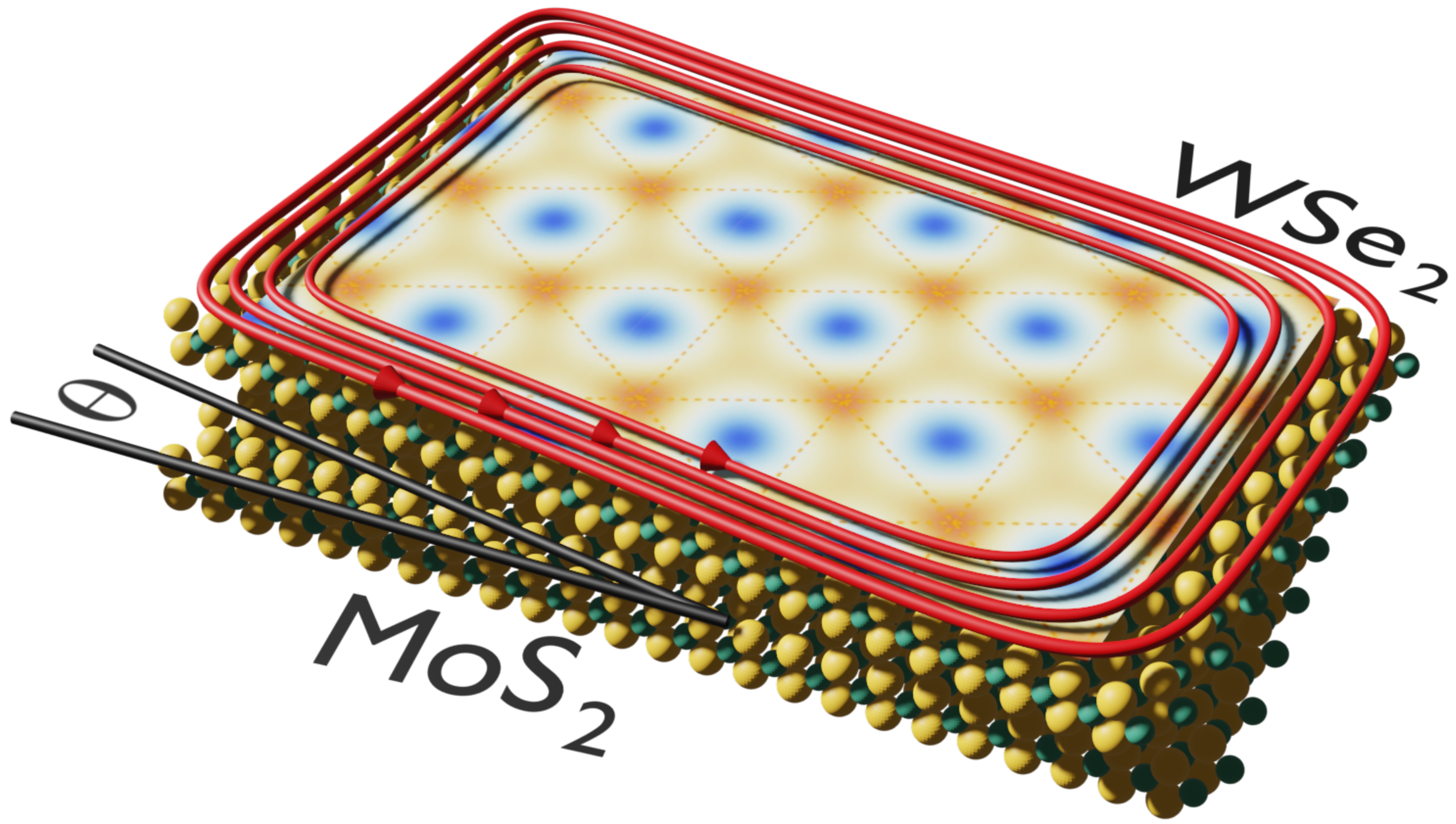

Scherer, Kennes, Classen, npj Quant. Mat. (2022)
Gneist, Classen, Scherer, PRB (2022)
Klebl *et al.*, arxiv:2204.00648 (2021)